ISSN 0103-5118 / e-ISSN 2446-6786

VOLUME 37 – Number 4
OCTOBER / NOVEMBER / DECEMBER 2026

JBNC

JORNAL BRASILEIRO DE NEUROCIRURGIA

BRAZILIAN JOURNAL OF NEUROSURGERY

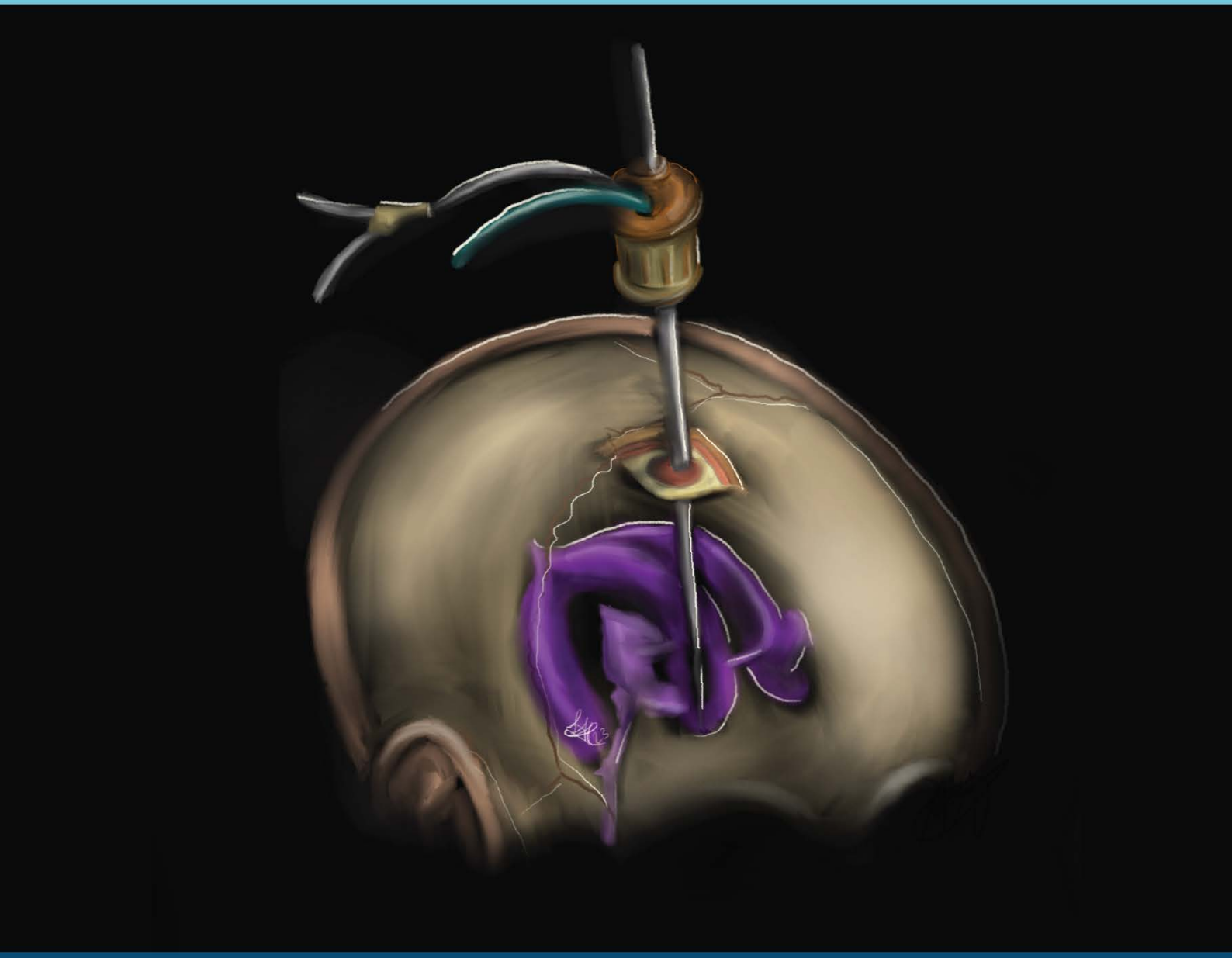

Official Journal of the Brazilian Academy of Neurosurgery ABNc

latindex

ISSN 2446-6786

JBNC Brazilian Journal of Neurosurgery
Jornal Brasileiro de Neurocirurgia

Official Journal of the
Brazilian Academy of Neurosurgery

Indexed in LATINDEX Database

Volume 37 **Number 4** **Biennium 2025-2027**

JBNC
JORNAL BRASILEIRO DE NEUROCIRURGIA
BRAZILIAN JOURNAL OF NEUROSURGERY

INTERNATIONAL EDITORIAL BOARD

JBNC
JORNAL BRASILEIRO DE NEUROCIRURGIA
BRAZILIAN JOURNAL OF NEUROSURGERY

NATIONAL EDITORIAL BOARD

EDITOR-IN-CHIEF
The Editor-in-Chief oversees the entire editorial process and reviews the recommendations made by the scientific editors regarding the acceptance or rejection of submissions. He is responsible for the final decision ensuring the quality and integrity of the journal's content.

EXECUTIVE EDITOR
The Executive Editor is responsible for the operational aspects of the journal. This includes managing policies related to editorial matters, addressing allegations of misconduct, and overseeing contracts with sponsors and service providers in order to uphold the journal's smooth running and maintaining its ethical standards.

SCIENTIFIC EDITOR
The Scientific Editor focuses specifically on the scientific aspects of the submissions. Their responsibility is to assess the scientific merit and validity of the research presented in the submissions. This role is key to ensuring that the content published by the journal is both scientifically accurate and contributes meaningfully to the field.

EXECUTIVE SECRETARY
The executive secretary is responsible for addressing all matters related to the editorial workflow from sub-mission to publication, making sure that requests and complaints are sent to the proper channels and prop-erly handled.

SCIENTIFIC ASSOCIATED EDITORS
They play a supportive role to both the Editor-in-Chief and the Scientific Editor. Their primary responsibility is managing the peer review process of submissions. This involves overseeing the review workflow, ensuring that each submission is evaluated fairly and thoroughly by qualified peers in the field.

ASSOCIATED EXECUTIVE EDITORS
They assist the Executive Editor in managing processes related to the adoption and implementation of new editorial policies and best practices. They also play a vital role during investigations of allegations of miscon-duct. Their work ensures that the journal not only stays current with evolving standards in scholarly publishing but also upholds ethical practices and addresses issues proactively.

EDITORIAL BOARD

The editorial board's role is more focused on giving advice on strategic journal development matters, its members might be requested to assist both the executive and scientific editors, should their expertise in their respective academic fields be required. This can involve:

Advising on specific submissions, contributing to discussions on content areas, and providing insights that help maintain the journal's academic rigor. Provide operational support to the executive editor in implement-ing policies and procedures, or assisting the scientific editor in overseeing the scientific quality and integrity of the journal.

Assist in strategic planning and development of the journal by evaluating and recommending best practices, organizing and suggesting calls for special or thematic issues, while ensuring that the journal's direction aligns with current trends and needs in the field.

JBNC
JORNAL BRASILEIRO DE NEUROCIRURGIA
BRAZILIAN JOURNAL OF NEUROSURGERY

INSTRUCTIONS FOR AUTHORS

1. MISSION AND SCOPE

The Brazilian Journal of Neurosurgery – JBNc (ISSN print 0103-5118, ISSN online 2446-6786) is an online journal published by the Academia Brasileira de Neurocirurgia (https://www.abnc.org.br/). The journal is fully open access, peer reviewed and accepts submissions written in English, Portuguese, or Spanish. Accepted contributions are published in a quarterly issue-based model with four issues per year, and licensed under the Creative Commons Attribution 4.0 International (CC BY 4.0) (https://creativecommons.org/licenses/by/4.0/deed.en_US) license. JBNc does not charge submission or publication fees.

2. MANUSCRIPT PREPARATION GUIDELINES

SECTION SPECIFIC REQUIREMENTS

Submissions must follow the limits and specific requirements outlined on the table below, according to their section.

Section	Abstract	Text sections	Text length	Tables & Figures	References (max)
Original article	structured not excee-ding 200 words	introduction, methods, results, discussion, conclusion and references	4000 words	10	75
Review (preferably systematic review)	non-structured not exceeding 200 words	introduction, method, results, discussion, conclusion and references	4000 words	10	75
Case Report (preferably with systematic review)	non-structured not exceeding 200 words	introduction (with brief literature review), clinical case presentation, discussion, final comments and references	3500 words	8	45
Brief Note	non-structured not exceeding 200 words	no requirement	1500 words	3	30
Clinical Images	non-structured not exceeding 200 words	no requirement	1500 words	5	30
Letter to the editor	non-structured not exceeding 200 words	no requirement	1500 words	0	15

NUMBER OF AUTHORS

The number of authors should be proportional to the complexity and scientific nature of the submitted manuscript. In general, case reports and technical notes are recommended to include between 3 and 6 authors; case series between 4 and 8 authors; and original articles between 5 and 10 authors. Multicenter studies, complex prospective investigations, research involving advanced statistical analysis, innovative technologies, or multidisciplinary collaboration may justify a higher number of authors. All authors must fully meet internationally accepted authorship criteria, including substantial contribution to the conception of the study, data collection or analysis, drafting or critical revision of the manuscript, final approval of the submitted version, and full intellectual responsibility for the published content. The inclusion of authors without effective scientific contribution is strongly discouraged.

Section	Authors (max)
Original article	5-10
Review (preferably systematic review)	5-8
Case Report (preferably with systematic review)	3-6
Case series (preferably with systematic review)	4-8
Brief Note	3-5
Clinical Images	3-5
Letter to the editor	3
Multicenter studies, complex prospective investigations, research involving advanced statistical analysis, innovative technologies, or multidisciplinary collaboration	Justify more authors

INTRODUCTION

In the Introduction section we state the motivation for the work presented in the manuscript. Its contents could be:

1) context (to orient readers who are less familiar with the topic and to establish the importance of the manuscript),
2) need (to state the need for the work, as an opposition between what the scientific community currently has and what it wants), 3) task (to indicate what was done in the effort to address the need), and 4) object of the document (to prepare the readers for its structure).

CLINICAL CASE PRESENTATION

Patient's clinical data in comprehensive account of the presenting features, with medical, and social, family history, if needed are presented. All crucial investigations to the management of decisions should be discussed. Images of the case: Choose appropriate images being aware of removing any detail that can identify the patient. If relevant, describe the treatment or surgery. Outcomes and follow up are described elsewhere.

METHODS

In Materials and Methods section, the technical specifications and quantities and source or method of preparation are described. Attention to the use only scientific names of drugs; inclusion of the manufacturer in brackets when describing equipment. Discuss statistical methods if needed.

RESULTS

In Results section, the results of the paper are presented in logical order, using tables and graphs as necessary. Remember that results must be presented and then explained. The results are explained showing how they help to answer the research questions (already cited in the Introduction section).

DISCUSSION

In Discussion section, the principles, relationships and generalizations shown by the results are presented. Also, exceptions or lack of correlations are pointed out. The authors show how their results agree or disagree with pre-vious published papers, and discuss the theoretical implications as well as practical applications of the paper, and the significance of their results.

CONCLUSIONS

In Conclusions section the most important outcome of the work is stated, and interpretation of the findings also. If the authors have succeeded, or not, in addressing the need stated in the Introduction is reported here.

PRODUCT NAMES

If any product is cited in the manuscript the usage of ® or ™, and manufacturer data are mandatory. Use only scientific names of drugs. Include the manufacturer in brackets when describing equipment.

UNITS OF MEASUREMENT

Units of measurements should follow the primary language used (Portuguese/Spanish or English).

ABBREVIATIONS AND SYMBOLS

Abbreviatons should follow the first mention of the term in the manuscript. The list of abbreviations is waived.

FOOTNOTES

Footnotes are used only in Tables/Boxes.

3. USE OF COLORS

Although the use of color is permitted, it is important that authors (or professionals hired for editing) make an effort to ensure that the use of color does not impair understanding for readers with some form of visual impairment. We recommend consulting the following resources before preparing figures or tables using colors:

How to make scientific figures accessible to readers with color-blindness (https://www.ascb.org/science-news/how-to-make-scientific-figures-accessible-to-readers-with color-blindness/) (2019, Science News,The American Society for Cell Biology).

Wong, B. Points of view: Color blindness. Nat Methods 8, 441 (2011). https://doi.org/10.1038/nmeth.1618 (https://doi.org/10.1038/nmeth.1618).

4. FIGURES PREPARATION GUIDELINES

Graphs, photographs, diagrams, illustrations, and similar content should be referred to as figures (e.g., Figure 1, Figure 2, Figures 1, 2, 5-7) in ascending order according to their appearance in the text. Authors are strongly advised to adhere to the guidelines specified in the 'Use of Colors' and 'Preparation and Manipulation of Figures' sections below, in line with the International Committee of Medical Journal Editors (ICMJE) (https://www.icmje.org/recommendations/browse/manuscript-preparation/preparing for-submission.html#i) recommendations.

When using arrows, symbols, letters, or numbers to highlight specific parts of the figures, authors must clearly describe their purpose in the corresponding figure caption. Additionally, in compliance with privacy concerns and ICMJE recommendations for the protection of research participants (https://www.icmje.org/recommendations/browse/roles-and-responsibilities/protection-of-research participants.html), images containing photographs of people must ensure that individuals cannot be identified unless their explicit permission for publication has been obtained. This ensures the protection of individual privacy and aligns with ethical standards in scholarly publication.

PREPARATION AND MANIPULATION OF FIGURES

We strongly recommend that authors (or professionals hired for editing) follow the guidelines outlined below.

RESOLUTION AND FORMATS

Graphics, photographs, diagrams, illustrations, etc., should be submitted in TIFF or JPG formats, with high resolution (see recommended minimum image sizes below). Consider whether the figure will be published occupying the full width of the page or column, and then ensure that it allows for the perfect readability of all texts and symbols used.

RECOMMENDED MINIMUM IMAGE SIZES

Between 2500 and 5000 pixels in width: For full page width images or panels.
Between 1200 and 2400 pixels in width: For column or half page width images.

EDITING AND MANIPULATION

When preparing your images, be careful when using filters or other types of editing to include highlights, etc. Images should not be manipulated or adjusted excessively in a way that could lead to misinterpretation of the information.

The following recommendations must be observed:

Photographs or images generated digitally or by programs and equipment should be of the highest quality possible.

Before-and-after photographs should have the same dimensions, orientation, framing, lighting, and color balance.

Micrographs and similar images should indicate the magnification and include a scale bar. Histological sections should indicate the type of staining, magnification, and include a scale bar. Photographs and images, when necessary, should include (in a standardized manner) arrows or other markings to identify the information in their caption.

Additionally, we strongly encourage authors (or professionals hired for editing) to observe and follow these additional recommendations:

“What’s in a picture? The temptation of image manipulation (https://doi.org/10.1083/jcb.200406019)” (Mike Rossner, Kenneth M. Yamada. J Cell Biol 5 July 2004; 166 (1): 11–15. doi: https://doi.org/10.1083/jcb.200406019 (https://doi.org/10.1083/jcb.200406019)).

Digital Images and Misconduct (https://www.councilscienceeditors.org/resource library/editorial-policies/white-paper-on-publication-ethics/3-4-digital-images-and misconduct/). (Council of Science Editors, White Paper on Publication Ethics).

Preparing a Manuscript for Submission to a Medical Journal > Illustrations (Figures) (http://www.icmje.org/recommendations/browse/manuscript-preparation/preparing-for submission.html#i). (International Committee of Medical Journal Editors).

5. TABLES PREPARATION GUIDELINES

Never build tables using spaces or tabs. Tables and Boxes must be created using the text editor built-in table creation tool and follow the following guidelines:

Identify tables (Table 1, Table 2, Tables 1, 2, 5-7, etc.) in ascending order according to their first in text citation.

Avoid using colors to convey meaning, as screen readers and people with visual impairments may be disadvantaged. When absolutely necessary the use of colors should follow the guidelines in the “Use of colors” section.

When using arrows, symbols (*, ‡, §, ǂ, #, ¢, £, etc.), letters or numbers to include notes, be sure to clearly identify their use in the respective caption or table footnote.

The use of decimal markers and the thousand separators must be observed and follow the text language.

To maximize interoperability the use of diagonal cell splits is forbidden as these are not properly translated into

XML and other electronic formats.

TABLE CAPTIONS AND FOOTNOTES

Captions should be explanatory, starting with the identification in bold (Table 1, Table 2, Tables 1, 2, 5-7, etc.), followed by a period and descriptive text. Explanation about acronyms or other information must be done using symbols (*, ‡, §, ǂ, #, ¢, £, etc.), letters, numbers, etc., and be inserted in the footer of the table.

Every table must include an indication of the source and citations whenever relevant, and authors are responsible for obtaining the correct authorization for use (or adaptation of data) from other sources, as appropriate, directly from the copyright owner.

6. REFERENCES AND CITATIONS

REFERENCES LIST

References should adhere to the Vancouver system. List all references in consecutive order as they appear in the text. For publications with up to six authors, list all authors. For publications with more than six authors, list the first six followed by 'et al.'. Whenever available insert the PMIDs (PubMed identifier) and the full DOI URL (e.g., https://doi.org/[...]). Personal communications should not be included in the references list but may be mentioned in the text.

For examples and detailed guidelines, refer to the "Samples of formatted references for authors of journal articles" available at http://www.nlm.nih.gov/bsd/uniform_requirements.html (http://www.nlm.nih.gov/bsd/uniform_requirements.html).

Authors that have deposited their data in a public data repository must cite and include a full reference providing a direct link (preferably a DOI) to the dataset.

REFERENCES CITATION

In the text, cite references in consecutive order using Arabic numerals (1,2,3...) in superscripT 1,2,3. Ensure that each citation corresponds accurately to a numbered reference in the references list (in citation order). This system allows readers to locate the source easily in the references list.

7. SUBMISSION GUIDELINES

SUBMISSION CHECKLIST

Before submitting your manuscript to the Brazilian Journal of Neurosurgery (JBNc), please ensure that you have followed all policies and instructions detailed in our submission guidelines. Carefully review each of the following items in the checklist to ensure a thorough and compliant submission:

Read Policies and Instructions for Authors: Thoroughly read and understand the journal's policies and the detailed instructions for authors to ensure compliance with all requirements. Title Page: A properly formatted title page containing essential details about your manuscript as outlined in the submission instructions.

Cover Letter: A letter introducing your manuscript, its importance, and confirming its originality. Author Statements: Ensure that all required declarations and statements are provided according to their respective policies.

Main Manuscript: The complete manuscript prepared according to the journal's formatting and structuring requirements. Note: This file MUST NOT have any author data, and MUST HAVE the titles in English/Portuguese, English/Spanish, Spanish/Portuguese

References and Citations: Ensure that all sources referenced in their work are cited accurately and formatted correctly.

Original Figures: High-resolution images (if applicable), each submitted as a separate file. Tables: Make sure your tables are editable and designed using your text editor table tool. Disclosure Forms: Completed forms disclosing any potential conflicts of interest for all authors. License Agreement: A signed agreement form from all authors, granting necessary publishing rights to the journal.

Reporting Guideline Files: Relevant checklists (e.g., CARE, PRISMA) filled out as per the type of your study.

Revision Comments File: (If submitting a revised version) A document addressing reviewers' and editors' comments from previous submission rounds.

Please review each of these components carefully to ensure compliance with our standards. Complete and accurate submission of these documents is essential for the effective handling of your manuscript.

REQUIRED FILES

As part of your submission to the Brazilian Journal of Neurosurgery (JBNc), you are required to upload various files. Each file serves a specific purpose in the submission and review process. Please refer to the table below for a detailed overview of the required files, their designations, filenames, and the necessity of each file.

File designation	Filename	Required?
Title page	titlepage.docx	Yes.
Cover letter	coverletter.docx	Yes.
Main manuscript	manuscript.docx	Yes.
Original figure	figure1.jpg, figure2.jpg etc.	Yes, if images are used.
Disclosure forms	disclosurefiles.zip	Yes.
License agreement	agreement.pdf	Yes.
Reporting guideline files	care-checklist.pdf, prisma-checklist.pdf etc.	Yes, depending on the type of work.
Revision comments file	revisioncomments.pdf	Yes, when sending the revised version of your manuscript

Please ensure that each file is prepared according to the guidelines provided below. Accurate and complete file submission is crucial for the efficient processing and review of your manuscript.

TITLE PAGE

The title page is a critical component of your submission and should include the following information, organized clearly and in order:

Submission Type (in English): Indicate the manuscript type as per JBNc section policies. Institutional Affiliation: Provide the name of the institution where the study was conducted, including city and country.

Title: Provide the title of the manuscript in English, and in the original language if the main text is not English.

Authors list: Include the full names of all authors, along with their highest degree, e-mail, institutional affiliations, and ORCID ID. The order of the names should be as it will be published. Abstract: Present a concise abstract of the manuscript in English, and in the original language if the main text is not English.

Keywords: List relevant keywords in English, and in the original language if the main text is not English.

Corresponding author's information: Provide the full name, postal and electronic addresses of the corresponding author.

Conflicts of interest statement (in English): Disclose any potential conflicts of interest. Financial support statement (in English): Acknowledge any financial support or grants received in relation to the study.

Authors' responsibility and contributions declaration (in English): Declare each author's specific contributions to the work.

Institutional ethics committee approval (in English): Include a statement of approval or waiver from the Institutional Ethics Committee.

Data availability statement: Include a concise data availability statement detailing whether their research data is publicly accessible.

Clinical trials approval and registration statement (in English): If applicable, provide the registration statement and approval for clinical trials.

JBNC
JORNAL BRASILEIRO DE NEUROCIRURGIA
BRAZILIAN JOURNAL OF NEUROSURGERY

COVER LETTER

The cover letter should introduce your manuscript and explain its importance to the field of neurosurgery. It must include a declaration that the work is original, has not been published elsewhere, and is not under consideration by any other journal. The letter should briefly outline the major findings of your study and how they contribute to the existing knowledge. Additionally, any potential conflicts of interest or important points not covered in the manuscript or in other submission files should be disclosed. The cover letter is also an opportunity to suggest preferred or opposed reviewers and to provide any other information that may assist the editorial process.

MAIN MANUSCRIPT FILE

The main manuscript file **must NOT** contain any data from the institution or the authors.

The main manuscript file must contain TITLE, ABSTRACT/RESUMO and the full text and be structured according to the requirements described in our Section Policies and the Manuscript preparation guidelines section.

Please also make sure to follow all of our instructions for authors.

ORIGINAL FIGURES FILES

Each figure must be submitted as a separate file. Ensure that all figures are of high resolution and clearly labeled to correspond with their citations in the manuscript text.

Please also make sure each figure adheres to the journal's guidelines for figure preparation, including any specifications for file format, resolution, and size.

DISCLOSURE FORMS

This file should contain completed disclosure forms for all authors, declaring any potential conflicts of interest. These forms are essential for maintaining transparency and upholding the integrity of the publication process. Ensure that each author's form is included and that all information is current and accurate.

Please also make sure that each author reviews and follows our authorship and ethics policies. Attention: Each author must fill and sign their own disclosure form individually.

LICENSE AGREEMENT

All authors must sign the Authorship Responsibility and License Agreement. By signing this form, the authors accept that they have contributed significantly to the work, agree to the terms of publication, and grant the journal the necessary publishing rights. This agreement is crucial for copyright management and clarifies the permissions for reproducing and distributing the work.

REPORTING GUIDELINE FILES

For manuscripts that follow specific reporting guidelines such as CARE for case reports or PRISMA for systematic reviews, the corresponding completed checklist must be submitted. This ensures adherence to the highest standards of transparency and detail in reporting. The checklist should be filled out comprehensively, indicating where in the manuscript each guideline item is addressed. The filename should clearly correspond to the relevant guideline.

Please also make sure to review and follow our reporting guidelines policies.

REVISION COMMENTS FILE

In response to the editorial review, authors must submit a file detailing how they have addressed each comment or suggestion. This file should systematically list the reviewers' and editors' comments, followed by the authors' response and explanation of the corresponding changes made in the manuscript. The document should be structured to make it easy for reviewers and editors to verify that all feedback has been considered and appropriately addressed.

Please also make sure to review and follow our peer review process.

JBNC
JORNAL BRASILEIRO DE NEUROCIRURGIA
BRAZILIAN JOURNAL OF NEUROSURGERY

Contents

Original

Review

Case Report

Clinical Images

Letter to the Editor

Endovascular Treatment of Middle Cerebral Artery Aneurysms

Tratamento Endovascular de Aneurismas de Artéria Cerebral Média

Leandro José Haas[1,2]
Guilherme Wandall[1]
Douglas Cipriano de Souza[1]
Wesley Severino[1]
Amanda Junges Derlam[1]
Eduarda Alves[1]
Ana Boaventura[1]
André Felipe Kroenke[1]
Gabriela Scheidt[1]
Camila Ceruti dos Santos[3]

ABSTRACT

Introduction: *The middle cerebral artery (MCA) can develop aneurysmal formations, which may occur as single or multiple along its course, influenced by predisposing factors and prevalent sites. Endovascular approaches allow for more delicate treatments, though they also carry the risk of complications. Therefore, screening these aneurysms in target populations is crucial for patient survival.* **Objective:** *To analyze cases of patients with middle cerebral artery aneurysms treated using the endovascular method in a specialized center.* **Methods:** *A retrospective observational study with a quantitative approach, including 368 patients with MCA aneurysms treated with endovascular techniques in an endovascular neurosurgery center from 2005 to 2023.* **Results:** *The female gender was most affected (73.91%), with a mean age of 55.1 years, and a significant prevalence of hypertension (74.18%). Small saccular aneurysms (94.29% / 83.97%) were most common, predominantly located at the MCA bifurcation (79.89%) and mostly unruptured (64.67%), corresponding to Fisher Grade 1 and Hunt & Hess Grade 0. Endovascular intervention was the treatment of choice, with coil embolization being the predominant technique (70.65%).* **Conclusion:** *Female, middle-aged, hypertensive patients should be investigated for the presence of MCA aneurysmal disease, as the probability of rupture is uncertain. The treatment focus should be on endovascular procedures, which are safe and have low failure rates, ensuring better survival outcomes.*

Keywords: *Intracranial aneurysm; MCA; Middle cerebral artery; Neurosurgery; Endovascular Procedures; Aneurysmal disease*

RESUMO

Introdução: *A artéria cerebral média (ACM) revela formações aneurismáticas, podendo se manifestar de forma única ou múltipla ao longo de seu leito, havendo fatores predisponentes para seu desenvolvimento e sítios prevalentes. Através da abordagem endovascular é possível realizar um tratamento mais delicado, assim como a ocorrência de complicações. Dessa forma, a triagem destes aneurismas na população alvo é relevante para a sobrevida destes pacientes.* **Objetivo:** *Analisar casos de pacientes com aneurisma de artéria cerebral média tratados por método endovascular em serviço de referência.* **Métodos:** *Estudo observacional retrospectivo com abordagem quantitativa de 368 pacientes com aneurismas de ACM submetidos a tratamento endovascular em serviço de neurocirurgia endovascular no período de 2005 a 2023.* **Resultados:** *O sexo feminino foi o mais acometido (73,91%), de meia idade (55,1 anos), com hipertensão arterial (74,18%). Prevaleceu o aneurisma sacular pequeno (94,29% / 83,97%) na bifurcação da ACM (79,89%), predominantemente não rotos (64,67%) correspondendo a escala de Fisher 1 e Grau 0 na escala de Hunt & Hess. A abordagem endovascular foi o procedimento de escolha em que a utilização de Coils prevaleceu (70,65%).* **Conclusão:** *Pacientes do sexo feminino, de meia idade, com hipertensão devem ser investigadas quanto a presença de doença aneurismática em ACM, uma vez que a probabilidade de não rotura é incerta, e a abordagem destas pacientes deve ter como foco o tratamento endovascular por ser uma conduta segura, com baixas taxas de insucesso, a fim da manutenção da vida destes.*

Palavras-Chave: *Aneurisma intracraniano; ACM; Artéria cerebral média; Neurocirurgia; Procedimentos Endovasculares; Doença aneurismática*

[1]Endovascular Neurosurgery, Hospital Santa Isabel, Blumenau, Santa Catarina (SC), Brasil
[2]Fundação Universidade Regional de Blumenau (FURB), Blumenau - Santa Catarina, Brazil
[3]Universidade Regional de Blumenau (Medicine), Blumenau - Santa Catarina, Brazil

Received Jun 1, 2026
Accepted Jun 25, 2026

INTRODUCTION

The middle cerebral artery (MCA) exhibits aneurysmal formations, either as single or multiple occurrences along its course[1-5]. Predisposing factors for their development include arterial structural characteristics, such as a shorter M1 segment[6], and more significant factors like a wide bifurcation angle, high-volume blood flow in the parent vessel, and a low junction exponent[7].

The most prevalent site for these structures, whether intact or ruptured[1], is the bifurcation of the middle cerebral artery (MCA bifurcation)[1-5]. These aneurysms often present as multiple[1] and spherical formations, with a higher likelihood of rupture. The average age at diagnosis is 56 years, predominantly in females, and while younger patients have a higher risk of rupture, female smokers show the highest rupture rates[4].

Endovascular approaches allow for more delicate treatments, either through intrasaccular or endoluminal techniques, with similar outcomes for both ruptured and unruptured aneurysms[4,8]. Most interventions are performed before rupture and show low rates of retreatment or complications, such as bleeding, thromboembolic events, and recanalization. This procedure enables the exclusion of aneurysms using stents, coils, or clipping, and for MCA bifurcation aneurysms, both coil embolization and clipping have proven to be effective treatments[4,8].

Thus, this study aims to investigate the epidemiological characteristics of patients with MCA aneurysms, their prevalent comorbidities, and the endovascular methodologies employed, to provide a better clinical and epidemiological understanding of this type of aneurysm.

METHODS

A retrospective observational study with a quantitative approach, based on data from medical records of patients with MCA aneurysms.

The initial sample included all patients diagnosed with intracranial aneurysms treated at a reference endovascular neurosurgery service in the city of Blumenau between 2005 and 2023. From this group, only patients with MCA aneurysms who had complete and analyzed variables recorded in their medical records were selected.

Patients with incomplete records, incorrectly filled information, or conflicting notes were excluded.

The epidemiological variables analyzed included patient sex, age range, associated comorbidities, and smoking status. Aneurysmal configuration, size, and location within MCA segments were also considered.

Patients were assessed using the Fisher scale and the Hunt & Hess scale to characterize rupture status, followed by an evaluation of the chosen treatment type, associated materials, and success rates.

The project adhered to current ethical standards and was approved by the local ethics committee under CAAE: 61294422.0.0000.5370. The authors declare there were no conflicts of interest and received no funding.

RESULTS

Among the 2,049 cases of intracranial aneurysms treated by the endovascular neurosurgery service at Hospital Santa Isabel between October 2005 and December 2023, 17.95% were classified as middle cerebral artery aneurysms. Of these, 73.91% were female, with an average age of 55.10 years, while 26.08% were male, with an average age of 54.70 years. The overall average age for the sample of 368 cases was 55 years (Table 1).

Regarding the presence of comorbidities, systemic arterial hypertension (SAH) was the most prevalent, found in 74.18% of cases, of which 25.87% were male and 74.12% female, followed by dyslipidemia in 23.91% of patients, with 24.76% male and 75.23% female, and diabetes mellitus in 10.05% of patients, of which 30.76% were male and 69.23% female. A history of smoking, either past or present, was reported in 30.71% of cases, with 27.27% male and 72.72% female.

Saccular aneurysms were observed in 94.29% of cases, fusiform in 4.35%, mammillary in 1.09%, and dissecting in 0.27%. No infundibular aneurysms were recorded in the sample.

In terms of aneurysm size, 83.97% of cases were small aneurysms, of which 25.39% were male and 74.60% female. Large aneurysms represented 12.23% of cases, with 23.91% male and 76.08% female. Giant aneurysms made up 3.80% of cases, with 71.42% male and 28.57% female.

As for aneurysm topography, 79.89% were located at the Middle Cerebral Artery Bifurcation, with 26.53% male and 73.46% female. Middle Cerebral Artery Trifurcation aneurysms accounted for 6.25% of cases, with 21.73% male and 78.26% female. Middle cerebral artery M1 segment aneurysms represented 9.23% of cases, with 26.47% male and 73.52% female. M2 segment aneurysms accounted for 3.53% of cases, with 23.07% male and 76.92% female. M3 segment aneurysms represented 0.54% of cases, all in females (100%). M4 segment aneurysms accounted for 0.54% of cases, equally distributed between males and females (50% each) (Table 2).

In the analysis using the Fisher scale, Fisher 1 was identified in 64.67% of individuals, of which 25.63% were male and 74.36% female. Fisher 2 was observed in 7.60% of individuals, with 25% male and 75% female. Fisher 3 was identified in 10.32% of individuals, with 39.47% male and 60.52% female. Fisher 4 was identified in 17.39% of individuals, with 20.31% male and 79.68% female.

Table 1. Age distribution of patients with middle cerebral artery aneurysms, by sex, from October 2005 to December 2023, at Hospital Santa Isabel, Blumenau, 2023.

Age Groups	Male	Female	Total Individuals
(00 – 10)	0	0	0
(11 – 20)	02	02	04
(21 – 30)	02	07	09
(31 – 40)	08	25	33
(41 – 50)	19	66	85
(51 – 60)	31	70	101
(61 – 70)	25	67	92
(71 – 80)	08	32	40
(81 – 90)	01	03	04
(91 – 100)	0	0	0
Total	96	272	368

Source: Hospital Santa Isabel, Neurosurgery Department, 2023.

Table 2. Intracranial aneurysm locations in patients with middle cerebral artery aneurysms, by sex, from October 2005 to December 2023, at Hospital Santa Isabel, Blumenau, 2023.

Aneurysm Locations	Male	Female	Total Cases
Middle Cerebral Artery Bifurcation	78	216	294
Middle Cerebral Artery Trifurcation	05	18	23
M1 Segment of the Middle Cerebral Artery	09	25	34
M2 Segment of the Middle Cerebral Artery	03	10	13
M3 Segment of the Middle Cerebral Artery	0	02	02
M4 Segment of the Middle Cerebral Artery	01	01	02
Total	**96**	**272**	**368**

Source: Hospital Santa Isabel, Neurosurgery Department, 2023.

In the analysis using the Hunt & Hess scale, 64.67% of individuals were classified as grade 0, with 25.63% male and 74.36% female. Grade 1 was observed in 2.71% of individuals, with 30% male and 70% female. Grade 2 was identified in 16.57% of individuals, with 32.78% male and 67.21% female. Grade 3 was identified in 9.78% of individuals, with 25% male and 75% female. Grade 4 was observed in 4.89% of individuals, with 5.55% male and 94.44% female. Grade 5 was identified in 1.35% of individuals, with 40% male and 60% female.

Thus, it was found that 64.67% of cases were non-ruptured aneurysms, corresponding to Fisher scale 1 and Grade 0 in the Hunt & Hess scale, of which 25.63% were male and 74.36% female. In contrast, 35.32% of the aneurysms were ruptured, corresponding to Fisher scale 2 or higher, and Hunt & Hess scale 1 or higher, with 26.92% male and 73.07% female (Table 3).

Regarding the treatment of middle cerebral artery aneurysms, it was observed that 100% of the sample underwent endovascular procedures. It was found that, in 70.65%, the approach involved only Coils. In 1.36%, the treatment involved only Stents. In 25%, the treatment of choice was the combination of Coils and Stents. In 0.81%, the Y-shaped Stent technique and Coils were used. In 1.35%, only a flow diverter Stent was used. In 0.54%, the intrasaccular device technique (WEB™) was employed. In 0.27%, there were treatment failures, occurring 100% in females (Tables 4 and 5).

Regarding morbidity and mortality, we observed that 25% of patients with ruptured cerebral aneurysms showed vasospasm when carrying out an angiographic study, with 15% being asymptomatic and 10% symptomatic, mainly in patients with Fisher 3 on tomography. Patients with Fisher 4 on the Fisher scale and 4 and 5 on the Hunt & Hess scale had worse outcomes. On the other hand, patients with intact aneurysms had a complication rate of 2.5%, with embolic effects, hemorrhagic complications during the procedure, and hematomas at the puncture site being the main complications (Figures 1 and 2).

Table 3. Integrity of middle cerebral artery aneurysms, by sex, from October 2005 to December 2023, at Hospital Santa Isabel, Blumenau, 2023.

Aneurysm Integrity	Male	Female	Total
Non-ruptured aneurysms (Fisher scale = 1 and Hunt & Hess scale = 0)	61	177	238
Ruptured aneurysms (Fisher scale ≥ 2 and Hunt & Hess scale ≥ 1)	35	95	130
Total	96	272	368

Source: Hospital Santa Isabel, Neurosurgery Department, 2023.

Table 4. Endovascular treatments in patients with middle cerebral artery aneurysms, by sex, from October 2005 to December 2023, at Hospital Santa Isabel, Blumenau, 2023.

Endovascular Treatments	Male	Female	Total
Only Coils	64	196	260
Only Stents	03	02	05
Stents associated with Coils	26	66	92
Only Flow Diverter Stent	01	04	05
Y-shaped Stent and Coils	02	01	03
Intrasaccular Device (WEB™)	01	01	02
Failure	0	01	01
Total	96	272	368

Source: Hospital Santa Isabel, Neurosurgery Department, 2023.

Table 5. Comparative analysis between ruptured and unruptured middle cerebral artery aneurysms (n = 368).

Age by age group	Unruptured	Ruptured
< 70 years	200/238 (84%)	111/130 (85%)
71-90 years	27/238 (11%)	19/130 (15%)
> 90 years	11/238 (5%)	0/130 (0)
Comorbidities – total number / n (%)		
SAH*	152/238 (63%)	121/130 (93%)
Dyslipidemia	50/238 (21%)	38/130 (29%)
Diabetes mellitus	11/238 (5%)	26/130 (20%)
Smoking	43/238 (25%)	70/130 (53%)
Aneurysmal morphology – total number / n (%)		
Saccular	226/238 (95%)	121/130 (93%)
Fusiform	9/238 (3%)	7/130 (5%)
Mammillary	2/238 (1%)	2/130 (1%)
Dissecting	1/238 (0,5%)	0/130 (0)
Infundibular	0/238 (0)	0/130 (0)
Aneurysmal size – total number / n (%)		
Small	198/238 (83%)	111/130 (85%)
Large	32/238 (13%)	13/130 (10%)
Giant	8/238 (3%)	6/130 (4%)

*SAH = Systemic Arterial Hypertension. Source: Hospital Santa Isabel, Neurosurgery Department, 2023.

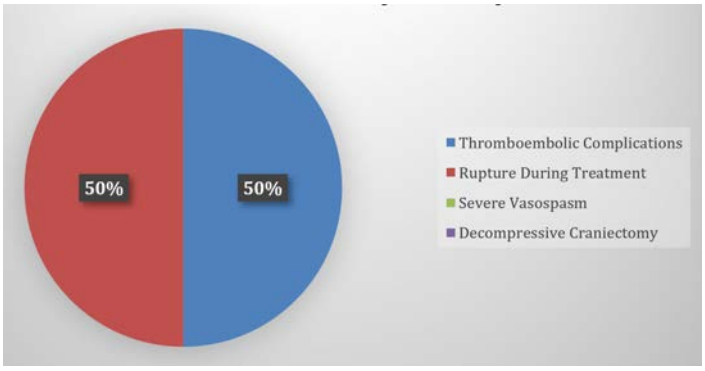

Figure 1. Complications in non-ruptured middle cerebral artery aneurysms.
Source: Hospital Santa Isabel, Neurosurgery Department, 2023.

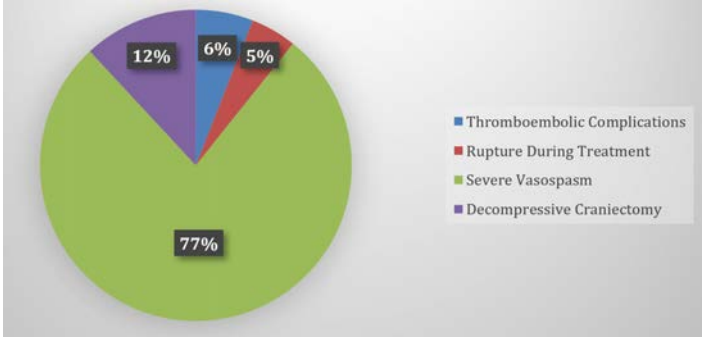

Figure 2. Complications in ruptured middle cerebral artery aneurysms.
Source: Hospital Santa Isabel, Neurosurgery Department, 2023.

DISCUSSION

Aneurysmal disease is documented in scientific literature as a condition with higher incidence in the middle-aged population[9], with values between 60 and 70 years. Moreover, there is a higher predisposition for females to develop cerebral aneurysms[10], a factor that, when combined with a prior history, leads to middle-aged women being the main candidates for aneurysmal development. In this context, the data previously observed suggest that middle cerebral artery (MCA) aneurysms present similarly to other typical topographies of cerebral aneurysms, meaning that women showed the pre-established dominance in the literature regarding the sex most likely to develop the disease, surpassing 70% of all cases. Furthermore, the typical age observed mirrored what was found in other texts on the subject, showing that MCA aneurysms do not diverge in terms of typical age.

When investigating the most common comorbidities in aneurysms, it is evident that the main conditions exacerbating the aneurysm tend to recur in most patients. Among these comorbidities, the most observed, and unfortunately the most disastrous, is systemic arterial hypertension (SAH), as its presence creates a high hemodynamic stress environment. In short, hypertension tends to be the primary comorbidity in patients with cerebral aneurysms, and its presence is strongly associated with aneurysmal rupture[11,12].

As reported by Brown and Broderick[13], the most common aneurysm configuration found in a general population would be a small saccular aneurysm, and clearly, using data to track the history of patients at risk of developing a ruptured aneurysm would be a valuable tool for medical professionals. In this context, the conclusions made by the previous authors seem to align with what was observed in the study of MCA aneurysms, where vascular configurations match the main findings in literature, meaning a small, saccular aneurysm would be the most likely case to develop in the studied vessel.

Regarding aneurysmal topographies, there was a significant dominance in the bifurcation area of the MCA, accounting for nearly 80% of all registered cases. This might appear to be a peculiar characteristic of the vessel itself, but when considering the hemodynamic stress process previously discussed, the bifurcation area would undoubtedly be the largest aneurysmal hotspot. This is due to physical events such as increased flow velocity and blood pressure within bifurcation areas due to the reduced diameter of the vessel[14]. Additionally, the primary topography also showed a significant disproportion relative to the most common sex, and similarly, this can be explained by the fact that the female vascular configuration has less muscular tissue in its tunica media[15], reducing the arterial diameter and increasing the chance of an aneurysmal event.

Aneurysmal integrity refers to an aneurysm not rupturing. There is a possibility for an individual to maintain their arterial dilation intact, avoiding for a while the harm associated with aneurysmal rupture and subarachnoid hemorrhage[16]. However, the probability of an aneurysm remaining intact is highly uncertain. In the general population, the chance of aneurysmal integrity ranges from 2% to 6%[17], a very ambiguous figure that does not warrant ignoring endovascular intervention when diagnosed. Following this reasoning, even though MCA aneurysms have demonstrated many cases of aneurysmal integrity, the number of such patients still requires endovascular intervention to ensure a positive outcome for their condition.

The Fisher and Hunt & Hess scales demonstrated a wide range of patients in the more moderate positions of both scales, meaning that Fisher 1 and Hunt & Hess 0 had the highest incidence, which can be attributed to the large number of intact aneurysms mentioned earlier. Still, in cases of subarachnoid hemorrhage, the main Fisher scale was 2.

With the development of endovascular intervention, and the availability of new materials, this treatment option continues to grow in terms of its use in MCA aneurysm treatment, providing greater safety and efficacy. The advancement of digital angiography techniques with 3D reconstruction has enabled better visualization of aneurysms, their characteristics, and their anatomical relations. Additionally, the emergence of new stents[18] and coils[19] has allowed safer navigation through intracranial vessels, facilitating the embolization of aneurysms. Another key factor in the spread of this technique for treating aneurysms in this artery is the increasing qualification and certification of professionals, which will consequently shorten the learning curve for new neurosurgeons who will use endovascular therapy multiple times as the treatment of choice for aneurysms in this topography[19].

During the study, the most common intervention was the use of coils in 70% of total treatments, demonstrating the good response of MCA aneurysms to this type of endovascular intervention[20]. The second most common treatment was the combination of coils and stents, used in 25% of patients. Both interventions with the exclusive use of stents and endoluminal flow diverters, or the intra-aneurysmal device WEB™, showed lower incidence rates of around 2%. Regardless of the chosen device, treatment planning in this territory depends on a precise angiographic reading of the MCA and its bifurcation branches. The angiographic classifications proposed for endovascular procedures in this artery reinforce how a systematic assessment of the M1 and M2 segments guides access strategy and device selection.[21]

Regarding morbidity and mortality, it was observed that 25% of patients with ruptured cerebral aneurysms showed vasospasm in the angiographic study, with 15% being asymptomatic and 10% symptomatic, mainly in patients with Fisher 3 on CT. Patients with Fisher 4 and Hunt & Hess scales 4 and 5 had worse outcomes. Meanwhile, patients with intact aneurysms had a complication rate of 2.5%, with embolic effects, hemorrhagic complications during the procedure, and hematomas at the puncture site as the main complications. It should also be noted that a subset of MCA aneurysms occurs in association with underlying vasculopathies, such as moyamoya disease, a scenario in which the hemodynamic overload imposed on the parent and collateral vessels favors aneurysm formation and demands individualized endovascular planning.[22]

CLINICAL CASES

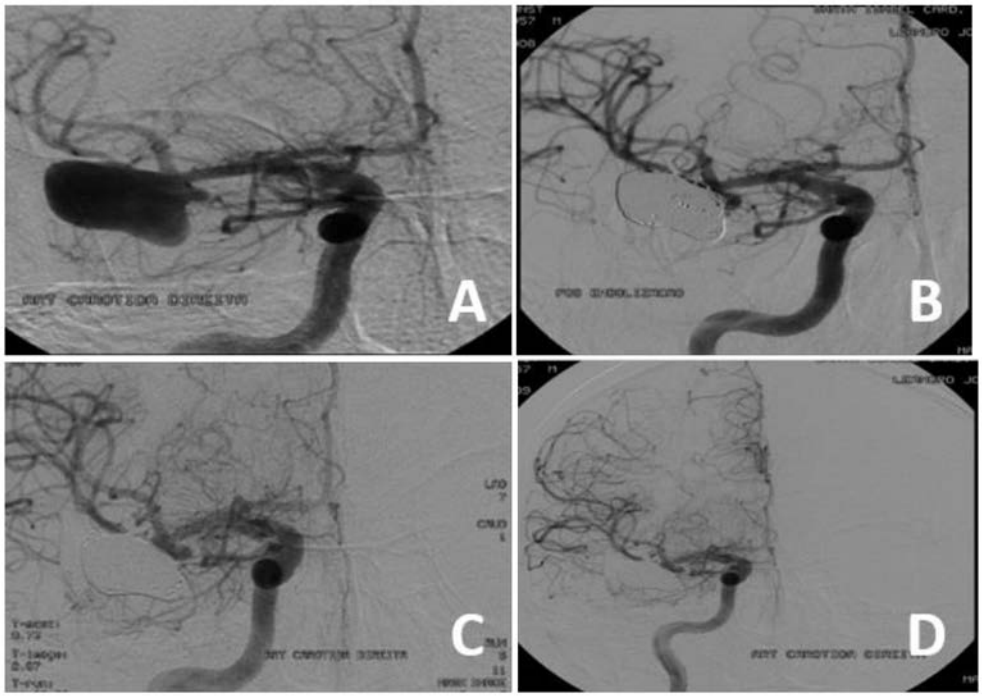

Figure 3. Case 1. Right middle cerebral artery (MCA) aneurysm treated by endovascular embolization with platinum coils, with a 1-year follow-up. A. Pre-treatment digital subtraction angiography (DSA) of the right internal carotid artery (ICA), working projection, showing a large saccular aneurysm of the right MCA. B. Immediately after embolization, in the same projection: the coil mass conforms to the sac, with complete exclusion of the aneurysm. C. Post-embolization control run demonstrating the coil mass in position and preservation of flow in the parent vessel and distal MCA branches. D. One-year follow-up right ICA angiogram showing stable occlusion, without residual filling or recanalization, and normal opacification of the MCA territory.
Source: Personal collection, 2023.

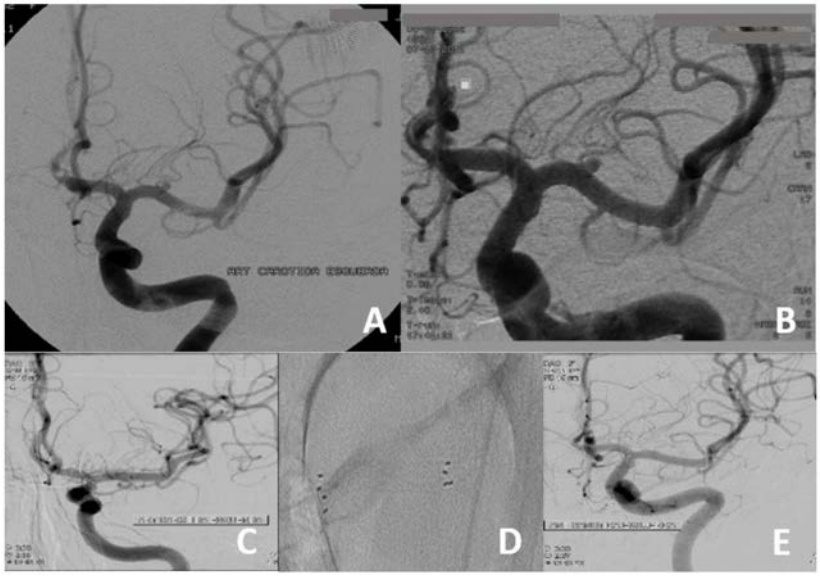

Figure 4. Case 2. Aneurysm of the M1 segment of the left MCA treated with a Neuroform™ stent, with a 2-year follow-up. A. Pre-treatment DSA of the left ICA, lateral projection, showing the aneurysm of the M1 segment. B. Magnified working projection detailing the aneurysm, its neck and the relationship with the M1 segment and adjacent branches. C. Angiographic control after stent deployment, showing exclusion of the aneurysm with patency of the M1 segment. D. Unsubtracted image demonstrating the radiopaque markers of the Neuroform™ stent across the aneurysm neck. E. Two-year follow-up left ICA angiogram showing a stable result, with a patent stent and no residual filling of the aneurysm.
Source: Personal collection, 2023.

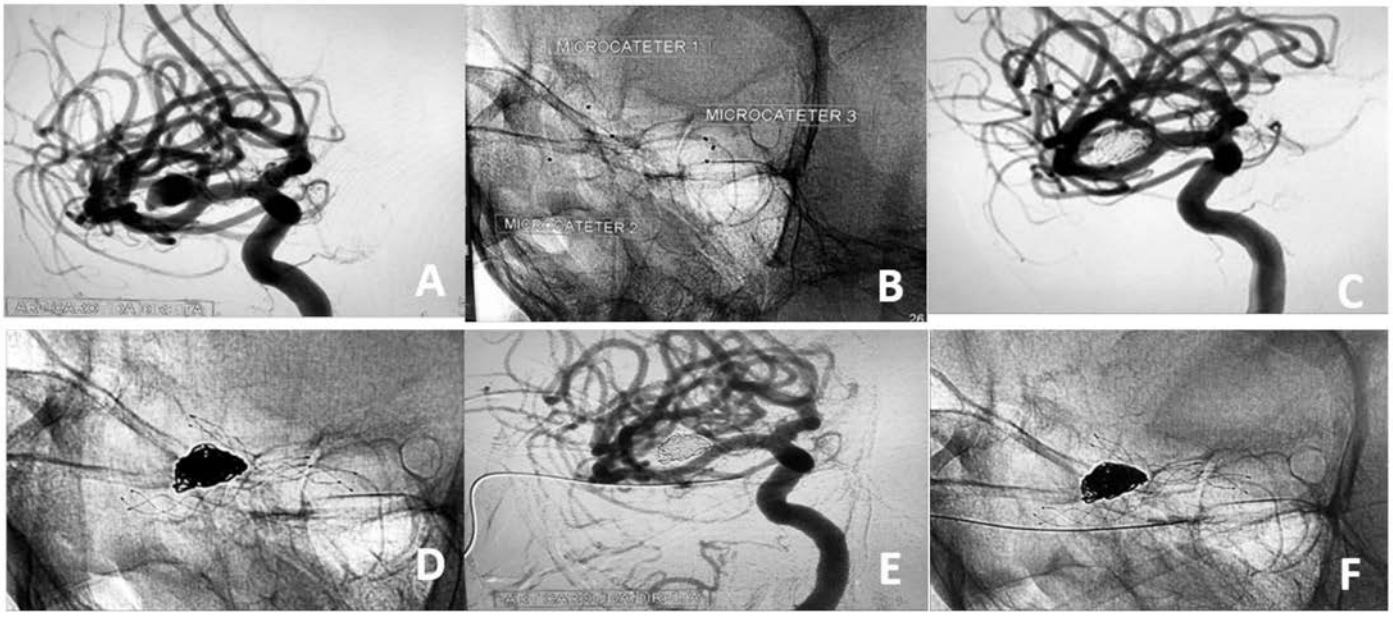

Figure 5. Case 3. Aneurysm of the right MCA trifurcation treated with a Y-configured LVIS Jr.™ stent and coils, with a 1-year follow-up. A. Pre-treatment DSA of the right ICA showing the aneurysm at the trifurcation of the right MCA. B. Unsubtracted intraprocedural image showing the three microcatheters (microcatheters 1, 2 and 3) positioned for the Y-stent and coiling technique. C. Angiographic control after Y-stenting and coiling, with the coil mass within the sac and patency of the trifurcation branches. D. Unsubtracted image showing the final coil mass at the trifurcation. E. Post-treatment control run demonstrating exclusion of the aneurysm with preserved distal flow. F. One-year follow-up showing a stable coil mass, without recanalization.
Source: Personal collection, 2023.

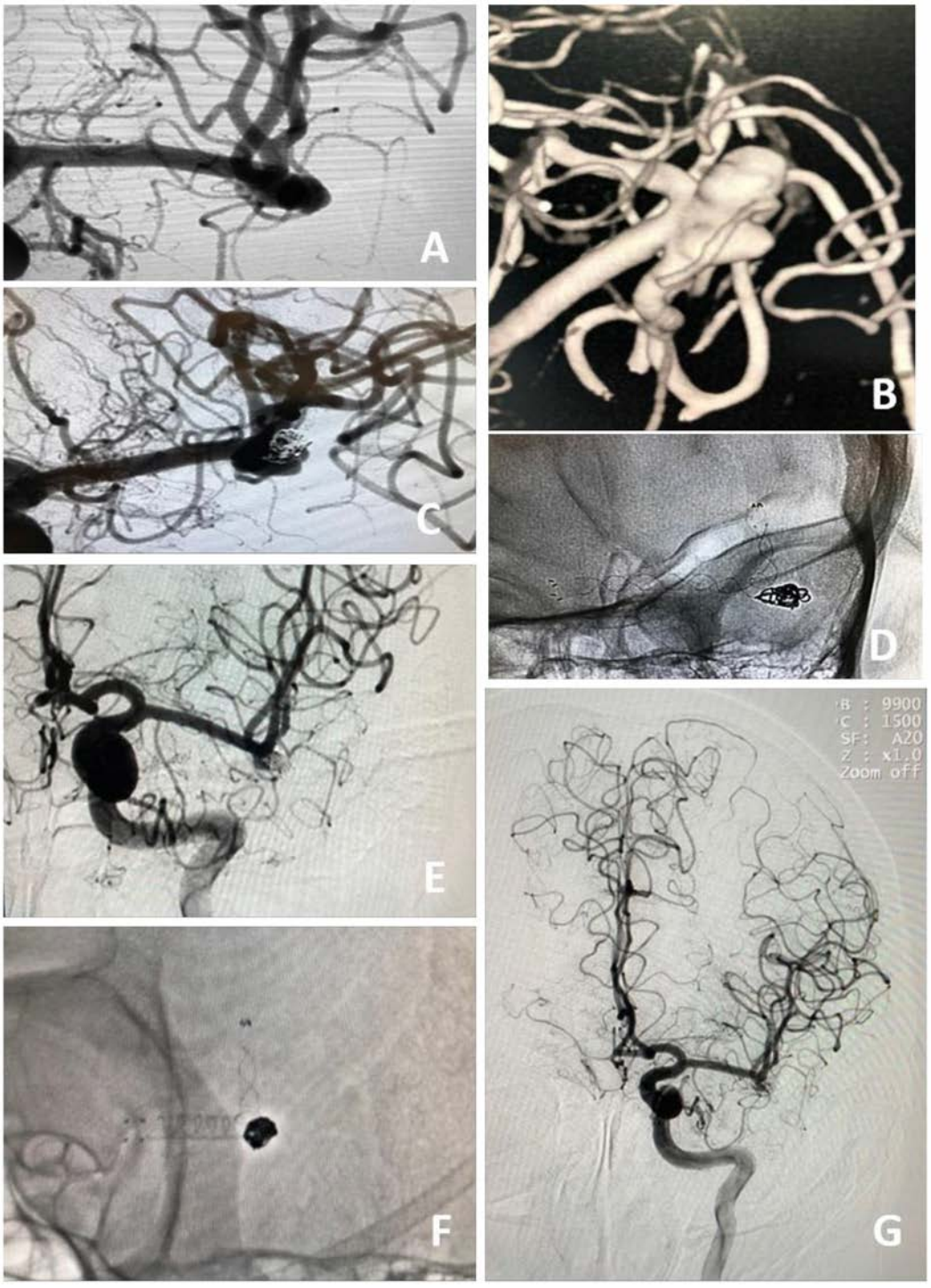

Figure 6. Case 4. Aneurysm of the left MCA trifurcation treated with a FRED™ flow-diverter stent and coils, with a 1-year follow-up. A. Pre-treatment DSA of the left ICA, magnified view, showing the aneurysm at the trifurcation of the left MCA. B. Three-dimensional rotational angiography reconstruction demonstrating the morphology of the aneurysm and its relationship with the efferent branches. C. Angiographic control after treatment, showing the coil mass within the sac. D. Unsubtracted image showing the braid of the FRED™ flow-diverter stent across the aneurysm neck, associated with the coil mass. E. Post-treatment control angiogram, lateral projection, showing preserved filling of the MCA branches. F. Unsubtracted spot image of the final coil mass. G. One-year follow-up left ICA angiogram showing complete exclusion of the aneurysm, with patency of the parent vessel and of the distal branches. **Source:** Personal collection, 2023.

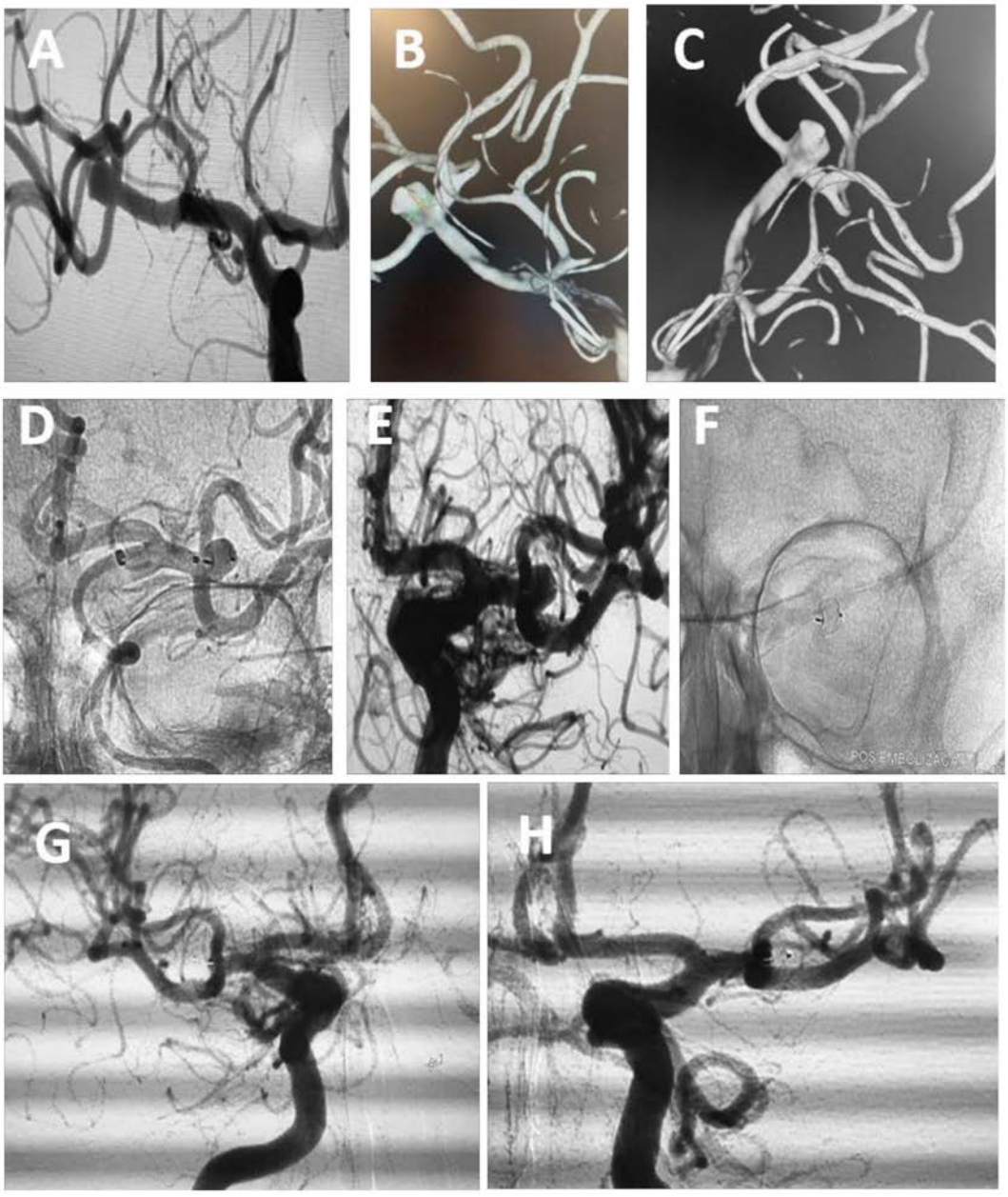

Figure 7. Case 5. Aneurysm of the left MCA bifurcation treated with the WEB™ intrasaccular device, with a 1-year follow-up. A. Pre-treatment DSA of the left ICA, magnified view, showing the aneurysm of the left MCA bifurcation. B. Three-dimensional rotational angiography with measurement of the sac and of the neck for device sizing. C. Three-dimensional reconstruction in a complementary projection, showing the relationship of the aneurysm with the bifurcation branches. D. Unsubtracted working projection showing the radiopaque markers of the WEB™ device during deployment within the sac. E. Angiographic control immediately after deployment, with the device in position and exclusion of the aneurysm. F. Unsubtracted image after embolization, showing the WEB™ device within the sac. G. One-year follow-up angiogram showing stable occlusion, with patency of the bifurcation branches. H. One-year follow-up in a complementary projection, confirming the absence of residual filling of the aneurysm.
Source: Personal collection, 2023.

CONCLUSION

The patient affected by a middle cerebral artery aneurysm showed considerable similarity to the general epidemiology of aneurysmal disease worldwide. The prominent comorbidity associated is arterial hypertension, with a focus on the female sex, along with age and tobacco use, which together increase the likelihood of aneurysmal disease. Since the probability of non-rupture is uncertain, these patients should be managed, with endovascular treatment being a safe approach due to its minimal failure rates. The use of Coils shows good resolution, and Stents can be added when necessary, maintaining resolution rates.

REFERENCES

1. Liu J, Chen Y, Zhu D, et al. A nomogram to predict rupture risk of middle cerebral artery aneurysm. Neurol Sci. 2021;42(12):5289-96. https://doi.org/10.1007/s10072-021-05255-6. PMid:33860397.

2. Brasileira R, Fillus IC, Solana De Oliveira C, Conte T, Frederico C, Rodrigues A. Artigos de revisão análise dos aneurismas intracranianos operados no Hospital Policlínica Pato Branco-PR. Revista Brasileira de Neurologia e Psiquiatria. [Internet]. 2017 [Accessed: 6/1/2026];21(1): 51-9. Available from: http://www.revneuropsiq.com.br

3. Liang F, Yang Y, Luo L, et al. Endovascular treatment of complex middle cerebral artery aneurysms using TuBridge flow diverters. Interv Neuroradiol. 2020;26(5):539-46. https://doi.org/10.1177/1591019920946216. PMid:32722987.

4. Brzegowy P, Polak J, Wnuk J, et al. Endovascular treatment of middle cerebral artery aneurysms – single-centre results. Pol J Radiol. 2020;85(1): 650-6. https://doi.org/10.5114/pjr.2020.103204. PMid:33552317.

5. Zaidat OO, Castonguay AC, Teleb MS, et al. Middle cerebral artery aneurysm endovascular and surgical therapies: comprehensive literature review and local experience. Neurosurgery Clinics. 2014;25(3):455-69. PMid:24994084.

6. Cunha CEG, Correia CC. Middle cerebral artery extension and the risk for aneurysmal disease. J Neurol Sci. 2018;390:219-21. https://doi.org/10.1016/j.jns.2018.04.040. PMid:29801892.

7. Kaspera W, Ćmiel-Smorzyk K, Wolański W, et al. Morphological and hemodynamic risk factors for middle cerebral artery aneurysm: a case-control study of 190 patients. Sci Rep. 2020;10(1):2016. https://doi.org/10.1038/s41598-019-56061-2. PMid:32029748.

8. Santiago-Dieppa DR, Pannell JS, Khalessi AA. Endovascular and surgical options for ruptured middle cerebral artery aneurysms: review of the literature. Stroke Res Treat. 2014;2014(1):315906. https://doi.org/10.1155/2014/315906. PMid:25097795.

9. Brisman JL, Song JK, Newell DW. Cerebral aneurysms. N Engl J Med. 2006;355(9):928-39. https://doi.org/10.1056/NEJMra052760. PMid:16943405.

10. Ikawa F, Abiko M, Ishii D, et al. Effect of actual age on outcome at discharge in patients by surgical clipping and endovascular coiling for ruptured cerebral aneurysm in Japan. Neurosurg Rev. 2018;41(4): 1007-11. https://doi.org/10.1007/s10143-017-0942-9. PMid:29335886.

11. Wiebers DO, Whisnant JP, Huston J 3rd, et al. Unruptured intracranial aneurysms: natural history, clinical outcome, and risks of surgical and endovascular treatment. Lancet. 2003;362(9378):103-10. https://doi.org/10.1016/S0140-6736(03)13860-3. PMid:12867109.

12. Lawton MT, Vates GE. Subarachnoid Hemorrhage. N Engl J Med. 2017;377(3):257-66. https://doi.org/10.1056/NEJMcp1605827. PMid:28723321.

13. Brown RD Jr, Broderick JP. Unruptured intracranial aneurysms: epidemiology, natural history, management options, and familial screening. Lancet Neurol. 2014;13(4):393-404. https://doi.org/10.1016/S1474-4422(14)70015-8. PMid:24646873.

14. Stefani MA, Schneider FL, Marrone ACH, Severino AG. Influence of the gender on cerebral vascular diameters observed during the magnetic resonance angiographic examination of willis circle. Braz Arch Biol Technol. 2013;56(1):45-52. https://doi.org/10.1590/S1516-89132013000100006.

15. Galvao J, Lima DD, Haas LJ. Prevalência de aneurismas cerebrais incidentais entre homens e mulheres. Saude Pesqui. 2020;13(2):309-16. https://doi.org/10.17765/2176-9206.2020v13n2p309-316.

16. Nielsen R, Hauerberg J, Munthe S, et al. Screening for intracranial aneurysms. Ugeskr Læger. 2019;181(2). PMid:30618370.

17. Weir B. Unruptured intracranial aneurysms: a review. J Neurosurg. 2002;96(1):3-42. https://doi.org/10.3171/jns.2002.96.1.0003. PMid:11794601.

18. Lanzino G, Fraser K, Kanaan Y, Wagenbach A. Treatment of ruptured intracranial aneurysms since the International Subarachnoid Aneurysm Trial: practice utilizing clip ligation and coil embolization as individual or complementary therapies. J Neurosurg. 2006;104(3): 344-9. https://doi.org/10.3171/jns.2006.104.3.344. PMid:16572645.

19. Jiang B, Paff M, Colby GP, Coon AL, Lin LM. Cerebral aneurysm treatment: modern neurovascular techniques. Stroke Vasc Neurol. 2016;1(3):93-100. https://doi.org/10.1136/svn-2016-000027. PMid:28959469.

20. Brinjikji W, Lanzino G, Cloft HJ, Rabinstein A, Kallmes DF. Endovascular treatment of middle cerebral artery aneurysms. Neurosurgery. 2011;68(2): 397-402. https://doi.org/10.1227/NEU.0b013e318201d7f4. PMid:21135730.

21. Gao F, Guo X, Han J, Sun X, Zhou Z, Miao Z. Endovascular recanalization for symptomatic non-acute middle cerebral artery occlusion: proposal of a new angiographic classification. J Neurointerv Surg. 2021;13(10):900-5. https://doi.org/10.1136/neurintsurg-2020-016692. PMid:33122350.

22. Sumi T, Kawamoto S, Fukaya S, Ueki K, Kim P. Middle cerebral artery aneurysm associated with moyamoya disease. World Neurosurg. 2020;140:233-6. https://doi.org/10.1016/j.wneu.2020.05.111. PMid:32434024.

CORRESPONDING AUTHOR

Guilherme Wandall, MS
Medical student
Universidade Regional de Blumenau – FURB
Blumenau, Santa Catarina, Brasil
E-mail: wandallguilherme@gmail.com

Funding: *nothing to disclose.*
Conflicts of interest: *nothing to disclose.*
Ethics Committee Approval: *approved by under CAAE: 61294422.0.0000.5370.*

CRediT

Leandro José Haas: Conceptualization, Formal analysis, Data Curation, Supervision. Guilherme Wandall: Conceptualization, Validation, Writing – Review & editing, Project administration. Douglas Cipriano de Souza: Methodology. Wesley Severino: Investigation, Writing – Original Draft. Amanda Junges Derlam: Resources, Writing – Review & editing. Eduarda Alves: Visualization. Ana Boaventura: Software. André Felipe Kroenke: Investigation, Writing – Original Draft. Gabriela Scheidt: Writing – Original Draft, Writing – Review & editing. Camila Ceruti dos Santos: Validation, Writing – Review & editing.

Topographic Classification of Middle Cerebral Artery M1 Segment Aneurysms: anatomical and microsurgical findings from a retrospective surgical series

Classificação Topográfica dos Aneurismas do Segmento M1 da Artéria Cerebral Média: achados anatômicos e microcirúrgicos de uma série cirúrgica retrospectiva

Daniel Serfaty Fonseca[1,2]
Hung Tzu Wen[1]
Saul Almeida da Silva[1]
Deisiane da Silva Mesquita Serfaty[3]
Lucianna Serfaty de Holanda[4]
Eberval Gadelha Figueiredo[1]

ABSTRACT

Introduction: *M1 segment aneurysms remain challenging because of anatomical variability, perforator proximity, and limited standardized topographic descriptions for operative planning.* **Objective**: *To describe a four-quadrant posteroanterior (PA) classification for M1 aneurysms and evaluate its association with sagittal projection, M1 morphology, and intraoperative rupture (IOR).* **Methods**: *We retrospectively reviewed 86 patients who underwent microsurgical clipping by a single senior surgeon between 2006 and 2018. Aneurysms were classified as superolateral, inferolateral, inferomedial, or superomedial on PA imaging. Sagittal projection and M1 morphology were independently assessed.* **Results**: *The inferolateral quadrant was the most frequent location (62.3%). PA topography was associated with sagittal projection (p=0.034); medial aneurysms were predominantly anterior compared with lateral lesions (88.9% vs. 50.0%; p=0.035). Overall IOR occurred in 10.5% of cases. Curved M1 morphology showed a non-significant trend toward higher IOR (15.4% vs. 6.4%; OR 3.18; p=0.075), whereas temporary clipping was significantly associated with IOR (33.3% vs. 6.8%; OR 6.80; p=0.020).* **Conclusion**: *This PA-based classification offers a simple descriptive framework for M1 aneurysms. Surgical risk appears more closely related to parent-vessel morphology and intraoperative technical complexity than to quadrant position alone.*

Keywords: *Intracranial aneurysm; Middle cerebral artery; Microsurgery; Neurosurgical procedures; Intraoperative complications; Anatomy*

RESUMO

Introdução: *Os aneurismas do segmento M1 apresentam desafios microcirúrgicos relacionados à variabilidade anatômica, à proximidade dos ramos perfurantes e à escassez de descrições topográficas padronizadas.* **Objetivo**: *Descrever uma classificação em quatro quadrantes no plano posteroanterior (PA) para aneurismas de M1 e avaliar sua associação com projeção sagital, morfologia do M1 e ruptura intraoperatória (RIO).* **Métodos**: *Revisamos retrospectivamente 86 pacientes submetidos à clipagem microcirúrgica por um único cirurgião sênior entre 2006 e 2018. Os aneurismas foram classificados como superolaterais, inferolaterais, inferomediais ou superomediais em imagens PA. Projeção sagital e morfologia do M1 foram avaliadas independentemente.* **Resultados**: *O quadrante inferolateral foi o mais frequente (62,3%). A topografia PA associou-se à projeção sagital (p=0,034); aneurismas mediais foram predominantemente anteriores em comparação aos laterais (88,9% vs. 50,0%; p=0,035). A RIO ocorreu em 10,5% dos casos. A morfologia curva do M1 mostrou tendência não significativa de maior RIO (OR 3,18; p=0,075), enquanto a clipagem temporária associou-se significativamente à RIO (OR 6,80; p=0,020).* **Conclusão**: *A classificação PA oferece uma estrutura simples para descrição dos aneurismas de M1. O risco cirúrgico parece estar mais relacionado à morfologia do vaso parental e à complexidade intraoperatória do que à posição em quadrante isoladamente.*

Palavras-Chave: *Aneurisma intracraniano; Artéria cerebral média; Microcirurgia; Procedimentos neurocirúrgicos; Complicações intraoperatórias; Anatomia*

[1]Division of Neurosurgery, Hospital das Clínicas, Faculdade de Medicina, Universidade de São Paulo – USP, São Paulo, SP, Brasil.
[2]Graduate Program in Neurology, Faculdade de Medicina, Universidade de São Paulo – USP, São Paulo, SP, Brasil.
[3]Graduate Program in Public Health and Environment – PPGSPMA, Oswaldo Cruz Foundation – FIOCRUZ, Rio de Janeiro, RJ, Brasil.
[4]Hospital das Clínicas Gaspar Vianna, Belém, PA, Brasil.

Received May 25, 2026
Accepted May 30, 2026

INTRODUCTION

Middle cerebral artery (MCA) aneurysms are frequent, anatomically-diverse lesions. Although most arise at or near the bifurcation, aneurysms related to the M1 segment represent a demanding subgroup because of their relationship with the proximal sylvian fissure, the anterior perforated substance, and the lenticulostriate arteries[1-6].

Variation in M1 length, curvature, course, and dome orientation may affect surgical exposure, proximal control, clip application, and the risk of perforator injury[7-11]. For this reason, preoperative description of M1 aneurysms should be simple enough for routine use, but sufficiently anatomical to support operative planning.

Despite advances in endovascular therapy, microsurgical clipping remains an important treatment for selected MCA aneurysms, particularly lesions with wide necks, incorporated branches, complex morphology, or associated hematomas[12,13]. Intraoperative rupture (IOR) remains one of the most relevant technical complications of aneurysm surgery, as it may abruptly transform a planned dissection into urgent hemorrhage control under impaired visualization[14-17].

Classic microsurgical anatomy of the MCA is well established[8,11,13]; however, practical topographic models focused specifically on M1 aneurysms remain limited. In daily surgical reasoning, the dome position in the posteroanterior (PA) plane, the sagittal projection, and the morphology of the parent M1 segment are often considered together, but they are not always described in a standardized way.

The objective of this study was to describe a four-quadrant PA-based topographic classification for M1 segment aneurysms and to evaluate its association with sagittal dome projection, M1 morphology, and intraoperative findings, with particular attention to IOR.

METHODS

Study design

This was a retrospective, single-center observational study conducted as an institutional surgical series. The study followed the Strengthening the Reporting of Observational Studies in Epidemiology (STROBE) recommendations[18].

Study population and setting

We retrospectively reviewed 107 consecutive records of patients treated for MCA aneurysms at a tertiary academic center between 2006 and 2018. To reduce technical heterogeneity, only patients operated on under the supervision of the same senior neurosurgeon were considered for inclusion.

Inclusion and exclusion criteria

Inclusion criteria were: age 18 years or older; diagnosis of a saccular aneurysm located primarily in the MCA M1 segment; treatment by transcranial microsurgical clipping; and preoperative planning based on computed tomography angiography and/or three-dimensional digital subtraction angiography. Exclusion criteria were incomplete medical records, unavailable imaging, fusiform, mycotic, or traumatic aneurysms, aneurysms treated by endovascular techniques, and cases with insufficient records for reliable anatomical characterization.

Case series and analytic subgroups

Demographic and intraoperative rupture analyses were performed in 86 eligible patients. PA topographic classification and sagittal projection were available in 69 and 70 cases, respectively, according to imaging quality and documentation. Denominators are reported for each analysis to avoid overstatement of missing data.

Data collection and variables

Data were obtained from medical records, digital imaging studies, and operative records. Variables included sex, age group, aneurysm size, lobulations, rupture status at presentation, M1 length and course, PA quadrant, sagittal projection, use of temporary clipping, number of clips, and occurrence of IOR. Variables that could not be standardized across the full series, such as the exact perforator-neck relationship, were not included in the analytic model.

Surgical technique

Patients underwent standard or mini-pterional craniotomies according to aneurysm characteristics and surgeon preference. Sylvian fissure dissection was tailored to the individual anatomy. Clipping strategies prioritized proximal control, perforator preservation, and arterial reconstruction with the least necessary manipulation.

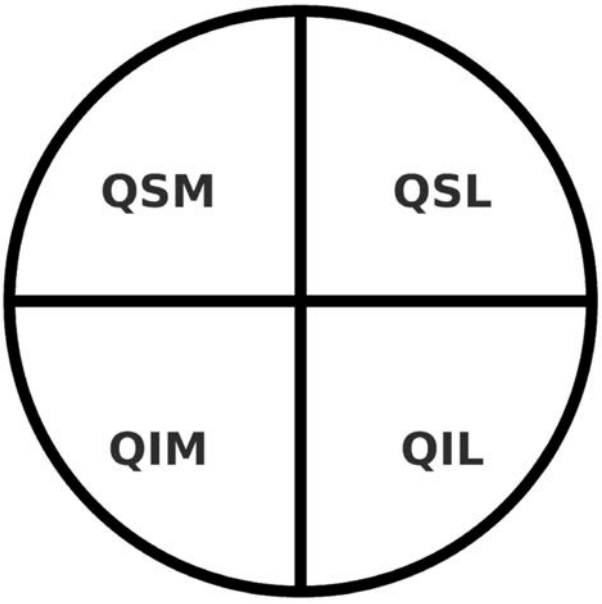

Figure 1. Schematic representation of the four-quadrant PA classification for left-sided M1 segment aneurysms.

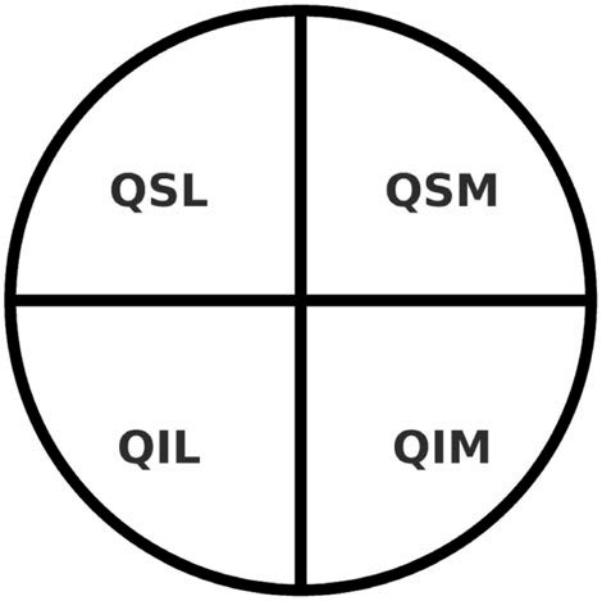

Figure 2. Schematic representation of the four-quadrant PA classification for right-sided M1 segment aneurysms.

Topographic classification and operational definitions

The proposed classification was based on the dome position in the PA plane. Aneurysms were assigned to one of four quadrants relative to the M1 axis: superolateral, inferolateral, inferomedial, or superomedial. Sagittal projection was assessed independently on lateral imaging and classified as anterior or posterior. Figures 1 and 2 illustrate the quadrant distribution for left- and right-sided lesions.

Complementary anatomical variables

M1 morphology was categorized according to length and course. Course was dichotomized as straight or curved. Curved M1 morphology was analyzed because it may limit linear visualization of the neck, restrict proximal control, and modify the clip application angle.

Statistical analysis

Categorical variables were described as absolute frequencies and percentages. Associations between categorical variables were assessed using Fisher's exact test, the likelihood ratio test, or the linear-by-linear association test, as appropriate. Associations with binary outcomes were estimated using odds ratios (ORs) and 95% confidence intervals (CIs). Statistical analysis was performed using IBM SPSS Statistics®, version 25.0 (IBM Corp., Armonk, NY, USA). Statistical significance was set at $p<0.05$. Values between 0.05 and 0.10 were interpreted as exploratory trends.

Ethical aspects

The study protocol was approved by an institutional Research Ethics Committee (CAAE 14176919.5.0000.0068). Because the study was based on retrospective secondary data, waiver of informed consent was requested. Patient confidentiality was preserved in accordance with applicable ethical regulations.

RESULTS

The final demographic and intraoperative rupture cohort included 86 patients. Overall IOR frequency was 10.5% (9/86). Most patients were female (76.7%). IOR was proportionally more frequent in males than in females (20.0% vs. 7.6%; OR 3.05; 95% CI 0.73-12.68; p=0.203), and in patients younger than 60 years compared with those aged 60 years or older (13.6% vs. 3.7%; OR 0.24; 95% CI 0.03-2.06; p=0.262). These differences did not reach statistical significance (Table 1).

PA topographic classification was available in 69 cases. The inferolateral quadrant was the most frequent location (43/69; 62.3%), followed by the superolateral (17/69; 24.6%), inferomedial (6/69; 8.7%), and superomedial quadrants (3/69; 4.3%).

Although no statistically significant association was found between quadrant position and the tested morphological or clinical variables, superolateral aneurysms had the highest proportion of large aneurysms (41.2%) and posterior sagittal projection (58.8%). Inferomedial aneurysms showed the highest proportion of ruptured presentation (50.0%), but the subgroup was small (Table 2).

Sagittal projection was available in 70 cases: 39 (55.7%) were anterior and 31 (44.3%) were posterior. PA topography was associated with sagittal projection (p=0.034). Medial aneurysms were predominantly anterior when compared with lateral aneurysms (88.9% vs. 50.0%; p=0.035). In contrast, lateral lesions were evenly distributed between anterior and posterior projection. No significant association was found between sagittal projection and IOR (p=1.000) or ruptured presentation with subarachnoid hemorrhage (p=0.410). Large or giant aneurysms showed an exploratory tendency toward anterior projection (72.2%; p=0.096), while lobulated aneurysms tended toward posterior projection (55.6%; p=0.095) (Table 3).

In the analysis of anatomical and technical variables associated with IOR, curved M1 morphology showed a non-significant trend toward higher rupture frequency compared with straight M1 morphology (15.4% vs. 6.4%; OR 3.18; 95% CI 0.73-13.7; p=0.075). Temporary clipping was significantly associated with IOR: rupture occurred in 33.3% of cases with temporary clipping and in 6.8% of cases without temporary clipping (OR 6.80; 95% CI 1.50-30.7; p=0.020). Inferior projection axis, posterior sagittal projection, multiple clips, and short M1 segment were not significantly associated with IOR (Table 4).

Table 1. Epidemiological profile and association with intraoperative rupture (N=86).

Demographic Variables	No Rupture n (%)	Rupture n (%)	Total (n)	p-value	OR (95% CI)
Gender				0.203[1]	3.05 (0.73-12.68)
Female	61 (92.4%)	5 (7.6%)	66		Ref.
Male	16 (80.0%)	4 (20.0%)	20		
Age Group				0.262[1]	0.24 (0.03-2.06)
<60 years	51 (86.4%)	8 (13.6%)	59		Ref.
≥60 years	26 (96.3%)	1 (3.7%)	27		

[1]Fisher's exact test.
Source: study data.

Table 2. Morphological and clinical profile of M1 aneurysms according to topographic classification in the posteroanterior plane (N=69).

Variables	QSL (1) n=17	QIL (2) n=43	QIM (3) n=6	QSM (4) n=3	p-value
Posterior sagittal projection	10 (58.8%)	20 (46.5%)	0 (0%)	1 (33.3%)	0.093
Large aneurysm	7 (41.2%)	10 (23.3%)	1 (16.7%)	0 (0%)	0.071
Curved M1	11 (64.7%)	16 (37.2%)	4 (66.7%)	1 (33.3%)	0.515
Short M1	4 (23.5%)	15 (34.9%)	3 (50.0%)	0 (0%)	0.386
Ruptured aneurysm (SAH)	3 (17.6%)	11 (25.6%)	3 (50.0%)	0 (0%)	0.317
Presence of lobulations	7 (41.2%)	16 (37.2%)	2 (33.3%)	2 (66.7%)	0.204

Source: study data.

Table 3. Analysis of morphological and clinical characteristics according to sagittal dome projection (N=70).

Associated Variables	Anterior Profile n (%)	Posterior Profile n (%)	Total (n)	p-value
Topographic PA classification (n=69)				0.034[1]
QSL (Superolateral)	7 (41.2%)	10 (58.8%)	17	
QIL (Inferolateral)	23 (53.5%)	20 (46.5%)	43	
QIM (Inferomedial)	6 (100.0%)	0 (0.0%)	6	
QSM (Superomedial)	2 (66.7%)	1 (33.3%)	3	
Position in the PA plane (n=69)				0.035[2]
Lateral (QSL + QIL)	30 (50.0%)	30 (50.0%)	60	
Medial (QIM + QSM)	8 (88.9%)	1 (11.1%)	9	
Size (n=70)				0.096[1]
Small	26 (50.0%)	26 (50.0%)	52	
Large / Giant	13 (72.2%)	5 (27.8%)	18	
Lobulations (n=70)				0.095[3]
Absent (0)	27 (62.8%)	16 (37.2%)	43	
Present (1, 2, or 3)	12 (44.4%)	15 (55.6%)	27	
Intraoperative rupture	3 (7.7%)	3 (9.7%)	6	1.000[2]
Integrity (Ruptured/SAH)	12 (30.8%)	6 (19.4%)	18	0.410[2]

[1]Likelihood ratio. [2]Fisher's exact test. [3]Linear-by-linear association.
Source: study data.

Table 4. Association between anatomical and technical variables and intraoperative rupture (N=86).

Risk Factors	No Rupture n=77	Rupture n=9	p-value	OR (95% CI)
Inferior projection axis	45 (91.8%)	4 (8.2%)	1.000	1.68 (0.17-16.1)
Curved M1	33 (84.6%)	6 (15.4%)	0.075[2]	3.18 (0.73-13.7)
Temporary clipping (Yes)	8 (66.7%)	4 (33.3%)	0.020[1]*	6.80 (1.50-30.7)
Posterior sagittal projection	28 (90.3%)	3 (9.7%)	1.000	1.28 (0.24-6.86)
Use of multiple clips	23 (85.2%)	4 (14.8%)	0.453	1.87 (0.46-7.63)
Short M1	25 (96.1%)	1 (3.9%)	0.261	0.25 (0.03-2.07)

[1] Fisher's exact test; [2] linear-by-linear association.*p<0.05.
Source: study data.

DISCUSSION

This study evaluated M1 segment aneurysms using a simple PA-based topographic classification complemented by independent assessment of sagittal projection and parent-vessel morphology. Three main findings deserve emphasis. First, aneurysms were most often located in the inferolateral quadrant. Second, PA topography was associated with sagittal projection, especially when medial and lateral positions were compared. Third, IOR appeared to be more closely related to M1 curvature and intraoperative technical complexity, particularly temporary clipping, than to quadrant position alone[11,13,16,17].

The predominance of the inferolateral quadrant suggests that M1 aneurysms in this series were not randomly distributed. This pattern may reflect the interaction between the geometry of the M1 segment, local branching, curvature, and hemodynamic forces[3,7,10]. Although the present study was not designed to evaluate flow dynamics, the observed distribution supports the value of a standardized topographic language for describing these lesions.

A central point of the proposed model is the distinction between PA topography and sagittal projection. The quadrant classification was intentionally restricted to the PA plane, while sagittal orientation was analyzed separately. This preserves simplicity, avoids excessive geometric assumptions, and makes the classification easier to apply in routine preoperative planning.

The association between PA topography and sagittal projection has practical implications. Medial aneurysms were predominantly anterior, while lateral aneurysms were divided between anterior and posterior projections. Superolateral aneurysms had the highest proportion of posterior projection. These observations should not be interpreted as deterministic rules, but they may help anticipate the likely dissection corridor, direction of dome exposure, and relationship between the dome, neck, and parent vessel during microsurgical planning[7,13,14,19,20].

Some morphological tendencies were also observed. Superolateral aneurysms had the highest proportion of large aneurysms, whereas lobulated lesions tended to project posteriorly. These findings did not reach statistical significance and should be interpreted cautiously, particularly because some subgroups were small. Nonetheless, they are consistent with the broader concept that angiographic morphology may influence both preoperative risk assessment and intraoperative behavior[11].

In the IOR analysis, M1 curvature appeared clinically relevant. Although statistical significance was not reached, curved M1 morphology was associated with a higher frequency of IOR and an OR above 3. This finding is anatomically plausible. A curved parent vessel may reduce the direct line of sight to the aneurysm neck, hinder proximal control, and make clip positioning less straightforward[9,15,16,21-24]. Because the number of IOR events was small, this result should be treated as exploratory rather than definitive.

Temporary clipping was the strongest variable associated with IOR. This association should not be interpreted as simple causality. In this series, temporary clipping most likely functioned as an intraoperative marker of complex or hostile anatomy, difficult proximal control, tense aneurysm behavior, or limited exposure[17,23,25,26]. Adjunctive intraoperative tools, including flow assessment and clip readjustment after flow verification, illustrate how complex neck anatomy may require real-time technical refinement, although these strategies were not specifically analyzed in the present series[14,27].

It is equally important to state what was not demonstrated. IOR was not significantly associated with posterior sagittal projection, inferior projection axis, multiple clip use, or short M1 segment. Therefore, the proposed quadrant system should be viewed primarily as a descriptive and planning tool, not as a standalone predictor of intraoperative rupture.

This study has limitations. It is a retrospective, single-center surgical series with a limited sample size and only nine IOR events, which reduces statistical power and widens confidence intervals. Not all cases had sufficient imaging documentation for PA topographic classification or sagittal analysis, resulting in different denominators across analyses. The proposed classification has not yet undergone external validation. Finally, relevant anatomical variables, such as the exact relationship between the neck and perforators or the precise proximal-distal position along M1, could not be standardized across the entire cohort.

CONCLUSION

The proposed PA-based quadrant classification provides a simple and reproducible framework for describing M1 segment aneurysms. In this retrospective surgical series, the inferolateral quadrant was the most frequent location, and PA topography was associated with sagittal dome projection.

Surgical risk, particularly IOR, appeared to be more closely related to parent-vessel morphology and intraoperative technical complexity than to quadrant position alone. Curved M1 morphology showed an exploratory association with higher IOR frequency, whereas temporary clipping was significantly associated with IOR as an intraoperative marker.

These findings should be interpreted cautiously and validated in larger external cohorts.

REFERENCES

1. Zhou Z, Lan W, Yu J. Endovascular treatment of middle cerebral artery aneurysms: current status and future prospects. Front Neurol. 2023;14:1239199. https://doi.org/10.3389/fneur.2023.1239199. PMid:38033773.

2. Yang W, Huang J. Treatment of middle cerebral artery (MCA) aneurysms: a review of the literature. Chin Neurosurg J. 2015;1(1):1. https://doi.org/10.1186/s41016-015-0001-8.

3. Campbell E, Burklund CW. Aneurysms of the middle cerebral artery. Ann Surg. 1953;137(1):18-28. https://doi.org/10.1097/00000658-195301000-00003. PMid:12996963.

4. Gibo H, Lenkey C, Rhoton AL Jr. Microsurgical anatomy of the supraclinoid portion of the internal carotid artery. J Neurosurg. 1981;55(4):560-74. https://doi.org/10.3171/jns.1981.55.4.0560. PMid:7277004.

5. Tsutsumi K, Horiuchi T, Nagm A, Toba Y, Hongo K. Clinical characteristics of ruptured distal middle cerebral artery aneurysms: review of the literature. J Clin Neurosci. 2017;40:14-7. https://doi.org/10.1016/j.jocn.2016.12.019. PMid:28087184.

6. Cardozo LCM Jr, Barros BP, Holanda MFDC. Fatores de risco em pacientes com aneurismas intracranianos atendidos em um hospital de referência de Belém - PA. J Bras Neurocir. 2018;22(3):95-9. https://doi.org/10.22290/jbnc.v22i3.1011.

7. Paulo MS, Edgardo S, Fernando M, Pablo P, Alejandro T, Verónica V. Aneurysms of the middle cerebral artery proximal segment (M1): anatomical and therapeutic considerations; revision of a series. Asian J Neurosurg. 2010;5(2):57-63. PMid:22028759.

8. Alreshidi M, Cote DJ, Dasenbrock HH, et al. Coiling versus microsurgical clipping in the treatment of unruptured middle cerebral artery aneurysms: a meta-analysis. Neurosurgery. 2018;83(5):879-89. https://doi.org/10.1093/neuros/nyx623. PMid:29438551.

9. Adamou A, Alexandrou M, Roth C, Chatziioannou A, Papanagiotou P. Endovascular treatment of intracranial aneurysms. Life. 2021;11(4):335. https://doi.org/10.3390/life11040335. PMid:33920264.

10. Ribas Escosteguy J, Bertuol I. Tratamento endovascular de aneurismas intracranianos rotos em pacientes submetidos a craniotomia descompressiva: pode ser viável? J Bras Neurocir. 2019;29(3):559-65. https://doi.org/10.22290/jbnc.v29i3.1785.

11. Estevão IA, Camporeze B, Araujo AS Jr, et al. Middle cerebral artery aneurysms: aneurysm angiographic morphology and its relation to pre-operative and intra-operative rupture. Arq Neuropsiquiatr. 2017;75(8):523-32. https://doi.org/10.1590/0004-282x20170082. PMid:28813082.

12. Sharma U, Verma S, Adithan S, Khobragade A. Morphology and variations of middle cerebral artery: systematic review and meta-analysis. Anat Cell Biol. 2024;57(4):481-97. https://doi.org/10.5115/acb.24.005. PMid:39317447.

13. Ni W, Yang H, Xu B, et al. Proximal middle cerebral artery aneurysms: microsurgical management and therapeutic results. World Neurosurg. 2019;122:e907-16. https://doi.org/10.1016/j.wneu.2018.10.174. PMid:30404066.

14. Fagundes-Pereyra WJ, Hoffman WE, Misra M, Charbel FT. Clip readjustment in aneurysm surgery after flow evaluation using the ultrasonic perivascular probe: case report. Arq Neuropsiquiatr. 2005;63(2A):339-44. https://doi.org/10.1590/S0004-282X2005000200028. PMid:16100988.

15. Yasargil MG. Microneurosurgery. CNS tumors: surgical anatomy, neuropathology, neuroradiology, neurophysiology, clinical considerations, operability, treatment options. New York: Thieme; 1994. (vol. 4A).

16. Gibo H, Carver CC, Rhoton AL Jr, Lenkey C, Mitchell RJ. Microsurgical anatomy of the middle cerebral artery. J Neurosurg. 1981;54(2):151-69. https://doi.org/10.3171/jns.1981.54.2.0151. PMid:7452329.

17. Chen SF, Kato Y, Kumar A, et al. Intraoperative rupture in the surgical treatment of patients with intracranial aneurysms. J Clin Neurosci. 2016;34:63-9. https://doi.org/10.1016/j.jocn.2016.01.045. PMid:27692502.

18. von Elm E, Altman DG, Egger M, et al. The Strengthening the Reporting of Observational Studies in Epidemiology (STROBE) statement: guidelines for reporting observational studies. PLoS Med. 2007;4(10):e296. https://doi.org/10.1371/journal.pmed.0040296. PMid:17941714.

19. Lawton MT. Seven aneurysms: tenets and techniques for clipping. New York: Thieme; 2011. https://doi.org/10.1055/b-002-66278.

20. Wiebers DO, Whisnant JP, Huston J 3rd, et al. Unruptured intracranial aneurysms: natural history, clinical outcome, and risks of surgical and endovascular treatment. Lancet. 2003;362(9378):103-10. https://doi.org/10.1016/S0140-6736(03)13860-3. PMid:12867109.

21. Morita A, Kirino T, Hashi K, et al. The natural course of unruptured cerebral aneurysms in a Japanese cohort. N Engl J Med. 2012;366(26):2474-82. https://doi.org/10.1056/NEJMoa1113260. PMid:22738097.

22. Rhoton AL Jr. The supratentorial arteries. Neurosurgery. 2002;51(4, Suppl):S53-120. PMid:12234447.

23. Dugani SM. Management of intraoperative rupture of intracranial aneurysms: agony and ecstasy. In: Turel KE, Chernov MF, Sarkar H, editors. Complications in neurosurgery II. Cham: Springer; 2023. p. 65-79. https://doi.org/10.1007/978-3-030-12887-6_9.

24. Żurada A, Gielecki J, Tubbs RS, et al. Three-dimensional morphometrical analysis of the M1 segment of the middle cerebral artery: potential clinical and neurosurgical implications. Clin Anat. 2011;24(1):34-46. https://doi.org/10.1002/ca.21051. PMid:20949492.

25. Doddamani R, Chandra PS. Intraoperative rupture of aneurysms: better avoid than mitigate. Neurol India. 2024;72(1):2-3. https://doi.org/10.4103/neurol-india.neurol-india_79_24. PMid:38442992.

26. Kim D, Park SK, Chung J. Outcomes and predictors of intraprocedural rupture in patients with cerebral aneurysm. Acta Neurochir. 2024;166(1):370. https://doi.org/10.1007/s00701-024-06262-0. PMid:39283335.

27. Amin-Hanjani S, Meglio G, Gatto R, Bauer A, Charbel FT. The utility of intraoperative blood flow measurement during aneurysm surgery using an ultrasonic perivascular flow probe. Neurosurgery. 2006;58(4, Suppl 2): ONS-305-12. https://doi.org/10.1227/01.NEU.0000209339.47929.34. PMid:16582654.

CORRESPONDING AUTHOR

Daniel Serfaty Fonseca, MD, PhD
Universidade de São Paulo – USP
Hospital das Clínicas
Division of Neurosurgery
São Paulo, São Paulo, Brasil
E-mail: drdanielserfaty@gmail.com

Funding: *nothing to disclose.*

Conflicts of interest: *nothing to disclose.*

Ethics Committee Approval: *The study protocol was approved by the institutional Research Ethics Committee (CAAE 14176919.5.0000.0068). A waiver of informed consent was requested due to the retrospective nature of the study.*

CRediT

Daniel Serfaty Fonseca: Conceptualization, Data Curation, Formal Analysis, Investigation, Methodology, Project Administration, Visualization, Writing – original draft. Hung Tzu Wen: Conceptualization, Methodology, Supervision, Writing – review & editing. Saul Almeida da Silva: Formal Analysis, Writing – original draft, Writing – review & editing. Deisiane da Silva Mesquita Serfaty: Methodology, Formal Analysis, Writing – review & editing. Lucianna Serfaty de Holanda: Data Curation, Investigation, Writing – original draft. Eberval Gadelha Figueiredo: Project Administration, Supervision, Writing – review & editing.

SAVE THE DATE

INOVAÇÃO PARA A EVOLUÇÃO DA NEUROCIRURGIA

XXII CABNc

CONGRESSO DA ACADEMIA BRASILEIRA DE NEUROCIRURGIA

21-24 | abril | 2027

CURITIBA | PR

Machine Learning Prediction of Six-month Functional Outcome Across the Full Severity Spectrum of Traumatic Brain Injury: a TRACK-TBI study

Predição por Aprendizado de Máquina do Desfecho Funcional em Seis Meses no Espectro Completo de Gravidade do Traumatismo Cranioencefálico: um estudo TRACK-TBI

Samuel Pedro Pereira Silveira[1]
Gustavo del Rio Lima[2]
Luiza Carolina Moreira Marcolino[3]
Larissa Batista Xavier[3]
Kioshe Rodrigues Siracava[3]
João Ricardo Sousa Vasconcellos[3]
Murillo Martins Correia[3]
Danilo Otávio de Araújo Silva[4]
Carlos Umberto Pereira[5]
Roberto Alexandre Dezena[3]

ABSTRACT

Introduction: *Prognostic models for traumatic brain injury (TBI), such as IMPACT, were derived in moderate-to-severe cohorts and do not apply to predominant mild injuries.* **Objective:** *To develop a machine-learning model predicting six-month functional outcome across the TBI severity spectrum.* **Methods:** *Of 2,545 TRACK-TBI adults, 1,749 had a valid six-month outcome. An XGBoost model used demographics, clinical examination, 13 CT findings, and five blood biomarkers to predict unfavorable outcome (GOSE-TBI 1–4), evaluated by cross-validation and benchmarked against IMPACT in the moderate-to-severe subset.* **Results:** *Unfavorable outcomes occurred in 242 patients (13.8%). Calibration was good (Brier 0.051; slope 0.95). Within-severity AUROC was 0.85 (mild) and 0.89 (moderate-to-severe); the pooled 0.944 was severity-inflated. Discrimination rose with each added modality (AUPRC 0.751→0.787→0.814) and exceeded IMPACT in this in-cohort benchmark (ΔAUROC +0.108 Core; +0.070 Extended), remaining more accurate after in-cohort recalibration (Brier 0.134 vs 0.189); a pre-specified decomposition attributed this advantage to the multimodal predictor set.* **Conclusion:** *A single calibrated, interpretable model predicts six-month outcome across the TBI severity spectrum, discriminates better than IMPACT, and provides calibrated risk estimates for the mild-TBI majority, for which IMPACT produces none. The prevalent mild-TBI endpoint (incomplete recovery) was not modeled, and external validation is required before clinical use.*

Keywords: *Brain Injuries, Traumatic; Machine Learning; Prognosis; Glasgow Outcome Scale; Biomarkers*

RESUMO

Introdução: *Modelos prognósticos de traumatismo cranioencefálico (TCE), como o IMPACT, derivam de coortes moderadas-a-graves e não se aplicam às lesões leves, que são predominantes.* **Objetivo:** *Desenvolver um modelo de aprendizado de máquina para prever o desfecho funcional em seis meses no espectro de gravidade do TCE.* **Métodos:** *Dos 2.545 adultos do TRACK-TBI, 1.749 tinham desfecho válido em seis meses. Um XGBoost usou demografia, exame clínico, 13 achados tomográficos e cinco biomarcadores sanguíneos para prever desfecho desfavorável (GOSE-TBI 1–4), com validação cruzada e comparação ao IMPACT no subgrupo moderado a grave.* **Resultados:** *O desfecho desfavorável ocorreu em 242 pacientes (13,8%). Calibração boa (Brier 0,051; slope 0,95). AUROC intra-estrato: 0,85 (leve) e 0,89 (moderado a grave); a agrupada (0,944), inflada pela gravidade. A discriminação aumentou a cada modalidade (AUPRC 0,751→0,787→0,814) e superou o IMPACT neste benchmark intra-coorte (ΔAUROC +0,108 Core; +0,070 Extended), permanecendo mais acurada após recalibração na coorte (Brier 0,134 vs 0,189); decomposição pré-especificada atribuiu a vantagem aos preditores multimodais.* **Conclusão:** *Um único modelo calibrado e interpretável prediz o desfecho em seis meses no espectro de gravidade do TCE, discrimina melhor que o IMPACT e fornece estimativas de risco calibradas para a maioria leve, para a qual o IMPACT não gera nenhuma. A recuperação incompleta, desfecho prevalente no TCE leve, não foi modelada; validação externa é necessária antes do uso clínico.*

Palavras-Chave: *Lesões Encefálicas Traumáticas; Aprendizado de Máquina; Prognóstico; Escala de Resultado de Glasgow; Biomarcadores*

[1]Faculty of Medicine, Universidade Federal do Triângulo Mineiro – UFTM, Uberaba, MG, Brazil.
[2]Center for Mathematics, Computing and Cognition – CMCC, Universidade Federal do ABC – UFABC, Santo André, SP, Brazil.
[3]Neurosurgery Division, Clinics Hospital, Universidade Federal do Triângulo Mineiro – UFTM, Uberaba-MG, Brazil.
[4]Department of Neurosurgery, Northwell Health, New Hyde Park, NY, USA.
[5]Neurosurgery Division, Universidade Federal do Sergipe – UFS, Aracaju, SE, Brazil.

Received Jul 11, 2026
Accepted Jul 21, 2026

INTRODUCTION

Traumatic brain injury (TBI) is a leading cause of death and acquired disability worldwide, and its clinical heterogeneity is a central obstacle to prognosis and to the design of clinical trials[1]. For the neurosurgeon and neurointensivist, an early, accurate estimate of long-term functional outcome informs monitoring intensity, anchors family counseling and goals-of-care discussions, and underpins trial stratification. A prognostic instrument that is accurate, calibrated, and applicable to the patients seen in practice would therefore be of direct clinical value.

The most widely validated prognostic instruments — the International Mission for Prognosis and Analysis of Clinical Trials in TBI (IMPACT) model[2] and the Corticosteroid Randomization After Significant Head injury (CRASH) model[3] — were derived in cohorts dominated by moderate-to-severe injury: IMPACT in patients with a Glasgow Coma Scale (GCS) ≤ 12, and CRASH in patients with GCS ≤ 14. IMPACT is therefore, by construction, undefined for mild TBI (GCS 13–15), and even CRASH excludes the GCS-15 patients who constitute most mild presentations; neither model is calibrated for the mild-injury majority reaching medical attention. This is consequential: many mild-TBI patients do not return to their pre-injury baseline even a year after injury — only ~47% report full recovery at 12 months[4] — yet no established quantitative tool stratifies their risk. Compounding this, both IMPACT and CRASH were derived from data collected between 1984 and 2004, and recent work shows they can be miscalibrated in contemporary cohorts, systematically overestimating mortality[5]. There is thus a dual gap: existing tools neither span the severity spectrum nor reflect contemporary outcomes.

Two developments now make a unified, spectrum-wide prognostic model feasible. First, large, harmonized, multimodal datasets such as Transforming Research and Clinical Knowledge in TBI (TRACK-TBI) capture demographics, structured clinical examination, standardized head computed tomography (CT) findings, and acute blood biomarkers in a single cohort[6]. Acute glial and neuronal blood biomarkers — notably glial fibrillary acidic protein (GFAP) and ubiquitin C-terminal hydrolase L1 (UCH-L1) — carry independent diagnostic information after TBI and are now clinically deployed to rule out intracranial injury[7]. Second, modern machine-learning (ML) methods — in particular, gradient-boosted decision trees — accommodate non-linear interactions, mixed data types, and the informative missingness that is intrinsic to acute trauma care (not every patient undergoes every assessment), while remaining interpretable through post-hoc attribution methods. Prior ML models for TBI, however, have largely been confined to moderate-to-severe injury and have not consistently outperformed logistic regression[8]; whether flexible models add value across the full spectrum — and, if so, whether that value comes from the algorithm or from richer data — remains unresolved.

Therefore, we set out to (i) develop an ML model that predicts six-month functional outcome across the entire TBI severity spectrum; (ii) quantify the incremental prognostic value of CT findings and acute blood biomarkers over clinical variables; (iii) interrogate the model's behavior with SHapley Additive exPlanations (SHAP) to ensure clinical plausibility; and (iv) benchmark it head-to-head against IMPACT in the subgroup where it is defined, decomposing any advantage into algorithm- and data-attributable components.

METHODS

This study is reported in accordance with the TRIPOD+AI statement for the development of multivariable prediction models using machine learning[9].

Data source and participants

We used the publicly available TRACK-TBI "Acute Imaging, Blood Biomarker, and Clinical Indicators of TBI Severity" dataset (Open Data Commons for TBI, ODC-TBI:1168; DOI 10.34945/F5088C)[10], comprising 2,545 adults (≥ 17 years) enrolled with TBI at U.S. level 1 trauma centers. The dataset was de-identified at source; this secondary analysis of openly available, de-identified data was exempt from additional institutional ethics committee approval (ethics waiver).

Outcome

The primary outcome was the six-month Glasgow Outcome Scale-Extended attributable to TBI (GOSE-TBI)[11], dichotomized as unfavorable (GOSE 1–4: death through upper severe disability) versus favorable (GOSE 5–8), consistent with the established IMPACT endpoint. We used the TBI-attributable GOSE rather than the all-injury variant so that the target reflects disability due to the brain injury itself rather than concomitant extracranial trauma.

The unfavorable dichotomy was chosen for direct comparability with IMPACT; incomplete recovery (GOSE < 8), although highly prevalent in mild TBI, is a distinct endpoint beyond the present scope. Records with an invalid GOSE code (n = 106) or a missing six-month outcome (n = 690) were excluded from the modeling cohort (analytic n = 1,749).

Predictors

Acute predictors available within 24 hours of injury were organized into three modality blocks (the CT findings, blood biomarkers, and clinical signs among them correspond to the TRACK-TBI acute severity framework[6]):

- **Clinical / demographic** — age, sex, race, ethnicity, years of education, health insurance, admission GCS total and reverse-coded eye/verbal/motor subscores, loss-of-consciousness duration, post-traumatic amnesia duration, mechanism of injury, highest level of care, and CT-positive status.
- **CT findings** — 13 binary National Institute of Neurological Disorders and Stroke (NINDS) Common Data Element findings (skull fracture, contusion, traumatic axonal/shear injury, extra-axial hematoma, epidural/subdural/subarachnoid/intraventricular hemorrhage, edema, downward and upward herniation, Duret hemorrhage, midline shift). Some of these elements overlap by definition (e.g., extra-axial hematoma subsumes epidural and subdural hemorrhage); the gradient-boosting model accommodates such collinearity without harm to prediction.
- **Blood biomarkers** — day 1 GFAP, UCH-L1, neuron-specific enolase (NSE), S100 calcium-binding protein B (S100B), and high-sensitivity C-reactive protein (hsCRP), provided as deciles.

The binary CT-positive flag was grouped with the clinical block as a bedside imaging summary, the 13 detailed findings forming the separate CT block; grouping it with imaging instead left the modality-ablation result unchanged. To avoid leakage, severity categories (e.g., GCS-based grouping) and the IMPACT linear predictors were reserved as reference/benchmark variables and not used as model inputs, as were the two-week and all-injury GOSE outcome variants.

Missing data

Missingness ranged from 0% (age, sex) to 31% (post-traumatic amnesia duration) and was treated as potentially informative — failure to assess a variable (e.g., amnesia in an intubated patient) is itself clinically meaningful. XGBoost handles missing values natively and was trained on the unimputed data; for logistic regression, numeric gaps were median-imputed within each training fold and "unknown" categories were kept as explicit levels.

Models and validation

We compared penalized logistic regression with a gradient-boosted tree ensemble (XGBoost[12]), the latter with conservative settings fixed in advance to limit overfitting. Performance was estimated by repeated stratified five-fold cross-validation (10 repeats), so each patient was scored only by models that had not seen them; 95% confidence intervals came from patient-level bootstrapping. We report discrimination — the area under the receiver operating characteristic curve (AUROC, the c-statistic) and, given the 13.8% event rate, the more informative area under the precision–recall curve (AUPRC) — together with calibration (Brier score and calibration slope/intercept[13]) and clinical utility (decision-curve net benefit[14]). With 242 events for 33 candidate predictors (56 parameters, since categorical variables expand into multiple binary indicator terms) — i.e. ~4 events per parameter, below the usual minimum of ten[15] — overfitting was countered by regularization and shown to be minimal by nested cross-validation and a near-ideal calibration slope. Paired comparisons were pre-specified but exploratory (unadjusted for multiple testing).

Incremental value, interpretation, and benchmarking

We added CT findings and then blood biomarkers to the clinical variables, testing each gain by paired bootstrap, and interpreted predictor contributions with SHAP values[16], a method that quantifies how much each variable pushes an individual prediction toward or away from an unfavorable outcome. In the moderate-to-severe subset where IMPACT applies, we compared the model against the IMPACT Core (n = 358) and Extended (n = 260) linear predictors, supplied pre-computed from the published IMPACT weights[2] — IMPACT as originally specified. CRASH could not be benchmarked, as its linear predictor is absent from this release.

Sensitivity analyses

Pre-specified checks examined robustness: decomposing the advantage over IMPACT into algorithm- and data-attributable components; recalibrating IMPACT's intercept and slope in this cohort by cross-validated logistic recalibration, so the calibration comparison would not merely reward in-cohort fitting; nested cross-validation to confirm the fixed settings were not optimistic; inverse-probability weighting for non-random

loss to follow-up; refitting without "level of care" and without the loss-of-consciousness/amnesia variables (to probe reverse causation and "too-sick-to-assess" effects); and refitting without socioeconomic variables. Analyses used Python 3.11 (scikit-learn, XGBoost, SHAP); code is available at https://github.com/silveirasamuel/odc-tbi-track-tbi.

RESULTS

Cohort

Of 2,545 enrolled patients, 1,749 had a valid six-month GOSE-TBI and formed the modeling cohort (Figure 1; 106 excluded for an invalid GOSE code and 690 for a missing six-month outcome). The median age was 39 years (interquartile range [IQR] 26–56) and 68% were male; mild injury (GCS 13–15) predominated (1,339 of 1,749, 77%). An unfavorable outcome occurred in 242 patients (13.8%), including 125 deaths (7.1%). Patients with unfavorable outcomes were older (median 51 vs 37 years), more frequently CT-positive (85.5% vs 42.0%), and more often required intensive care (91.7% vs 37.2%) (Table 1).

The burden of incomplete recovery was high and graded by severity: 60.3% of mild, 83.5% of moderate, and 88.7% of severe patients had a GOSE < 8 at six months, whereas the classical unfavorable endpoint was rare in mild TBI (3.6%) (Figure 2). This dissociation motivates modeling across the full severity spectrum rather than within a single severity band.

Model performance and clinical utility

The full XGBoost model achieved an AUROC of 0.944 (95% CI 0.925–0.959) and an AUPRC of 0.814 (0.767–0.856), outperforming penalized logistic regression at every modality level (full-model AUROC 0.944 vs 0.927; AUPRC 0.814 vs 0.767) (Table 2, Figure 3). This pooled AUROC is inflated by the mixing of mild and severe cases; the within-stratum estimates reported below are the fairer measure of discrimination.

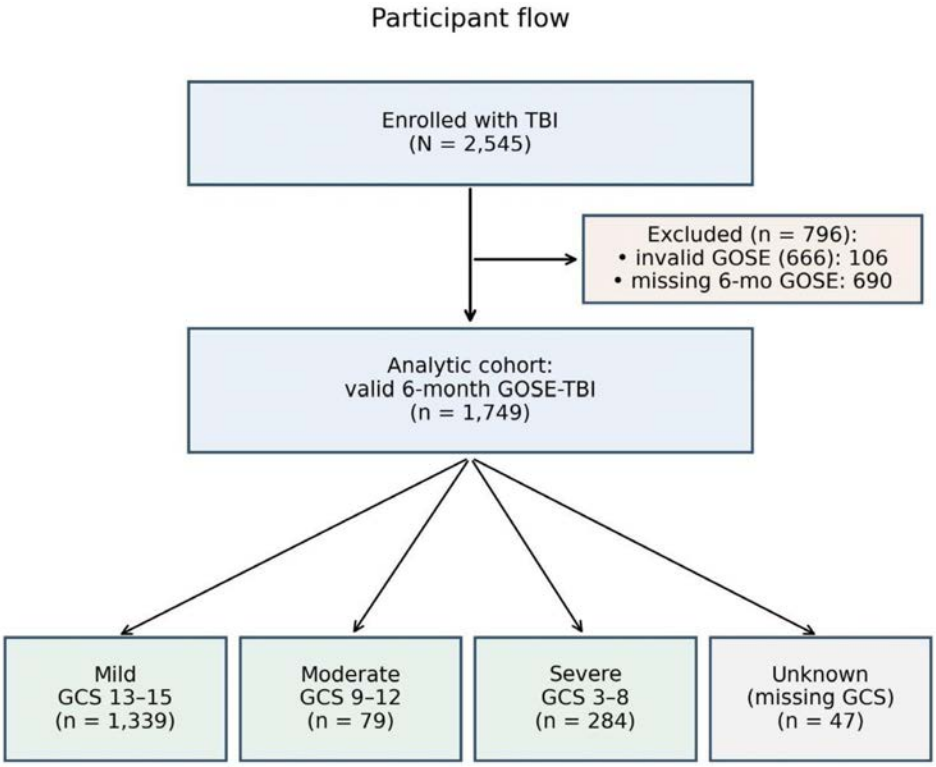

Figure 1. Participant flow. Of 2,545 adults enrolled with TBI, 796 were excluded (106 with an invalid GOSE code and 690 with a missing six-month outcome), leaving an analytic cohort of 1,749 with a valid six-month GOSE-TBI, partitioned into admission-severity strata: mild (GCS 13–15, n = 1,339), moderate (GCS 9–12, n = 79), severe (GCS 3–8, n = 284), and a group with missing admission GCS (n = 47). GOSE-TBI = TBI-attributable Glasgow Outcome Scale-Extended; GCS = Glasgow Coma Scale.

Table 1. Cohort characteristics overall and by six-month outcome (n = 1,749). n (%) gives each group's share of the analytic cohort; Death at 6 mos. (GOSE 1) is a component of the unfavorable endpoint.

Characteristic	Overall	Favorable (GOSE 5–8)	Unfavorable (GOSE 1–4)	SMD	Missing, %
n (%)	1,749 (100.0)	1,507 (86.2)	242 (13.8)	—	—
Death at 6 mos., n (%)	125 (7.1)	0 (0.0)	125 (51.7)	—	—
Demographics					
Age, median [IQR]	39 [26–56]	37 [25–53]	51 [33–65]	0.53	0.0
Male, %	68.0	67.0	74.8	0.17	0.0
White, %	76.8	76.5	78.5	0.05	0.9
Black, %	16.0	16.7	11.6	−0.15	0.9
Hispanic, %	15.7	15.8	15.3	−0.01	0.0
Education, yrs, median [IQR]	13 [12–16]	13 [12–16]	12 [12–14]	−0.43	4.5
Uninsured, %	18.0	18.6	14.0	−0.12	0.0
Injury mechanism					
Road traffic, %	56.8	56.8	57.0	0.00	0.0
Fall, %	26.9	26.6	28.9	0.05	0.0
Violence/assault, %	6.0	6.1	5.4	−0.03	0.0
Clinical severity					
Admission GCS, median [IQR]	15 [14–15]	15 [14–15]	5 [3–10]	−1.68	2.7
Severe (GCS 3–8), %	16.2	9.4	59.1	1.23	2.7
CT positive, %	48.0	42.0	85.5	1.02	3.3
Highest level of care					
Emergency department only, %	22.4	25.6	2.5	−0.71	0.0
Intensive care unit, %	44.8	37.2	91.7	1.39	0.0
Blood biomarkers (deciles)					
GFAP, median [IQR]	6 [3–8]	5 [3–7]	10 [8–10]	1.46	3.2
UCH-L1, median [IQR]	6 [3–8]	5 [3–7]	9 [8–10]	1.48	3.2
S100B, median [IQR]	6 [3–8]	5 [3–7]	9 [8–10]	1.46	10.5
NSE, median [IQR]	5 [3–8]	5 [3–7]	8 [6–9]	0.90	10.5
hsCRP, median [IQR]	5 [3–8]	5 [3–7]	9 [6–10]	0.95	16.5

SMD = standardized mean difference (favorable → unfavorable); |SMD| > 0.1 indicates meaningful imbalance. Percentages are computed among non-missing values, and the Missing column reports per-predictor missingness in the analytic cohort; post-traumatic amnesia and loss-of-consciousness duration (not tabulated) had the highest missingness (~30%; see Methods, Missing data). Blood biomarkers are reported as population deciles (1–10).

It was well calibrated (Brier 0.051; calibration slope 0.95, intercept 0.05; Figure 4A). Decision-curve analysis confirmed clinical utility: the full model showed positive net benefit across the entire evaluated range of threshold probabilities (1–60%) and exceeded both treat-all and treat-none strategies throughout (for example, net benefit 0.11 versus 0.04 for treat-all at a 10% risk threshold) (Figure 4B).

Incremental value of imaging and biomarkers

Adding modalities improved discrimination at each step. For XGBoost, AUPRC rose from 0.751 (clinical) to 0.787 (+CT) to 0.814 (+biomarkers); AUROC rose from 0.933 to 0.943 with CT and plateaued at 0.944 with biomarkers. Increments were tested by paired bootstrap (rather than judged from overlapping marginal intervals).

CT findings improved both overall discrimination and precision (ΔAUROC +0.010, paired p<0.001; ΔAUPRC +0.035, p=0.005), whereas blood biomarkers contributed almost exclusively to precision (ΔAUPRC +0.027, p=0.021) with AUROC already saturated (ΔAUROC +0.001, p=0.79). Thus, biomarkers sharpened identification of the infrequent poor-outcome patients rather than overall ranking — a modest but statistically supported contribution, tempered by their collinearity with GCS- and CT-defined severity.

Performance within severity strata

Because pooled discrimination mixes mild with severe cases, we evaluated it within each admission-severity stratum (Table 3, Figure 5). The model retained substantial within-stratum discrimination (AUROC 0.849 in mild, 0.886 in moderate, 0.886 in severe) and remained reasonably calibrated within each stratum (Table 3), with intercept drift confined to the small moderate stratum (n = 79), confirming that performance is not merely a re-expression of the GCS. As expected, mild TBI was the hardest stratum, and its estimates rest on only 48 events: the AUROC confidence interval was wide (0.780–0.911) and the AUPRC (0.436 vs a 0.036 prevalence baseline) should be read

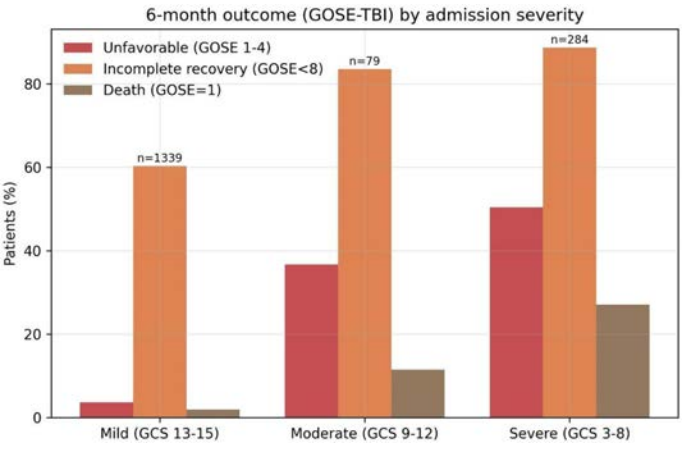

Figure 2. Six-month outcome by admission severity. Grouped bars show, within each severity stratum, the percentage of patients with an unfavorable outcome (GOSE 1–4), with incomplete recovery (GOSE < 8), and who died (GOSE 1); stratum sizes are annotated above the bars. Incomplete recovery is highly prevalent even in mild TBI (60%), whereas the classical unfavorable endpoint is rare there (3.6%), motivating modeling across the full severity spectrum.

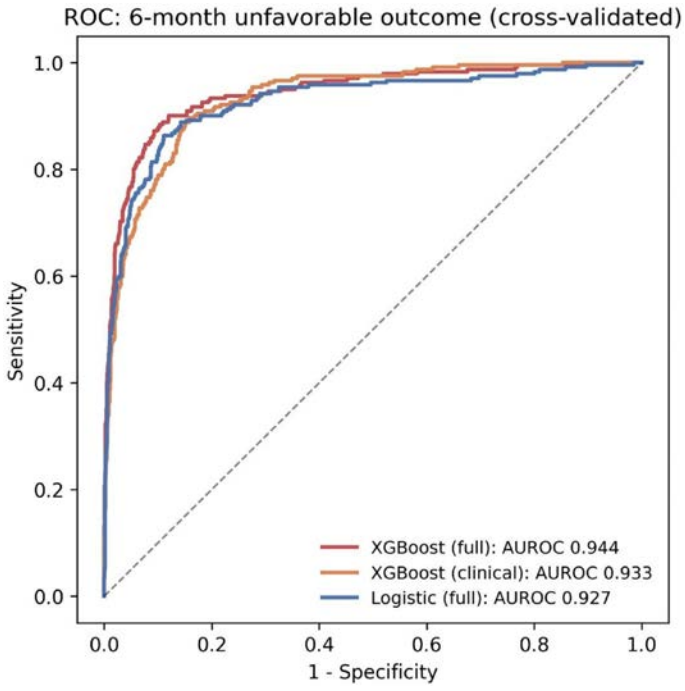

Figure 3. Cross-validated receiver-operating-characteristic curves for the six-month unfavorable outcome, from repeated stratified five-fold cross-validation. Curves are shown for the full XGBoost model (all modalities), the clinical-only XGBoost model, and the full penalized logistic-regression model; the dashed diagonal denotes chance, and areas under the curve (AUROC) are given in the legend.

Table 2. Cross-validated performance by model and modality block.

Model	Features	AUROC (95% CI)	AUPRC (95% CI)	Brier
Logistic	Clinical	0.913 (0.891–0.933)	0.722 (0.666–0.774)	0.066
XGBoost	Clinical	0.933 (0.916–0.949)	0.751 (0.699–0.800)	0.062
Logistic	+ CT	0.923 (0.901–0.943)	0.742 (0.684–0.795)	0.061
XGBoost	+ CT	0.943 (0.926–0.958)	0.787 (0.740–0.833)	0.055
Logistic	+ Biomarkers (full)	0.927 (0.904–0.947)	0.767 (0.714–0.817)	0.058
XGBoost	+ Biomarkers (full)	0.944 (0.925–0.959)	0.814 (0.767–0.856)	0.051

Table 3. Discrimination within admission-severity strata (full XGBoost, cross-validated).

Stratum	n	Events (%)	AUROC (95% CI)	AUPRC (95% CI)	AUPRC baseline	Cal. slope	Cal. intercept
Mild (GCS 13–15)	1,339	48 (3.6)	0.849 (0.780–0.911)	0.436 (0.295–0.573)	0.036	0.95	0.07
Moderate (GCS 9–12)	79	29 (36.7)	0.886 (0.804–0.951)	0.834 (0.706–0.925)	0.367	0.84	0.31
Severe (GCS 3–8)	284	143 (50.4)	0.886 (0.844–0.921)	0.889 (0.839–0.930)	0.504	0.90	−0.05
Unknown (missing GCS)	47	22 (46.8)	0.940 (0.862–0.993)	0.919 (0.794–0.994)	0.468	1.51	0.16
Overall	1,749	242 (13.8)	0.944 (0.925–0.959)	0.814 (0.767–0.856)	0.138	0.95	0.05

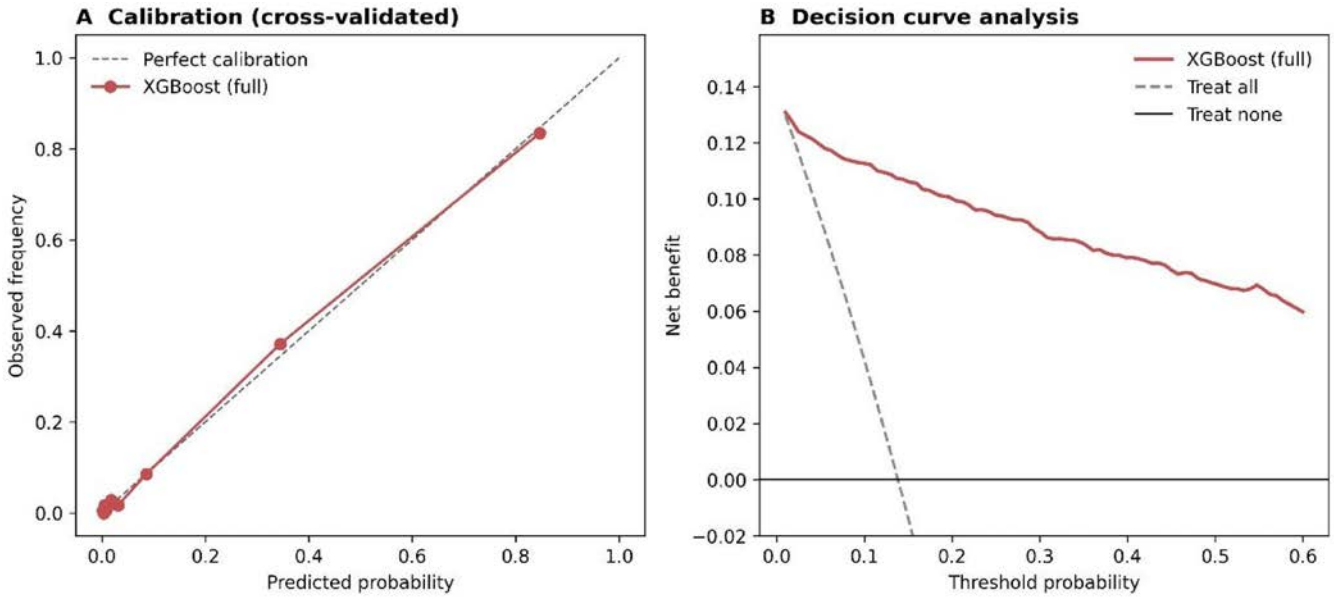

Figure 4. Calibration and clinical utility of the full XGBoost model (cross-validated). **A.** Reliability diagram: mean predicted probability (x-axis) versus observed frequency of the unfavorable outcome (y-axis), binned by predicted risk; the dashed diagonal denotes perfect calibration. **B.** Decision-curve analysis: net benefit (y-axis) across threshold probabilities from 1% to 60% (x-axis) for the full model versus the default treat-all (dashed) and treat-none (horizontal line) strategies.

as encouraging but provisional. A small group with missing admission GCS (n = 47, 22 events) could not be assigned a severity stratum and is reported separately in Table 3.

Benchmarking against IMPACT

In the moderate-to-severe subset where IMPACT is defined, our model exceeded both IMPACT variants on the identical patients (Table 4): versus IMPACT Core, AUROC 0.894 vs 0.785 (paired ΔAUROC +0.108, 95% CI +0.062 to +0.154, p<0.001); versus IMPACT Extended, 0.909 vs 0.838 (ΔAUROC +0.070, 95% CI +0.024 to +0.117, p=0.002).

Beyond discrimination, the model was also better calibrated than IMPACT in this subset — the property our framework emphasizes and that legacy models are known to lose in contemporary cohorts[5]. IMPACT systematically overestimated risk, whereas our model was near-ideal (Table 4). Three checks address the fairness of the comparison. First, because a frozen external model is expected to miscalibrate, we recalibrated IMPACT's intercept and slope in this cohort (cross-validated). This corrected its calibration slope and intercept (Table 4), confirming that part of the miscalibration reflects its 1984–2004 coefficients. Its Brier score, however, was essentially unchanged and remained well above ours: the residual gap is driven by discrimination (refinement), which recalibration

Table 4. Head-to-head performance versus IMPACT in the moderate-to-severe subset (cross-validated). "XGBoost full" is our full model on the identical patients; "recalibrated" re-estimates IMPACT's intercept and slope in this cohort, which corrects calibration while leaving discrimination (AUROC) essentially unchanged. The Extended linear predictor requires additional inputs and is therefore computable in fewer patients (n = 260) than Core (n = 358).

Model	n	AUROC (95% CI)	Brier	Cal. slope	Cal. intercept	Paired ΔAUROC vs ours (95% CI; p)
IMPACT Core (frozen)	358	0.785 (0.737–0.832)	0.190	1.12	−0.19	+0.108 (0.062–0.154; p<0.001)
IMPACT Core (recalibrated)	358	0.784	0.189	0.98	≈0.00	—
XGBoost full (same subset)	358	0.894 (0.859–0.923)	0.134	0.94	+0.06	—
IMPACT Extended (frozen)	260	0.838 (0.791–0.883)	0.167	1.32	−0.22	+0.070 (0.024–0.117; p=0.002)
IMPACT Extended (recalibrated)	260	0.834	0.166	0.97	≈0.00	—
XGBoost full (same subset)	260	0.909 (0.871–0.941)	0.120	1.01	−0.02	—

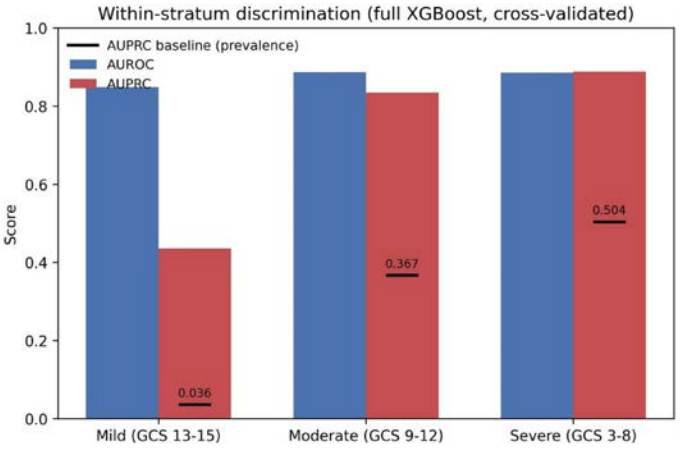

Figure 5. Within-stratum discrimination of the full XGBoost model (cross-validated). Bars show AUROC and AUPRC within each admission-severity stratum; the horizontal mark on each AUPRC bar is the stratum event prevalence — the no-skill AUPRC baseline against which precision must be read. Because prevalence is low in mild TBI (3.6%), its AUPRC baseline is correspondingly low. The unknown-GCS stratum (Table 3) is omitted.

leaves untouched. Second, the endpoint mismatch does not explain the gap: IMPACT discriminated its native all-cause endpoint essentially identically to the TBI-attributable endpoint (Core 0.788 vs 0.785; Extended 0.835 vs 0.838). Third, as detailed below, the advantage decomposes into separately attributable algorithm and data components. The discrimination gap nonetheless remains an in-cohort benchmark that structurally favors the developed model (see Discussion). Our model additionally yields risk estimates for the 1,339 mild-TBI patients for whom IMPACT, by construction, produces none.

Model interpretation

SHAP attribution (Figure 6) ranked age and admission GCS as the dominant predictors. The remaining leading predictors, in descending order of mean |SHAP|, were post-traumatic amnesia duration, S100B, UCH-L1, health-insurance status, years of education, loss-of-consciousness duration, CT downward herniation, hsCRP, and GFAP. Effect directions were physiologically coherent (lower GCS, higher age, and higher biomarker deciles increased predicted risk). Four of the five blood biomarkers — S100B, UCH-L1, hsCRP, and GFAP — ranked among the top 15 predictors despite their modest AUROC contribution, consistent with their role in sharpening precision rather than coarse discrimination; the fifth, NSE, ranked just outside (16th). Socioeconomic proxies (insurance status, years of education) carried measurable signal, a finding we interpret cautiously and revisit in the Discussion. Because SHAP importances were scored per one-hot column (in-sample TreeSHAP on the full model), multi-level categorical predictors such as insurance and mechanism are split across their levels, so their aggregate importance is understated relative to single-column predictors such as age and GCS.

Sensitivity and robustness

Pre-specified analyses supported the main results. A decomposition attributed the improvement to the predictor set rather than the algorithm: relative to a logistic model fit to the same IMPACT-like inputs, the flexible algorithm added little discrimination (ΔAUROC +0.07 Core, +0.05 Extended), whereas expanding to the full multimodal predictor set added substantially more (+0.11 Core, +0.12 Extended). On matched IMPACT-like inputs the gradient-boosted model only matched IMPACT (Core AUROC 0.784 vs

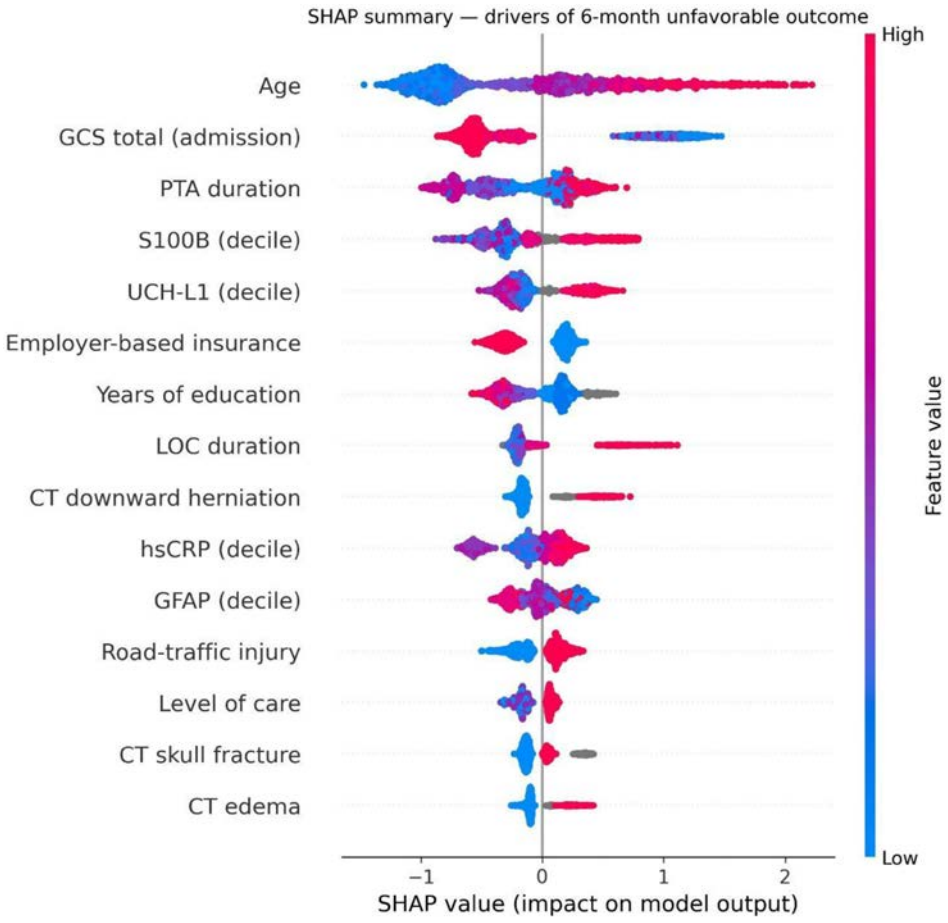

Figure 6. SHAP summary (beeswarm) plot for the full XGBoost model, showing the 15 predictors with the largest mean absolute SHAP value, ordered top to bottom by importance. Each point is one patient; its horizontal position is the SHAP value — the contribution to the model's log-odds of an unfavorable outcome, with points further right increasing predicted risk. Point color encodes the predictor's value (red = high, blue = low; grey = missing). SHAP = SHapley Additive exPlanations; PTA = post-traumatic amnesia; LOC = loss of consciousness.

0.785) and did not exceed it (Extended 0.792 vs 0.838), so essentially all of the advantage over IMPACT is attributable to the richer data rather than the algorithm. Model settings (hyperparameters) fixed in advance were not optimistic: nested cross-validation reproduced the headline performance (AUROC 0.942 vs 0.944), and the cross-validated calibration slope (0.95) indicated minimal overfitting despite the low events-per-variable. Discrimination was essentially unchanged when potentially problematic variables were removed or neutralized — level of care (AUPRC 0.814→0.812), the loss-of-consciousness/amnesia variables whose missingness may mark "too sick to assess" (→0.809–0.812), and the socioeconomic proxies (→0.799) — so the headline is not an artifact of leakage or informative missingness. Finally, loss to follow-up was only weakly predictable from baseline features (propensity AUROC 0.597), and inverse-probability weighting left performance unchanged (AUROC 0.944→0.943), arguing against meaningful selection bias.

DISCUSSION

In a multicenter cohort spanning the entire TBI severity spectrum, a single, post-hoc–interpretable machine-learning model predicted six-month functional outcome with high discrimination and good calibration, discriminated better than IMPACT within its own moderate-to-severe domain, and — unlike IMPACT — produced calibrated risk estimates across the spectrum, including the mild-injury majority.

Three findings merit emphasis. First, the modality-resolved analysis disentangles where prognostic information resides: clinical variables carry most of the discriminative signal, CT findings add both discrimination and precision, and acute blood biomarkers contribute

almost exclusively to incremental precision. The dissociation between AUROC (plateauing) and AUPRC (improving) with biomarkers illustrates why precision–recall metrics are essential when events are infrequent and why headline AUROC alone can understate biomarker value. Second, the model showed higher discrimination than IMPACT on identical patients, and a pre-specified decomposition traced this advantage almost entirely to the richer multimodal predictor set rather than the algorithm — on IMPACT-like inputs the flexible model merely matched (Core) or underperformed (Extended) IMPACT. The comparison is, however, in-cohort — our model was developed here, whereas IMPACT is an external, older, fixed-coefficient instrument built for a different (all-cause) endpoint — and is best read as benchmarking, not proof of universal superiority. Third, spectrum-wide applicability: severity-stratified analysis showed that discrimination is preserved within each severity level (AUROC 0.85–0.89) and that the model remained calibrated within the mild stratum (slope 0.95), so the pooled performance is not an artifact of the model simply rediscovering the GCS. We are deliberately careful about the mild-TBI claim, however. The present endpoint is unfavorable outcome (GOSE 1–4), which is rare in mild TBI (3.6%); the prevalent mild-TBI problem — incomplete recovery (GOSE < 8), affecting ~60% — is a distinct endpoint we did not model here. Our mild-TBI contribution is therefore a calibrated, spectrum-wide risk estimate including these patients, not a validated tool for predicting incomplete recovery, which requires dedicated modeling.

Relation to prior work. The established models discriminate only moderately in contemporary cohorts and are prone to miscalibration in present-day patients[5]; this matches the IMPACT performance we observed in-cohort (AUROC 0.79 Core, 0.84 Extended) and its systematic overestimation of risk. Earlier head-to-head comparisons found machine learning was no better than logistic regression for TBI prognosis[8]; our findings refine rather than contradict that conclusion, since the advantage we observe traces predominantly to multimodal predictors and full-spectrum coverage rather than to the algorithm itself. Most directly, a recent TRACK-TBI analysis using the same acute indicators derived a latent item-response-theory severity score and showed it predicts outcome incrementally beyond GCS and IMPACT[6]; our aim is complementary but distinct — we train directly on the six-month GOSE endpoint across the full spectrum, quantify each modality's incremental value, and benchmark head-to-head against IMPACT on identical patients. To our knowledge, this is among the first spectrum-wide models to provide calibrated risk estimates extending into mild TBI, a group the reference models exclude by construction.

Clinical implications. A single calibrated model spanning the severity spectrum could anchor several acute decisions: risk estimates to inform monitoring and triage, an objective adjunct for family counseling and goals-of-care discussions, and a basis for trial enrichment and stratification. Calibration — often subordinated to discrimination — is decisive here, because threshold-based decisions and risk communication require numerically accurate probabilities, not merely correct rank ordering; the model's near-diagonal reliability and positive net benefit support this use. Equally important, discrimination was retained within the mild stratum, precisely where clinicians lack quantitative tools and prognostic uncertainty is greatest.

The prominence of socioeconomic proxies in the SHAP ranking warrants caution: in observational data such signals may reflect confounding, access-to-care effects, or residual severity coding rather than causal determinants. We present them descriptively and do not advocate their use for individual decisions; reassuringly, removing insurance and education cost little discrimination (AUPRC 0.814→0.799), so a deployed model could omit them to avoid encoding socioeconomic disadvantage. We did not, however, formally evaluate predictive performance or error balance across demographic subgroups (for example by sex, race, or age); given the prominence of these proxies, a prospective fairness audit across strata is an important prerequisite to clinical deployment.

Limitations. First, this is an internal cross-validation in a single (albeit multicenter) cohort; external and prospective validation are required before clinical deployment. The present data release does not include an enrolling-site identifier, precluding even a leave-one-site-out internal–external validation; obtaining the site-resolved TRACK-TBI release or an independent cohort (e.g., CENTER-TBI) is a next step priority. Second, only IMPACT could be benchmarked: a CRASH linear predictor was not provided in this release, and the decomposition relied on an "IMPACT-mappable" reconstruction (lacking pupillary reactivity, hypoxia, hypotension, glucose, and hemoglobin), so its algorithm-versus-data split is indicative rather than exact. Third, "highest level of care" may reflect the admission course rather than a purely baseline triage decision, raising a reverse-causation concern; reassuringly, removing it left performance essentially unchanged (AUPRC 0.814→0.812), but residual leakage cannot be

fully excluded. Fourth, loss-of-consciousness and post-traumatic amnesia duration cannot be assessed in intubated or comatose patients, so their missingness partly encodes "too sick to assess" and correlates with poor outcome; treating it as informative may inflate apparent discrimination and limit transportability to settings with different assessment practices. Fifth, biomarkers were available only as deciles, limiting analysis of continuous concentration–risk relationships. Sixth, although outcome missingness (~27%) appeared near-random and results were stable under inverse-probability weighting, residual unmeasured selection cannot be excluded. Finally, we deliberately excluded post-baseline variables to preserve an acute-prognosis use case, and the endpoint was dichotomized for comparability with IMPACT, discarding ordinal information; ordinal modeling is a natural extension.

Future directions. Focused extensions include prediction of incomplete recovery in mild TBI, where no validated tool exists; the continuous prognostic value of acute biomarkers; temporal-trajectory modeling from two weeks to six months; and ordinal formulations of the full GOSE.

CONCLUSION

A calibrated, post-hoc–interpretable gradient-boosting model predicts six-month functional outcome across the full TBI severity spectrum, showed higher discrimination than IMPACT in this cohort, and provides risk estimates across the spectrum — including mild TBI, whose clinically relevant endpoint (incomplete recovery) remains to be modeled directly. These results support spectrum-wide, multimodal machine-learning prognostication as a promising approach to neurotrauma outcome estimation and trial design, pending external validation before any clinical use.

REFERENCES

1. Maas AIR, Menon DK, Adelson PD, et al. Traumatic brain injury: integrated approaches to improve prevention, clinical care, and research. Lancet Neurol. 2017;16(12):987-1048. https://doi.org/10.1016/S1474-4422(17)30371-X. PMid:29122524.

2. Steyerberg EW, Mushkudiani N, Perel P, et al. Predicting outcome after traumatic brain injury: development and international validation of prognostic scores based on admission characteristics. PLoS Med. 2008;5(8):e165, discussion e165. https://doi.org/10.1371/journal.pmed.0050165. PMid:18684008.

3. Perel P, Arango M, Clayton T, et al. Predicting outcome after traumatic brain injury: practical prognostic models based on large cohort of international patients. BMJ. 2008;336(7641):425-9. https://doi.org/10.1136/bmj.39461.643438.25. PMid:18270239.

4. Nelson LD, Temkin NR, Dikmen S, et al. Recovery after mild traumatic brain injury in patients presenting to US level I trauma centers: a Transforming Research and Clinical Knowledge in Traumatic Brain Injury (TRACK-TBI) study. JAMA Neurol. 2019;76(9):1049-59. https://doi.org/10.1001/jamaneurol.2019.1313. PMid:31157856.

5. Yue JK, Lee YM, Sun X, et al. Performance of the IMPACT and CRASH prognostic models for traumatic brain injury in a contemporary multicenter cohort: a TRACK-TBI study. J Neurosurg. 2024;141(2):417-29. https://doi.org/10.3171/2023.11.JNS231425. PMid:38489823.

6. Nelson LD, Magnus BE, Yue JK, et al. Beyond mild, moderate, and severe traumatic brain injury: modelling severity from clinical, neuroimaging, and blood-based indicators. EBioMedicine. 2025;121:106001. https://doi.org/10.1016/j.ebiom.2025.106001. PMid:41192220.

7. Bazarian JJ, Biberthaler P, Welch RD, et al. Serum GFAP and UCH-L1 for prediction of absence of intracranial injuries on head CT (ALERT-TBI): a multicentre observational study. Lancet Neurol. 2018;17(9):782-9. https://doi.org/10.1016/S1474-4422(18)30231-X. PMid:30054151.

8. Gravesteijn BY, Nieboer D, Ercole A, et al. Machine learning algorithms performed no better than regression models for prognostication in traumatic brain injury. J Clin Epidemiol. 2020;122:95-107. https://doi.org/10.1016/j.jclinepi.2020.03.005. PMid:32201256.

9. Collins GS, Moons KGM, Dhiman P, et al. TRIPOD+AI statement: updated guidance for reporting clinical prediction models that use regression or machine learning methods. BMJ. 2024;385:e078378. https://doi.org/10.1136/bmj-2023-078378. PMid:38626948.

10. Nelson LD, Magnus BE, Yue JK, et al. TRACK-TBI Acute Imaging, Blood Biomarker, and Clinical Indicators of TBI Severity in Humans [dataset]. Open Data Commons for Traumatic Brain Injury; 2025. ODC-TBI:1168. https://doi.org/10.34945/F5088C.

11. Wilson JT, Pettigrew LE, Teasdale GM. Structured interviews for the Glasgow Outcome Scale and the Extended Glasgow Outcome Scale: guidelines for their use. J Neurotrauma. 1998;15(8):573-85. https://doi.org/10.1089/neu.1998.15.573. PMid:9726257.

12. Chen T, Guestrin C. XGBoost: a scalable tree boosting system. In: Proceedings of the 22nd ACM SIGKDD International Conference on Knowledge Discovery and Data Mining (KDD '16);

2016; New York. New York: ACM; 2016. p. 785-94. https://doi.org/10.1145/2939672.2939785.

13. Van Calster B, McLernon DJ, van Smeden M, et al. Calibration: the Achilles heel of predictive analytics. BMC Med. 2019;17(1):230. https://doi.org/10.1186/s12916-019-1466-7. PMid:31842878.

14. Vickers AJ, Elkin EB. Decision curve analysis: a novel method for evaluating prediction models. Med Decis Making. 2006;26(6):565-74. https://doi.org/10.1177/0272989X06295361. PMid:17099194.

15. Riley RD, Ensor J, Snell KIE, et al. Calculating the sample size required for developing a clinical prediction model. BMJ. 2020;368:m441. https://doi.org/10.1136/bmj.m441. PMid:32188600.

16. Lundberg SM, Lee SI. A unified approach to interpreting model predictions. In: Guyon I, von Luxburg U, Bengio S, et al., editors. Advances in Neural Information Processing Systems 30: Annual Conference on Neural Information Processing Systems; 2017 Dec 4-9; Long Beach, CA. Red Hook (NY): Curran Associates, Inc.; 2017. p. 4765-74.

ACKNOWLEDGMENTS

Data were obtained from the Open Data Commons for TBI (ODC-TBI:1168, https://doi.org/10.34945/F5088C) supported by the TRACK-TBI investigators and the U.S. National Institutes of Health/NINDS.

CORRESPONDING AUTHOR

Samuel Pedro Pereira Silveira, MS
Medical Student
Faculty of Medicine
Universidade Federal do Triângulo Mineiro - UFTM
Uberaba, Minas Gerais, Brazil
E-mail: sppsilveira.md@gmail.com

Funding: *Nothing to disclose.*
Conflicts of interest: *Nothing to disclose.*
Ethics Committee Approval: *This is a secondary analysis of de-identified, publicly available data (Open Data Commons for TBI, ODC-TBI:1168; https://doi.org/10.34945/F5088C). The study was exempt from additional institutional ethics committee approval (waived).*

CRediT

Samuel Pedro Pereira Silveira: Conceptualization, Data curation, Formal analysis, Investigation, Writing – original draft. Gustavo del Rio Lima: Methodology, Software, Formal analysis, Validation, Writing – review & editing.

Luiza Carolina Moreira Marcolino: Investigation, Writing – review & editing. Larissa Batista Xavier: Investigation, Writing – review & editing. Kioshe Rodrigues Siracava: Investigation, Writing – review & editing. João Ricardo Sousa Vasconcellos: Investigation, Writing – review & editing. Murillo Martins Correia: Investigation, Writing – review & editing. Danilo Otávio de Araújo Silva: Supervision, Writing – review & editing. Carlos Umberto Pereira: Validation, Supervision, Writing – review & editing. Roberto Alexandre Dezena: Supervision, Resources, Writing – review & editing.

Challenging the Odds: anterior odontoid screw fixation for type II odontoid fractures without neuronavigation — a free-hand technique experience from a tertiary care centre in India

Desafiando as Probabilidades: fixação com parafuso odontoide anterior para fraturas odontoides tipo II sem neuronavegação — uma experiência de técnica livre em um centro de cuidados terciários na Índia

Siddharth Vrajesh Jindal[1]
Akyam Lakshman Rao[1]
Devi Chendira Pemmaiah[1]
Srikanth Dhadavai[1]
Ambarapu Mastan Reddy[1]

ABSTRACT

Introduction: *Type II odontoid fractures account for most odontoid injuries and carry a high risk of non-union with conservative treatment. Anterior odontoid screw fixation (AOSF) is the accepted surgical standard, but resource constraints in developing countries often preclude neuronavigation or intraoperative CT. We report our experience with the free-hand technique using minimal fluoroscopic guidance.* **Methods:** *We retrospectively reviewed ten consecutive patients who underwent single-screw AOSF for Type II fractures between January 2023 and December 2024 at a tertiary neurosurgical unit in Deccan India. All procedures used the free-hand technique under conventional C-arm fluoroscopy, without neuronavigation or O-arm assistance.* **Results:** *The cohort included eight males and two females, with a mean age of 32.8 years (range 20–52). Road traffic accidents caused 70% of injuries. Eight patients (80%) had excellent immediate postoperative outcomes. Two patients with cord contusion showed no immediate neurological improvement but reached ASIA Grade D by three months. Bony union was achieved in nine patients (90%). One screw malposition required revision surgery.* **Conclusion:** *Free-hand AOSF is safe, feasible, and effective even where advanced intraoperative imaging is unavailable. It demands meticulous preoperative planning, precise patient positioning, and thorough knowledge of surgical anatomy.*

Keywords: *Cervical vertebrae; Spine*

RESUMO

Introdução*: Fraturas do odontoide tipo II são as mais comuns dessa região e alto risco de não-consolidação com tratamento conservador. A fixação anterior do odontoide com parafuso (FAOP) é o padrão cirúrgico aceito, mas limitações de recursos em países em desenvolvimento frequentemente impedem acesso à neuronavegação ou tomografia intraoperatória. Apresentamos a experiência com a técnica "free-hand" para FAOP usando orientação fluoroscópica mínima.* **Métodos***: Revisão retrospectiva de dez pacientes consecutivos submetidos à FAOP com parafuso único para fraturas tipo II (janeiro/2023 a dezembro/2024) em unidade terciária de neurocirurgia no Deccan, Índia. Todos os procedimentos utilizaram técnica free-hand sob fluoroscopia convencional com arco em C, sem neuronavegação ou O-arm.* **Resultados***: Esta coorte incluiu oito homens e duas mulheres, com idade média de 32,8 anos (20-52 anos). Acidentes de trânsito causaram 70% das lesões. Oito pacientes (80%) apresentaram desfechos excelentes no pós-operatório imediato. Dois com contusão medular não obtiveram melhora neurológica imediata, mas alcançaram ASIA grau D em três meses. Nove pacientes (90%) obtiveram consolidação óssea. Um mau posicionamento do parafuso exigiu cirurgia de revisão.* **Conclusão***: A FAOP free-hand é segura, viável e eficaz mesmo sem imagem intraoperatória avançada, exigindo planejamento pré-operatório meticuloso, posicionamento preciso do paciente e profundo conhecimento da anatomia cirúrgica.*

Palavras-Chave: *Vértebras cervicais; Coluna vertebral*

[1]Department of Neurosurgery, Osmania Medical College and Osmania General Hospital, Hyderabad, Telangana, India

Received Jul 10, 2026
Corrected Jul 30, 2026
Accepted Aug 4, 2026

INTRODUCTION

Fractures of the odontoid process (dens) account for 9–20% of all cervical spine fractures and represent one of the most clinically challenging injuries encountered in spinal surgery[1]. Among the three types defined by the Anderson–D'Alonzo classification, Type II fractures — occurring at the base of the dens — are the most prevalent, constituting nearly two-thirds of all odontoid fractures, and carry the highest propensity for non-union[2].

Non-operative management with halo-vest immobilisation has historically yielded fusion rates ranging from 53% to 93%, while the attendant morbidity — including pin-site infection, swallowing dysfunction, and complications related to recumbency — renders it suboptimal for many patients[3]. Posterior C1–C2 fusion, though effective, sacrifices the 50% of axial rotation attributable to the atlantoaxial joint, significantly impairing cervical kinematics.

Anterior odontoid screw fixation (AOSF), first described by Nakanishi in 1980 and subsequently popularised by Böhler in 1982, addresses these limitations by achieving direct osteosynthesis at the fracture site while preserving atlantoaxial rotation[4,5]. Contemporary series employing neuronavigation or intraoperative three-dimensional fluoroscopy report fusion rates of 87–100% with low complication profiles[3,6].

Despite these advances, neuronavigation and O-arm fluoroscopy remain largely unavailable in peripheral and government-sector neurosurgical centres across India and other low- to middle-income countries. The conventional free-hand technique, relying on biplanar C-arm fluoroscopy and anatomical landmarks, therefore, retains substantial clinical relevance. We present our institutional experience with AOSF using this technique, comparing outcomes with published international and Indian series.

METHODS

Study design and patient selection

This is a retrospective, single-institution case series. All patients who underwent anterior single-screw odontoid fixation for Type II odontoid fractures at the Department of Neurosurgery, Osmania General Hospital, Hyderabad, between January 2023 and December 2024, were included. Written informed consent was obtained from every patient. Ethical approval was obtained from the institutional review committee.

Patients were excluded if they had: (a) disrupted transverse ligament with atlanto-dens interval greater than 4 mm; (b) associated Jefferson's fracture with lateral mass overhang exceeding 7 mm; (c) an oblique anterior fracture line unfavourable for lag-screw purchase; (d) severe osteopaenia; or (e) a chronic fracture older than six months.

Preoperative evaluation

All patients underwent plain radiographs of the cervical spine, computed tomography (CT) with thin-slice axial and sagittal reconstructions, and magnetic resonance imaging (MRI) to assess ligamentous integrity and spinal cord status. Neurological grading was performed using the American Spinal Injury Association (ASIA) Impairment Scale.

Surgical technique

All operations were performed under general anaesthesia with orotracheal intubation using a fibre-optic technique to avoid uncontrolled neck manipulation. The patient was positioned supine on a radiolucent table with the neck in gentle extension. The tip of the nose, suprasternal notch, and xiphisternum were aligned in a single anatomical plane to ensure the trajectory window for the screw was not impeded by the chin.

A vertical skin incision was made along the anterior border of the sternocleidomastoid at the C2–C3 level. Blunt dissection was carried through the platysma, and the prevertebral space was accessed by retracting the carotid sheath laterally and the trachea-oesophagus medially. A limited median C2–C3 discectomy was performed to create a small gutter in the superior cortex of the C3 body, providing a stable bony shelf for the cannulated drill guide.

Fluoroscopic guidance was employed at defined steps: an initial lateral view confirmed that the guide-wire projected posterior to the anterior cortex of C2 to prevent blowout; an AP view verified midline entry into the C2 body and the dens; and a final lateral view confirmed that the screw crossed the fracture line and its tip lay just proximal to the cortex of the odontoid tip. Controlled neck flexion or extension was used intraoperatively to reduce

the fracture and restore odontoid alignment. A single 3.5 mm cannulated, partially threaded lag screw from the Medtronic implant system was placed in all cases.

Early mobilization was encouraged from the second postoperative day in a Philadelphia cervical collar, which was worn for six weeks.

Postoperative follow-up

A dynamic cervical spine radiograph was obtained four weeks postoperatively. Patients were reviewed at one, two, three, six, and twelve months. Bony union was defined as the absence of motion at the fracture site on dynamic radiographs and bridging callus on CT. Clinical outcome was assessed by ASIA grade and resolution of neck pain.

RESULTS

Demographic and clinical profile

Ten patients were treated during the study period. Eight were male (80%) and two were female (20%). The mean age was 32.8 years (range 20–52 years), with 80% of patients being between 20 and 40 years of age. Road traffic accidents were the commonest mechanism (70%), followed by falls from height (20%) and crush injury from falling heavy objects (10%). All patients reported neck pain; five (50%) had restricted cervical range of motion; and four (40%) presented with quadriparesis. Cord contusion at the C2–C3 level was identified on MRI in two patients (20%) (Table 1).

Operative and postoperative outcomes

Eight of ten patients (80%) demonstrated excellent neurological and functional outcomes in the immediate postoperative period. The two patients presenting with cord contusion (ASIA grades C and D) showed no neurological deterioration after surgery; both improved to ASIA Grade D at the three-month follow-up, suggesting gradual neural recovery rather than operative harm.

One patient (Case 6, the only ASIA C patient) had a screw placed in an incorrect trajectory, which was identified on the postoperative radiograph and successfully revised in a second operative sitting with no additional neurological deficit. A second patient (Case 9) demonstrated delayed bony union, with bridging callus ultimately confirmed at the six-month CT. No cases of pseudoarthrosis or screw breakage were observed at final follow-up. There were no

Table 1. Clinical profile of patients.

No.	Age/ Sex	Mechanism	Symptoms	ASIA Grade	Associated Injury	Outcome
1	35/M	RTA	Neck pain, restricted movement	E	None	Excellent — union at 3 months
2	26/M	RTA	Neck pain	E	None	Union at 3 months
3	45/M	Crush injury	Quadriparesis, neck pain	D	C2–C3 cord contusion	Improved to ASIA D→ E at 3 months
4	28/M	Fall from height	Quadriparesis, neck pain, restricted movement	D	None	Improved to ASIA D→ E, union at 3 months
5	22/M	RTA	Neck pain, restricted movement	E	None	Union at 3 months
6	38/F	RTA	Quadriparesis, neck pain	C	C2–C3 cord contusion	Improved ASIA C→D; screw revision required
7	32/M	Fall from height	Neck pain	E	None	Union at 3 months
8	30/F	RTA	Neck pain	E	None	Union at 3 months
9	52/M	RTA	Quadriparesis, neck pain, restricted movement	D	None	Improved to ASIA D→ E, union at 3 months; delayed union at 6 months confirmed
10	20/M	RTA	Neck pain, restricted movement	E	None	Union at 3 months

wound-related complications, postoperative dysphagia, vascular injury, or perioperative mortality.

DISCUSSION

The management of Type II odontoid fractures continues to generate considerable debate. While the superiority of surgical over conservative management in preventing non-union is broadly accepted, the optimal surgical strategy — and the role of technology within it — remains a subject of ongoing discussion[6,7].

In the present series, a 90% fusion rate was achieved, which is consistent with the published range of 87–100% from centres that routinely employ neuronavigation or intraoperative CT guidance[3,8]. Sawarkar and colleagues, reporting from a level-one Indian trauma centre with 142 cases, recorded a fusion rate of 91.2%[9]. The similarity of our outcomes reinforces the premise that, when properly executed, the free-hand technique is not intrinsically inferior to image-guided approaches.

The single screw malposition in our series (10%) resulted in revision surgery without any lasting deficit. This is comparable to re-operation rates reported by Chiba et al. (11%) and Sawarkar et al.[9] (7%), and it underscores that even experienced surgeons operating with advanced technology encounter this complication[9,10]. The key learning from our case was the critical importance of the AP fluoroscopic view confirming midline wire entry — a step that must not be abbreviated regardless of operative time pressures.

Two patients with cord contusion did not demonstrate immediate (within one month) neurological improvement, though both improved to ASIA Grade D by three months. This trajectory of delayed recovery is well recognised in the context of spinal cord contusion and should not be attributed to surgical failure. Platzer and colleagues observed a mortality rate of 9.3% in their elderly cohort, likely reflecting the impact of medical comorbidities; our cohort was younger (mean age 32.8 years) and yielded zero mortality, consistent with the lower operative risk expected in a young demographic[6].

From a technical standpoint, several nuances deserve emphasis. Adequate chin–chest distance and the alignment landmark (nose–sternum–xiphisternum) are indispensable for creating the oblique fluoroscopic window without mandibular interference. The guttering of the C3 superior end plate is often underappreciated but is critical for providing a stable platform for the drill guide, preventing a slip that can precipitate misangulation. Intraoperative reduction of the fracture through controlled neck positioning — rather than through instrument manipulation — achieves alignment without jeopardising the fracture site.

The cost implications cannot be overlooked. Neuronavigation systems represent a capital expenditure that is prohibitive for most district-level hospitals in India. The free-hand technique requires only a standard C-arm, a cannulated screw set, and a radiolucent table — equipment that is widely available even in resource-limited settings. The scalability of this technique therefore carries a significant public health argument in favour of its continued practice and teaching (Table 2).

Table 2. Comparison of outcomes with published literature.

Parameter	Chiba et al. (1996)[10]	Sawarkar et al. (2015)[9]	Platzer et al. (2007)[6]	Present Series
n	90	85	43	10
Male: Female	80:20	89:11	—	80:20
Mean age (years)	38	30	—	32.8
RTA (%)	71.1	69.4	—	70
Bony union (%)	93	91.2	79.1	90
Delayed union (%)	4.4	3.7	—	10
Re-operation (%)	11	7	—	10
Mortality (%)	0	1.1	9.3	0

CONCLUSION

Anterior odontoid screw fixation using the free-hand technique, guided by biplanar C-arm fluoroscopy, is a safe and reproducible surgical option for appropriately selected Type II odontoid fractures. The outcomes in this series are comparable to those reported from technologically advanced centres, affirming that meticulous surgical technique, sound anatomical knowledge, and careful patient selection can together substitute for expensive adjuncts. With growing neurosurgical workloads in resource-constrained environments, continued training in and dissemination of this technique remains both clinically and socioeconomically relevant.

REFERENCES

1. Anderson LD, D'Alonzo RT. Fractures of the odontoid process of the axis. J Bone Joint Surg Am. 1974;56(8):1663-74. https://doi.org/10.2106/00004623-197456080-00017. PMid:4434035.

2. Hadley MN, Browner CM, Liu SS, Sonntag VKH. New subtype of acute odontoid fractures (Type IIA). Neurosurgery. 1989;22(1):67-71. https://doi.org/10.1227/00006123-198801000-00010. PMid:3344089.

3. Fountas KN, Kapsalaki EZ, Karampelas I, et al. Results of long-term follow-up in patients undergoing anterior screw fixation for type II and rostral type III odontoid fractures. Spine. 2005;30(6):661-9. https://doi.org/10.1097/01.brs.0000155415.89974.d3. PMid:15770182.

4. Nakanishi T. Internal fixation of the odontoid fracture. Central Japan Journal of Orthopaedic and Traumatological Surgery. 1980;23:399-406.

5. Böhler J. Anterior stabilization for acute fractures and non-unions of the dens. J Bone Joint Surg Am. 1982;64(1):18-27. https://doi.org/10.2106/00004623-198264010-00004. PMid:7033229.

6. Platzer P, Thalhammer G, Oberleitner G, Schuster R, Vecsei V, Gaebler C. Surgical treatment of dens fractures in elderly patients. J Bone Joint Surg Am. 2007;89(8):1716-22. https://doi.org/10.2106/00004623-200708000-00007. PMid:17671009.

7. Goel A. Treatment of odontoid fractures. Neurol India. 2015;63(1):7-8. https://doi.org/10.4103/0028-3886.152657. PMid:25751462.

8. Moon MS, Moon JL, Sun DH, Moon YW. Treatment of dens fracture in adults: A report of thirty-two cases. Bull Hosp Jt Dis. 2006;63(3–4):108-12. PMid:16878829.

9. Sawarkar D, Singh P, Siddique S, et al. Surgical management of odontoid fracture at a level one trauma center: A single-center surgical series of 142 cases. Neurol India. 2015;63(1):40-8. https://doi.org/10.4103/0028-3886.152633. PMid:25751468.

10. Chiba K, Fujimura Y, Toyama Y, Fujii E, Nakanishi T, Hirabayashi K. Treatment protocol for fractures of the odontoid process. J Spinal Disord. 1996;9(4):267-76. https://doi.org/10.1097/00002517-199608000-00001. PMid:8877952.

CORRESPONDING AUTHOR

Siddharth Vrajesh Jindal, MD
Osmania General Hospital
Department of Neurosurgery
Hyderabad, Telangana, India
E-mail: siddharthjindal345@gmail.com

Funding: *nothing to disclose.*
Conflicts of interest: *nothing to disclose.*
Ethics Committee Approval: *approved by the IEC of Osmania Medical College [ECR/300/Inst/AP/2013/RR-24].*

CRediT

Siddharth Vrajesh Jindal: Data Curation, Writing - Original Draft. Akyam Lakshman Rao: Validation, Formal Analysis. Devi Chendira Pemmaiah: Conceptualization, Methodology. Srikanth Dhadavai: Supervision, Visualization, Writing - Review & Editing. Ambarapu Mastan Reddy: Supervision, Visualization, Writing - Review & Editing.

BioNeuro

Precisão e Tecnologia

FUJI
HEALTH

Inovação, Acurácia e Excelência

Clinical and Pain Outcomes Following Transforaminal Endoscopic Lumbar Discectomy

Resultados Clínicos e de Dor Após Discectomia Lombar Endoscópica Transforaminal

Reinaldo Rodrigues Pamplona[1]
Vinicius Santos Baptista[2]

ABSTRACT

Introduction: *Transforaminal endoscopic lumbar discectomy (TELD) is a minimally invasive treatment for lumbar disc herniation, although Brazilian data remain limited.* **Objective:** *To evaluate pain relief, perioperative morbidity, and clinical outcomes after TELD.* **Methods:** *This retrospective study included 55 adults who underwent TELD at a single Brazilian center between May 2021 and October 2025. Outcomes included Visual Analog Scale (VAS) pain scores, paresthesia, sympathetic changes, epidural hematoma, infection, reoperation, dural sac or nerve root injury, operative time, and estimated blood loss.* **Results:** *Mean age was 49.5 years, and most procedures involved a single level at L4–L5. No dural sac or nerve root injuries occurred. Mean operative time was 97.0 minutes, and mean estimated blood loss was 14.54 mL. Mean VAS score decreased from 9.38 preoperatively to 3.94 postoperatively ($p < 0.0001$). Paresthesia occurred in 14 patients (25.5%) and resolved spontaneously during follow-up. One epidural hematoma occurred without requiring drainage. No infections, sympathetic changes, or reoperations were recorded.* **Conclusion:** *TELD provided significant pain relief with low perioperative morbidity and was a safe, effective minimally invasive treatment for lumbar disc herniation.*

Keywords: *Endoscopic Discectomy; Lumbar Vertebrae; Intervertebral Disc Displacement; Minimally Invasive Surgical Procedures; Pain Management; Treatment Outcome*

RESUMO

Introdução: *A discectomia lombar endoscópica transforaminal (TELD) é uma alternativa minimamente invasiva para hérnia de disco lombar, embora dados brasileiros sejam limitados.* **Objetivo:** *Avaliar o alívio da dor, a morbidade perioperatória e os desfechos clínicos após TELD.* **Métodos:** *Estudo retrospectivo com 55 adultos submetidos à TELD em um centro brasileiro entre maio de 2021 e outubro de 2025. Foram avaliados escores de dor pela Escala Visual Analógica (EVA), parestesia, alterações simpáticas, hematoma epidural, infecção, reoperação, lesão do saco dural ou da raiz nervosa, tempo operatório e perda sanguínea estimada.* **Resultados:** *A idade média foi de 49,5 anos, e a maioria dos procedimentos envolveu um nível em L4–L5. Não ocorreram lesões do saco dural ou da raiz nervosa. O tempo operatório médio foi de 97,0 minutos, e a perda sanguínea média foi de 14,54 mL. A EVA diminuiu de 9,38 para 3,94 ($p < 0,0001$). Parestesia ocorreu em 14 pacientes (25,5%) e regrediu espontaneamente. Houve um hematoma epidural sem necessidade de drenagem. Não ocorreram infecções, alterações simpáticas ou reoperações.* **Conclusão:** *A TELD proporcionou alívio significativo da dor, com baixa morbidade perioperatória*

Palavras-Chave: *Discectomia Endoscópica; Vértebras Lombares; Deslocamento do Disco Intervertebral; Procedimentos Cirúrgicos Minimamente Invasivos; Manejo da Dor; Resultado do Tratamento.*

[1]Instituto do Cérebro, Fundação de Neurologia e Neurocirurgia, Salvador, BA, Brazil.
[2]Department of Neurology and Neurosurgery, Universidade Federal de São Paulo, São Paulo, SP, Brazil

Received Mar 25, 2026
Accepted May 7, 2026

INTRODUCTION

Lumbar disc herniation remains one of the most common causes of lumbosciatica and radicular pain, with substantial impact on physical function, quality of life, and healthcare utilization[1,2]. Although most symptomatic patients improve with nonoperative management, a relevant subgroup continues to experience persistent disabling pain and functional limitation, eventually requiring surgical treatment after failure of conservative measures[1,3].

In parallel with the broader evolution of spine surgery, operative treatment for lumbar disc herniation has progressively shifted from conventional open procedures toward minimally invasive strategies aimed at reducing soft-tissue disruption while preserving decompressive efficacy[4]. Over the last decades, endoscopic lumbar surgery has emerged from earlier percutaneous intradiscal techniques and evolved into a mature therapeutic platform supported by advances in optics, instrumentation, surgical access, and training[5-7]. Among these techniques, transforaminal endoscopic lumbar discectomy (TELD) has become one of the most established full-endoscopic approaches for lumbar disc herniation.

The transforaminal route provides access to the disc through the posterolateral corridor of Kambin's triangle and has been particularly favored for foraminal and extraforaminal herniations, as well as for selected upper lumbar and central/subarticular lesions, depending on anatomy and surgeon experience[8,9]. Potential advantages of TELD include a smaller incision, less paravertebral muscle injury, reduced perioperative morbidity, shorter hospitalization, and, in selected cases, the possibility of surgery under local anesthesia with sedation[7-9]. At the same time, the approach is technically demanding, highly anatomy-dependent, and associated with a learning curve that continues to influence case selection and outcomes[7,9].

Current evidence suggests that TELD provides clinical results comparable to those of conventional microdiscectomy in appropriately selected patients. A systematic review and meta-analysis comparing percutaneous transforaminal endoscopic discectomy with open microdiscectomy found no significant differences in leg pain relief or functional outcomes at intermediate and long-term follow-up[10]. Likewise, comparative studies with 5-year follow-up have demonstrated sustained improvement in pain and function, with potential advantages for endoscopic surgery in hospital stay, recovery profile, and return to daily activities[11,12]. From a safety standpoint, available evidence indicates that full-endoscopic lumbar discectomy has an acceptable complication profile and may even present lower overall complication and dural injury rates in some comparative analyses[13]. However, specific concerns remain relevant, particularly postoperative dysesthesia related to dorsal root ganglion irritation and the possibility of higher revision or reoperation rates in some series and population-based studies[13-15].

Despite the increasing international acceptance of TELD, the published Brazilian experience with the exclusively transforaminal technique remains limited, and additional data from national centers are still valuable to determine whether outcomes observed in the international literature are reproducible in our setting[16]. In this context, the present study aimed to evaluate pain improvement, clinical outcomes, and perioperative morbidity in a Brazilian cohort of patients undergoing transforaminal endoscopic lumbar discectomy for lumbar disc herniation.

METHODOLOGY

Study design and patient selection

This retrospective observational study analyzed patients treated at the Fundação de Neurologia e Neurocirurgia – Instituto do Cérebro. Data were retrospectively extracted from an institutional surgical database including procedures performed between May 2021 and October 2025. Although the present investigation was retrospective, the database had been prospectively populated at the time of surgery as part of routine clinical documentation and secure procedural record keeping, rather than being originally designed for research purposes.

All consecutive patients who underwent transforaminal endoscopic lumbar discectomy (TELD) for lumbar disc herniation during the study period were considered eligible. The only exclusion criterion was age younger than 18 years.

Data collection and follow-up

Demographic and perioperative variables collected for analysis included the total number of patients, sex, age, body mass index (BMI), and operated lumbar levels. All patients were retrospectively

followed for a minimum of 6 months after surgery through standardized institutional postoperative visits scheduled at 1 week, 1 month, and 6 months.

Outcomes

The primary outcomes of interest were postoperative paresthesia, sympathetic alterations, epidural hematoma, infection, reoperation, and pain improvement. Paresthesia was assessed using the Leeds Assessment of Neuropathic Symptoms and Signs (LANSS) scale. Pain improvement was evaluated using the Visual Analog Scale (VAS), based on the comparison between preoperative and postoperative scores.

Secondary outcomes included dural sac injury, nerve root injury, estimated blood loss, and operative time. Injuries to neural structures were defined as any insult involving the dural sac or nerve roots, including inadvertent incision or inappropriate manipulation resulting in intraoperative or postoperative clinical consequences. Operative time was defined as the interval from skin incision to skin closure and was estimated according to recorded operative time intervals. Estimated blood loss was obtained from operative records based on the volume collected in suction devices and the assessment of blood loss absorbed by surgical sponges.

Statistical analysis

Statistical analysis was performed to systematically evaluate the collected data and interpret study outcomes with methodological rigor. Descriptive statistics were calculated for all variables. Continuous variables were summarized as mean and standard deviation or median and interquartile range, as appropriate, whereas categorical variables were expressed as absolute and relative frequencies.

Normality of continuous variables was assessed using the Shapiro–Wilk test. Preoperative and postoperative VAS scores were compared using the paired Student's t test when data were normally distributed and the Wilcoxon signed-rank test otherwise. A two-sided p value of less than 0.05 was considered statistically significant. All confidence intervals were reported at the 95% level. Statistical analyses were performed using R software, version 4.3.1, to ensure reproducibility and analytical accuracy.

RESULTS

A total of 55 patients were included in the study. The mean age was 49.5 years (SD 12.83), with a median of 46 years and an age range from 20 to 72 years. There was a slight predominance of female patients (32 women and 23 men). The mean body mass index was 26.69 kg/m² (SD 4.58) (Table 1).

Most procedures were performed at the lower lumbar levels, with L4–L5 representing the most frequently treated segment. Single-level surgery predominated, accounting for 45 cases, whereas 10 patients underwent two-level procedures; no patient underwent surgery at three or more levels.

No intraoperative nerve root injury or dural sac injury was observed in this series. Mean operative time was 97.0 minutes (SD 45.27), and mean estimated blood loss was low, at 14.54 mL (SD 29.61) (Table 2).

Pain improved significantly after surgery. Mean VAS score decreased from 9.38 (SD 0.56) preoperatively to 3.94 (SD 1.10) postoperatively, corresponding to a statistically significant reduction ($p < 0.0001$) (Table 2).

Regarding postoperative morbidity, paresthesia was the most frequent adverse event, occurring in 14 patients (25.0%). Among these cases, the mean LANSS score was 16.33 (SD 4.11). Importantly, all cases of postoperative paresthesia were transient and resolved spontaneously during follow-up. Sympathetic changes, postoperative infection, and reoperation were not observed. One patient (1.81%) developed epidural hematoma, with an estimated volume of 50 mL; however, no surgical drainage was required. Length of stay was minimal overall, supporting a near-ambulatory postoperative profile in most patients (Table 3).

Table 1. Demographic data.

General characteristics	
Number of Patients, n	55
Mean age, y (SD)	49.50 (12.83)
Age range, y	20 - 72
Median age, y	46
Sex (male/female), n	23 / 32
Mean BMI, kg/m2 (SD)	26.69 (4.58)

Description: BMI = Body Mass Index; SD = Standard Deviation.

Table 2. Intraoperative parameters.

Operated Levels	
L1-L2-L3	1
L2-L3	4
L2-L3-L4	1
L3-L4	4
L4-L5	34
L4-L5-S1	8
L5-S1	3
Number of Operated Levels	**n**
1	45
2	10
3 or more	0
Intraoperative injury	
Nerve root involvement, n (%)	0
Dural sac injury, n (%)	0
Operative time, min (SD)	97.00 (45.27)
Bleeding, mL (SD)	14.54 (29.61)

Description: SD = Standard Deviation.

Table 3. Postoperative parameters.

VAS Scale	
Before surgery, SD	9.38 (0.56)
After surgery, SD	3.94 (1.10)
p-value	< 0.0001
Postoperative complications	**n**
Paresthesia, %	14 (0.25)
Lanss Scale, SD	16.33 (4.11)
Sympathetic changes, %	0
Epidural hematoma, %	1 (1.81)
Infection, %	0
Reoperation, %	0
Length of stay, days (SD)	0.09 (0.68)

Description: VAS = Visual Analog Scale; SD = Standard Deviation. We defined $p < 0.05$ as the threshold for statistical significance.

DISCUSSION

The present study adds to the growing body of evidence supporting transforaminal endoscopic lumbar discectomy as an effective and safe option for selected patients with lumbar disc herniation. In this Brazilian series, TELD was associated with a marked reduction in pain, very low estimated blood loss, minimal length of stay, absence of intraoperative dural or nerve root injury, and low rates of major postoperative morbidity. Taken together, these findings are consistent with the current understanding that the transforaminal endoscopic approach can provide adequate decompression with limited tissue aggression when performed in appropriately selected cases[5-10].

The most relevant clinical finding of the present cohort was the significant improvement in pain, with mean VAS decreasing from 9.38 preoperatively to 3.94 postoperatively. This magnitude of improvement is in line with prior comparative and long-term studies showing that transforaminal endoscopic discectomy achieves pain relief and overall clinical outcomes comparable to those of conventional microdiscectomy or microendoscopic discectomy[10-12]. In particular, the systematic review and meta-analysis by Gadjradj et al. found no significant differences between percutaneous transforaminal endoscopic discectomy and open microdiscectomy in leg pain relief or functional status at intermediate- and long-term follow-up, supporting the interpretation that the endoscopic technique can reproduce the effectiveness of conventional surgery while preserving the advantages of a less invasive access route[10].

Our perioperative findings also reinforce the minimally invasive profile of TELD. Mean estimated blood loss was only 14.54 mL, and postoperative hospital stay was nearly negligible, which is coherent with prior literature highlighting reduced soft-tissue disruption, faster recovery, and shorter hospitalization after endoscopic lumbar discectomy[7-12]. The predominance of lower lumbar surgery, especially at L4-L5, also reflects the expected epidemiological distribution of lumbar disc herniation treated surgically in routine practice[1,2]. From a technical standpoint, the transforaminal route offers a well-established posterolateral corridor and may be particularly attractive because it avoids the extensive posterior muscle dissection and bony removal classically associated with open exposure[8,9].

An important safety finding in the present series was the absence of intraoperative nerve root injury and dural sac injury. This result compares favorably with the available literature and is especially noteworthy because dural injury remains one of the traditional concerns in lumbar discectomy. In the meta-analysis by Yang et al., full-endoscopic lumbar discectomy was associated

with a lower rate of dural injury than open microdiscectomy, suggesting that the magnified visualization and tissue-sparing nature of endoscopic surgery may contribute to reducing some intraoperative complications[13]. Although our sample size does not allow definitive conclusions, the absence of these injuries in the current cohort supports the technical safety of the transforaminal approach in experienced hands.

Postoperative paresthesia was the most frequent complication in our study, occurring in 25% of patients. At first glance, this rate may appear relatively high; however, interpretation should take into account the known relationship between the transforaminal route and transient irritation of the dorsal root ganglion[14]. This pattern has already been well described in the literature. Lewandrowski et al.[14], for example, reported postoperative dysesthesia in 21.5% of patients undergoing lumbar transforaminal endoscopy, with even higher rates in more complex scenarios such as foraminal stenosis and recurrent herniation. Likewise, the meta-analysis by Yang et al.[13] suggested that although full-endoscopic procedures may have lower overall complication rates, they can be associated with a higher frequency of transient dysesthesia and residual symptoms requiring close postoperative observation. In this context, one of the most clinically reassuring aspects of our data is that all cases of paresthesia were transient and resolved spontaneously during follow-up, indicating that these events were self-limited rather than structurally disabling.

The incidence of more serious postoperative events in our cohort was low. Only one patient developed an epidural hematoma, with an estimated volume of 50 mL, and no surgical drainage was required. No cases of infection, sympathetic alteration, or reoperation were observed. These findings are broadly concordant with previous comparative studies showing low infection rates after endoscopic lumbar discectomy and overall acceptable perioperative safety[13,15]. At the same time, caution is warranted when interpreting the absence of reoperation in the present series. Larger database studies have suggested that although endoscopic discectomy may offer favorable short-term morbidity and lower infection rates, reoperation can remain a concern in some settings[15]. Therefore, our zero reoperation rate should be viewed as encouraging but not definitive, particularly given the modest sample size and the relatively limited follow-up window.

Another relevant aspect of the present study is its national contribution. Although TELD is already a consolidated technique in the international literature, published Brazilian data remain limited[16]. In this sense, our findings help expand the local evidence base by showing that the favorable pain and safety outcomes reported internationally can also be reproduced in a Brazilian center. This point is particularly important because real-world outcomes may be influenced by differences in referral patterns, case selection, healthcare organization, perioperative protocols, and the local stage of adoption of endoscopic spine surgery. Rather than presenting TELD as a novel technique, our study supports its reproducibility and feasibility in the national context.

This study has limitations that should be acknowledged. Its retrospective design makes it inherently subject to selection and information bias, and the institutional database was not originally created specifically for research purposes. In addition, the sample was derived from a single center, and there was no control group. Even so, the study also has strengths, including a consecutive real-world cohort, standardized institutional follow-up, and a focused evaluation of the exclusively transforaminal technique.

CONCLUSION

Transforaminal endoscopic lumbar discectomy was associated with significant postoperative pain improvement, minimal blood loss, short hospital stays, and a low rate of major complications in this Brazilian series. No intraoperative dural or nerve root injuries, infections, sympathetic changes, or reoperations were observed. Although postoperative paresthesia was the most frequent adverse event, all cases were transient and resolved spontaneously during follow-up. These findings support TELD as a safe and effective minimally invasive option for the treatment of lumbar disc herniation in appropriately selected patients.

REFERENCES

1. Deyo RA, Mirza SK. Herniated lumbar intervertebral disk. N Engl J Med. 2016;374(18):1763-72. https://doi.org/10.1056/NEJMcp1512658. PMid:27144851.

2. Hincapié CA, Kroismayr D, Hofstetter L, et al. Incidence of and risk factors for lumbar disc herniation with radiculopathy in adults:

a systematic review. Eur Spine J. 2025;34(1):263-94. https://doi.org/10.1007/s00586-024-08528-8. PMid:39453541.

3. Bailey CS, Rasoulinejad P, Taylor D, et al. Surgery versus conservative care for persistent sciatica lasting 4 to 12 months. N Engl J Med. 2020;382(12):1093-102. https://doi.org/10.1056/NEJMoa1912658. PMid:32187469.

4. Momin AA, Steinmetz MP. Evolution of minimally invasive lumbar spine surgery. World Neurosurg. 2020;140:622-6. https://doi.org/10.1016/j.wneu.2020.05.071. PMid:32434014.

5. Heo DH, Kim HS, Whang YH, Lee DC, Lim K. History of endoscopic spine surgery: where did it all begin? Development of indications and techniques. Spine J. 2026;26(3):467-78 https://doi.org/10.1016/j.spinee.2025.07.031. PMid:40653021.

6. Ahn Y. A historical review of endoscopic spinal discectomy. World Neurosurg. 2021;145:591-6. https://doi.org/10.1016/j.wneu.2020.08.008. PMid:32781148.

7. Kwon B, Moon A. Advances in endoscopic lumbar spine surgery: a comprehensive review of the techniques used for the treatment of lumbar disc herniations and spinal stenosis and lumbar spinal fusion. Spine J. 2026;26(3):457-66. https://doi.org/10.1016/j.spinee.2025.06.004. PMid:40578443.

8. Kotheeranurak V, Liawrungrueang W, Quillo-Olvera J, et al. Full-endoscopic lumbar discectomy approach selection: a systematic review and proposed algorithm. Spine. 2023;48(8):534-44. https://doi.org/10.1097/BRS.0000000000004589. PMid:36745468.

9. Ju CI. technical considerations of the transforaminal approach for lumbar disk herniation. World Neurosurg. 2021;145:597-611. https://doi.org/10.1016/j.wneu.2020.08.229. PMid:32916343.

10. Gadjradj PS, Harhangi BS, Amelink J, et al. Percutaneous transforaminal endoscopic discectomy versus open microdiscectomy for lumbar disc herniation: a systematic review and meta-analysis. Spine. 2021;46(8):538-49. https://doi.org/10.1097/BRS.0000000000003843. PMid:33290374.

11. Chen Z, Zhang L, Dong J, et al. Percutaneous transforaminal endoscopic discectomy versus microendoscopic discectomy for lumbar disk herniation: five-year results of a randomized controlled trial. Spine. 2023;48(2):79-88. https://doi.org/10.1097/BRS.0000000000004468. PMid:36083850.

12. Ahn Y, Lee SG, Son S, Keum HJ. Transforaminal endoscopic lumbar discectomy versus open lumbar microdiscectomy: a comparative Cohort Study With a 5-Year Follow-Up. Pain Physician. 2019;22(3):295-304. https://doi.org/10.36076/ppj/2019.22.295. PMid:31151337.

13. Yang CC, Chen CM, Lin MH, et al. Complications of full-endoscopic lumbar discectomy versus open lumbar microdiscectomy: a systematic review and meta-Analysis. World Neurosurg. 2022;168:333-48. https://doi.org/10.1016/j.wneu.2022.06.023. PMid:36527213.

14. Lewandrowski KU, Dowling Á, Calderaro AL, et al. Dysesthesia due to irritation of the dorsal root ganglion following lumbar transforaminal endoscopy: analysis of frequency and contributing factors. Clin Neurol Neurosurg. 2020;197:106073. https://doi.org/10.1016/j.clineuro.2020.106073. PMid:32683194.

15. Kang TW, Park SY, Oh H, Lee SH, Park JH, Suh SW. Risk of reoperation and infection after percutaneous endoscopic lumbar discectomy and open lumbar discectomy: a nationwide population-based study. Bone Joint J. 2021;103-B(8):1392-9. https://doi.org/10.1302/0301-620X.103B8.BJJ-2020-2541.R2. PMid:34334035.

16. Asano LYJ, Bergamaschi JPM, Dowling Á, Rodrigues LMR. Transforaminal endoscopic lumbar discectomy: clinical outcomes and complications. Rev Bras Ortop (Sao Paulo). 2020;55(1):48-53. https://doi.org/10.1055/s-0039-1700822. PMid:32123445.

CORRESPONDING AUTHOR

Vinicius Santos Baptista, MS
Medical student
Universidade Federal de São Paulo
Department of Neurology and Neurosurgery
São Paulo, São Paulo, Brazil
E-mail: vinicius.baptista@unifesp.br

Funding: *nothing to disclose.*
Conflicts of interest: *nothing to disclose.*
Ethics Committee Approval: *approved by the Hospital Geral Roberto Santos – BA Ethics Committee (CAAE: 89685025.7.0000.5028).*

CRediT

Reinaldo Rodrigues Pamplona: Conceptualization, Methodology, Supervision, Writing – Original Draft, Review & Editing. Vinicius Santos Baptista: Investigation, Methodology, Project Administration, Validation, Writing – Original Draft, Review & Editing.

Analysis of Patients with Acute Ischaemic Stroke Treated Via Endovascular Approach

Análise de Pacientes com Acidente Vascular Cerebral Isquêmico Agudo Tratados por Via Endovascular

Leandro José Haas[1]
Rayana Amanda Nazario[1]
André Felipe Kroenke[1]
Carolina Santanielo Vidote[1]
Carolina Schmitt Testoni[1]
Gabriele Babel[1]
Nathalia Wisniewski Setter[1]
Julia Westarb Buss[1]

ABSTRACT

Introduction: *Stroke is one of the leading causes of death and disability worldwide, occurring primarily in middle-aged adults. Among the various types of strokes, ischemic stroke is the most common and recurrent. Therefore, given the high rate of morbidity and mortality, certain risk factors must be considered, in addition to appropriate treatment.* **Objective**: *To quantify the clinical improvement observed in patients diagnosed with ischemic stroke who underwent mechanical thrombectomy at a referral neurosurgery center.* **Methods**: *The study is a retrospective observational study based on an analysis of data from October 2020 to December 2024 in an endovascular neurosurgery unit.* **Results:** *There were 52 patients diagnosed with ischemic stroke who underwent mechanical thrombectomy; the group was equally divided between men and women, ranging in age from 20 to 89 years. Furthermore, a single treatment was sufficient in most cases, and the TICI (Thrombolysis in Cerebral infarction) score was predominantly 3.* **Conclusion**: *Endovascular treatment of patients with ischemic stroke using thrombectomy proved to be effective and resulted in excellent patient outcomes. The TICI scale demonstrated complete recanalization with normal reperfusion of the branches.*

Keywords: *Endovascular; TICI; Ischemic stroke*

RESUMO

Introdução: *O Acidente Vascular Cerebral (AVC) é uma das principais causas de morte e incapacidade no mundo, ocorrendo majoritariamente em adultos de meia-idade. Dentre as diversas classificações, o isquêmico é o mais frequente e mais recorrente. Assim, alguns fatores de risco devem ser levados em consideração, devido à alta taxa de morbimortalidade, além do adequado tratamento.* **Objetivo**: *Quantificar a melhora clínica obtida em pacientes com diagnóstico de AVC isquêmico tratados por trombectomia mecânica em um serviço de referência em neurocirurgia.* **Métodos**: *Trata-se de um estudo observacional retrospectivo baseado na análise de dados no período de outubro de 2020 a dezembro de 2024 em serviço de neurocirurgia endovascular.* **Resultados**: *Houve 52 pacientes com diagnóstico de AVC isquêmico, os quais realizaram o procedimento de trombectomia mecânica, sendo igualmente do sexo feminino e masculino, com idade entre 20-89 anos. Ademais, um único tratamento foi suficiente para a maioria dos casos e com escala TICI (Thrombolysis in Cerebral Ischemia) predominantemente 3.* **Conclusão**: *O tratamento endovascular de pacientes com AVC isquêmico com o uso de trombectomia mostrou uma boa aplicação e ótima evolução dos pacientes. Demonstrando por meio da escala TICI uma recanalização completa com reperfusão normal dos ramos.*

Palavras-Chave: *Endovascular; TICI; Isquêmico*

[1]Universidade Regional de Blumenau - FURB (Medicina), Blumenau, SC, Brazil.

Received Jun 29, 2026
Corrected Jul 23, 2026
Accepted Jul 28, 2026

INTRODUCTION

According to the World Health Organization (WHO), a stroke is characterized as one of the leading causes of death and disability worldwide. This acute episode is diagnosed based on clinical signs caused by spontaneous hemorrhage or infarction in a specific affected area of the brain, spinal cord, or retina, lasting longer than 24 hours or confirmed by imaging tests such as computed tomography (CT)[1]. The condition occurs primarily in the elderly and middle-aged adults[2].

Based on the classification, a stroke can be characterized as ischemic—an alteration in cerebral blood flow due to an arterial blockage—or hemorrhagic—a collection of blood within the brain parenchyma or a subarachnoid hemorrhage. According to this classification, management is carried out in a specific manner, with ischemic stroke being the most prevalent form[3]. Given this, ischemic stroke presents some distinctions among events, considering clinical signs and additional investigations, based on the TOAST classification in the Acute Stroke Treatment (Trial OS 10172) study, which categorizes the event by causes such as atherosclerosis of large arteries (which may be embolic or thrombogenic); small vessel occlusion; cardioembolic events; or stroke of undetermined cause[4].

Recognizing certain risk factors is essential for implementing targeted interventions aimed at reducing the global stroke rate. According to the INTERSTROKE study, certain risk factors were present in most of the stroke cases, such as hypertension, physical inactivity, smoking, and poor diet[5]. Thus, cerebrovascular diseases represent a significant public health concern, as they are associated with high morbidity and mortality rates and high costs for treatment, rehabilitation, and patient follow-up[6]. Consequently, one of the possible treatments for stroke is endovascular, such as mechanical thrombectomy. This is an option when there is proximal occlusion of the anterior portion of arteries, allowing for recanalization of the obstructed site[6].

METHODS

This study is based on a descriptive observational study, involving an analysis of data from a hospital database in the Endovascular Neurosurgery Department at Santa Isabel Hospital in Blumenau, Santa Catarina. This study was approved by the ethics committee of Hospital Santa Isabel, with approval number 31682920.2.0000.5370. The study includes a total of 52 individuals diagnosed with and treated for acute ischemic stroke, analyzed using the TICI (Thrombolysis in Cerebral infarction) scale, from October 2020 through December 2024. The variables used in the study were: gender, age group, comorbidities such as systolic hypertension, diabetes mellitus, dyslipidemia, smoking, previous stroke and/or transient ischemic attack, previous symptoms such as headache, dizziness, nausea, vomiting, psychomotor agitation, aphasia, paresthesia, motor deficit, and altered level of consciousness. Additionally, the location of the stroke, the imaging method used to aid and confirm the diagnosis, the time between the stroke and treatment, and symptoms following the procedure.

The TICI (Thrombolysis in Cerebral infarction) scale is used to classify recanalization following intra-arterial thrombolysis in acute ischemic stroke, such that TICI 0 = no reperfusion/ TICI 1 = minor reperfusion / TICI 2a = partial recanalization with reperfusion < 50% / TICI 2b = partial recanalization with reperfusion > 50% / TICI 3 = complete reperfusion.

RESULTS

The sample consisted of 52 individuals and was characterized by an equal distribution between the sexes (Table 1), with 26 females (N = 26; 50%) and 26 males (N = 26; 50%). The sample was most concentrated in the 50–59 (N = 16; 30.76%) and 60–69 (N = 12; 23.07%) age groups, with the group's mean age being 61.59 years. Regarding comorbidities, most of the study population had at least one comorbidity (N = 44; 84.61%), with the highest prevalence being hypertension (HTN) (N = 34; 77.27%), followed by diabetes mellitus (N = 13; 29.54%) and dyslipidemia (N = 8; 18.18%). Approximately 7% (N = 4) of the patients had a history of previous stroke. Motor deficit was the most common clinical finding (N = 49; 94.23%). This was followed by aphasia (N = 25; 48.07%) and altered level of consciousness (N = 12; 23.07%). The mean Glasgow Coma Scale (GCS) score was 13 points upon arrival at the Emergency Department.

Table 1. Summary of demographic and clinical characteristics.

Characteristics	
Gender	
Female	26 (50%)
Male	26 (50%)
Comorbidities	
Hypertension	34 (77.27%)
Diabetes Mellitus	13 (29.54%)
Dyslipidemia	08 (18.18%)
Smoking	13 (25%)
Previous Stroke	04 (7%)
Previous TIA	01 (1.92%)
Age Group	
20-29 years	01(1.92%)
30-39 years	01(1.92%)
40-49 years	08 (15.32%)
50-59 years	16 (30.76%)
60-69 years	12 (23,07%)
70-79 years	06 (11.53%)
80-89 years	08 (15.32%)
Symptoms	
Headache	02 (3.84%)
Nausea	1 (1.92%)
Vomiting	2 (3.84%)
Anisocoria	2 (3.84%)
Psychomotor agitation	1 (1.92%)
Aphasia	25 (48.07%)
Paresthesia	2 (3.84%)
Motor deficit	49 (94.23%)
Altered level of consciousness	12 (23.07%)

Only 1 patient had cerebral venous thrombosis; the others had strokes of arterial origin (N = 51, 98.07%). The total number of occluded segments was 66, with multiple segments affected in only 18.8% of cases. Regarding the topography of the occlusions (Table 2), it was observed that the most affected territory was the middle cerebral artery (MCA), with N = 42 (63.63%); notably, within the MCA, the M1 segment was the most affected (N = 26; 39.39%). Regarding laterality, the prevalence between the right and left sides occurred with equal frequency (N = 21; 40.38%).

For diagnosis, CT and CT angiography of the extracranial and intracranial vessels were performed upon the patient's admission to the emergency department in all cases (N = 52; 100%).

Of the 52 patients included in the study, 45 (N = 86.5%) underwent mechanical thrombectomy, 3 (N = 28.20%) underwent intra-arterial thrombolysis, and 4 patients (N = 7.69%) underwent intravenous thrombolysis combined with mechanical thrombectomy. Among the patients who underwent mechanical thrombectomy (N = 49), the Solitaire® stent (Medtronic) was used in 6 patients (N = 12.24%) and direct aspiration with the Sofia® aspiration catheter (Microvention) in 46 patients (N = 93.87%).

Of the 52 patients who underwent the procedure, successful recanalization by mechanical thrombectomy (TICI 2b/3) was achieved in 43 patients (N = 82.69%) (Table 3). In addition, the median NIHSS score at the time of the stroke was 19 points, with 12 patients (23.07%) having a score below 16 and 40 patients (76.92%) having a score above 16. Of the 52 patients, most had a door-to-needle time of 3–4 hours (N = 20, 38.46%); furthermore, only 7 patients presented with wake-up stroke (N = 13.46%), making it impossible to determine the exact time between symptom onset and the procedure.

Table 2. Distribution of the topography of occlusions according to laterality.

Segments	Left	Right	No lateralization	Total (n)
Basilar Artery	0	0	4	4
Anterior Cerebral Artery	2	1	0	3
Common Carotid Artery	1	0	0	1
Internal Carotid Artery	6	8	0	14
Middle Cerebral Artery	24	18	0	42
Posterior Cerebral Artery	0	1	0	1
Transverse Sinus	0	0	1	1
Total	33	28	5	66

Source: Hospital Santa Isabel, Department of Neurosurgery, 2024.

Table 3. Outcome of vascular recanalization, as measured by the TICI scale.

	TICI 0	TICI 1	TICI 2A	TICI 2B	TICI 3	Total (n)
Intra-arterial fibrinolysis	0	0	0	2	1	3
Intravenous fibrinolysis + anterior circulation AC thrombectomy	0	0	2	2	0	4
Thrombectomy SS	1	0	0	0	1	2
SS Thrombectomy + Pre-treatment	0	0	0	0	1	1
SS Thrombectomy + AC Thrombectomy	0	1	0	0	2	3
AC Thrombectomy	3	0	2	6	26	37
AC Thrombectomy + Pre-treatment	0	0	0	1	1	2
TOTAL	4	1	4	11	32	52

Source: Hospital Santa Isabel, Department of Neurosurgery, 2024.

DISCUSSION

In the present study, 52 cases of patients with ischemic stroke were analyzed. The sample consisted of an equal number of female and male individuals, with each group accounting for 50% of the cases, which is consistent with data from the literature. Regenhardt et al.[7] found a similar proportion, with 52% of patients being female. In contrast, data from the study by Ohya et al. indicated a higher prevalence among males (58%)[8]. The mean age of the sample was 61.59 years. This value is slightly lower than that observed in other publications, in which the mean age ranged from 68 to 73.5 years[7].

Regarding comorbidities in patients with ischemic stroke, the present study identified a predominance of hypertension (77.27%), followed by diabetes mellitus (29.54%) and dyslipidemia (18.18%). The observational study with multicenter data by Ohya et al. presented similar findings, in which HTN was the most prevalent risk factor across all age groups (58–81%), followed by dyslipidemia (48–52%) and DM (23–32%)[8]. The same study demonstrated that, particularly in the under-50 age group, lifestyle factors (smoking, alcohol abuse, and obesity) play an important role in the risk of ischemic stroke, with 25% of patients in the present study being smokers.

In addition, 7% of the patients in this study had a history of stroke, indicating a lower recurrence rate than that observed in a meta-analysis on recurrent stroke, in which rates ranged from 12% to 14%[9]. This discrepancy can be explained by the difference in the patients' age range between the studies: while the predominant age group in the present study was 50 to 59 years, in the studies included in the meta-analysis it ranged from 62 to 75 years. With advancing age, there is a natural increase in the probability of recurrent ischemic events.

High NIHSS scores are associated with worse functional outcomes and higher risks of dependency. However, these patients tend to benefit from mechanical thrombectomy, as demonstrated in the clinical trial by Martins et al.[10], which showed a higher probability of recanalization and significant functional recovery at 90 days post-procedure. Regarding initial clinical severity, it was observed that most patients in the present study had NIHSS scores above 16 points. This finding is consistent with the data from the aforementioned trial, which predominantly included patients with high NIHSS scores, with a median of 18 points, very close to the median observed in our sample (19 points). Thus, the NIHSS serves as a marker of severity and as a tool for the selection and rapid management of patients who benefit most from mechanical thrombectomy.

For diagnosis, extracranial and intracranial CT and CT angiography were used upon the patient's admission to the department. The prospective study by Powers et al. demonstrated a higher use of cranial CT (63%), followed by cranial MRI (33%) and cranial CT angiography (16.5%). The study, however, considered only the initial radiographic examination prior to endovascular treatment, excluding arteriography, which is performed at the time of the intervention itself[3].

Regarding the location of the arterial occlusion, the study demonstrated a higher incidence of middle cerebral artery (MCA) occlusion (64%), predominantly in the M1 territory (50%), followed by the anterior cerebral artery (ACA) (20%).

The study by Regenhardt et al.[7] showed consistent findings, with 66% of patients presenting ACM-M1 occlusion and 19% presenting ACI occlusion.

The success of endovascular treatment for ischemic stroke is measured using the TICI (Thrombolysis in Cerebral infarction) classification, which assesses the therapeutic response based on the degree of recanalization of the affected vessel, ranging from TICI 0 (no recanalization) to TICI 3 (complete recanalization). In the present study, TICI scores were obtained for 57 patients, of whom 94.73% had a satisfactory response (TICI 2b to 3). A similar finding was observed in a study by Regenhardt et al.[7], based on data from Massachusetts General Hospital in the United States, in which 84% of patients undergoing endovascular treatment achieved satisfactory recanalization.

CONCLUSION

Ischemic stroke, when properly assessed and diagnosed correctly and in a timely manner, has a good prognosis. In the present study, thrombectomy treatment proved effective, with most patients classified on the TICI scale as having complete recanalization and normal reperfusion of distal branches. Among these patients, a second procedure was not necessary, with only one AC thrombectomy treatment required. Given this, this study demonstrated the success of the procedures performed, with good clinical outcomes and low rates of post-treatment complications. However, further studies are needed to provide in-depth follow-up for the long-term analysis of patients treated with thrombectomy.

REFERENCES

1. Protocolo Clínico e Diretrizes Terapêuticas do Acidente Vascular Cerebral Isquêmico Agudo [Internet]. Available from: https://www.gov.br/conitec/pt-br/midias/consultas/relatorios/2021/20211230_relatorio_recomendacao_avci_agu do_cp110.pdf. Accessed: 4/12/2024.

2. Naghavi M, Abajobir AA, Abbafati C, et al. Global, regional, and national age-sex specific mortality for 264 causes of death, 1980-2016: a systematic analysis for the Global Burden of Disease Study 2016. Lancet. 2017;390(10100):1151-210. https://doi.org/10.1016/S0140-6736(17)32152-9. PMid:28919116.

3. Powers WJ, Rabinstein AA, Ackerson T, et al. Guidelines for the Early Management of Patients With Acute Ischemic Stroke: A Guideline for Healthcare Professionals From the American Heart Association/American Stroke Association. Stroke. 2018;49(3):e46-110. https://doi.org/10.1161/STR.0000000000000158. PMid:29367334.

4. Pazuello GB. Trombectomia para tratamento do acidente vascular cerebral isquêmico agudo causado por oclusões do segmento m2 da artéria cerebral média [dissertation]. Ribeirão Preto: Faculdade de Medicina de Ribeirão Preto, University of São Paulo; 2019. https://doi.org/10.11606/D.17.2020.tde-18082020-215725.

5. O'Donnell MJ, Xavier D, Liu L, et al. Risk factors for ischaemic and intracerebral haemorrhagic stroke in 22 countries (the INTERSTROKE study): a case-control study. Lancet. 2010;376(9735):112-23. https://doi.org/10.1016/S0140-6736(10)60834-3. PMid:20561675.

6. Alves AESR, Cese BC, Reyna CFO, et al. Trombectomia mecânica no acidente vascular cerebral isquêmico agudo: revisão de literatura. Arq Med Hosp Fac Cienc Med St Casa S Paulo. 2018;63(2):110-4. https://doi.org/10.26432/1809-3019.2018.63.2.110.

7. Regenhardt RW, Bonkhoff AK, Bretzner M, et al. Association of infarct topography and outcome after endovascular thrombectomy in patients with acute ischemic stroke. Neurology. 2022;98(11):e1094-103. https://doi.org/10.1212/WNL.0000000000200034. PMid:35101908.

8. Ohya Y, Matsuo R, Sato N, et al. Causes of ischemic stroke in young adults versus non-young adults: a multicenter hospital-based observational study. PLoS One. 2022;17(7):e0268481. https://doi.org/10.1371/journal.pone.0268481. PMid:35830430.

9. Kolmos M, Christoffersen L, Kruuse C. Recurrent ischemic stroke - a systematic review and meta-analysis. J Stroke Cerebrovasc Dis. 2021;30(8):105935. https://doi.org/10.1016/j.jstrokecerebrovasdis.2021.105935. PMid:34153594.

10. Martins SO, Schochat C, Carvalho JJF, et al. Thrombectomy for stroke in the public health care system of Brazil. N Engl J Med. 2020;382(24):2316-26. https://doi.org/10.1056/NEJMoa2000120. PMid:32521133.

CORRESPONDING AUTHOR

André Felipe Kroenke, MS
Universidade Regional de Blumenau - FURB (Medicina)
Blumenau, Santa Catarina, Brazil
E-mail: kandrefk@gmail.com

Funding: *nothing to disclose.*
Conflicts of interest: *nothing to disclose.*
Ethics Committee Approval: *Ethics Committee of Hospital Santa Isabel, under number 31682920.2.0000.5370.*

CRediT

Leandro José Haas: Conceptualization, Methodology, Investigation, Supervision, Project administration, Writing - Original Draft, Writing - Review & Editing. Rayana Amanda Nazario: Investigation, Writing - Original Draft, Writing - Review & Editing. André Felipe Kroenke: Writing - Review & Editing. Carolina Santanielo Vidote: Investigation, Validation, Writing - Review & Editing. Carolina Schmitt Testoni: Investigation, Validation, Writing - Review & Editing. Gabriele Babel: Data Curation, Visualization, Writing - Review & Editing. Nathalia Wisniewski Setter: Data Curation, Formal analysis, Writing - Review & Editing. Julia Westarb Buss: Supervision, Validation, Writing - Review & Editing.


PDT
Responsável Técnico
Dr. André Giacomelli Leal
CRM-PR 21874
O Hospital INC foi pioneiro nas Américas ao utilizar a Terapia Fotodinâmica Intraoperatória (PDT) – LASER que destroi células tumorais cerebrais.
INC
HIGH·TECH
Hospital INC:
pioneiro em
novas tecnologias
hospitalinc.com.br
Sede Hospital INC | Rua Jeremias Maciel Perretto, 300
Campo Comprido | Curitiba/PR | CEP 81210-310 | Fone 41 3028.8545
Filiais Pátio Batel, Eurobusiness & Jockey Plaza
HOSPITAL
INC
INSTITUTO DE
NEUROLOGIA
DE CURITIBA

3D Bioprinting Applied to Neurosurgery: a scoping review and systematic review of preclinical evidence

Bioimpressão 3D Aplicada à Neurocirurgia: revisão de escopo e revisão sistemática da evidência pré-clínica

Mhaedra Comin Galvan[1]
Lorena Maria Dering[2]
André Giacomelli Leal[3]

ABSTRACT

Three-dimensional bioprinting enables the controlled deposition of cells, biomaterials, and bioactive molecules and has potential applications in central nervous system (CNS) modeling and repair. This study mapped CNS applications of 3D bioprinting and synthesized preclinical evidence on cell-laden constructs produced by direct bioprinting. A two-stage review was conducted, comprising a scoping review reported in accordance with PRISMA-ScR and a systematic review reported in accordance with PRISMA 2020. Searches of PubMed, Scopus, and Web of Science identified 445 records. Sixty studies were included: 25 reviews or technical syntheses, 17 in vitro or methodological studies, and 18 in vivo studies. Of these, 49 remained exclusive to the scoping review, and 11 met the systematic review criteria. Spinal cord injury accounted for 14 of the 18 in vivo studies. Among the 11 systematically reviewed studies, GelMA was used in seven constructs, and neural stem cells were the most frequent cell population. Of 110 SYRCLE risk-of-bias judgments, 98 were classified as unclear risk, 11 as low risk, and one as high risk. Three-dimensional bioprinting showed regenerative potential, but methodological heterogeneity and predominantly unclear judgments continue to limit clinical translation.

Keywords: *3D bioprinting; Central nervous system; Spinal cord injury; Neural tissue engineering; Regenerative medicine; Neurosurgery*

RESUMO

A bioimpressão tridimensional permite a deposição controlada de células, biomateriais e moléculas bioativas e apresenta aplicações potenciais na modelagem e no reparo do sistema nervoso central (SNC). Este estudo mapeou as aplicações da bioimpressão 3D no SNC e sintetizou as evidências pré-clínicas sobre construtos celularizados produzidos por bioimpressão direta. Foi realizada uma revisão em duas etapas, compreendendo uma revisão de escopo conforme o PRISMA-ScR e uma revisão sistemática conforme o PRISMA 2020. As buscas no PubMed, Scopus e Web of Science identificaram 445 registros. Foram incluídos 60 estudos: 25 revisões ou sínteses técnicas, 17 estudos in vitro ou metodológicos e 18 estudos in vivo. Destes, 49 permaneceram exclusivamente na revisão de escopo e 11 preencheram os critérios da revisão sistemática. A lesão medular representou 14 dos 18 estudos in vivo. Entre os 11 estudos incluídos na revisão sistemática, GelMA foi utilizado em sete construtos, e células-tronco neurais foram a população mais frequente. Dos 110 julgamentos de risco de viés pelo SYRCLE, 98 foram classificados como risco incerto, 11 como baixo risco e um como alto risco. A bioimpressão 3D demonstrou potencial regenerativo, mas a heterogeneidade metodológica e o predomínio de julgamentos incertos ainda limitam a translação clínica.

Palavras-Chave: *Bioimpressão 3D; Sistema nervoso central; Lesão medular; Engenharia de tecidos neurais; Medicina regenerativa; Neurocirurgia*

[1]Universidade Positivo, Curitiba, PR, Brazil.
[2]INC 3D, Instituto de Neurologia de Curitiba – INC, Curitiba, PR, Brazil.
[3]Department of Neurosurgery, Instituto de Neurologia de Curitiba – INC, Curitiba, PR, Brazil.

Received Aug 3, 2026
Accepted Aug 16, 2026

INTRODUCTION

Regeneration of the central nervous system (CNS) is constrained by its low intrinsic repair capacity and by an inhibitory microenvironment characterized by glial scarring, extracellular matrix disorganization, and myelin-associated molecules that restrict axonal growth[1]. Three-dimensional (3D) bioprinting has therefore been investigated as a means of filling tissue defects, organizing biological components, and supporting neural repair.

Three-dimensional bioprinting enables the controlled deposition of cells, biomaterials, and bioactive molecules in predefined architectures[2]. Unlike isolated cell administration, which is limited by poor retention, dispersion, and reduced survival, cell-laden constructs provide mechanical support, biochemical signals, and topographical cues[3]. They may therefore reproduce relevant cell–matrix interactions and serve regenerative, disease-modeling, and drug-screening applications[4,5].

Construct performance depends on the interaction among bioink composition, cell population, architecture, and manufacturing technique. Neural bioinks must balance printability, biocompatibility, mechanical stability, degradation, and cell viability while supporting differentiation and axonal growth[6,7]. Common matrices include GelMA, alginate, hyaluronic acid, collagen, and decellularized extracellular matrix, sometimes combined with bioactive or electroconductive components[8]. These variables jointly determine whether a construct can be fabricated reproducibly while maintaining a permissive microenvironment after implantation.

Applications range from in vitro neural and disease models to implantable constructs. Spinal cord injury predominates in vivo, likely because tissue cavities and longitudinal anatomy permit the use of aligned fibers and microchannels to bridge the lesion[9]. Traumatic brain injury, other brain injuries, and neurodegenerative conditions remain less represented[10]. Reproducing regional brain architecture and distributed connectivity is also more difficult than guiding growth along a longitudinal tract.

The literature nevertheless combines reviews, methodological and in vitro studies, acellular printed scaffolds, and constructs directly bioprinted with living cells, with substantial variation in materials, models, comparators, follow-up, and outcomes[11].

To delineate this heterogeneous field, we first mapped CNS bioprinting technologies, biomaterials and bioinks, models, and applications through a scoping review. We then systematically reviewed preclinical in vivo studies using direct cell-laden bioprinting to repair structural CNS injuries and synthesized their biological and functional outcomes and translational limitations.

MATERIAL AND METHODS

A two-stage review was conducted. The scoping review followed the PRISMA Extension for Scoping Reviews (PRISMA-ScR)[12] and mapped 3D bioprinting and construct fabrication for CNS applications. The systematic review was conducted and reported in accordance with PRISMA 2020[13].

PubMed, Scopus, and Web of Science were searched in February 2026 without date or language restrictions. Database-specific strategies combined terms for bioprinting; neural regeneration or nervous system injury; and tissue engineering or biofabrication, including bioink, cell viability, and cell differentiation. Searches were adapted to the indexing and syntax of each database to capture both bioprinting-specific and broader neural tissue-engineering terminology.

The search identified 445 records (PubMed, 112; Scopus, 228; Web of Science, 105). After 184 duplicates were removed, 261 records underwent title and abstract screening, and 157 were excluded. Of 104 full texts sought, eight could not be retrieved, and 96 were assessed for eligibility.

The scoping review included primary in vitro, preclinical in vivo, methodological, review, and technical-perspective publications in which 3D bioprinting, scaffold printing, a bioink, or a 3D construct was central to the objective, method, intervention, or technical discussion and was explicitly applied to neural cells or tissues, brain or spinal cord injury, or CNS tissue engineering. Contextual publications were retained only when they mapped an otherwise underrepresented CNS application. This broad framework was selected to characterize different stages of technological development rather than restrict the mapping to implantation studies.

The systematic review included only primary in vivo studies addressing repair of a structural CNS injury through direct cell-laden bioprinting, defined as the presence of living cells in the bioink during fabrication. Reviews, exclusively in vitro studies, scaffolds seeded after printing, constructs carrying only drugs, factors, exosomes, or extracellular vesicles, and neurodegenerative models without structural injury were excluded. The scoping review additionally excluded predominantly peripheral nervous system studies, incidental mentions of printing, generic biomaterials without an explicit CNS application, and publications lacking extractable technical content. Full texts available only in a language not understood by the reviewer were excluded when a reliable translation could not be obtained to confirm eligibility and extract data.

Sixty studies formed the scoping corpus; 11 met the systematic-review criteria, and 49 remained exclusive to the scoping review. Screening, full-text assessment, and extraction were performed by one reviewer using a standardized matrix covering study type, technique, biomaterial or bioink, cells, model, comparators, animal numbers, follow-up, application, and biological and functional outcomes.

One reviewer assessed risk of bias in the 11 preclinical studies using the 10 original SYRCLE domains[14]: sequence generation, baseline characteristics, allocation concealment, random housing, blinding of caregivers and investigators, random outcome assessment, blinding of outcome assessors, incomplete outcome data, selective reporting, and other sources of bias. Each domain was judged as low, high, or unclear risk from the articles and available supplements; insufficient reporting was classified as unclear. No overall score was assigned. Judgments were displayed with robvis[15]. Findings were synthesized narratively, and meta-analysis was not undertaken because of heterogeneity in designs, materials, models, cells, follow-up periods, and outcomes (Figure 1).

RESULTS

Scoping review results

The scoping review included 60 studies: 25 reviews or technical syntheses, 17 primary in vitro or methodological studies, and 18 preclinical in vivo studies. Eleven in vivo studies met the systematic review criteria; the remaining 49 publications contributed only to the scoping review.

The mapped literature covered in vitro neural models, disease modeling, drug screening, biomaterial and manufacturing assessment, and preclinical tissue repair. Spinal cord injury dominated in vivo applications, whereas brain, traumatic brain injury, and neurodegenerative models were less frequent[16-29].

Frequently investigated materials included GelMA, alginate, hyaluronic acid, collagen, chitosan, fibrin, and decellularized extracellular matrix, alone or combined with conductive components, nanomaterials, growth factors, drugs, exosomes, or extracellular vesicles. Cell populations included neural stem and progenitor cells, iPSC-derived cells, mesenchymal cells, astrocytes, Schwann cells, and PC12 cells[30,31].

Extrusion-based bioprinting predominated, including microextrusion, coaxial, multimaterial, and embedded approaches. Stereolithography, digital light processing (DLP), laser-assisted bioprinting, inkjet printing, fused deposition modeling (FDM), and 4D printing were also reported. Table 1 summarizes the corpus by biomaterials and functional properties, neural models, manufacturing and spatial organization, and preclinical applications.

Biomaterials, decellularized matrices, and electroconductivity

Formulations ranged from conventional hydrogels to multifunctional matrices intended to reproduce biochemical, mechanical, or electrical properties of neural tissue. GelMA, alginate, and hyaluronic acid were used alone or with collagen, fibrin, chitosan, or tissue-derived components. Decellularized spinal cord matrix preserved neural biochemical cues and showed cellular compatibility and neural phenotype-associated protein expression, supporting its feasibility as a bioink component[32].

Electroconductive strategies incorporated gold nanorods, conductive polymers, or graphene derivatives and were assessed for conductivity, mechanics, cell viability, and neural differentiation[7,33]. Direct comparison remained inappropriate because composition, concentration, and crosslinking differed among formulations.

Neural models and in vitro applications

Seventeen studies developed in vitro neural models or examined methodological aspects of bioprinting. Platforms included neurospheroid–astrocyte co-cultures, spatially organized neural and glial tissues, and constructs containing neural stem or progenitor cells, iPSC-derived cells, Schwann cells, astrocytes, or PC12 cells in collagen, fibrin, GelMA, and other hydrogels.

Table 1. Categorical mapping of technologies, materials, and applications identified in the scoping review (n = 60).

Mapping Category	Technological and Biological Elements Identified in the Corpus
Biomaterials and Natural Matrices	Gelatin methacryloyl (GelMA), alginate (including alginate dialdehyde - ADA), hyaluronic acid (HA and HAMA), collagen (type I and NorCol), chitosan, fibrin, and decellularized spinal cord extracellular matrix (DSCT).
Additives, Drugs, and Smart Materials	Conductive polymers (PEDOT:CSMA, PEDOT:PSS), graphene derivatives, gold nanorods (GNRs), thermoresponsive hydrogels (polyurethane - PU2), OSMI-4 delivery, isoliquiritigenin (ISL), and extracellular vesicles/exosomes (plant-, MSC-, and NSC-derived).
Cell Populations	**Stem cells:** NSCs (neural), MSCs (bone marrow, umbilical cord), iPSCs (induced pluripotent), and hDPSCs (dental pulp). **Somatic/tumor cells:** Schwann cells, GSCs (glioblastoma stem cells), astrocytes, macrophages, and endothelial cells.
In Vitro Applications and Models	Construction of functional 3D neural networks (demonstrated by calcium imaging), biomimetic brain organoids for Alzheimer's and Parkinson's diseases, vascularized tumor microenvironments (glioblastoma for chemotherapeutic screening), and blood-brain barrier models (BBB-on-a-chip).
Translational In Vivo Applications	**Primary focus:** complete and hemisection spinal cord injury (SCI) and traumatic brain injury (TBI). **Secondary scoping-review applications:** experimental models of neurodegenerative disease (dementia/Alzheimer's disease) and ischemic stroke.
Bioprinting Technologies	**Nozzle-based:** conventional extrusion, microextrusion, and coaxial extrusion (multimaterial). **Light-/photochemistry-based:** digital light processing (DLP) and stereolithography (SLA). **Other:** inkjet (acoustic/thermal droplet printing), laser-assisted bioprinting (LAB), fused deposition modeling (FDM), and transition to 4D printing.

Outcomes focused on printability, mechanics, viability, differentiation, and cellular organization[4,6,34-37].

Other studies tested how bioink composition, layered or multimaterial architecture, and microchannels influenced neuronal differentiation[38-40]. The mapping also identified neurodegenerative-disease and organoid models, drug-screening systems, and constructs reproducing elements of the glioblastoma microenvironment[41-46]. These applications broadened the field beyond regeneration but addressed outcomes distinct from those of implantable preclinical constructs.

Manufacturing techniques and spatial organization

Extrusion was chiefly used for macroscopic scaffolds containing longitudinal fibers or channels; some constructs incorporated microchannels of approximately 150–300 μm to guide cellular organization and growth. Light-based approaches enabled smaller-scale fabrication, although use of such a technique did not by itself satisfy the systematic-review definition.

Qian et al.[47] fabricated hDPSC-containing GelMA microspheres by DLP, but the platform was developed and evaluated primarily for dental pulp regeneration, with spinal cord repair as a secondary application. Lee et al.[48] and Zhou et al.[49] produced scaffolds by stereolithography and seeded cells after fabrication. These studies remained in the scoping review because they did not use direct cell-laden bioprinting as defined for the systematic review.

Preclinical in vivo applications

Fourteen of the 18 in vivo studies used spinal cord injury models; the remainder addressed traumatic brain injury or experimental neurodegenerative conditions. Models varied in lesion type, anatomical level, implant, and follow-up. Interventions included cell-laden constructs, acellular scaffolds carrying bioactive agents, extracellular-vesicle delivery systems, and scaffolds seeded after printing. Ischemic stroke appeared only in a synthesis publication.

Among the seven in vivo studies retained only in the scoping review, four used acellular constructs containing oxymatrine, plant-derived exosomes with isoliquiritigenin, extracellular vesicles, or signals intended to recruit endogenous neural stem cells[10,50-52]. One combined a printed collagen/heparan sulfate and growth-factor scaffold with mesenchymal cells added after printing[53]. The other two evaluated a brain-like transplant in an Alzheimer-like model and the predominantly dental-regeneration platform noted above[47,54].

The remaining 11 studies incorporated living cells into the bioink during fabrication and evaluated the constructs in vivo for structural CNS repair; these formed the systematic review.

Systematic review results

The systematic review included 10 rat spinal cord injury studies and one zebrafish study of embryonic neural injury and traumatic cerebellar injury. Complete thoracic transection predominated in rats, with defects of 3–10 mm; one study used hemisection. Follow-up ranged from four to 12 weeks in rodents and was eight days in adult zebrafish.

Extrusion and its conventional, microextrusion, coaxial, multimaterial, multicellular spatial printing, and nanoengineered extrusion-aligned tract (NEAT) variants predominated. One custom platform used FDM to deposit thermoresponsive polyurethane containing neural stem cells.

GelMA was present in seven of the 11 studies, alone or with hyaluronic acid, PEGDA, β-cyclodextrin, bioactive peptides, or other components. Neural stem cells were the most frequent population; other constructs used mesenchymal, ectodermal mesenchymal, bone marrow-derived mesenchymal, or Schwann cells.

Species, lesion severity, bioink, technique, cells, comparators, and follow-up varied substantially. Randomization and blinding were reported only in a subset, and no main article reported a prospective sample-size calculation. Tables 2 and 3 present the methodological characteristics and outcomes.

Table 2. Methodological characteristics of studies included in the systematic review.

Study	Model, Groups, and Follow-up	Technique and Bioink	Cells
Cao et al. (2025)[9]	Male SD rats; 3-mm complete transection at T10; 5 groups, n = 8/group; 8 weeks.	Extrusion-based multimaterial bioprinting; GelMA with regionally distributed factors.	EMSCs
Hsieh et al. (2015)[55]	Zebrafish; ethanol-induced embryonic neural injury and traumatic cerebellar injury in adults; 3 adult groups, n = 11/group; 8 days.	FDM (fused deposition manufacturing) on a custom platform; thermoresponsive polyurethane hydrogel (PU2 at 25-30%).	NSCs
Huang et al. (2026)[2]	SD rats; 4-mm complete T9-T10 transection; sham, SCI, nonaligned NorCol, and aligned NorCol; n = 8/group; 8 weeks.	Extrusion-based NEAT; NorCol.	hNSCs
Jiu et al. (2025)[11]	Female SD rats; 3-mm complete thoracic transection at T10; sham, SCI, scaffold, and MRSCC; n = 36 (9/group); 4 weeks.	Extrusion; GelMA with gelatin microcarriers.	MSCs
Li et al. (2025)[56]	SD rats; T9-T11 laminectomy with complete 3- and 10-mm defects; no implant, microfibers, and microfibers + exosomes; 4 weeks (small defect) and 8 weeks (large defect).	Coaxial extrusion; OHA-CMC-Matrigel core and 3% alginate sheath.	NSCs; ucMSC-exos as an adjuvant
Liu et al. (2021)[5]	Female SD rats; 4-mm complete transection at T8-T9; no implant, acellular scaffold, and NSC-containing scaffold; n = 8/group; 12 weeks.	Single-step extrusion; functionalized chitosan/hyaluronic acid/Matrigel.	NSCs
Liu et al. (2022)[57]	Female SD rats; T7-T10 laminectomy with 4-mm transection at T8-T9; control, NSC scaffold, and NSC + OSMI-4 scaffold; n = 6/group; 8 weeks.	Extrusion; GelMA/β-cyclodextrin with OSMI-4 delivery.	NSCs
Song et al. (2023)[58]	Female SD rats; 4-mm complete T8-T9 transection; control, GP scaffold, and conductive GPP-TA scaffold; n = 5/group; 8 weeks.	Microextrusion; GelMA/PEGDA/PEDOT:CSMA,TA.	NSCs
Wang et al. (2021)[3]	Female SD rats; hemisection between T10 and T11; sham, control, acellular scaffold, cell-containing hydrogel, and printed scaffold; n = 6/group; 4 weeks.	Multicellular spatial printing; GelMA/LAP.	BMSCs and Schwann cells
Yang et al. (2023)[59]	Female SD rats; 4-mm complete T9-T10 transection; SCI, acellular scaffold, and NSC-containing scaffold; n = 72 (24/group); 12 weeks.	Neural-fiber extrusion; GelMA/HAMA.	NSCs
Yang et al. (2025)[8]	Female SD rats; 4-mm complete T9-T10 transection; control, acellular GHP, and GHP@NSC; n = 90 (30/group); 12 weeks.	Extrusion; GelMA/OHA with HAVDI and RGI peptides.	NSCs

Abbreviations: BMSC, bone marrow-derived mesenchymal stem cell; EMSC, ectodermal mesenchymal stem cell; GelMA, gelatin methacryloyl; HAMA, hyaluronic acid methacrylate; hNSC, human neural stem cell; MSC, mesenchymal stem cell; NEAT, nanoengineered extrusion-aligned tract; NSC, neural stem cell; OHA, oxidized hyaluronic acid; PEGDA, polyethylene glycol diacrylate; SCI, spinal cord injury; ucMSC-exos, umbilical cord mesenchymal stem cell-derived exosomes.

Table 3. Main outcomes of studies included in the systematic review.

Study	Main Biological Findings	Functional Outcome
Cao et al. (2025)[9]	Tuj-1 density of 16 ± 3 neurites/mm², GFAP 7 ± 3%, GAP43 ~40%, and nestin ~35%, with improved tissue preservation and regeneration.	BBB 13.5 ± 1.2, with improvement in inclined-plane and open-field tests.
Hsieh et al. (2015)[55]	Greater viability and neural differentiation with PU2; construct integration and neurogenesis in the adult model.	Improved swimming speed; BBB not applicable.
Huang et al. (2026)[2]	Greater axonal alignment, neuronal differentiation, graft retention, synaptic markers, and vascularization; reduced glial reactivity.	Improved BBB score from week 3 and improved gait; approximate final score of 9.
Jiu et al. (2025)[11]	Increased MAP-2 and MBP, marked reductions in GFAP and MMP13, and findings consistent with neuronal regeneration and myelination.	Improved BBB score, approximately 8-9, and improved sensory threshold relative to injured controls.
Li et al. (2025)[56]	Higher Tuj-1 (~14%), Olig2 (~13%), and angiogenesis (CD31+). A more favorable inflammatory profile (reduced IL-6 and TNF-α) in the exosome-combination group.	Better BBB, open-field, swimming, and electromyography outcomes in smaller defects; structural tissue fusion in the 10-mm defect.
Liu et al. (2021)[5]	Greater neuronal differentiation and axonal regeneration, reduced glial scar deposition, and graft survival.	BBB 7.4 ± 0.5; improved joint movement and hindlimb strength.
Liu et al. (2022)[57]	Greater neuronal differentiation (14 ± 4%), GAP43 expression, and axonal growth; reduced astrocytic differentiation (GFAP 4 ± 2%) and inflammation.	BBB 7.5 ± 0.8 in the OSMI-4 group versus 5.3 ± 0.5 in the drug-free scaffold group.
Song et al. (2023)[58]	Tuj-1: 17.4 ± 3.7%; GFAP: 4.3 ± 0.4%; organized NF200 fibers (~30.5%) and greater myelination.	BBB 6.8 ± 0.4; improved inclined-plane test performance.
Wang et al. (2021)[3]	Directed differentiation, myelinated fibers, nodes of Ranvier, and improved anatomical tissue organization.	Greater locomotor recovery with the printed scaffold; peak BBB recovery reached 17-18.
Yang et al. (2023)[59]	NF+ 20.75 ± 3.9%; 20,225 ± 2,747 nerve fibers/mm² and a g-ratio of 0.42; axonal regeneration, angiogenesis, immune modulation, and myelination.	Median BBB = 9; improved gait, climbing, and evoked potentials.
Yang et al. (2025)[8]	Increased Tuj-1 (~30%), NF (~30%), and MBP (~75%); reduced GFAP/CS-56; revascularization and tract reconstruction.	Improved BBB, gait, sensitivity, and evoked potentials; approximate final score of 10.

Abbreviations: BBB, Basso-Beattie-Bresnahan; CD31, cluster of differentiation 31; GAP43, growth-associated protein 43; GFAP, glial fibrillary acidic protein; MAP2, microtubule-associated protein 2; MBP, myelin basic protein; NF, neurofilament; NeuN, neuronal nuclear protein; Olig2, oligodendrocyte transcription factor 2; Tuj-1, beta-III tubulin.

Neurogenesis and neuronal differentiation

Most studies reported increased neuronal differentiation or axonal-growth markers, principally Tuj-1/βIII-tubulin, MAP-2, NeuN, and GAP43. Tuj-1-positive areas were approximately 30 ± 8% with dynamic GelMA/OHA, 17.4 ± 3.7% with the conductive GPP-TA scaffold, and about 14% with OSMI-4- or exosome-enhanced platforms[8,56-58]. Regionalized cell and factor distribution produced 16 ± 3 βIII-tubulin-positive neurites/mm²[9].

Other constructs increased MAP-2, neuronal differentiation, axonal growth, or cell and neurite alignment[2,5,11]. Because outcomes were expressed as positive area, intensity, neurite density, or qualitative observations and were measured in different regions and periods, effect magnitudes could not be compared.

Astrocytic response and glial scar

Reduced GFAP or other scar-associated markers were frequently reported. In treated groups, GFAP-positive values ranged from approximately 1.5% to 7 ± 3%: about 1.5% with microfibers and exosomes, 4 ± 2% with OSMI-4, 4.3 ± 0.4% with GPP-TA, and 7 ± 3% with regionalized cells and factors, compared with 13 ± 2% after homogeneous distribution[9,56-58].

Dynamic, microcarrier-containing, and bioprinted neural-tissue constructs also reduced GFAP, CS-56, MMP13, or glial scar deposition[5,8,11]. Variation in immunolabeling, regions of interest, and time points prevented quantitative comparison.

Axonal growth, synapse formation, and myelination

Treated groups generally showed greater NF-, NF200-, GAP43-, or Tuj-1-positive fiber density or organization, accompanied in several studies by MBP, synaptic markers, or morphometric evidence of myelination. Longitudinal living neural fibers yielded an NF-positive area of 20.75 ± 3.9%, 20,225 ± 2,747 myelinated fibers/mm², and a g-ratio of 0.42[59]. GPP-TA constructs produced approximately 30.5% NF200 and 17.5% MBP[58], whereas dynamic GelMA/OHA produced about 30% NF and 75% MBP[8].

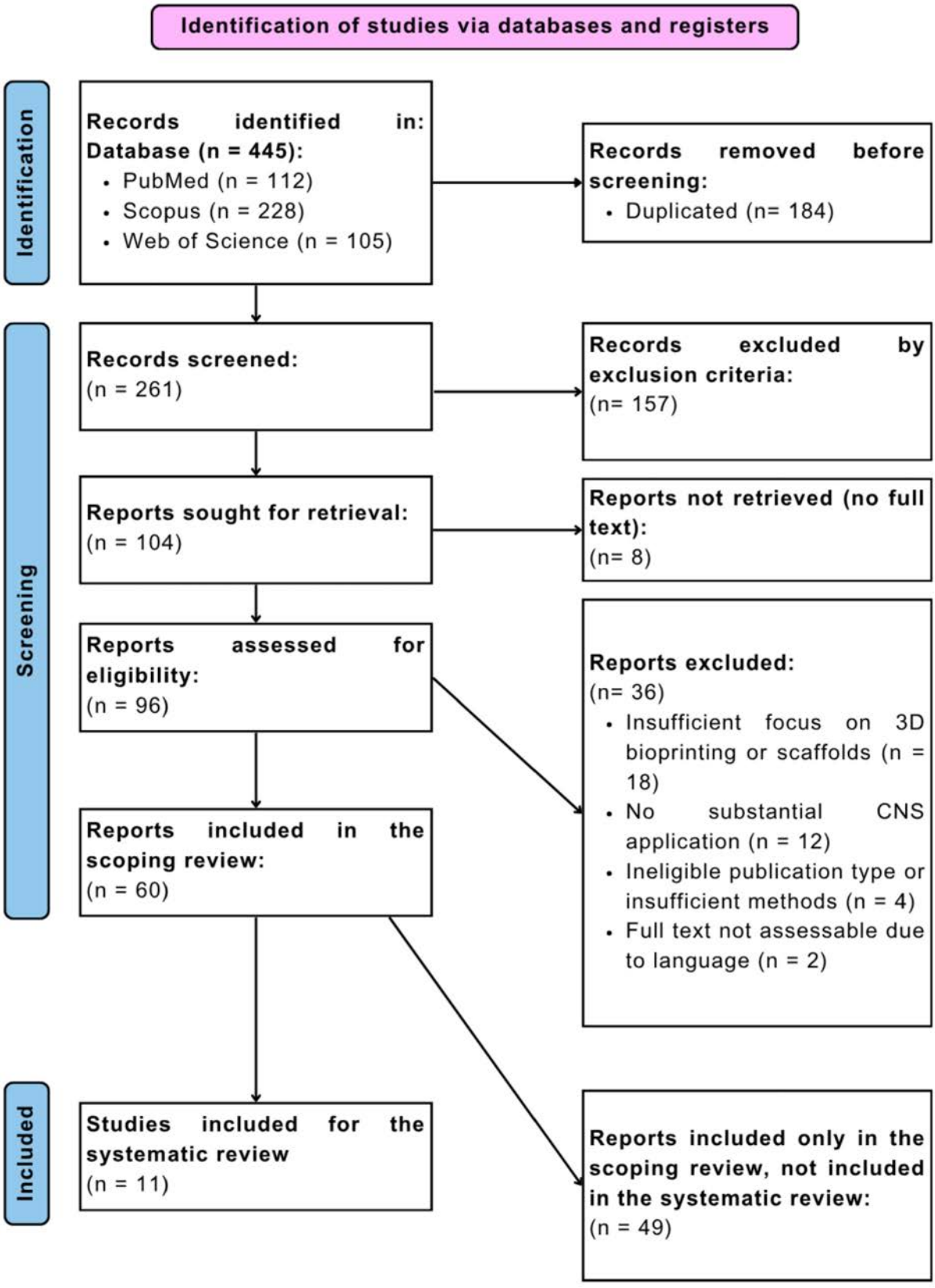

Figure 1. Flowchart diagram of study identification, screening, and inclusion.

Regionalized cells and factors were associated with approximately 40% GAP43 and 35% nestin[9]. Other studies reported axonal alignment, MAP-2 and MBP expression, synaptic markers, myelinated fibers, or nodal structures[2,3,11]. Differences in techniques, units, and follow-up precluded ranking the constructs.

Functional recovery

All rat studies reported functional improvement relative to their respective injured controls. The BBB scale predominated and was supplemented by gait, inclined-plane, open-field, climbing, swimming, sensory, electromyographic, and evoked-potential assessments.

Peak BBB scores were approximately 17–18 after hemisection and approximately 6.8–13.5 after complete transection. Regionalized cells and factors achieved 13.5 ± 1.2, and microfibers combined with exosomes achieved a value close to 12; most remaining results ranged from 7 to 10[3,9,56]. A 10-mm defect showed structural integration but less functional recovery than smaller lesions. These values were not directly comparable because lesion severity, follow-up, and protocols differed.

The zebrafish study assessed spontaneous contraction, hatching, swimming speed, and locomotor recovery after cerebellar injury. Its findings were not numerically compared with rodent outcomes because of differences in species, regenerative capacity, lesions, and instruments.

Risk-of-bias assessment

Of 110 SYRCLE judgments, 98 (89.1%) were unclear, 11 (10.0%) were low risk, and one (0.9%) was high risk. Low-risk judgments occurred mainly for baseline characteristics, random outcome assessment, assessor blinding, and incomplete outcome data. Hsieh et al.[55] received the only high-risk judgment because mortality differed among groups and the analysis included survivors only. Insufficient reporting accounted for most unclear judgments (Figure 2).

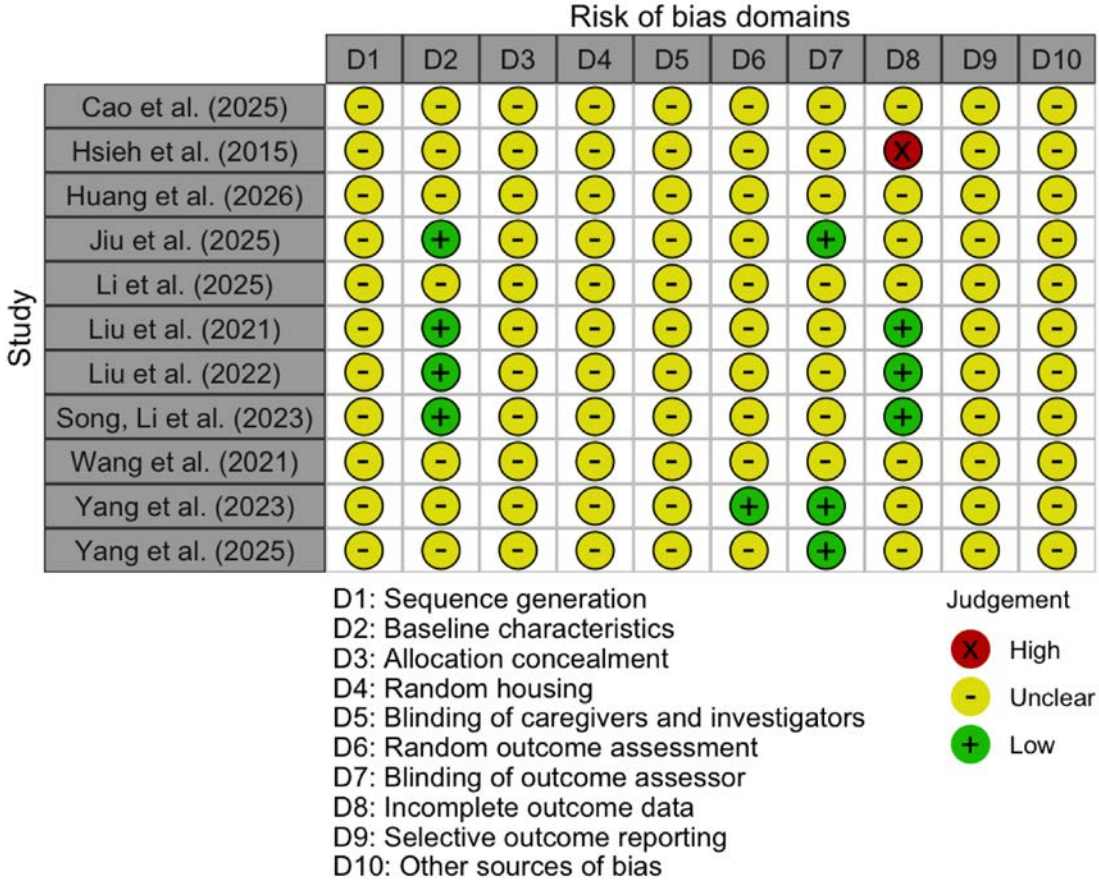

Figure 2. Risk-of-bias assessment of the 11 preclinical studies using the SYRCLE tool. Green indicates low risk, yellow indicates unclear risk, and red indicates high risk.

DISCUSSION

This two-stage review distinguishes the breadth of CNS bioprinting from the more restricted evidence on direct cell-laden constructs for structural repair. The scoping review identified neural models, disease and drug-screening platforms, methodological investigations, acellular or post-seeded scaffolds, and implantable cell-laden constructs. The systematic review included only the latter when evaluated in vivo. Similar diversity has been reported in previous neural-bioprinting reviews[60], and separating these bodies of evidence avoids treating different objectives and mechanisms as equivalent.

Spinal cord injury accounted for 14 of the 18 in vivo studies. Its longitudinal organization and focal tissue cavities favor aligned fibers, microchannels, and cellular or molecular gradients that can bridge a lesion, features already emphasized in the spinal cord bioprinting literature[61]. This concentration limits generalizability: the brain has greater regional heterogeneity, distributed circuits, and more complex three-dimensional connectivity[43]. Hsieh et al.[55] broadened the models by examining zebrafish neural and cerebellar injury, but the species' high regenerative capacity limits extrapolation to mammals.

The anatomical concentration of the evidence also affects the clinical questions that can be addressed. Most constructs bridged acute, defined defects, whereas neurosurgical practice includes irregular, chronic, ischemic, neoplastic, and treatment-related lesions. Feasibility in a standardized spinal cord gap is therefore proof of principle rather than evidence that the same architecture will repair diverse clinical injuries.

The biomaterial landscape has progressed from relatively simple hydrogels to multifunctional formulations intended to combine printability, structural support, and biochemical, mechanical, or electrical signaling[62]. GelMA appeared in seven of the 11 systematic-review studies, plausibly because of its cell-adhesion domains, tunable properties, and photopolymerization compatibility[63]. Frequency of use does not demonstrate superiority: concentrations, photoinitiators, crosslinking, cell density, and added components differed substantially. NorCol, functionalized chitosan–hyaluronic acid–Matrigel, and thermoresponsive polyurethane illustrate how material selection was tailored to the printing method, cell type, architecture, and implantation site[2,5,55]. Accordingly, the frequent presence of GelMA indicates technical versatility rather than comparative effectiveness. None of the included studies compared GelMA with all relevant alternatives while holding architecture, cells, mechanics, and additives constant. Claims of material superiority will require head-to-head designs with matched cell density, printing parameters, degradation profiles, and lesion models.

Decellularized spinal cord matrix may provide tissue-specific biochemical signals, but variation in source tissue, decellularization, and processing complicates reproducibility and quality control[32]. Conductive components may support neural signaling, yet they also alter rheology, stiffness, and swelling, preventing conductivity from being interpreted independently[7]. The neuronal, axonal, and functional improvements reported with the conductive neural stem cell scaffold of Song et al.[58] are encouraging, but controls isolating conductivity from chemical composition and architecture remain necessary.

Architecture was likewise an active therapeutic variable rather than merely structural support. Aligned tracts, longitudinal fibers, microchannels, coaxial compartments, and regionalized deposition can guide migration and axonal growth or position cells and signals within specific regions, consistent with the importance of spatial patterning in neural repair[64]. Aligned constructs were associated with axonal orientation, retention, vascularization, myelination, and functional recovery[2,59]. More complex regionalized or coaxial platforms also produced favorable outcomes, but factorial comparators are needed to determine the separate and interactive contributions of architecture, cells, and bioactive agents.

These observations favor evaluating each construct as an integrated system. A material that improves print fidelity may simultaneously alter stiffness and differentiation, while aligned geometry may affect cell retention, vascular ingrowth, and axonal direction. Multicomponent designs can demonstrate therapeutic potential but cannot establish which element is necessary, sufficient, or principally responsible for the effect.

Neural stem cells predominated, although mesenchymal, ectodermal mesenchymal, bone marrow-derived mesenchymal, and Schwann cells were also used. No optimal population could be identified because source, differentiation status, cell density, preimplantation culture, and follow-up varied, and cell behavior depends on its interaction with the matrix, signals, and host tissue[65].

The addition of drugs, growth factors, exosomes, or extracellular vesicles further transformed scaffolds into multifactorial platforms, but greater complexity also weakened causal attribution to any individual component.

The scoping review therefore retained clinically relevant strategies that did not satisfy the systematic-review definition. Acellular constructs can provide structural support and controlled local delivery of drugs, growth factors, or extracellular vesicles[66], acting mainly through pharmacological, paracrine, or immunomodulatory mechanisms. Cell-laden constructs additionally pursue cell replacement and integration. Neither approach avoids requirements for stability, sterility, reproducibility, and appropriate controls.

This distinction is illustrated by two 2023 studies by Song and colleagues. Song et al.[50] printed an oxymatrine-loaded scaffold without living cells in the material during fabrication; subsequent in vitro cell testing and in vivo recruitment of endogenous cells did not constitute direct cell-laden bioprinting, so the study remained scoping-only. Song et al.[58] incorporated neural stem cells into a conductive bioink during fabrication; therefore, their study was included in the systematic review.

Across the 11 systematically reviewed studies, findings converged qualitatively toward greater neuronal-marker expression, axonal growth, angiogenesis, synapse formation, myelination, and functional recovery. This direction of effect does not establish comparable magnitude or platform superiority. Histological outcomes used different markers, units, regions, and time points. Similarly, lower GFAP was often interpreted as attenuated scarring, although chondroitin sulfate proteoglycans can inhibit axonal growth[67] and reactive astrocytes may also limit injury spread and support repair[68]. GFAP should therefore be interpreted with scar-matrix, axonal, myelin, and functional measures rather than as an isolated surrogate of benefit.

The same caution applies to numerical histology. Percent-positive area, staining intensity, fiber density, and cell counts represent different biological quantities and vary with image selection, thresholding, region of interest, and tissue preservation. Even use of the same marker does not permit direct comparison unless acquisition and quantification procedures are equivalent.

Functional outcomes were also sensitive to lesion anatomy and assessment timing. Higher BBB scores after hemisection than after complete transection cannot be interpreted as superiority of a material or technique because spontaneous-recovery potential and maximum attainable function differ. Variation across four-, eight-, and 12-week follow-up further affects apparent recovery. The combined influence of printing method, geometry, biomaterial, cells, and supplements has been highlighted elsewhere[69]. Prespecified histological and functional protocols, common outcome sets, comparable follow-up, sample-size calculations, randomization, and blinded assessment would improve reproducibility and future quantitative synthesis.

A common outcome framework should combine behavioral testing with electrophysiology and predefined histological measures. Functional improvement without organized host–graft connectivity may differ mechanistically from recovery accompanied by axonal continuity and remyelination; conversely, favorable staining without durable functional benefit is insufficient to support clinical development.

Translation additionally depends on manufacturing scale-up, sterility, stability, tissue integration, and cell safety. Cell-laden bioprinting combines features of cell therapy, a medical device, and a tissue-engineered product, creating complex regulatory and quality-control requirements[70,71]. Clinically relevant volumes intensify constraints involving nutrient diffusion, vascularization, cell viability, and mechanical integrity[72]. Current lesions are smaller and more standardized than human injuries, and the absence of large-animal studies leaves surgical implantation, long-term integration, immune responses, cell persistence, and unwanted differentiation insufficiently examined.

Large-animal work must test operative handling, fixation within irregular cavities, vascular support over clinically relevant distances, tissue motion, and loading. Long-term studies should address graft overgrowth, migration, immune compatibility, tumorigenicity, and stability of the intended cellular phenotype.

This review also has limitations. One reviewer conducted screening, full-text assessment, extraction, and risk-of-bias evaluation, increasing the possibility of error, selection bias, and subjective judgment. Ninety-eight of 110 SYRCLE judgments were unclear, principally because randomization, allocation concealment, random housing, blinding, and sample-size planning were insufficiently described. Unclear risk does not confirm bias but prevents firm assessment of internal validity.

The single high-risk judgment reflected differential mortality and analysis of surviving animals. Some numerical values were estimated from graphs, reducing precision, and publication bias is possible because favorable results predominated. Finally, methodological heterogeneity precluded meta-analysis, and the concentration on rodent spinal cord injury limits generalization to other CNS conditions.

Overall, 3D bioprinting may support cell retention and organization, neuronal differentiation, axonal growth, myelination, and functional recovery, but bioink, cells, spatial architecture, and bioactive signals act interdependently. The evidence cannot yet identify an optimal combination or support clinical inference. Progress toward neurosurgical translation will require transparent and standardized comparisons, independent risk-of-bias assessment, large-animal models, long-term safety evaluation, and broader investigation of brain injuries.

CONCLUSION

This review mapped CNS applications of 3D bioprinting and synthesized preclinical in vivo evidence on directly bioprinted cell-laden constructs for structural repair. Favorable findings—particularly in spinal cord injury—involved neuronal differentiation, glial modulation, axonal growth, myelination, and motor recovery. However, methodological heterogeneity, predominantly unclear risk-of-bias judgments, and the absence of human evidence indicate that the technology remains experimental. Standardized protocols and outcomes, large-animal models, and broader study of brain and other CNS injuries are needed before clinical translation.

REFERENCES

1. Cafferty WBJ, Duffy P, Huebner E, Strittmatter SM. MAG and OMgp synergize with Nogo-A to restrict axonal growth and neurological recovery after spinal cord trauma. J Neurosci. 2010;30(20):6825-37. https://doi.org/10.1523/JNEUROSCI.6239-09.2010. PMid:20484625.

2. Huang W, Chen S, Li K, et al. Nanoengineered extrusion-aligned tract bioprinting enables functional repair of spinal cord injuries. Cell Stem Cell. 2026;33(2):340-354.e7. https://doi.org/10.1016/j.stem.2025.12.021. PMid:41534522.

3. Wang J, Kong X, Li Q, et al. The spatial arrangement of cells in a 3D-printed biomimetic spinal cord promotes directional differentiation and repairs the motor function after spinal cord injury. Biofabrication. 2021;13(4):045016. https://doi.org/10.1088/1758-5090/ac0c5f. PMid:34139682.

4. Joung D, Truong V, Neitzke CC, et al. 3D printed stem-cell derived neural progenitors generate spinal cord scaffolds. Adv Funct Mater. 2018;28(39):1801850. https://doi.org/10.1002/adfm.201801850. PMid:32595422.

5. Liu X, Hao M, Chen Z, et al. 3D bioprinted neural tissue constructs for spinal cord injury repair. Biomaterials. 2021;272:120771. https://doi.org/10.1016/j.biomaterials.2021.120771. PMid:33798962.

6. Haring AP, Thompson EG, Tong Y, et al. Process- and bio-inspired hydrogels for 3D bioprinting of soft free-standing neural and glial tissues. Biofabrication. 2019;11(2):025009. https://doi.org/10.1088/1758-5090/ab02c9. PMid:30695770.

7. Kiyotake EA, Thomas EE, Homburg HB, et al. Conductive and injectable hyaluronic acid/gelatin/gold nanorod hydrogels for enhanced surgical translation and bioprinting. J Biomed Mater Res A. 2022;110(2):365-82. https://doi.org/10.1002/jbm.a.37294. PMid:34390325.

8. Yang J, Kim K, Liu Y, et al. 3D bioprinted dynamic bioactive living construct enhances mechanotransduction-assisted rapid neural network self-organization for spinal cord injury repair. Bioact Mater. 2025;46:531-54. https://doi.org/10.1016/j.bioactmat.2024.12.028. PMid:39886605.

9. Cao X, Li X, Shi W, et al. 3D-Bioprinted Scaffolds with Precise Factor Delivery for Spinal Cord Injury Repair. ACS Appl Mater Interfaces. 2025;17(30):42586-601. https://doi.org/10.1021/acsami.5c03076. PMid:40673827.

10. Zhang L, Chen G, Pang J, et al. 3D bioprinted NSC-EVs hydrogel scaffold promotes sustained functional repair via autophagy activation after TBI in mice. Chem Eng J. 2025;522:167836. https://doi.org/10.1016/j.cej.2025.167836.

11. Jiu J, Liu H, Li D, et al. 3D Mechanical Response Stem Cell Complex Repairs Spinal Cord Injury by Promoting Neurogenesis and Regulating Tissue Homeostasis. Adv Healthc Mater. 2025;14(7):e2404925. https://doi.org/10.1002/adhm.202404925. PMid:39853962.

12. Tricco AC, Lillie E, Zarin W, et al. PRISMA Extension for Scoping Reviews (PRISMA-ScR): checklist and explanation. Ann Intern Med. 2018;169(7):467-73. https://doi.org/10.7326/M18-0850. PMid:30178033.

13. Page MJ, McKenzie JE, Bossuyt PM, et al. The PRISMA 2020 statement: an updated guideline for reporting systematic reviews. BMJ. 2021;372(71):n71. https://doi.org/10.1136/bmj.n71. PMid:33782057.

14. Hooijmans CR, Rovers MM, de Vries RBM, Leenaars M, Ritskes-Hoitinga M, Langendam MW. SYRCLE's risk of bias tool for animal studies. BMC Med Res Methodol. 2014;14(1):43. https://doi.org/10.1186/1471-2288-14-43. PMid:24667063.

15. McGuinness LA, Higgins JPT. Risk-of-bias VISualization (robvis): an R package and Shiny web app for visualizing risk-of-bias assessments. Res Synth Methods. 2021;12(1):55-61. https://doi.org/10.1002/jrsm.1411. PMid:32336025.

16. Knefel M, Kantor M, Kępka K, Owczarzy A, Kulig K, Maciążek-Jurczyk M. Applications of bio-printing to promote spinal cord regeneration. Polim Med. 2024;54(2):127-34. https://doi.org/10.17219/pim/196553. PMid:39639728.

17. Benedek A, Cernica D, Mester A, et al. Modern concepts in regenerative therapy for ischemic stroke: from stem cells for promoting angiogenesis to 3D-bioprinted scaffolds customized via carotid shear stress analysis. Int J Mol Sci. 2019;20(10):2574. https://doi.org/10.3390/ijms20102574. PMid:31130624.

18. He W, Xu C, Wu W, et al. The promising applications of 3D printing technology in neurotrauma. Int J Bioprint. 2024;10(3):2311. https://doi.org/10.36922/ijb.2311.

19. Li S, Meng X, Zhong Z, Li C. Advances in 3D bioprinting of functional biomaterials for neural tissue engineering. Tissue Cell. 2025;96:103024. https://doi.org/10.1016/j.tice.2025.103024. PMid:40578149.

20. Joung D, Lavoie NS, Guo SZ, Park SH, Parr AM, McAlpine MC. 3D printed neural regeneration devices. Adv Funct Mater. 2020;30(1):1906237. https://doi.org/10.1002/adfm.201906237. PMid:32038121.

21. Pokharel R, Leipzig ND. 3D bioprinting for spinal cord injury: engineering scaffolds for functional recovery. ACS Biomater Sci Eng. 2026;12(2):757-72. https://doi.org/10.1021/acsbiomaterials.5c01474. PMid:41505565.

22. Bedir T, Ulag S, Ustundag CB, Gunduz O. 3D bioprinting applications in neural tissue engineering for spinal cord injury repair. Mater Sci Eng C. 2020;110:110741. https://doi.org/10.1016/j.msec.2020.110741. PMid:32204049.

23. Lu D, Yang Y, Zhang P, et al. Development and application of three-dimensional bioprinting scaffold in the repair of spinal cord injury. Tissue Eng Regen Med. 2022;19(6):1113-27. https://doi.org/10.1007/s13770-022-00465-1. PMid:35767151.

24. Kim DY, Liu Y, Kim G, An SB, Han I. Innovative strategies in 3D bioprinting for spinal cord injury repair. Int J Mol Sci. 2024;25(17):9592. https://doi.org/10.3390/ijms25179592. PMid:39273538.

25. Wang L, Zhou X, Wang S, et al. Bioinks used in the repair of nerve injury in vivo. Prog Mater Sci. 2026;158:101643. https://doi.org/10.1016/j.pmatsci.2025.101643.

26. Zarepour A, Hooshmand S, Gökmen A, Zarrabi A, Mostafavi E. Spinal cord injury management through the combination of stem cells and implantable 3D bioprinted platforms. Cells. 2021;10(11):3189. https://doi.org/10.3390/cells10113189. PMid:34831412.

27. St Clair-Glover M, Yue Z, Dottori M. 3D Printing for Neural Repair: Bridging the Gap in Regenerative Medicine. Adv Mater. 2025;37(36):e07590. https://doi.org/10.1002/adma.202507590. PMid:40736088.

28. Thomas M, Willerth SM. 3-D bioprinting of neural tissue for applications in cell therapy and drug screening. Front Bioeng Biotechnol. 2017;5:69. https://doi.org/10.3389/fbioe.2017.00069. PMid:29204424.

29. Dhar S, Ahmad F, Deshpande A, Rana SS, Ahmed TA, Priyadarsini S. 3-Dimensional printing and bioprinting in neurological sciences: applications in surgery, imaging, tissue engineering, and pharmacology and therapeutics. J Mater Sci Mater Med. 2025;36(1):32. https://doi.org/10.1007/s10856-025-06877-4. PMid:40205004.

30. Oliveira EP, Malysz-Cymborska I, Golubczyk D, et al. Advances in bioinks and in vivo imaging of biomaterials for CNS applications. Acta Biomater. 2019;95:60-72. https://doi.org/10.1016/j.actbio.2019.05.006. PMid:31075514.

31. Rotaru-Zavaleanu AD, Bica M, Dinescu SN, et al. Bioactive hydrogels for spinal cord injury repair: emphasis on gelatin and its derivatives. Gels. 2025;11(7):497. https://doi.org/10.3390/gels11070497. PMid:40710658.

32. dos Santos MG, França FS, Prestes JP, et al. Production of a bioink containing decellularized spinal cord tissue for 3D bioprinting. Tissue Eng Part A. 2024;30(1-2):61-74. https://doi.org/10.1089/ten.tea.2023.0078. PMid:37772706.

33. Song S, Liu X, Huang J, Zhang Z. Neural stem cell-laden 3D bioprinting of polyphenol-doped electroconductive hydrogel scaffolds for enhanced neuronal differentiation. Biomater Adv. 2022;133:112639. https://doi.org/10.1016/j.msec.2021.112639. PMid:35527143.

34. Lee YB, Polio S, Lee W, et al. Bio-printing of collagen and VEGF-releasing fibrin gel scaffolds for neural stem cell culture. Exp Neurol. 2010;223(2):645-52. https://doi.org/10.1016/j.expneurol.2010.02.014. PMid:20211178.

35. Li YE, Jodat YA, Samanipour R, et al. Toward a neurospheroid niche model: optimizing embedded 3D bioprinting for fabrication of neurospheroid brain-like co-culture constructs. Biofabrication. 2021;13(1):015014. https://doi.org/10.1088/1758-5090/abc1be. PMid:33059333.

36. De la Vega L, Rosas Gómez DA, Abelseth E, Abelseth L, Allisson da Silva V, Willerth SM. 3D bioprinting human induced pluripotent stem cell-derived neural tissues using a novel lab-on-a-printer technology. Appl Sci (Basel). 2018;8(12):2414. https://doi.org/10.3390/app8122414.

37. Kwokdinata C, Chai KL, Lau K, Tan J, Chew SY. Bioprinted microchannel scaffolds modulate neuronal differentiation of encapsulated human spinal cord progenitor cells. ACS Appl Bio Mater. 2025;8(5):4337-50. https://doi.org/10.1021/acsabm.5c00441. PMid:40312827.

38. Cruz EM, Machado LS, Zamproni LN, et al. A gelatin methacrylate-based hydrogel as a potential bioink for 3D bioprinting and neuronal differentiation. Pharmaceutics. 2023;15(2):627. https://doi.org/10.3390/pharmaceutics15020627. PMid:36839949.

39. Hamid OA, Eltaher HM, Sottile V, Yang J. 3D bioprinting of a stem cell-laden, multi-material tubular composite: an approach for spinal cord repair. Mater Sci Eng C. 2021;120:111707. https://doi.org/10.1016/j.msec.2020.111707. PMid:33545866.

40. Lozano R, Stevens L, Thompson BC, et al. 3D printing of layered brain-like structures using peptide modified gellan gum substrates. Biomaterials. 2015;67:264-73. https://doi.org/10.1016/j.biomaterials.2015.07.022. PMid:26231917.

41. Bordoni M, Rey F, Fantini V, et al. From neuronal differentiation of iPSCs to 3D neuro-organoids: modelling and therapy of neurodegenerative diseases. Int J Mol Sci. 2018;19(12):3972. https://doi.org/10.3390/ijms19123972. PMid:30544711.

42. Zhuang P, Sun AX, An J, Chua CK, Chew SY. 3D neural tissue models: from spheroids to bioprinting. Biomaterials. 2018;154:113-33. https://doi.org/10.1016/j.biomaterials.2017.10.002. PMid:29120815.

43. Choi T, Park J, Lee S, et al. 3D Bioprinted Neural Tissues: Emerging Strategies for Regeneration and Disease Modeling. Pharmaceutics. 2025;17(9):1176. https://doi.org/10.3390/pharmaceutics17091176. PMid:41012512.

44. Rey F, Barzaghini B, Nardini A, et al. Advances in tissue engineering and innovative fabrication techniques for 3-D-structures: translational applications in neurodegenerative diseases. Cells. 2020;9(7):1636. https://doi.org/10.3390/cells9071636. PMid:32646008.

45. Samanipour R, Tahmooressi H, Rezaei Nejad H, Hirano M, Shin SR, Hoorfar M. A review on 3D printing functional brain model. Biomicrofluidics. 2022;16(1):011501. https://doi.org/10.1063/5.0074631. PMid:35145569.

46. Amiri E, Sanjarnia P, Sadri B, Jafarkhani S, Khakbiz M. Recent advances and future directions of 3D to 6D printing in brain cancer treatment and neural tissue engineering. Biomed Mater. 2023;18(5):052005. https://doi.org/10.1088/1748-605X/ace9a4. PMid:37478841.

47. Qian Y, Gong J, Lu K, et al. DLP printed hDPSC-loaded GelMA microsphere regenerates dental pulp and repairs spinal cord. Biomaterials. 2023;299:122137. https://doi.org/10.1016/j.biomaterials.2023.122137. PMid:37172537.

48. Lee SJ, Nowicki M, Harris B, Zhang LG. Fabrication of a highly aligned neural scaffold via a table top stereolithography 3D printing and electrospinning. Tissue Eng Part A. 2017;23(11-12):491-502. https://doi.org/10.1089/ten.tea.2016.0353. PMid:27998214.

49. Zhou X, Cui H, Nowicki M, et al. Three-dimensional-bioprinted dopamine-based matrix for promoting neural regeneration. ACS Appl Mater Interfaces. 2018;10(10):8993-9001. https://doi.org/10.1021/acsami.7b18197. PMid:29461046.

50. Song S, Zhou J, Wan J, et al. Three-dimensional printing of microfiber-reinforced hydrogel loaded with oxymatrine for treating spinal cord injury. Int J Bioprint. 2023;9(3):692. https://doi.org/10.18063/ijb.692. PMid:37273987.

51. Wang Q, Liu K, Cao X, et al. Plant-derived exosomes extracted from Lycium barbarum L. loaded with isoliquiritigenin to promote spinal cord injury repair based on 3D printed bionic scaffold. Bioeng Transl Med. 2024;9(4):e10646. https://doi.org/10.1002/btm2.10646. PMid:39036078.

52. Li Y, Cheng S, Wen H, et al. Coaxial 3D printing of hierarchical structured hydrogel scaffolds for on-demand repair of spinal cord injury. Acta Biomater. 2023;168:400-15. https://doi.org/10.1016/j.actbio.2023.07.020. PMid:37479156.

53. Chen M, Ye Y, Wang T, Zhang X, Chen J, Zhang J. Neural network reconstruction and motor function recovery in traumatic brain injury rat models via a 3D collagen/heparan/bFGF/NGF scaffold combined with mesenchymal stem cells. J Neural Eng. 2025;22(5):056022. https://doi.org/10.1088/1741-2552/ae09fd. PMid:40983084.

54. Gai K, Song Y, Gao D, et al. Advanced stem cell therapy: 3d-bioprinted brain-like transplants for Alzheimer's disease-like dementia. Adv Sci (Weinh). 2026;13(4):e10062. https://doi.org/10.1002/advs.202510062. PMid:41201135.

55. Hsieh FY, Lin HH, Hsu SH. 3D bioprinting of neural stem cell-laden thermoresponsive biodegradable polyurethane hydrogel and potential in central nervous system repair. Biomaterials. 2015;71:48-57. https://doi.org/10.1016/j.biomaterials.2015.08.028. PMid:26318816.

56. Li X, Zhang J, Zhang Y, et al. Conjugated therapy with coaxially printed neural stem cell-laden microfibers and umbilical cord mesenchymal stem cell derived exosomes on complete transactional spinal cord defects. Mater Today Bio. 2025;32:101639. https://doi.org/10.1016/j.mtbio.2025.101639. PMid:40160243.

57. Liu X, Song S, Chen Z, et al. Release of O-GlcNAc transferase inhibitor promotes neuronal differentiation of neural stem cells in 3D bioprinted supramolecular hydrogel scaffold for spinal cord injury repair. Acta Biomater. 2022;151:148-62. https://doi.org/10.1016/j.actbio.2022.08.031. PMid:36002129.

58. Song S, Li Y, Huang J, Cheng S, Zhang Z. Inhibited astrocytic differentiation in neural stem cell-laden 3D bioprinted conductive composite hydrogel scaffolds for repair of spinal cord injury. Biomater Adv. 2023;148:213385. https://doi.org/10.1016/j.bioadv.2023.213385. PMid:36934714.

59. Yang J, Yang K, Man W, et al. 3D bio-printed living nerve-like fibers refine the ecological niche for long-distance spinal cord injury regeneration. Bioact Mater. 2023;25:160-75. https://doi.org/10.1016/j.bioactmat.2023.01.023. PMid:36817821.

60. Cadena M, Ning L, King A, et al. 3D bioprinting of neural tissues. Adv Healthc Mater. 2021;10(15):e2001600. https://doi.org/10.1002/adhm.202001600. PMid:33200587.

61. Yuan TY, Zhang J, Yu T, Wu JP, Liu QY. 3D bioprinting for spinal cord injury repair. Front Bioeng Biotechnol. 2022;10:847344. https://doi.org/10.3389/fbioe.2022.847344. PMid:35519617.

62. Lee SJ, Esworthy T, Stake S, et al. Advances in 3D bioprinting for neural tissue engineering. Adv Biosyst. 2018;2(4):1700213. https://doi.org/10.1002/adbi.201700213.

63. Bupphathong S, Quiroz C, Huang W, Chung PF, Tao HY, Lin CH. Gelatin methacrylate hydrogel for tissue engineering applications – a review on material modifications. Pharmaceuticals (Basel). 2022;15(2):171. https://doi.org/10.3390/ph15020171. PMid:35215284.

64. Kwokdinata C, Chew SY. Additive manufacturing in spatial patterning for spinal cord injury treatment. Adv Drug Deliv Rev. 2025;218:115523. https://doi.org/10.1016/j.addr.2025.115523. PMid:39880332.

65. Ju D, Dong C. The combined application of stem cells and three-dimensional bioprinting scaffolds for the repair of spinal cord injury. Neural Regen Res. 2024;19(8):1751-8. https://doi.org/10.4103/1673-5374.385842. PMid:38103241.

66. Steele EM, Carr ZL, Dosmar E. Bioprinting of hydrogel-based drug delivery systems for nerve tissue regeneration. Biophysica. 2024;4(1): 58-73. https://doi.org/10.3390/biophysica4010004.

67. Bradbury EJ, Moon LD, Popat RJ, et al. Chondroitinase ABC promotes functional recovery after spinal cord injury. Nature. 2002;416(6881): 636-40. https://doi.org/10.1038/416636a. PMid:11948352.

68. Anderson MA, Burda JE, Ren Y, et al. Astrocyte scar formation aids central nervous system axon regeneration. Nature. 2016;532(7598): 195-200. https://doi.org/10.1038/nature17623. PMid:27027288.

69. Jiu J, Liu H, Li D, et al. 3D bioprinting approaches for spinal cord injury repair. Biofabrication. 2024;16(3):032003. https://doi.org/10.1088/1758-5090/ad3a13. PMid:38569491.

70. Mladenovska T, Choong PF, Wallace GG, O'Connell CD. The regulatory challenge of 3D bioprinting. Regen Med. 2023;18(8):659-74. https://doi.org/10.2217/rme-2022-0194. PMid:37403962.

71. Ng WL, An J, Chua CK. Process, Material, and Regulatory Considerations for 3D Printed Medical Devices and Tissue Constructs. Engineering (Beijing). 2024;36:146-66. https://doi.org/10.1016/j.eng.2024.01.028.

72. Ozbolat IT. Bioprinting scale-up tissue and organ constructs for transplantation. Trends Biotechnol. 2015;33(7):395-400. https://doi.org/10.1016/j.tibtech.2015.04.005. PMid:25978871.

CORRESPONDING AUTHOR

André Giacomelli Leal, MD, PhD
Instituto de Neurologia de Curitiba – INC
Department of Neurosurgery
Curitiba, Paraná, Brazil
E-mail andregiacomelli@inc-neuro.com.br

Funding: *nothing to disclose.*
Conflicts of interest: *nothing to disclose.*

CRediT

Mhaedra Comin Galvan: Methodology; Formal analysis; Investigation; Data curation; Writing - original draft; Visualization. Lorena Maria Dering: Supervision; Writing - review & editing. André Giacomelli Leal: Conceptualization; Supervision; Writing - review & editing.

Anatomy of the Lateral Femoral Cutaneous Nerve and its Clinical Implications: a narrative review

Anatomia do Nervo Cutâneo Femoral Lateral e suas Implicações Clínicas: uma revisão narrativa

Samuel Pedro Pereira Silveira[1]
Carlos Umberto Pereira[2]

ABSTRACT

The lateral femoral cutaneous nerve (LFCN) is a purely sensory nerve supplying the anterolateral thigh and the anatomical substrate of meralgia paresthetica, a compressive neuropathy causing pain, paresthesia and dysesthesia in that territory. Because of its vulnerability to compression and iatrogenic injury, detailed anatomical knowledge is essential for surgeons, anesthesiologists and neurologists. This narrative review synthesizes cadaveric, surgical and imaging data on its origin, course and clinical relevance. The nerve usually arises from the dorsal divisions of the L2–L3 ventral rami, emerges at the lateral border of psoas major, runs obliquely over the iliacus in the retroperitoneum, and crosses the inguinal region medial to the anterior superior iliac spine (ASIS), where compression is most likely. Variability is the rule: origin, pelvic exit, relationship to the ASIS and inguinal ligament (Aszmann types A–E), branching pattern and cutaneous territory all differ, with variants reported in up to 25% of individuals. We define the surgical "danger zone" around the ASIS relevant to inguinal herniorrhaphy, iliac bone-graft harvesting, abdominoplasty and direct anterior total hip arthroplasty, and discuss implications for ultrasound-guided blocks and decompression surgery. Recognizing this variability underpins injury prevention and accurate management of meralgia paresthetica.

Keywords: *Lateral femoral cutaneous nerve; Meralgia paresthetica; Anatomical variation; Lumbar plexus; Inguinal ligament; Peripheral nerve injuries*

RESUMO

O nervo cutâneo femoral lateral (NCFL) é um nervo exclusivamente sensitivo da face anterolateral da coxa e o substrato anatômico da meralgia parestésica, neuropatia compressiva que cursa com dor, parestesia e disestesia nesse território. Dada sua vulnerabilidade à compressão e à lesão iatrogênica, o conhecimento anatômico detalhado é essencial para cirurgiões, anestesiologistas e neurologistas. Esta revisão narrativa sintetiza dados cadavéricos, cirúrgicos e de imagem sobre sua origem, trajeto e relevância clínica. O nervo origina-se habitualmente das divisões dorsais dos ramos ventrais de L2–L3, emerge na borda lateral do psoas maior, cruza obliquamente o ilíaco no retroperitônio e alcança a região inguinal medialmente à espinha ilíaca anterossuperior (EIAS), onde a compressão é mais provável. A variabilidade é a regra: origem, saída pélvica, relação com a EIAS e o ligamento inguinal (tipos A–E de Aszmann), ramificação e território cutâneo variam amplamente, com variantes em até 25% dos indivíduos. Delimitamos a "zona de perigo" cirúrgica ao redor da EIAS, relevante para herniorrafia inguinal, enxerto ósseo ilíaco, abdominoplastia e artroplastia total do quadril por via anterior direta, além das implicações para bloqueios guiados por ultrassom e cirurgia descompressiva. Reconhecer essa variabilidade previne lesões e orienta o manejo da meralgia parestésica.

Palavras-Chave: *Nervo cutâneo femoral lateral; Meralgia parestésica; Variação anatômica; Plexo lombar; Ligamento inguinal; Lesões dos nervos periféricos*

[1]Faculty of Medicine, Universidade Federal do Triângulo Mineiro, Uberaba, MG, Brazil.
[2]Neurosurgery Division, Universidade Federal do Sergipe, Aracaju, SE, Brazil.

Received Jun 1, 2026
Accepted Jun 25, 2026

INTRODUCTION

The lateral femoral cutaneous nerve (LFCN) is an exclusively sensory nerve responsible for the innervation of the anterolateral aspect of the thigh. Its clinical relevance lies in the fact that it is the anatomical substrate of meralgia paresthetica (MP), a neuropathic condition characterized by pain, paresthesias, and dysesthesias in the corresponding cutaneous territory. Detailed knowledge of the anatomy of this nerve is fundamental for surgeons, anesthesiologists, and neurologists, since its vulnerability to compression and iatrogenic injury is widely documented in the literature[1].

The first report of the clinical syndrome associated with the LFCN was made by Martin Bernhardt, a German neuropathologist, in 1878. Independently, in 1895, the Russian neurologist Vladimir Karlovich Roth coined the term meralgia paresthetica — derived from the Greek meros (thigh) and algos (pain) — in a 24-page monograph in which he described the condition in horsemen who wore overly tight belts[2]. Curiously, Sigmund Freud also described his own MP symptoms in the Neurologisches Centralblatt in 1895, calling it a condition that was "harmless, although not uninteresting"[3]. Since then, the anatomy of the LFCN has been the subject of numerous cadaveric and surgical studies, revealing a remarkable variability that defies simplified descriptions and demands caution during procedures in the inguinal, pelvic, and hip regions. This narrative review aims to synthesize the current anatomical knowledge of the LFCN — its origin, course, variations, sensory territory and vascularization — and to relate these findings to the prevention of iatrogenic injury and to the diagnosis and management of meralgia paresthetica.

METHODS

This is a narrative review of the literature on the anatomy and clinical implications of the lateral femoral cutaneous nerve. Relevant cadaveric, surgical, radiological and clinical studies were identified through searches of the PubMed/MEDLINE and Google Scholar databases, complemented by review of the reference lists of the retrieved articles. Publications in English and Portuguese addressing the origin, course, anatomical variations, sensory territory, vascularization, surgical topography or clinical correlations of the nerve were considered. Given the descriptive nature of a narrative review, no formal protocol for systematic selection or quality appraisal was applied; studies were selected by the authors according to their anatomical and clinical relevance.

RESULTS AND DISCUSSION

Origin and formation of the nerve

The LFCN typically arises from the dorsal divisions of the ventral rami of L2 and L3 in the lumbar plexus. In a cadaveric study of 80 sides, Haládaj et al.[4] demonstrated that origin from L2–L3 was the most prevalent, occurring in 58.75% of specimens. However, variations include origin from L1–L2 or L3–L4, and even as a collateral branch of the femoral nerve. In rare cases, the LFCN may be absent, with its sensory territory supplied by the ilioinguinal nerve, the anterior femoral cutaneous nerve, or a branch of the genitofemoral nerve[1].

After its formation within the lumbar plexus, the nerve emerges at the lateral border of the psoas major muscle, a constant anatomical relationship of great importance for transpsoas surgical approaches to the lumbar spine[4].

Retroperitoneal course

Once it emerges from the lateral border of the psoas major, the LFCN takes an oblique course over the anterior surface of the iliacus muscle, covered by the iliac fascia. Along this retroperitoneal course, the nerve runs toward the anterior superior iliac spine (ASIS), maintaining relationships with visceral structures that differ according to the side. On the right, the nerve lies posterolateral to the cecum and the vermiform appendix; on the left, it passes posterior to the descending colon, providing, on both sides, sensory innervation to the parietal peritoneum of the iliac fossa[1].

Haládaj et al.[4] described that the iliac segment of the LFCN runs over the iliacus muscle between two layers of the iliac fascia, which makes the nerve relatively fixed in this segment and may predispose it to injury during laparoscopic procedures and iliac bone graft harvesting. Reinpold et al.[5] detailed the retroperitoneal relationships of the nerves of the lower abdominal wall, including the LFCN, and measured the distances between the nerves and bony landmarks, providing relevant data for the prevention of injuries during herniorrhaphies.

Dias et al.[6] described that, in the pelvis–thigh transition, the nerve runs through an "aponeurotic-fascial" tunnel that begins at the iliopubic tract and extends to the inguinal ligament, even observing the formation of pseudoneuromas at this point in some specimens.

Passage through the inguinal region

The passage of the LFCN through the inguinal region constitutes the most critical point of its vulnerability to compression. In the classic description, the nerve crosses beneath the inguinal ligament, medial to the ASIS, and enters the thigh (Figure 1). However, this simplified description does not reflect the actual anatomical diversity documented in the literature.

The meta-analysis by Tomaszewski et al.[7], which gathered 24 studies with 1,720 specimens, demonstrated that the most common pattern of pelvic exit is the nerve crossing medial to the sartorius muscle, as a single trunk, at a mean distance of 1.90 cm medial to the ASIS. Majkrzak et al[8] measured the depth of the nerve at the level of the inguinal ligament at 1.0 ± 0.6 cm, demonstrating that this depth is more variable than previously described. The authors recommend surgical caution, as the nerve may be found considerably more medial or lateral than expected. In 2017, Hanna[9] carried out a cadaveric study in 20 cadavers and described the existence of a complete fascial canal that surrounds the nerve from the inguinal ligament to its terminal branches. This fascial canal, when thickened or rigid, may constitute an additional mechanism of nerve entrapment, independent of direct compression by the inguinal ligament.

Anatomical variations

Anatomical variations of the LFCN are extremely frequent and clinically relevant, representing one of the greatest challenges for the surgeon. Anatomical studies show that variations in the origin, in the pelvic exit course, and in the branching pattern are found in up to 25% of individuals[10].

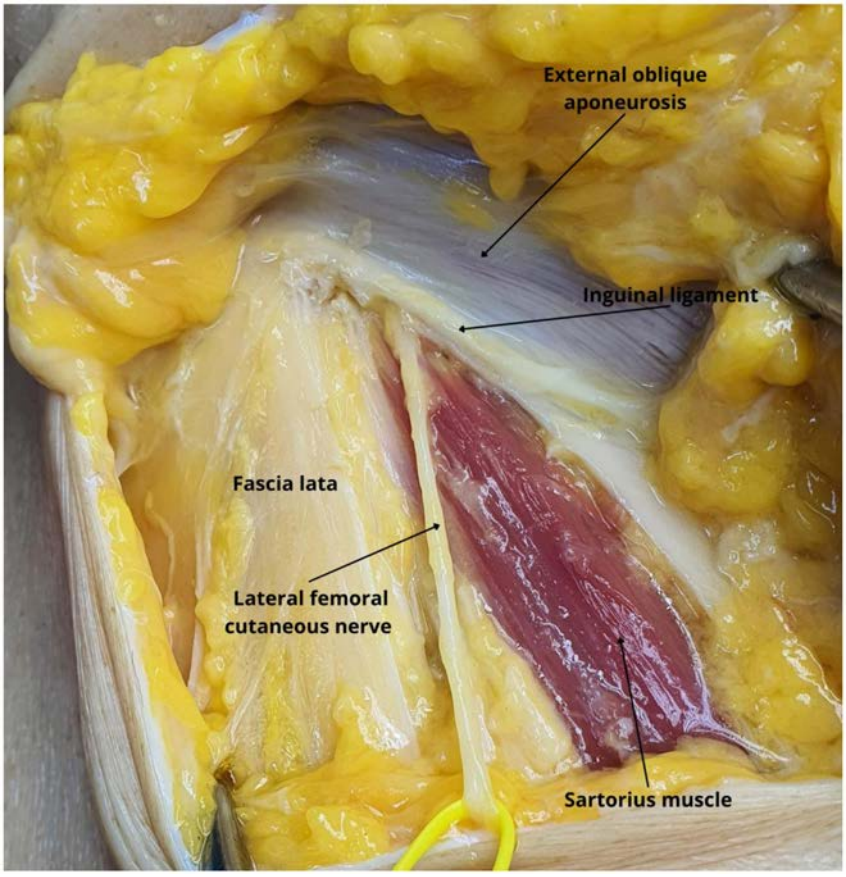

Figure 1. Right inguinal region dissected in an unembalmed adult cadaver. The lateral femoral cutaneous nerve crosses the inguinal ligament obliquely, medial to the anterior superior iliac spine, and enters the thigh. (Image courtesy of Dr. Mario Siqueira, Division of Neurosurgery, Hospital das Clínicas, FMUSP).

Aszmann classification

In 1997, Aszmann et al.[11] proposed a fundamental classification based on the study of 52 specimens, identifying five types of relationship between the nerve and the ASIS and inguinal ligament: type A — posterior to the ASIS, crossing the iliac crest (4%); type B — anterior to the ASIS, superficial to the origin of the sartorius, but within the substance of the inguinal ligament (27%); type C — medial to the ASIS, enveloped by the tendinous origin of the sartorius (23%); type D — medial to the origin of the sartorius, in the interval between the sartorius tendon and the iliopsoas fascia, deep to the inguinal ligament (26%); and type E — the most medial, embedded in loose connective tissue deep to the inguinal ligament (20%). Types A, B, and C are considered the most susceptible to mechanical trauma.

Variations in the number of branches and in the pelvic exit

Grothaus et al.[12] documented that up to five branches of the LFCN may be found, and that in 27.6% of cases the nerve divides before crossing the inguinal ligament. The meta-analysis by Tomaszewski et al.[7] demonstrated that the nerve emerges as a single trunk in 79.1% of cases. In the remainder, proximal bifurcation or trifurcation may occur, which increases the risk of injury during procedures in the inguinal region. Carai et al.[13], in their surgical series of 148 procedures, described less frequent findings such as early bifurcation, epifascial position, inferomedial direction, and exit from the pelvis through a canal in the iliac bone. In 8.8% of the operated cases, the nerve was not identified in the surgical field.

Variations in origin

Haládaj et al.[4], using retrograde fascicular microdissection in 80 cadaveric sides, identified multiple patterns of origin, including formation from a single root (L2 or L3), combined roots (L1–L2, L2–L3, L1–L2–L3), and origin from the femoral nerve. Erbil et al.[14] reported variants with multiple LFCNs in distinct cadavers, including a case with three lateral femoral cutaneous nerves on the same side, all perforating the psoas major muscle anterolaterally. Yeole et al.[15] described a previously unreported case of LFCN origin from the ilioinguinal nerve, further broadening the spectrum of possible variations.

Cutaneous distribution (sensory territory)

After crossing the inguinal ligament and entering the thigh, the LFCN typically divides into two terminal branches: anterior and posterior. The anterior branch becomes superficial approximately 10 cm below the inguinal ligament and is distributed to the skin of the anterior and lateral aspects of the thigh, possibly extending to the knee region, where it communicates with branches of the anterior femoral cutaneous nerve and with the infrapatellar branch of the saphenous nerve, forming the peripatellar plexus[1].

The posterior branch perforates the fascia lata and is distributed posteriorly, innervating the skin over the greater trochanter and the lateral aspect of the thigh down to the middle region. However, Dias et al.[6] demonstrated that in 36% of cases the posterior branch is absent, correlating this finding with the fact that the symptoms of MP are frequently limited to the territory of the anterior branch. The presence of an accessory nerve was documented in 30% of the specimens in the same study, which contributes to the great individual variability of the sensory distribution area.

Lee et al.[16] correlated the anatomy of the LFCN with clinical findings in MP, demonstrating that the extent of the territory of pain and paresthesias is directly related to the branching pattern of the nerve and to the level at which compression occurs. This individual variability in the sensory territory explains why the map of symptom distribution may differ substantially between patients.

Vascularization of the nerve (vasa nervorum)

The blood supply of the LFCN is provided by a complex network of vasa nervorum, which includes longitudinal extrinsic vessels and an intraneural microvasculature. The main arterial supply of the nerve in the proximal thigh region is derived from the superficial circumflex iliac artery, a branch of the femoral artery. Miyazaki et al.[17] described in detail the concept of the LFCN–SCIP (superficial circumflex iliac artery perforator) neurovascular flap, in which the superficial circumflex iliac artery consistently accompanies the LFCN, allowing the harvesting of vascularized nerve grafts more than 15 cm in length.

The relevance of nerve vascularization to MP lies in the fact that, at points of angulation or compression — such as the passage beneath the inguinal ligament — the intraneural blood flow may be compromised, potentiating local ischemia. Suami et al.[18] mapped the angiosomes of the nerves of the lower limb, demonstrating that the vascularization of the LFCN depends on multiple segmental sources that may be interrupted at points of anatomical fixation.

Topographic relationships with surgical structures

Knowledge of the topographic relationships of the LFCN is fundamental for the planning of various surgical approaches. At the level of the inguinal ligament, the nerve maintains a constant relationship with the sartorius muscle and with the tensor fasciae lata, which constitute the two main anatomical landmarks for surgical localization of the nerve.

Grothaus et al.[12] documented that the nerve may be found up to 7.3 cm medial to the ASIS along the inguinal ligament and up to 11.3 cm distal along the sartorius muscle from the ASIS. These data defined a "danger zone" that must be considered during inguinal herniorrhaphy, iliac bone graft harvesting, abdominoplasty, and total hip arthroplasty via the anterior approach. Tomaszewski et al.[7] recommend maintaining a minimum distance of 3 cm from the ASIS during surgical procedures to reduce the risk of injury to the LFCN.

Regarding the fascia lata, Dias et al.[6] observed that in the first 3 cm after leaving the pelvis, the LFCN lies deep to the fascia lata, which allows dissection in the subcutaneous plane to be carried out with relative safety in the immediate proximity of the ASIS. Hanna[9] confirmed that the fascial canal accompanying the nerve is a constant structure, which reinforces the importance of identifying and opening this canal during decompression procedures.

For total hip arthroplasty via the direct anterior approach, the LFCN is the neural structure at greatest risk of iatrogenic injury. de Ridder et al.[10], in a study of 200 cadavers, documented variations in about 25% of individuals and developed a perioperative protocol that included intraoperative neurolysis or transection when injury was identified, reducing the incidence of persistent MP to zero at 12-month follow-up.

Applied anatomy and clinical correlations

The integration of the anatomical data discussed throughout this review allows identification of the points of vulnerability of the LFCN along its course and the compression mechanisms associated with each segment:

Intrapelvic segment: within the psoas major muscle, the nerve may be compressed by retroperitoneal tumors, psoas hematomas, or during transpsoas surgical approaches to the lumbar spine. Fixation of the nerve by the iliac fascia makes it vulnerable to traction forces during hip extension[4].

Pelvis–thigh transition: the aponeurotic-fascial tunnel described by Dias et al.[6], located between the iliopubic tract and the inguinal ligament, constitutes the main point of compression (Figure 2).

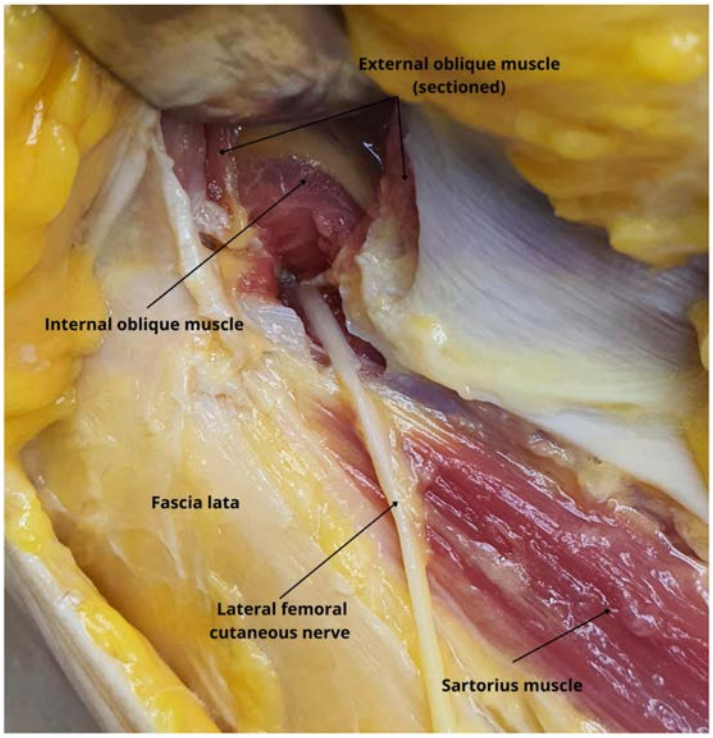

Figure 2. The tunnel formed by the iliopubic tract and the inguinal ligament at the pelvis–thigh transition is the main site of compression of the nerve. In this dissection of an unembalmed cadaver, a 360° decompression of the lateral femoral cutaneous nerve was simulated — one of the surgical techniques employed. Note that the inguinal ligament, the aponeurosis of the sartorius muscle, the aponeurosis of the external oblique muscle and the external oblique muscle itself were sectioned to allow wide decompression of the nerve. (Image courtesy of Dr. Mario Siqueira, Division of Neurosurgery, Hospital das Clínicas, FMUSP).

The formation of pseudoneuromas at this site attests to the existence of chronic microtrauma. Aszmann et al.[11] demonstrated that the anatomical types that position the nerve within the substance of the inguinal ligament or enveloped by the origin of the sartorius are at greater risk of compression.

Proximal thigh segment: the fascial canal described by Hanna et al.[9] may constitute an additional site of entrapment, particularly when thickened by inflammatory or fibrotic processes. In this segment, the superficial position of the nerve makes it vulnerable to extrinsic compression by belts, tight clothing, and personal protective equipment[19].

The incidence of MP has increased in recent decades, accompanying the growing prevalence of obesity, diabetes mellitus, and population aging. Parisi et al.[20] reported an incidence of 32.6 per 100,000 person-years, with significant associations with advanced age, elevated body mass index, and diabetes mellitus. The increase in abdominal volume promotes traction on the LFCN at its passage beneath the inguinal ligament, while metabolic neuropathy reduces the nerve's tolerance to mechanical compression, creating a synergistic scenario for the development of the syndrome.

From a therapeutic standpoint, anatomical knowledge of the variations of the LFCN is indispensable both for ultrasound-guided anesthetic block and for surgical decompression and neurectomy approaches. Becciolini et al.[21] reviewed the use of ultrasonography for identification of the nerve, highlighting that anatomical variations may significantly hinder echo-guided localization. The variability in the position of the nerve in relation to the inguinal ligament, described by Rossmann et al.[22], demonstrated that the ligament may function as an anatomical barrier that influences the dispersion of the local anesthetic during blocks.

CONCLUSION

The lateral femoral cutaneous nerve is anatomically simple in its classic textbook description but remarkably variable in reality. From its origin in the lumbar plexus to its terminal cutaneous branches, the nerve presents variability in its roots of origin, retroperitoneal course, relationship with the anterior superior iliac spine and inguinal ligament, number of branches, and sensory territory. This variability — reported in up to one quarter of individuals — underlies both the pathogenesis of meralgia paresthetica and the risk of iatrogenic injury during inguinal, pelvic, abdominal-wall and hip procedures. A thorough understanding of the danger zone around the ASIS, of the fascial tunnels that may entrap the nerve, and of the individual variability of its sensory distribution is therefore the cornerstone for safe surgery, accurate diagnosis, effective ultrasound-guided blockade and successful decompression. Future high-resolution imaging and anatomical studies may further refine the preoperative identification of these variations and reduce the burden of LFCN injury.

REFERENCES

1. Garg R, Li D, Bordoni B. Anatomy, bony pelvis and lower limb: lateral femoral cutaneous nerve. In: StatPearls [Internet]. Treasure Island (FL): StatPearls Publishing; 2025 [updated 2023 Aug 8]. Available from: https://www.ncbi.nlm.nih.gov/books/NBK532301/. Accessed: 1/6/2026.

2. Pearce JM. Meralgia paraesthetica (Bernhardt-Roth syndrome). J Neurol Neurosurg Psychiatry. 2006;77(1):84. https://doi.org/10.1136/jnnp.2005.072363. PMid:16361600.

3. Scholz C, Hohenhaus M, Pedro MT, Uerschels AK, Dengler NF. Meralgia paresthetica: relevance, diagnosis, and treatment. Dtsch Arztebl Int. 2023;120(39):655-61. PMid:37534445.

4. Haládaj R, Wysiadecki G, Macchi V, et al. Anatomic Variations of the Lateral Femoral Cutaneous Nerve: Remnants of Atypical Nerve Growth Pathways Revisited by Intraneural Fascicular Dissection and a Proposed Classification. World Neurosurg. 2018;118:e687-98. https://doi.org/10.1016/j.wneu.2018.07.021. PMid:30010076.

5. Reinpold W, Schroeder AD, Schroeder M, Berger C, Rohr M, Wehrenberg U. Retroperitoneal anatomy of the iliohypogastric, ilioinguinal, genitofemoral, and lateral femoral cutaneous nerve: consequences for prevention and treatment of chronic inguinodynia. Hernia. 2015;19(4):539-48. https://doi.org/10.1007/s10029-015-1396-z. PMid:26082397.

6. Dias LCFO, Valença MM, Guimarães FAF, et al. Lateral femoral cutaneous neuralgia: an anatomical insight. Clin Anat. 2003;16(4):309-16. https://doi.org/10.1002/ca.10106. PMid:12794914.

7. Tomaszewski KA, Popieluszko P, Henry BM, et al. The surgical anatomy of the lateral femoral cutaneous nerve in the inguinal region: a meta-analysis. Hernia. 2016;20(5):649-57. https://doi.org/10.1007/s10029-016-1493-7. PMid:27115766.

8. Majkrzak A, Johnston J, Kacey D, Zeller J. Variability of the lateral femoral cutaneous nerve: an anatomic basis for planning safe surgical approaches. Clin Anat. 2010;23(3):304-11. https://doi.org/10.1002/ca.20943. PMid:20169611.

9. Hanna A. The lateral femoral cutaneous nerve canal. J Neurosurg. 2017;126(3):972-8. https://doi.org/10.3171/2016.1.JNS152262. PMid:27104839.

10. de Ridder VA, de Lange S, Popta JV. Anatomical variations of the lateral femoral cutaneous nerve and the consequences for surgery. J Orthop Trauma. 1999;13(3):207-11. https://doi.org/10.1097/00005131-199903000-00009. PMid:10206253.

11. Aszmann OC, Dellon ES, Dellon AL. Anatomical course of the lateral femoral cutaneous nerve and its susceptibility to compression and injury. Plast Reconstr Surg. 1997;100(3):600-4. https://doi.org/10.1097/00006534-199709000-00008. PMid:9283556.

12. Grothaus MC, Holt M, Mekhail AO, Ebraheim NA, Yeasting RA. Lateral femoral cutaneous nerve: an anatomic study. Clin Orthop Relat Res. 2005;(437):164-8. https://doi.org/10.1097/01.blo.0000164526.08610.97. PMid:16056045.

13. Carai A, Fenu G, Sechi E, Crotti FM, Montella A. Anatomical variability of the lateral femoral cutaneous nerve: findings from a surgical series. Clin Anat. 2009;22(3):365-70. https://doi.org/10.1002/ca.20766. PMid:19173255.

14. Erbil KM, Sargon FM, Şen F, et al. Examination of the variations of lateral femoral cutaneous nerves: report of two cases. Anat Sci Int. 2002;77(4):247-9. https://doi.org/10.1046/j.0022-7722.2002.00014.x. PMid:12557420.

15. Yeole U, Zager EL, Hanna AS. A unique anatomical variation of the lateral femoral cutaneous nerve arising from the ilioinguinal nerve: illustrative case. J Neurosurg Case Lessons. 2025;9(10):CASE24790. https://doi.org/10.3171/CASE24790. PMid:40064014.

16. Lee SH, Shin KJ, Gil YC, Ha TJ, Koh KS, Song WC. Anatomy of the lateral femoral cutaneous nerve relevant to clinical findings in meralgia paresthetica. Muscle Nerve. 2017;55(5):646-50. https://doi.org/10.1002/mus.25382. PMid:27543938.

17. Miyazaki T, Tsukuura R, Yamamoto T, Daniel BW. Nerve vascularity in free vascularized nerve flaps. Glob Health Med. 2020;2(4):263-4. https://doi.org/10.35772/ghm.2020.01027. PMid:33330818.

18. Suami H, Taylor GI, Pan WR. Angiosome territories of the nerves of the lower limbs. Plast Reconstr Surg. 2003;112(7):1790-8. https://doi.org/10.1097/01.PRS.0000091161.95599.D8. PMid:14663222.

19. Cheatham SW, Kolber MJ, Salamh PA. Meralgia paresthetica: a review of the literature. Int J Sports Phys Ther. 2013;8(6):883-93. PMid:24377074.

20. Parisi TJ, Mandrekar J, Dyck PJ, Klein CJ. Meralgia paresthetica: relation to obesity, advanced age, and diabetes mellitus. Neurology. 2011;77(16):1538-42. https://doi.org/10.1212/WNL.0b013e318233b356. PMid:21975198.

21. Becciolini M, Pivec C, Riegler G. Ultrasound of the lateral femoral cutaneous nerve: a review of the literature and pictorial essay. J Ultrasound Med. 2022;41(5):1273-84. https://doi.org/10.1002/jum.15809. PMid:34387387.

22. Rossmann T, Zessner-Spitzenberg J, Sandurkov C, Heber UM, Weninger WJ, Meng S. Ultrasound-guided injections at the lateral femoral cutaneous nerve: the inguinal ligament as a Barrier. Pain Physician. 2020;23(4):E363-8. PMid:32709182.

CORRESPONDING AUTHOR

Samuel Pedro Pereira Silveira, MS
Medical Student
Faculty of Medicine, Universidade Federal do Triângulo Mineiro
Uberaba, Minas Gerais, Brazil
E-mail: sppsilveira.md@gmail.com

Funding: *nothing to disclose.*
Conflicts of interest: *nothing to disclose.*

CrediT

Samuel Pedro Pereira Silveira: Conceptualization; Investigation; Writing – Original Draft. Carlos Umberto Pereira: Conceptualization; Writing – Review & Editing.

Desde 1994

Jusimed

Produtos para Saúde

Tradição em dispositivos médicos.

Inovação em soluções para a saúde.

MIETHKE proGAV® 2.0

MIETHKE GAV®

Lyoplant®

Clipes Yasargil®

Matriz

(41) **3303-7661**

Rua Marcelino Nogueira, 419,
Bacacheri 82510-270 - Curitiba / PR

jusimed@jusimed.com.br

Filial

(51) **3058-5600**

Av. Carlos Gomes, 1155 - Auxiliadora
90480-004 - Porto Alegre / RS

administrativo.rs@jusimed.com.br

Angiocentric Glioma: a multidisciplinary diagnosis

Glioma Angiocêntrico: um diagnóstico multidisciplinar

Lygia Câmara[1]
Francisco Eduardo Penna Doutel de Andrade[2]
Almir Salgado Maurício[1]
Raphael Souza Ribeiro[1]
Matheus Guilherme Marques Vidal Barboza[2,3]
José Álvaro Bastos Pinheiro[2]

ABSTRACT

Introduction: *Study of a case of an invasive intraparenchymal frontal tumor with a difficult final diagnosis, Angiocentric Glioma (ACG).* **Objective:** *To present a rare case of difficult diagnosis, made possible through a multidisciplinary study, with clinical, neuroradiological, surgical and anatomopathological data.* **Method:** *Comparative study between the case presentation, with the findings of Magnetic Resonance Imaging (MRI) of the Skull, confronted with the anatomopathological results, using light microscopy (OM) as well as immunohistochemistry (IHC).* **Results:** *Comparing the neuroradiological and anatomopathological findings allowed the final diagnosis of ACG.* **Conclusion:** *Considering the clinical, neuroradiological and anatomopathological data, using the consulted literature, the diagnosis of a malignant glioma of a typical angiocentric subtype was possible, with implications not only for classification, but also for therapeutic conduct.*

Keywords: *Angiocentric Glioma (ACG); MRI; Anatomopathology.*

RESUMO

Introdução: *Estudo de um caso de tumor invasivo intraparenquimatoso frontal de difícil diagnóstico final, o Glioma Angiocêntrico (GAC).* **Objetivo:** *Apresentar um caso raro de difícil diagnóstico, possibilitado através do estudo multidisciplinar, com os dados clínicos, neurorradiológicos, cirúrgicos e anatomopatológicos.* **Método:** *Estudo comparativo entre a apresentação do caso, com os achados pela Ressonância Magnética (RM) do Crânio., confrontados com os resultados anatomopatológicos, usando microscopia óptica (MO) bem como imunohistoquímica (IHQ).* **Resultados:** *Comparando os achados neurorradiológicos e anatomopatológicos, permitiram o diagnóstico final de GAC.* **Conclusão:** *Considerando-se os dados clínicos, neurorradiológicos e anatomopatológicos, valendo-se da literatura consultada, o diagnóstico de um glioma maligno de típico subtipo angiocêntrico se fez possível, com implicações não só classificatórias, como na conduta terapêutica.*

Palavras-Chave: *Glioma Angiocêntrico; Ressonância Magnética; Anatomia Patológica.*

[1]Anatomopathological Service – APS, Hospital Municipal Salgado Filho – HMSF/RJ, Rio de Janeiro, RJ, Brazil.
[2]Neurosurgery Service – NSS, Hospital Municipal Salgado Filho – HMSF/RJ, Rio de Janeiro, RJ, Brazil.
[3]School of Medicine, Federal Fluminense University – UFF/RJ, Niteroi, RJ, Brazil.

Received Feb 27, 2026
Corrected Apr 6, 2026
Accepted Jun 11, 2026

INTRODUCTION

Angiocentric glioma (ACG) is considered a rare tumor[1-5]. It was described in 2002 by Wang as Angiocentric Bipolar Astrocytoma, in 2005 as Angiocentric Glioma, and in 2007 it was classified by the World Health Organization (WHO) as an isolated entity in the group "other neuroepithelial tumors" of uncertain origin[6,7]. In the 2021 classification (5th edition) of the World Health Organization as a "low grade" pediatric[7].

It is a slow-growing tumor usually in the frontal and temporal cortex, with a history of medication-refractory epileptic seizures[8-10]. Histopathologically, by light microscopy, it has a monotonous appearance of bipolar cells and a structure of cells radially arranged around vessels constituting a perivascular pseudorosette, which gives it the name Angiocentric glioma[4,7]. This structure is seen in other gliomas, mainly astrocytomas, oligodendrogliomas, ependymomas, and even glioblastomas, which leads to the difficulty of a precise histogenesis[7,11,12]. Added to this difficulty is the intratumoral heterogeneity of gliomas[7,10,13]. In the same tumor, we can have areas of "low grade" and areas of malignancy[10,13]. This is an aspect discussed in the literature, mainly among glioblastoma multiforme (GBM)[14]. The authors analyze what would be the pathognomonic characteristic to characterize it as an isolated identity.

Our objective is 1) to demonstrate the limitations of histopathological diagnoses using light microscopy, as observed in the literature when consensus with multiple neuropathologists is required; 2) to emphasize the importance of the neurosurgeon as the initial factor in choosing the specimen to be examined due to the heterogeneity of gliomas; and 3) to compare our case with the international literature.

MATERIALS AND METHODS

Case presentation and neuroradiological and neuropathological study, magnetic resonance imaging (MRI) of the skull compared with the histopathological analysis (AP) of the surgical specimen resulting from the frontal tumor excision, hematoxylin and eosin (H&E) study under light microscopy, and immunohistochemical study (IHC). A literature review of 142 cases of ACG was performed in PUBMED by NCBI.

CASE PRESENTATION

Patient MRF, female, 71 years old (born on 10/06/1952), brown-skinned, housewife, widowed, born and resident in the city of Rio de Janeiro, was admitted to Hospital Municipal Salgado Filho (HMSF) on 07/19/2023, Registration: 759317, accompanied by her daughter, reporting that since the end of June/23 she began to experience progressive loss of muscle strength on the right, dysarthria and disorientation. Initially treated at the Emergency Care Unit (UPA), where they requested a Magnetic Resonance Imaging (MRI) of the Skull (Figures 1 and 2), which was performed before being admitted to HMSF. Patient with systemic arterial hypertension (HAS), using Atenolol 50mg/day, Hydrochlorothiazide 25mg/morning and Enalapril 10mg 2X/day, in addition to Omeprazole 20mg/morning. Upon admission to the HMSF, the patient was awake, dysphasic, with right hemiparesis and partial cognitive impairment. Her Glasgow Coma Scale (GGS) was 14 points (Ocular 4, Verbal 4, Motor 6), was isochoric, and photoreactive.

The patient underwent left fronto-parieto-temporal craniotomy for resection of the expansile lesion. Lesion enucleation with a safety perimeter margin was performed, as per protocol. The surgical specimen was sent for pathological analysis. She spent the immediate postoperative period in the ICU, maintaining intubation and mechanical ventilation. On August 18, 2023, she was eupneic on room air, with a Glasgow Coma Scale (GGS) 12 points (Eye Opening 4, Verbal 2, Motor 6), aphasia, and right hemiplegia. She was discharged from the ICU on August 21, 2023, and returned to the ward. The patient developed progressive deterioration in consciousness, with secretions in the airways and an infectious condition, pneumonia, and was undergoing respiratory and antibiotic therapies. The patient maintained a 10-point Glasgow Coma Scale (Eye Opening 3, Verbal 2, Motor 5), aphasia, and right hemiplegia. SaO2 was 95% with a Hudson mask, macronebulization, and O_2 was 3 L/min. She died on September 3, 2023, from pneumonic sepsis.

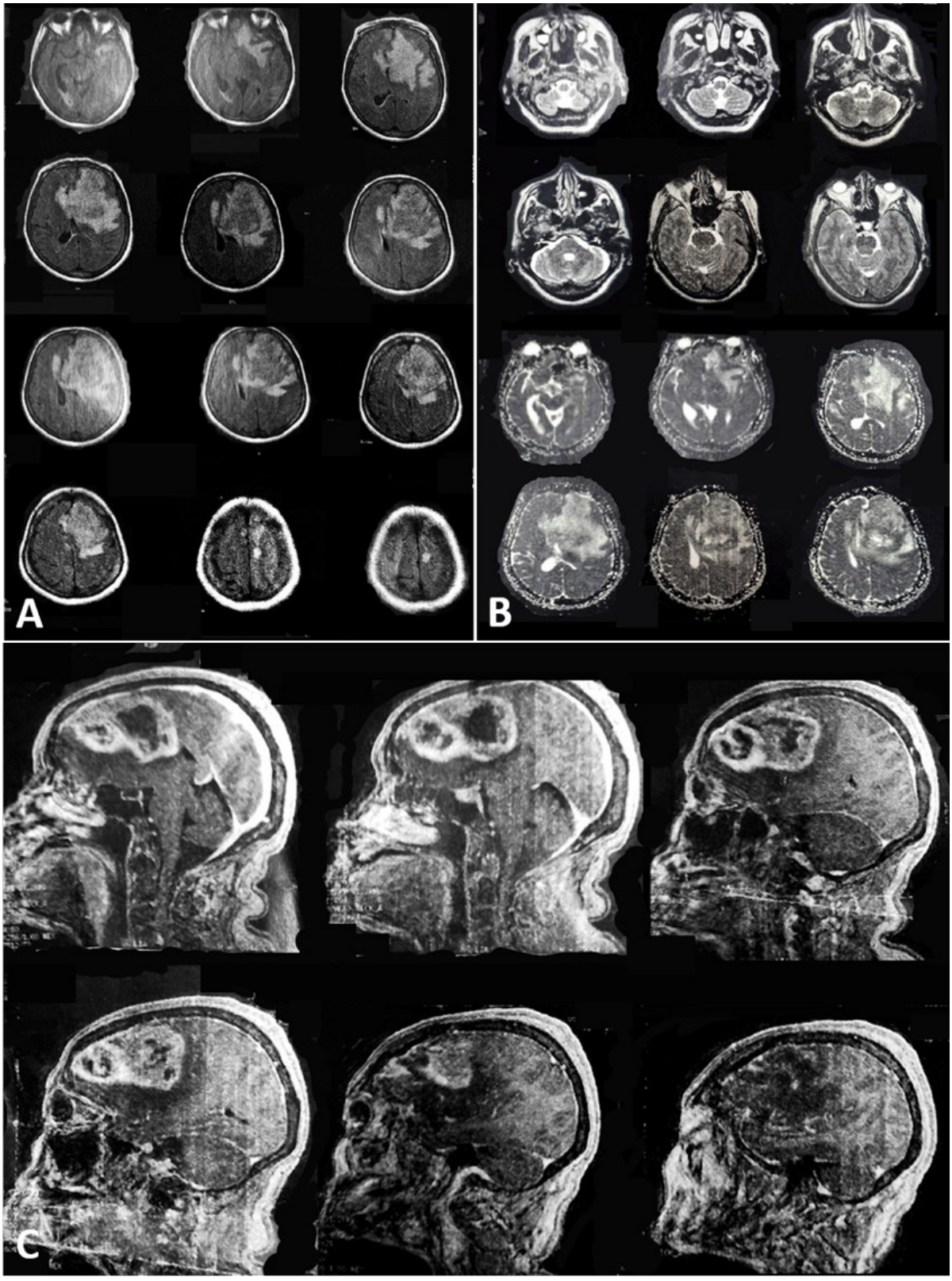

Figure 1. MRI. **A.** Axial Flair. **B.** Axial T2. **C.** Sagittal FLAIR. MRI showing the described lesion, infiltrative, invasive, with necrotic center and perilesional edema, accompanied by significant mass effect and anterior transcallosal expansion to the right hemisphere.

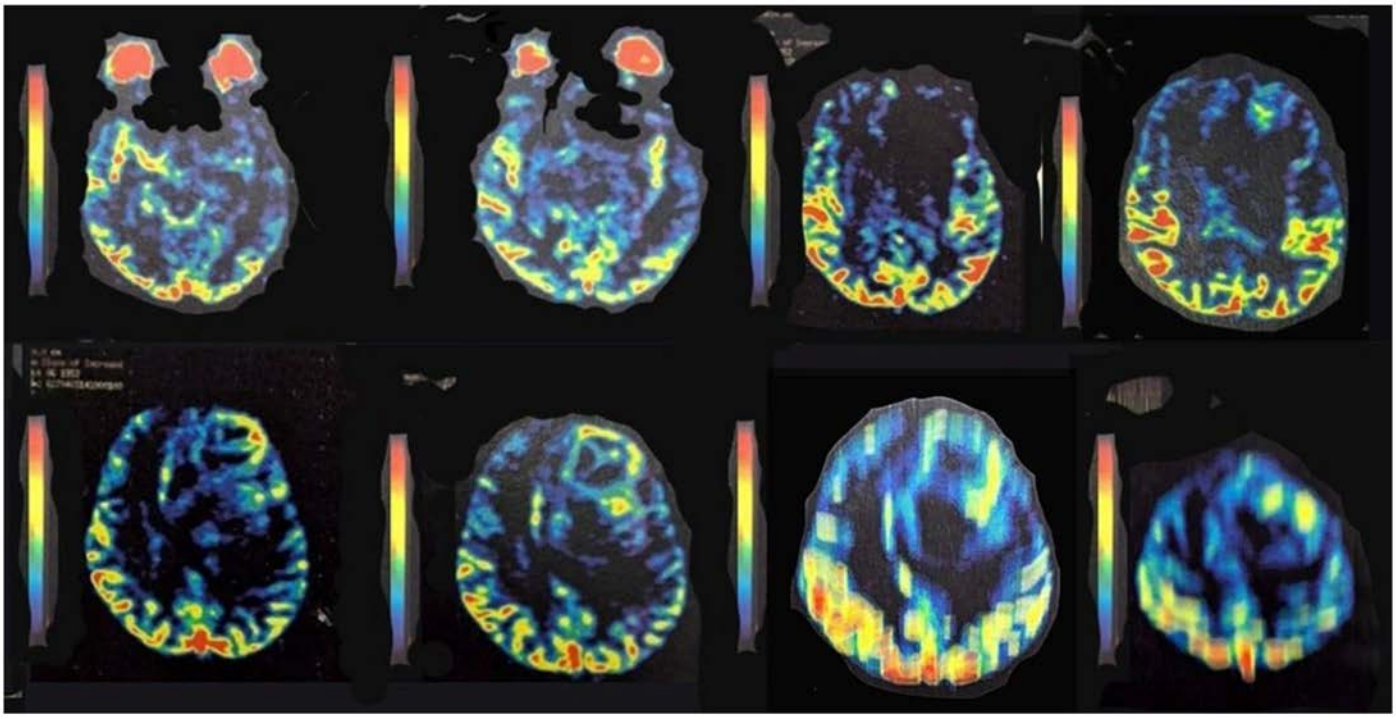

Figure 2. MRI with Perfusion Study using the ASL (Arterial Spin Labeling) technique, which eliminates the need for exogenous contrast injection. The study shows uptake with a pattern of high metabolic activity, with a low signal center (necrosis), as well as subcortical expansion, characterizing the high aggressiveness of the lesion in the white matter.

RESULTS

Clinical study

Patient with neurological findings suggestive of a brain injury involving the left hemisphere, with frontal topography, causing aphasia and right-sided motor deficits. Progressive onset and cognitive deterioration, suggesting the possibility of an intracranial expansive lesion, considering the patient's age.

Neuroradiological study

Cranial MRI, Labs (A+), Rio de Janeiro, RJ, BR. Registration: 6270403141

Examination performed using intravenous paramagnetic contrast. Large, expansive, heterogeneous infiltrative lesion with areas of necrosis and bleeding, restricted diffusion, contrast enhancement, and hyperperfusion, measuring approximately 8.5 x 6.5 cm in the largest transverse diameters, in the left frontal lobe, extending from the cortex deep to the periventricular region, where it infiltrates the corpus callosum and crosses into the right cerebral hemisphere. The infiltrative lesion extends anteriorly into the right frontal lobe to the straight and superior frontal gyri, where it is best identified, with hyperintense signal on FLAIR and T2-weighted images, and does not exhibit contrast enhancement, diffusion restriction, or hyperperfusion. Perilesional vasogenic edema. Contralateral midline shift of 2.3 cm with subfalcon herniation. Supratentorial ventricles are compressed, with associated periependymal edema, especially in the posterior extension of the right lateral ventricle. Brainstem and cerebellum show usual signal. Impression: Large, expansive infiltrative neoplasm in the left frontal lobe, extending through the corpus callosum to the right frontal lobe. Indicative of an aggressive, high-grade diffuse glioma (glioblastoma). Subfalcon herniation is present with significant contralateral midline shift (Figures 1 and 2).

Anatomopathological study

a. Macroscopic: fragments of brain tissue represented by cortex and white matter, yellowish areas, sometimes without a clear boundary between cortex and white matter, measuring 6.5 x 6.0 cm (Figure 3). The initial diagnostic hypothesis was low-grade glioma.

b. Light microscopy (LM) with hematoxylin and eosin (H&E): showed areas with monomorphic cells, some inflammatory, exuberant vascularization, gemistocytic-type astrocytes, recanalized vessels, and a radial arrangement of cells, but without a clear pseudorosette pattern. No palisade necrosis or glomeruloid-type vascular formations, as would be expected in GBM, were found. (Figure 4 A and B).

c. Considering the immunohistochemistry (IHC) study performed by DASA (Diagnóstico América S.A.), which was positive for GFAP (astrocytic fibrillary acidic protein), showing pseudorosettes, slightly reactive OLIG 2, positive ATRX (retained expression), and a dot pattern of EMA (epithelial membrane antigen), negative for P53 and IDH1 (isocitrate dehydrogenase), compatible with the diagnosis of angiocentric glioma, the second diagnostic hypothesis (Figures 5 and 6).

Figure 3. Macroscopic view. Tumor lesion measuring 6.5 x 5 cm. Cortical areas sometimes without precise borders and yellowish in color.

When comparing the neuroradiological findings (MRI and PET scan) with those of the BM and IHC, the third and definitive diagnostic hypothesis was considered: angiocentric glioma with malignant behavior. Likewise, with the anatomopathological examination correlating with the neuroimaging, the differential diagnostic hypotheses (metastasis, lymphoma, abscess) were excluded, corroborating that it was a GBM with the typical "butterfly" formation, with the final report of angiocentric glioma with radiological characteristics of malignancy.

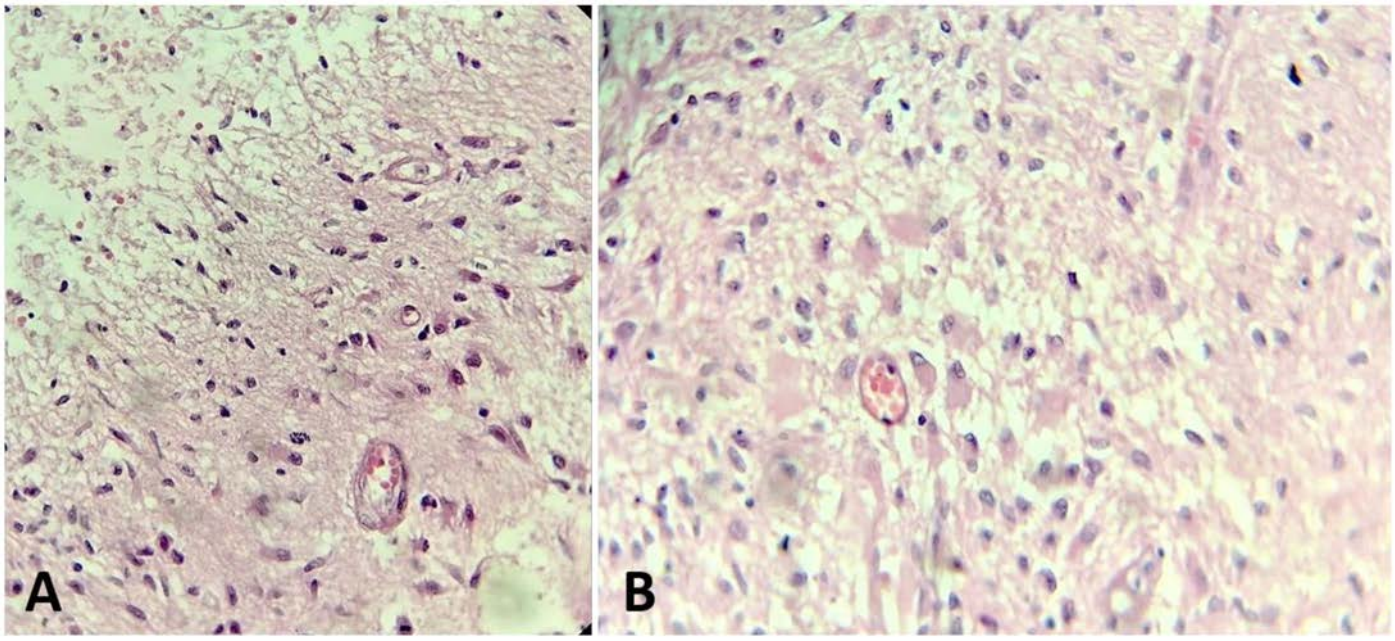

Figure 4. Optical Microscopy (OM). Hematoxylin-Eosin (H&E). 40X. **A.** Moderate cell density, a monomorphism of cells with elongated and some rounded nuclei. Vessel without evident angiocentrism. **B.** Area with gemestocytic astrocyte-type cells (nucleus pushed to the periphery and turgid and eosinophilic cytoplasm) in the center of the image.

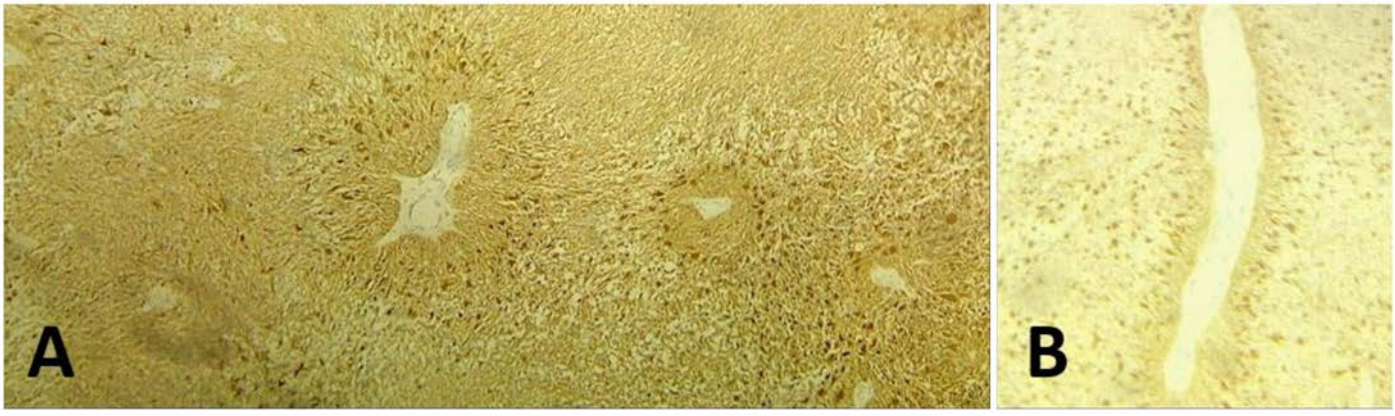

Figure 5. MO. Immunohistochemistry (IHC) GFAP. **A**. 40x. Vascular pseudorosettes (vessel in the center and astrocytic cells in a radial position to the vessel lumen). **B**. 100x. Shows the radial characteristic around the vessel, quite different from Flexner and Wright.

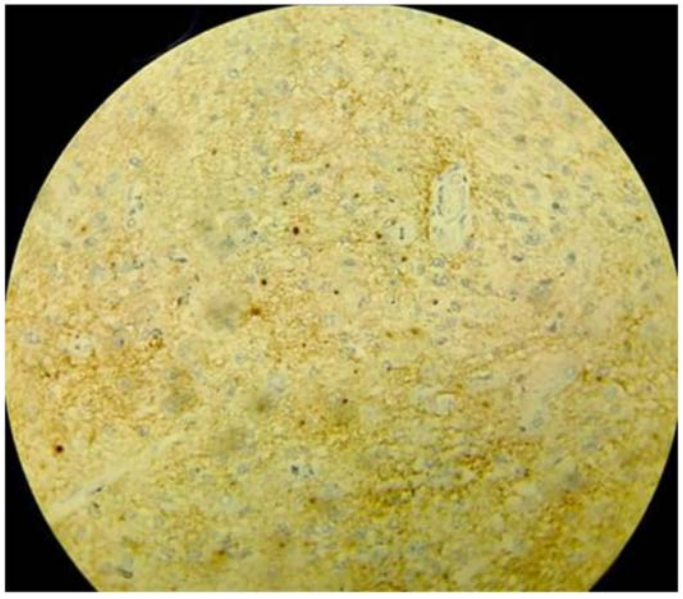

Figure 6. IHQ, EMA. 40x. Showing positivity in points.

DISCUSSION

The proposed surgery for a lesion with a neuroradiological appearance typical of an invasive lesion, including extension into the commissural white matter, forming an "anterior butterfly lesion" appearance through the corpus callosum's rostrum, was supported by the following factors:[3,15,16]

1. Karnoffsky score above 70%.
2. Accurate and reliable diagnosis of the lesion's nature.
3. Requirement for a histopathological report, which allows access to adjuvant therapies (radiation and/or chemotherapy).
4. Reduction in intracranial pressure and risk of death in the short term.
5. Possibility of improving quality of life and relatively prolonging its duration.

This is a very rare case of ACG in a patient (71 years old) with no history of epileptic seizures and with characteristics of high-grade glioma.

Until 1917, there was only one case reported in the literature involving a patient over 65 years of age[17,18].

The authors compared the isolated morphological diagnosis by optical microscopy with the multidisciplinary diagnosis by a neurosurgeon and complementary exams, confirming a necessary thesis of multidisciplinary diagnosis in cerebral gliomas.

1. Morphological heterogeneity of intratumoral glioma complicates the final diagnosis.
2. Is angiocentric glioma an isolated entity?
3. The diagnosis of gliomas requires multidisciplinary analysis in conjunction with a neurosurgeon.

We must consider that our case is extremely rare and, if diagnosed as angiocentric glioma, we would have many questions. We will focus on the issue that is currently the core of the diagnosis.

First, to understand the issues we have presented here, we will make some considerations in comparison with the literature. Gliomas are tumors originating from astrocytes, oligodendrocytes, and some authors include ependymoma[1,4-7,14]. We must consider that these cells will present with their own characteristics in any brain topography[1,7,14,19]. Their arrangements will give the tumor a particular appearance; for example, perivascular structures, pseudorosettes, multinucleated cells, cysts, myxoid appearance, etc[4,5,7,14,19].

In our particular case, pseudorosettes, which constitute a fundamental element in angiocentric glioma, can be present in astrocytomas, oligodendrogliomas, glioblastomas, and ependymomas[5,7,14,19-21].

We want to emphasize that this term will be found in structures that do not actually present tangentially as in ACG. For example, in lymphomas that are arranged circularly[14,22,23].

With a generally cortical topography, like other tumors, they can deviate from the norm and present in the brainstem, cerebellum, midbrain, and even the spinal cord. This presentation is justified by the fact that brain cells with structural tissue modifications are present throughout the brain and spinal cord[24-28].

Regarding the age group: although classified as pediatric tumors by the World Health Organization, they can be seen in the elderly[24,25,29,30].

Epilepsy is found in any tumor located in the temporal lobe, and the cellular specificity of the tumor is not commonly accepted[9,10,17,27,31]. However, the surrounding tissue that causes the epileptic seizure, such as ACG in the midbrain, does not cause epileptic seizures in the brainstem[24,25,27].

In terms of treatment, the best approach is total excision. It is not a unique aspect of ACG[28].

The potential for malignancy is another aspect common to gliomas. It is worth noting that in brain tumors, the following forms should be considered as the worst diagnosis that could be called malignant[7,10,29]: 1. Tumor morphology; 2. Biological behavior; and 3. Topography.

For example, a "low-grade" tumor in the midbrain or even the pons, despite benign histology, has a poor prognosis because complete resection is not possible[4,13,15,19]. Conversely, a GBM in the cerebral cortex with total excision has a better chance of biological behavior than the same tumor in the basal ganglia[7,14].

The anatomopathological examination best characterizes Angiocentric Glioma (ACG), as the name suggests[19,30,32,33]. Besides, the ACG can degenerate into anaplastic ependymoma[34].

The literature is unanimous in stating that in ACG, immunohistochemistry reveals positivity for GFAP, Oligo2, and EMA (epithelial membrane antigen), negativity for IDH1, and negative[11,32,35-41]. This was confirmed in the case presented, allowing a diagnosis compatible with ACG.

Of course, since it is considered rare in this age group and without epileptic seizures, as in our case, there are many questions, and molecular and genetic studies are needed[40-42].

Regarding molecular genetics, our study is limited to IDH testing, which showed negativity. While the diagnosis of ACG is consistent with the literature we consulted in this study, a striking feature of the latter classification is the classification of pediatric low-grade gliomas and adult low-grade gliomas as separate entities, precisely because it is negative in children, which is not generally the case in adults[12,33,42-45].

CONCLUSION

Our findings, both within the anatomopathological definition and the rarity of the age group (the patient was 71 years old), as well as the potential for malignancy, are consistent with the NCBI PubMed literature.

The diagnosis of a glioma, both in terms of its origin and its degree of malignancy, should be joint and/or multidisciplinary: a neuroradiologist, neurosurgeon, and neuropathologist, to ensure the three pillars that support the correct diagnosis: imaging, surgery, and histopathology.

Based on the type of surgery performed, gliomas are heterogeneous in their intralesional plurality. This requires sampling multiple areas of the lesion to ensure a broad and safer sample. Future studies are needed to determine whether ACG is an isolated tumor or simply a structural arrangement of gliomas, such as ependymoma, astrocytoma, and glioblastoma.

REFERENCES

1. Adamek D, Siwek GP, Chrobak AA, et al. Angiocentric glioma from a perspective of A-B-C classification of epilepsy associated tumors. Folia Neuropathol. 2016;54(1):40-9. https://doi.org/10.5114/fn.2016.58914. PMid:27179220.

2. Aguilar HN, Hung RW, Mehta V, Kotylak T. Imaging characteristics of an unusual, high-grade angiocentric glioma: a case report and review of the literature. J Radiol Case Rep. 2012;6(10):1-10. PMid:23378871.

3. Alexandru D, Haghighi B, Muhonen MG. The treatment of angiocentric glioma: case report and literature review. Perm J. 2013;17(1):e100-2. https://doi.org/10.7812/TPP/12-060. PMid:23596378.

4. Wang M, Tihan T, Rojiani AM, et al. Monomorphous angiocentric glioma: a distinctive epileptogenic neoplasm with features of infiltrating astrocytoma and ependymoma. 2005 Oct;64(10):875-81. PMid:16215459.

5. Kuncman W, Braun M, Kuncman L, et al. A malignant astrocytoma with uncommon angiocentric features and dot-like EMA expression. Contemp Oncol (Pozn). 2018;22(3):205-8. https://doi.org/10.5114/wo.2018.78944. PMid:30455594.

6. Miyata H, Ryufuku M, Kubota Y, Ochiai T, Niimura K, Hori T. Adult-onset angiocentric glioma of epithelioid cell-predominant type of the mesial temporal lobe suggestive of a rare but distinct clinicopathological subset within a spectrum of angiocentric cortical ependymal tumors. Neuropathology. 2011;32(5):479-91. https://doi.org/10.1111/j.1440-1789.2011.01278.x. PMid:22151480.

7. Patel T, Singh G, Goswami P. Recent updates in pediatric diffuse glioma classification: insights and conclusions from the WHO 5th edition. J Med Life. 2024;17(7):665-70. https://doi.org/10.25122/jml-2023-0515. PMid:39440342.

8. Chatterjee D, Gupta K, Singla N, Radotra BD. Angiocentric glioma of hippocampus-report of a rare intractable epilepsy-related tumor. Neurol India. 2016;64(2):340-3. https://doi.org/10.4103/0028-3886.177627. PMid:26954821.

9. Buccoliero AM, Caporalini C, Scagnet M, et al. Angiocentric glioma-associated seizures: the possible role of EAAT2, pyruvate carboxylase and glutamine synthetase. Seizure. 2021;86:152-4. https://doi.org/10.1016/j.seizure.2021.02.014. PMid:33621827.

10. Habberstad AH, Lind-Landström T, Sundstrøm S, Torp SH. Primary human glioblastomas - prognostic value of clinical and histopathological parameters. Clin Neuropathol. 2012;31(09):361-8. https://doi.org/10.5414/NP300439. PMid:22939176.

11. Satomi K, Shibayama T, Hibiya T, et al. MYB:QKI fusion-positive diffuse glioma of the cerebellum: A case report. Neuropathology. 2025;45(3):228-33. https://doi.org/10.1111/neup.13016. PMid:39569742.

12. Takada S, Iwasaki M, Suzuki H, Nakasato N, Kumabe T, Tominaga T. Angiocentric glioma and surrounding cortical dysplasia manifesting as intractable frontal lobe epilepsy – Case Report. Neurol Med Chir (Tokyo). 2011;51(7):522-6. https://doi.org/10.2176/nmc.51.522. PMid:21785249.

13. Buccoliero AM, Franchi A, Castiglione F, et al. Subependymal giant cell astrocytoma (SEGA): is it an astrocytoma? Morphological, immunohistochemical and ultrastructural study. Neuropathology. 2009;29(1):25-30. https://doi.org/10.1111/j.1440-1789.2008.00934.x. PMid:18564101.

14. Gupta S, Rangari KV, Mehrotra A, Pal L, Jaisawal AK, Kumar R. Temporal lobe angiocentric glioma with oligodendroglioma-like areas: a rare association of an uncommon tumor. A case report with review of literature. Childs Nerv Syst. 2020;36(3):641-6. https://doi.org/10.1007/s00381-019-04445-0. PMid:31897632.

15. Han G, Zhang J, Ma Y, Gui Q, Yin S. Clinical characteristics, treatment and prognosis of angiocentric glioma. Oncol Lett. 2020;20(2):1641-8. https://doi.org/10.3892/ol.2020.11723. PMid:32724405.

16. Ampie L, Choy W, DiDomenico JD, et al. Clinical attributes and surgical outcomes of angiocentric gliomas. J Clin Neurosci. 2016;28:117-22. https://doi.org/10.1016/j.jocn.2015.11.015. PMid:26778052.

17. Jin X, Abdullaev Z, Butman JA, et al. A 64-year-old woman with frontal lobe lesion and drug-resistant epilepsy. Brain Pathol. 2023;33(1):e13133. https://doi.org/10.1111/bpa.13133. PMid:36490308.

18. Gonzalez-Quarante LH, Carballal CF, Agarwal V, López AJ, Corral OLGS, Vendrell ES. angiocentric glioma in an elderly patient: case report and review of the literature. World Neurosurg. 2017;97:755. https://doi.org/10.1016/j.wneu.2016.10.034. PMid:27756673.

19. Amatya VJ, Akazawa R, Sumimoto Y, Takeshima Y, Inai K. Clinicopathological and immunohistochemical features of three pilomyxoid astrocytomas: comparative study with 11 pilocytic astrocytomas. Pathol Int. 2009;59(2):80-5. https://doi.org/10.1111/j.1440-1827.2008.02332.x. PMid:19154260.

20. Kurokawa R, Baba A, Emile P, et al. Neuroimaging features of angiocentric glioma: A case series and systematic review. J Neuroimaging. 2022;32(3):389-99. https://doi.org/10.1111/jon.12983. PMid:35201652.

21. Miyahara H, Toyoshima Y, Natsumeda M, et al. Anaplastic astrocytoma with angiocentric ependymal differentiation. Neuropathology. 2011;31(3):292-8. https://doi.org/10.1111/j.1440-1789.2010.01161.x. PMid:21062363.

22. Bhattacharjee R, Gupta M, Singh T, et al. Role of intra-tumoral vasculature imaging features on susceptibility weighted imaging in differentiating primary central nervous system lymphoma from glioblastoma: a multiparametric comparison with pathological validation. Neuroradiology. 2022;64(9):1801-18. https://doi.org/10.1007/s00234-022-02946-5. PMid:35435463.

23. Hiniker A, Lee HS, Chang S, Berger M, Perry A. Cortical ependymoma with unusual histologic features. Clin Neuropathol. 2013;32(4):318-23. https://doi.org/10.5414/NP300593. PMid:23458270.

24. Almubarak AO, Alahmari A, Hindi HA, AlShail E. Angiocentric glioma of brainstem. Neurosciences (Riyadh). 2020;25(5):416-20. https://doi.org/10.17712/nsj.2020.5.20200026. PMid:33459294.

25. Covington DB, Rosenblum MK, Brathwaite CD, Sandberg DI. Angiocentric Glioma-Like Tumor of the Midbrain. Pediatr Neurosurg. 2009;45(6):429-33. https://doi.org/10.1159/000277616. PMid:20110754.

26. D'Aronco L, Rouleau C, Gayden T, et al. Brainstem angiocentric gliomas with MYB-QKI rearrangements. Acta Neuropathol. 2017;134(4):667-9. https://doi.org/10.1007/s00401-017-1763-1. PMid:28803398.

27. Liu CQ, Zhou J, Qi X, Luan GM. Refractory temporal lobe epilepsy caused by angiocentric glioma complicated with focal cortical dysplasia: a surgical case series. J Neurooncol. 2012;110(3):375-80. https://doi.org/10.1007/s11060-012-0975-4. PMid:23065092.

28. Lu JQ, Patel S, Wilson BA, Pugh J, Mehta V. Malignant glioma with angiocentric features. J Neurosurg Pediatr. 2013;11(3):350-5. https://doi.org/10.3171/2012.11.PEDS12234. PMid:23240849.

29. Purkait S, Mahajan S, Sharma MC, Sarkar C, Suri V. Pediatric-type diffuse low grade gliomas: histomolecular profile and practical approach to their integrated diagnosis according to the WHO CNS5 classification. Indian J Pathol Microbiol. 2022;65(Suppl):S42-9. PMid:35562133.

30. Rosemberg S. Long-term epilepsy associated-tumors (LEATs): what is new? Arq Neuropsiquiatr. 2024;81(12):1146-51. PMid:38157880.

31. Kakkar A, Sharma MC, Suri V, et al. Angiocentric glioma: a treatable cause of epilepsy: report of a rare case. Neurol India. 2014;62(6):677-9. https://doi.org/10.4103/0028-3886.149405. PMid:25591686.

32. Ito T, Sato K, Oikawa M, et al. Clinicopathological study of pilomyxoid-spectrum astrocytomas: an analysis of the BRAF gene. Report of two cases. No Shinkei Geka. 2015;43(9):825-33. PMid:26321697.

33. Nagaishi M, Yokoo H, Hirato J, Yoshimoto Y, Nakazato Y. Clinicopathological feature of pilomyxoid astrocytomas: three case reports. Neuropathology. 2011;31(2):152-7. https://doi.org/10.1111/j.1440-1789.2010.01143.x. PMid:20667008.

34. McCracken JA, Gonzales MF, Phal PM, Drummond KJ. Angiocentric glioma transformed into anaplastic ependymoma: review of the evidence for malignant potential. J Clin Neurosci. 2016;34:47-52. https://doi.org/10.1016/j.jocn.2016.08.012. PMid:27742374.

35. Ferris SP, Hofmann JW, Solomon DA, Perry A. Characterization of gliomas: from morphology to molecules. Virchows Arch. 2017;471(2):257-69. https://doi.org/10.1007/s00428-017-2181-4. PMid:28674742.

36. Bandopadhayay P, Ramkissoon LA, Jain P, et al. MYB-QKI rearrangements in angiocentric glioma drive tumorigenicity through a tripartite mechanism. 2016 Mar 1;48(3):273-82.

37. Raghunathan A, Olar A, Vogel H, et al. Isocitrate dehydrogenase 1 R132H mutation is not detected in angiocentric glioma. Ann Diagn Pathol. 2012;16(4):255-9. https://doi.org/10.1016/j.anndiagpath.2011.11.003. PMid:22445362.

38. Pokharel S, Parker JR, Parker JC Jr, Coventry S, Stevenson CB, Moeller KK. Angiocentric glioma with high proliferative index: case report and review of the literature. Ann Clin Lab Sci. 2011;41(3):257-61. PMid:22075509.

39. Fuller LD, Prayson RA. Molecular immunohistochemical profile of angiocentric glioma. J Epilepsy Res. 2020;10(2):79-83. https://doi.org/10.14581/jer.20013. PMid:33659200.

40. Jesus-Ribeiro J, Rebelo O, Ribeiro IP, et al. The landscape of common genetic drivers and DNA methylation in low-grade (epilepsy-associated) neuroepithelial tumors: a review. Neuropathology. 2022;42(6):467-82. https://doi.org/10.1111/neup.12846. PMid:35844095.

41. Jain P, Saran RK, Singh D, Jagetia A, Srivastava AK, Singh H. Tanycytic ependymoma: highlighting challenges in radio-pathological diagnosis. Indian J Pathol Microbiol. 2021;64(4):633-7. https://doi.org/10.4103/IJPM.IJPM_1049_20. PMid:34673578.

42. Keser H, Barnes M, Moes G, Lee HS, Tıhan T. Well-differentiated pediatric glial neoplasms with features of oligodendroglioma, angiocentric glioma and dysembryoplastic neuroepithelial tumors: a morphological diagnostic challenge. Turk Patoloji Derg. 2014;30(1):23-9. https://doi.org/10.5146/tjpath.2013.01204. PMid:24448703.

43. Rho GJ, Kim H, Kim HI, Ju MJ. A case of angiocentric glioma with unusual clinical and radiological features. J Korean Neurosurg Soc. 2011;49(6):367-9. https://doi.org/10.3340/jkns.2011.49.6.367. PMid:21887397.

44. Wang H, Zhu J, Zhu P, Luo C. Angiocentric glioma: a case report and review of the literature. J Clin Neurosci. 2021;94:179-85. https://doi.org/10.1016/j.jocn.2021.10.016. PMid:34863434.

45. Shakur SF, McGirt MJ, Johnson MW, et al. Angiocentric glioma: a case series. J Neurosurg Pediatr. 2009;3(3):197-202. https://doi.org/10.3171/2008.11.PEDS0858. PMid:19338465.

CORRESPONDING AUTHOR

Lygia Câmara, MD
Neuropathologist
Anatomopathological Service – APS
Hospital Municipal Salgado Filho – HMSF/RJ
Rio de Janeiro, Rio de Janeiro, Brazil.
e-mail: lygiacamara3@gmail.com

Funding: *nothing to disclose.*
Conflicts of interest: *nothing to disclose.*
Ethics Committee *Approval: waived.*

Institution: *Hospital Municipal Salgado Filho (HMSF/RJ), Neurosurgery Service (NSS), Rio de Janeiro, RJ, Brazil. Hospital Naval Marcílio Dias. (HNMD), NSS, Rio de Janeiro, RJ, Brazil.*

CRediT

Lygia Câmara: Conceptualization, Investigation, Formal Analysis, Resources, Data Curation, Writing – Original draft, Supervision. Francisco Eduardo Penna Doutel de Andrade: Methodology, Software, Writing – Review & Editing, Supervision. Almir Salgado Maurício: Resources, Data Curation, Formal Analysis. Raphael Souza Ribeiro: Resources, Data Curation. Matheus Guilherme Marques Vidal Barboza: Investigation, Resources. José Álvaro Bastos Pinheiro: Resources, Validation,

Is Prophylactic Anticonvulsant Use Necessary in Chronic Subdural Hematoma? A case report and literature review

O Uso Profilático de Anticonvulsivante é Necessário em Caso de Hematoma Subdural Crônico? Relato de caso e revisão da literatura

Carlos Umberto Pereira[1]
Samuel Pedro Pereira Silveira[2]

ABSTRACT

Introduction: *Seizures are uncommonly reported in patients with chronic subdural hematoma (CSDH). The incidence of seizures in the postoperative period after burr-hole drainage of CSDH is considered low. The prophylactic use of anticonvulsant drugs in the pre- and postoperative period of CSDH remains controversial.* **Case presentation:** *We report a 79-year-old man with chronic alcoholism who, one month after a fall from his own height, presented with headache, a generalized seizure, drowsiness, and left hemiparesis. Cranial computed tomography showed a mixed-density subdural hematoma in the right hemisphere. He underwent burr-hole drainage but developed seizures in the immediate postoperative period, with neurological deterioration that progressed to death.* **Methods:** *A case report combined with a narrative review of the literature was conducted using the PubMed/MEDLINE, LILACS, and SciELO databases (1970-2024).* **Conclusion:** *The use of anticonvulsant drugs in patients with CSDH remains controversial, and no consensus has been reached regarding prophylaxis.*

Keywords: *Chronic subdural hematoma; Status epilepticus; Anticonvulsants; Seizures*

RESUMO

Introdução: *Convulsão é incomum ser relatada em paciente com hematoma subdural crônico (HSDC). A incidência de crises convulsivas no pós-operatório da drenagem do HSDC por trepanação (burr-hole) é considerada baixa. O uso profilático de drogas anticonvulsivantes no pré e pós-operatório do HSDC tem sido controverso.* **Descrição do caso:** *Homem de 79 anos, alcoolista crônico, que um mês após queda da própria altura apresentou cefaleia, crise convulsiva generalizada, sonolência e hemiparesia esquerda. A tomografia computadorizada de crânio evidenciou hematoma subdural de densidade mista no hemisfério cerebral direito. Foi submetido a drenagem por trepanação, porém apresentou crises convulsivas no pós-operatório imediato, com piora neurológica e evolução para óbito.* **Método:** *Relato de caso associado a revisão narrativa da literatura nas bases PubMed/MEDLINE, LILACS e SciELO (1970-2024).* **Conclusão:** *O uso de drogas anticonvulsivantes no paciente com HSDC permanece controverso, sem consenso quanto à profilaxia.*

Palavras-Chave: *Hematoma subdural crônico; Estado epiléptico; Anticonvulsivantes; Convulsões*

[1]Neurosurgery Division, Universidade Federal do Sergipe – UFS, Aracaju, SE, Brasil.
[2]Faculty of Medicine, Universidade Federal do Triângulo Mineiro – UFTM, Uberaba, MG, Brasil.

Received Jun 1, 2026
Accepted Jun 25, 2026

INTRODUCTION

Chronic subdural hematoma (CSDH) is a frequent condition in neurosurgical practice. Its incidence ranges from 7 to 30 per 100,000 inhabitants, affecting predominantly the elderly, with an increase in patients using antithrombotic medication, in those with repeated falls, and in chronic alcoholism[1,2]. Postoperative (PO) status epilepticus has been associated with increased morbidity and mortality rates in elderly patients undergoing neurosurgical procedures. Seizures are uncommonly reported in patients with CSDH. Seizures after CSDH surgery have been associated with postoperative complications, higher mortality, and poorer clinical outcomes at follow-up[3]. The incidence of seizures in the postoperative period of patients undergoing surgical drainage of CSDH via burr hole is considered low[4]. According to Goertz et al.[5], postoperative seizures are a potential complication in patients with CSDH. The routine use of prophylactic antiepileptic drugs has not been shown to be beneficial. When possible, patients with risk factors who could benefit from antiepileptic drug prophylaxis should be identified[5].

METHODS

This study comprises two components: a case report and a narrative review of the literature.

Case report

An illustrative clinical case of a patient with CSDH associated with seizures was documented from the medical records of the institution. The following data were collected: demographic characteristics (age, sex), comorbidities, seizure history, clinical presentation, neurological examination findings (Glasgow Coma Scale score, motor deficits, pupillary reactivity), neuroimaging findings (non-contrast cranial computed tomography), surgical treatment performed, postoperative course, complications, and clinical outcome.

Literature review

A narrative review of the literature was conducted using the PubMed/MEDLINE, LILACS, and SciELO databases, covering publications from 1970 to 2024. The following descriptors and Boolean operators were used: "Hematoma, Subdural, Chronic" AND "Status epilepticus" OR "Seizure" OR "Anticonvulsant agents" AND "Risk Factors". The reference lists of selected articles were also reviewed for additional relevant citations. Original articles, case reports, case series, systematic reviews, and meta-analyses addressing the association between seizures (or anticonvulsant use) and CSDH in adult patients were considered, with no language restrictions. Studies focusing exclusively on pediatric populations or on acute subdural hematoma without a chronic component were not emphasized. The selection and synthesis of the articles were performed by the authors by consensus.

The objective of this study was to review the epidemiology, pathophysiological mechanisms, risk factors, clinical and imaging features, treatment options, and prognosis of seizures in patients with CSDH, and to discuss the role of prophylactic anticonvulsant therapy in this setting.

CASE PRESENTATION

JFS, a 79-year-old retired man. Past medical history: chronic alcoholism, heart disease, malignant arterial hypertension, and diabetes mellitus. He had a history of a fall from his own height one month earlier and holocranial headache. He presented with a generalized seizure and was referred to the emergency department. Neurological examination: drowsy, isocoric pupils, left hemiparesis, Glasgow Coma Scale score of 9. He underwent non-contrast cranial computed tomography, which revealed a mixed-density subdural hematoma in the right cerebral hemisphere (Figure 1). He underwent trephination with two burr holes (right parietal and frontal) followed by drainage of the hematoma and irrigation of the cavity with saline solution. In the immediate postoperative period, he developed seizures and was treated with phenytoin. His neurological condition worsened, and he progressed to death.

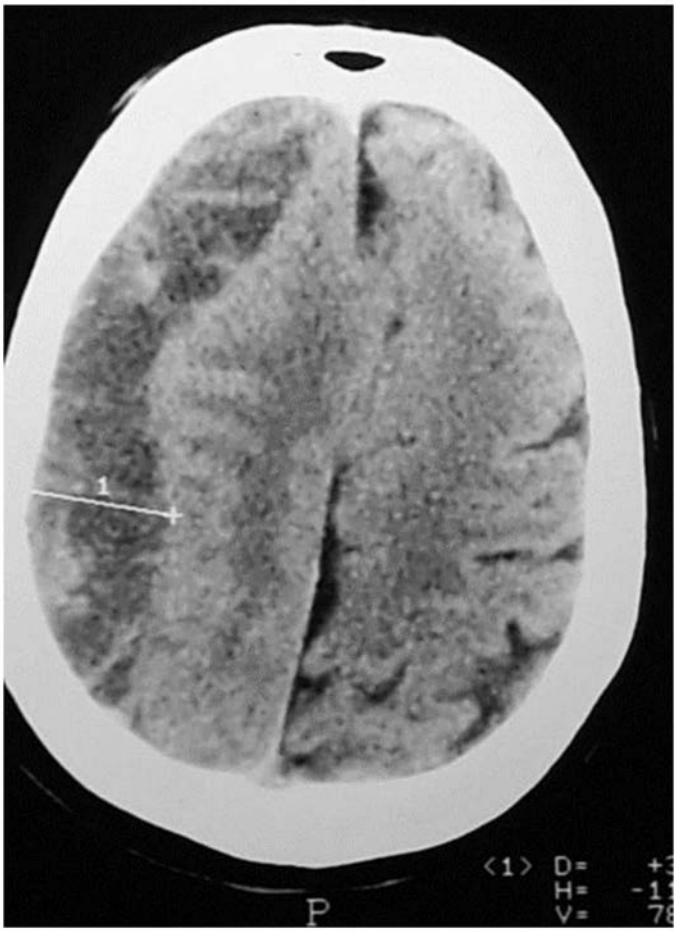

Figure 1. Non-contrast cranial computed tomography showing a mixed-density subdural hematoma in the right cerebral hemisphere with midline shift.

DISCUSSION

Seizures are one of the postoperative complications in patients with CSDH and may affect prognosis[3,6]. Clinical worsening after CSDH drainage is generally due to the occurrence of seizures, electrolyte disturbances, and infectious processes. The incidence of seizures in patients with CSDH ranges from 2.3% to 19%; however, the population characteristics and the description of the epileptic seizures vary widely[3,7-11]. The incidence of postoperative seizures ranges from 1% to 32%[3,4,12-15], thereby increasing morbidity and mortality rates[16-18]. According to Huang et al.[19], seizures occur within the first three months after CSDH surgery. According to Lee et al.[18], the incidence of postoperative seizures after burr-hole drainage of CSDH is unknown and also very low.

Seizures as a postoperative complication of CSDH are uncommon in clinical practice, particularly when the brain parenchyma is normal, as in most cases[20]. Postoperative seizures have an adverse effect on patient rehabilitation and may lead to increased morbidity and mortality[14,19,21-23].

The risk factors for seizures in patients with CSDH are: a previous history of seizures, chronic alcoholism, persistence of post-traumatic stress syndrome, and repeated traumatic brain injury (TBI)[24,25]. Cole and Spatz[25] reported that the seizure rate was above 47% in alcoholics with repeated TBI. Kotwica and Brzezinski[11] reported that irritation of the cerebral cortex by the hematoma provokes seizures; for this reason, drainage of the hematoma may reduce the rate of postoperative seizures. After TBI, the risk of seizures increases in proportion to the degree of associated brain injury, such as cerebral parenchymal injury, hemorrhage, and dural destruction[11,24]. In cases of hemorrhagic contusion or parenchymal hemorrhage combined with CSDH, seizures occur in more than 40%[26]. Seizures may occur in association with occult cortical injury, decreased cerebral blood flow, and hemoglobin degradation products[14,16,19,21-23,27]. Wu et al.[3] found that alcohol consumption, heart disease, cerebral infarction, and trabecular hematoma are independent risk factors for seizures. Preoperative imaging findings significantly associated with postoperative seizures are midline shift, membranectomy, and mixed density[5,21]. A randomized prospective study would be necessary to determine which subgroups of patients with CSDH could benefit from the use of prophylactic antiepileptic drugs. According to Goertz et al.[5], studies using subgroup analyses and risk scores are needed to determine which specific populations may benefit.

According to Seuk et al.[9], treatment of CSDH via burr hole offers good chances of recovery, but unexpected neurological complications may occasionally occur during the postoperative course. Brodersen and Gjerris[28] reported that drainage of the hematoma may decrease the occurrence of seizures, since cerebral compression causes decreased blood flow and ischemia. According to Pradhanang et al.[4], the incidence of postoperative seizures in patients undergoing burr-hole treatment for CSDH is low.

There is controversy regarding the need for anticonvulsant drugs in patients with CSDH[4,6,20,29-33]. Chen et al.[21] recommend the prophylactic use of antiepileptic drugs only in cases of CSDH in which the preoperative CT shows mixed density.

Other authors suggest that the use of prophylactic anticonvulsants before surgery is probably associated with a reduction in postoperative seizures in patients with CSDH treated surgically via burr hole[29,34]. Sabo et al.[14] demonstrated a significant increase in morbidity and mortality associated with respiratory complications and postoperative status epilepticus in CSDH, and recommended the prophylactic use of the anticonvulsant phenytoin in surgically treated cases. According to Wu et al.[3], there is no consensus on whether antiepileptic drugs should be prescribed prophylactically in patients with CSDH; other anticonvulsants such as phenobarbital, levetiracetam, and sodium valproate have been routine options. A 2013 Cochrane review found no conclusive evidence, owing to the limited number of observational studies and non-randomized trials[32]. According to Ratilal et al.[32], no formal recommendation can be made regarding prophylactic use in patients with CSDH based on the evaluated literature. According to Kramer et al.[30], the efficacy of prophylactic treatment with antiepileptic drugs has not been completely determined. According to Faruk et al.[6], the use of antiepileptic drugs in CSDH has been debated, with no consensus reached. While one retrospective study demonstrated a reduction in seizures with the prophylactic use of antiepileptic drugs, others found no benefit[14,15,34,35].

In the present case, the patient presented several of the risk factors described in the literature: advanced age, chronic alcoholism, heart disease, a mixed-density hematoma on preoperative computed tomography, and a generalized seizure at presentation. Despite surgical drainage via burr hole, he developed seizures in the immediate postoperative period, with neurological deterioration and an unfavorable outcome. This case illustrates the potential severity of postoperative seizures in patients harboring multiple risk factors and reinforces the discussion regarding the possible role of antiepileptic prophylaxis in this specific subgroup, in whom the risk–benefit balance might favor treatment.

This study has limitations. As a narrative review, it did not follow a systematic protocol with predefined search and selection criteria and is therefore subject to selection bias, so relevant studies may have been missed. The available evidence consists largely of retrospective series and case reports with heterogeneous populations, variable definitions of seizure, and differing surgical techniques and antiepileptic regimens, which limits the comparability of the reported incidence rates and the strength of any recommendation. In addition, the clinical experience is illustrated by a single case, which precludes generalization. These limitations reinforce the need for prospective, randomized studies stratified by risk factors.

CONCLUSION

The prophylactic use of anticonvulsant drugs to prevent seizures in the pre- and postoperative period of patients with CSDH has been widely debated, but no consensus has been reached. Prospective randomized studies stratifying patients by risk factors are needed to identify the subgroups most likely to benefit from prophylaxis.

REFERENCES

1. Rust T, Kiemer N, Erasmus A. Chronic subdural haematomas and anticoagulation or anti-thrombotic therapy. J Clin Neurosci. 2006;13(8):823-7. https://doi.org/10.1016/j.jocn.2004.12.013. PMid:16997707.

2. Hamou HA, Clusmann H, Schulz JB, Wiesmann M, Altiok E, Höllig A. Chronic subdural hematoma. Dtsch Arztebl Int. 2022;119(12): 208-13. PMid:35236548.

3. Wu L, Guo X, Ou Y, et al. Seizure after chronic subdural hematoma evacuation: associated factors and effect on clinical outcome. Front Neurol. 2023;14:1190878. https://doi.org/10.3389/fneur.2023.1190878. PMid:37228408.

4. Pradhanang AB, Sedain G, Shilpakar SK, Sharma MR. Prophylactic use of anti-epileptic drug (phenytoin) in preventing early postoperative seizure in patients with chronic subdural hematoma: a randomized control trial. Indian J Neurosurg. 2019;8(3):168-78. https://doi.org/10.1055/s-0039-1698478.

5. Goertz L, Speier J, Schulte AP, et al. Independent risk factors for postoperative seizures in chronic subdural hematoma identified by multiple logistic regression analysis. World Neurosurg. 2019;132: e716-21. https://doi.org/10.1016/j.wneu.2019.08.032. PMid:31421304.

6. Faruk MO, Kuddus MR, Sharif MS, Barua KK. Preventing post-operative seizures in chronic subdural hematoma surgery: role of antiepileptic drugs. Int J Clin Trials. 2025;12(2):74-9. https://doi.org/10.18203/2349-3259.ijct20251202.

7. Luxon LM, Harrison MJG. Chronic subdural haematoma. Q J Med. 1979;48(189):43-53. https://doi.org/10.1093/oxfordjournals.qjmed.a067565. PMid:482590.

8. Ohno K, Maehara T, Ichimura K, Suzuki R, Hirakawa K, Monma S. Low incidence of seizures in patients with chronic subdural haematoma. J Neurol Neurosurg Psychiatry. 1993;56(11):1231-3. https://doi.org/10.1136/jnnp.56.11.1231. PMid:8229039.

9. Seuk JW, Chun HJ, Yi HJ. Status epilepticus caused by small amount subacute to chronic subdural hematoma: case report and review of literatures. J Korean Neurotraumatol Soc. 2010;6(2):154-7. https://doi.org/10.13004/jknts.2010.6.2.154.

10. Cameron MM. Chronic subdural haematoma: a review of 114 cases. J Neurol Neurosurg Psychiatry. 1978;41(9):834-9. https://doi.org/10.1136/jnnp.41.9.834. PMid:690655.

11. Kotwica Z, Brzezinski J. Early and late results of the surgical treatment of chronic subdural hematoma. Neurol Neurochir Pol. 1987;21(4-5):376-80. PMid:3444508.

12. Grisoli F, Graziani N, Peragut JC, et al. Perioperative lumbar injection of Ringer's lactate solution in chronic subdural hematomas: a series of 100 cases. Neurosurgery. 1988;23(5):616-21. https://doi.org/10.1227/00006123-198811000-00012. PMid:3059219.

13. Hirakawa K, Hashizume K, Fuchinoue T, et al. Statistical analysis of chronic subdural hematoma in 309 adult cases. Neurol Med Chir. 1972;12(0):71-83. https://doi.org/10.2176/nmc.12.71. PMid:4135996.

14. Sabo RA, Hanigan WC, Aldag JC. Chronic subdural hematomas and seizures: the role of prophylactic anticonvulsive medication. Surg Neurol. 1995;43(6):579-82. https://doi.org/10.1016/0090-3019(95)00155-7. PMid:7482238.

15. Rubin G, Rappaport ZH. Epilepsy in chronic subdural haematoma. Acta Neurochir. 1993;123(1-2):39-42. https://doi.org/10.1007/BF01476283. PMid:8213276.

16. Won SY, Konczalla J, Dubinski D, et al. A systematic review of epileptic seizures in adults with subdural haematomas. Seizure. 2017;45:28-35. https://doi.org/10.1016/j.seizure.2016.11.017. PMid:27914224.

17. Flores G, Vicenty JC, Pastrana EA. Post-operative seizures after burr hole evacuation of chronic subdural hematomas: is prophylactic anti-epileptic medication needed? Acta Neurochir (Wien). 2017;159(11):2033-6. https://doi.org/10.1007/s00701-017-3298-6. PMid:28808801.

18. Lee KJ, Eom KS, Park JT, Kim TY. Fatal postoperative epilepticus after burr hole drainage for chronic subdural hematoma. Korean J Neurotrauma. 2015;11(2):144-6. https://doi.org/10.13004/kjnt.2015.11.2.144. PMid:27169081.

19. Huang YH, Yang TM, Lin YJ, et al. Risk factors and outcome of seizures after chronic subdural hematoma. Neurocrit Care. 2011;14(2):253-9. https://doi.org/10.1007/s12028-011-9509-8. PMid:21286854.

20. Nachiappan DS, Garg K. Role of prophylactic antiepileptic drugs in chronic subdural hematoma – a systematic review and meta-analysis. Neurosurg Rev. 2021;44(4):2069-77. https://doi.org/10.1007/s10143-020-01388-y. PMid:32910368.

21. Chen CW, Kuo JR, Lin HJ, et al. Early post-operative seizures after burr-hole drainage for chronic subdural hematoma: correlation with brain CT findings. J Clin Neurosci. 2004;11(7):706-9. https://doi.org/10.1016/j.jocn.2004.03.019. PMid:15337129.

22. Rabinstein AA, Chung SY, Rudzinski LA, Lanzino G. Seizures after evacuation of subdural hematomas: incidence, risk factors, and functional impact. J Neurosurg. 2010;112(2):455-60. https://doi.org/10.3171/2009.7.JNS09392. PMid:19698050.

23. Battaglia F, Lubrano V, Ribeiro-Filho T, Pradel V, Roche PH. Incidence and clinical impact of seizures after surgery for chronic subdural hematoma. Neurochirurgie. 2012;58(4):230-4. https://doi.org/10.1016/j.neuchi.2012.04.002. PMid:22626817.

24. Caveness WF, Portera A, Scheffner D. Epilepsy, a product of trauma in our time. Epilepsia. 1976;17(2):207-15. https://doi.org/10.1111/j.1528-1157.1976.tb03398.x. PMid:820549.

25. Cole M, Spatz E. Seizures in chronic subdural hematoma. N Engl J Med. 1961;265(13):628-31. https://doi.org/10.1056/NEJM196109282651304. PMid:13694560.

26. Chan AW. Alcoholism and epilepsy. Epilepsia. 1985;26(4):323-33. https://doi.org/10.1111/j.1528-1157.1985.tb05658.x. PMid:3891322.

27. Hamou H, Alzaiyani M, Rossmann T, et al. Seizure after surgical treatment of chronic subdural hematoma – associated factors and effect on outcome. Front Neurol. 2022;13:977329. https://doi.org/10.3389/fneur.2022.977329. PMid:36158969.

28. Brodersen P, Gjerris F. Regional cerebral blood flow in patients with chronic subdural hematomas. Acta Neurol Scand. 1975;51(3):233-9. https://doi.org/10.1111/j.1600-0404.1975.tb07604.x. PMid:125025.

29. Ghoneim MA, Abbass W. Anticonvulsants for preventing seizures in patients with chronic subdural haematoma: pilot study. Open J Mod Neurosurg. 2020;10(2):237-43. https://doi.org/10.4236/ojmn.2020.102025.

30. Kramer A, Degenhartt X, Gutenberg A, Ringel F. Risk factors for postoperative seizures in patients with chronic subdural haematomas. Neurosurg Rev. 2022;45(5):3291-8. https://doi.org/10.1007/s10143-022-01858-5. PMid:36097085.

31. Lavergne P, Labidi M, Brunet MC, et al. Efficacy of antiseizure prophylaxis in chronic subdural hematoma: a cohort study on routinely collected health data. J Neurosurg. 2019;132(1):284-8. https://doi.org/10.3171/2018.9.JNS182092. PMid:30660118.

32. Ratilal BO, Pappamikail L, Costa J, Sampaio C. Anticonvulsants for preventing seizures in patients with chronic subdural haematoma. Cochrane Database Syst Rev. 2013;2013(6):CD004893. https://doi.org/10.1002/14651858.CD004893.pub3. PMid:23744552.

33. Branco PM, Ratilal BO, Costa J, Sampaio C. Antiepileptic drugs for preventing seizures in patients with chronic subdural hematoma. Curr Pharm Des. 2017;23(42):6442-5. https://doi.org/10.2174/1381612823666171024144318. PMid:29076415.

34. Grobelny BT, Ducruet AF, Zacharia BE, et al. Preoperative antiepileptic drug administration and the incidence of postoperative seizures following bur hole-treated chronic subdural hematoma. J Neurosurg. 2009;111(6):1257-62. https://doi.org/10.3171/2009.6.JNS0928. PMid:19558304.

35. Temkin NR. Antiepileptogenesis and seizure prevention trials with antiepileptic drugs: meta-analysis of controlled trials. Epilepsia. 2001;42(4):515-24. https://doi.org/10.1046/j.1528-1157.2001.28900.x. PMid:11440347.

Funding: *nothing to disclose.*
Conflicts of interest: *nothing to disclose.*
Ethics Committee Approval: *waived.*

CORRESPONDING AUTHOR

Carlos Umberto Pereira, MD, PhD
Retired Professor
Universidade Federal do Sergipe – UFS
Department of Medicine
Aracaju, Sergipe, Brasil
E-mail: umberto@infonet.com.br

CRediT

Carlos Umberto Pereira: Conceptualization, Methodology, Supervision, Validation, Writing – review & editing. Samuel Pedro Pereira Silveira: Data curation, Formal analysis, Investigation, Writing – original draft, Writing – review & editing.

BIPLANO AZURION 7

COM CLARITY® PHILIPS

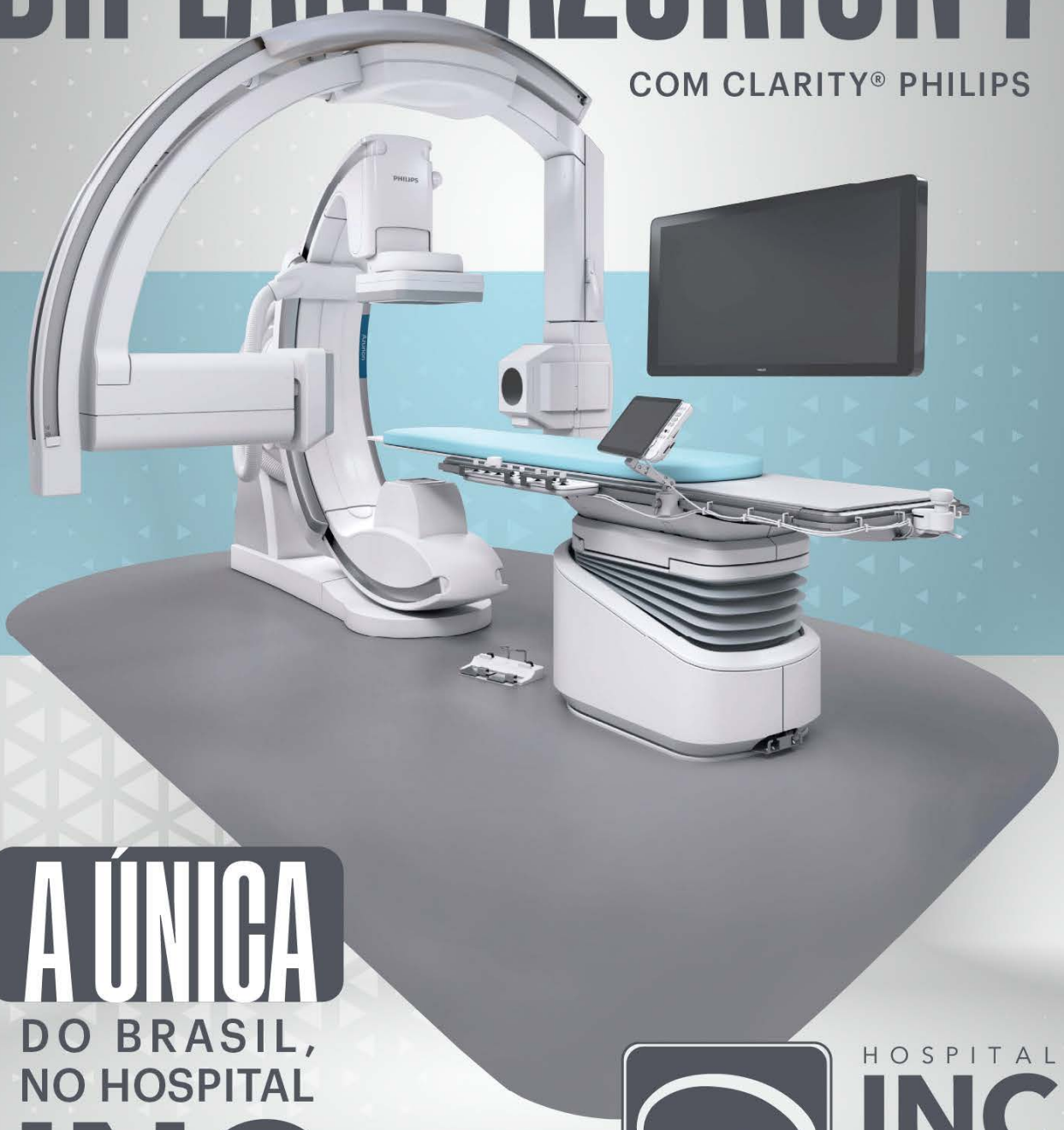

A ÚNICA

DO BRASIL,
NO HOSPITAL

INC

HOSPITAL
INC
INSTITUTO DE
NEUROLOGIA
DE CURITIBA

RESPONSÁVEL TÉCNICO / DR. ANDRÉ GIACOMELLI LEAL / CRM-PR 21874

Lateral Lumbar Interbody Fusion for Symptomatic Degenerative Disc Disease Secondary to a Retained Lumbar Spine Gunshot Wound

Fusão Intercorporal Lombar Lateral para Doença Degenerativa Discal Sintomática Secundária a Ferimento por Arma de Fogo na Coluna Lombar

Aécio Rubens Dias Pereira Filho[1]
Rubens Hajime Aratani[1]
Eduardo Fernandes Arruda[1]
Edjaimes Geitenes[1]
Maria Paula Loureiro de Oliveira Pereira[1]
Francisco Cialdine Frota Carneiro Júnior[1]

ABSTRACT

Introduction: *Degenerative disc disease (DDD) secondary to retained ballistic fragments is an uncommon but clinically significant cause of delayed spinal degeneration. Its management is technically challenging, as traditional anterior or posterior approaches may involve high operative risks.* **Case presentation:** *A 43-year-old man presented with progressive low back pain nearly twenty years after a lumbar gunshot wound initially treated by exploratory laparotomy. Imaging revealed a metallic fragment lodged in the right L3–L4 juxta-foraminal region, associated with disc collapse and a comminuted L4 superior endplate fracture. Due to the risk of anterior adhesions and posterior neural manipulation, a lateral lumbar interbody fusion (LLIF) at L3–L4 was chosen. With intraoperative assistance from a vascular surgeon, the projectile was completely removed and an interbody cage inserted without complications. Postoperative imaging confirmed satisfactory implant positioning and restoration of disc height and alignment. The patient recovered uneventfully, showing sustained improvement and preserved neurological function after six months. This report highlights LLIF as a safe and effective surgical alternative for post-traumatic DDD caused by retained spinal projectiles.*

Keywords: *Lateral lumbar interbody fusion; Degenerative disc disease; Gunshot wounds; Spinal injuries; Retained bullet; Case report*

RESUMO

Introdução: *A doença degenerativa do disco (DDD) secundária a fragmentos balísticos retidos é uma causa incomum, porém clinicamente relevante, de degeneração espinhal tardia. Seu manejo é tecnicamente desafiador, pois as abordagens tradicionais, anterior ou posterior, podem envolver alto risco cirúrgico.* **Descrição do Caso:** *Um homem de 43 anos apresentou dor lombar progressiva quase vinte anos após uma lesão por projétil na coluna lombar, tratada inicialmente com laparotomia exploradora. Os exames de imagem revelaram um fragmento metálico alojado na região juxta-foraminal direita de L3–L4, associado a colapso discal e fratura cominutiva da placa superior de L4. Devido ao risco de aderências anteriores e manipulação neural posterior, optou-se por uma fusão intersomática lombar lateral (LLIF) em L3–L4. Com apoio intraoperatório de um cirurgião vascular, o projétil foi completamente removido e uma gaiola intersomática foi implantada sem complicações. As imagens pós-operatórias confirmaram posicionamento adequado do implante e restauração da altura e do alinhamento discal. O paciente apresentou recuperação satisfatória, com melhora sustentada e função neurológica preservada após seis meses. Este relato destaca a LLIF como uma alternativa cirúrgica segura e eficaz para DDD pós-traumática causada por projéteis espinhais retidos.*

Palavras-Chave: *Fusão lombar lateral; Doença degenerativa do disco; Ferimentos por arma de fogo; Lesões da coluna vertebraL; Projétil retido; Relato de caso*

[1]Instituto de Acessos à Coluna Aécio Dias – IAAD, São Paulo, SP, Brasil.

Received Nov 3, 2025
Accepted Dec 10, 2025

INTRODUCTION

Degenerative disc disease (DDD) may arise from diverse etiologies, including age-related degeneration, biomechanical stress, or inflammatory responses to injury. Among these, penetrating trauma with retained foreign bodies—such as gunshot wounds (GSWs)—represents a particularly insidious mechanism of disc degeneration. The introduction of metallic fragments into the disc or adjacent tissues may disrupt vascular perfusion, impair nutrient diffusion, and trigger chronic inflammatory cascades, thereby accelerating structural and biochemical deterioration[1-3]. In individuals with retained ballistic fragments adjacent to the intervertebral space, the degenerative process may evolve silently over years, culminating in discogenic pain, segmental instability, or neural compromise. These sequelae are rarely immediate but represent a delayed and underrecognized consequence of spinal trauma. Clinical suspicion should be heightened in patients with a history of GSW and new-onset axial pain or neurological decline, particularly when imaging reveals localized degeneration near the trajectory of the retained projectile[3].

When surgical intervention becomes necessary in these contexts—due to progressive neurological symptoms or mechanical instability—the choice of approach must be tailored to anatomical constraints and prior surgical history. Conventional anterior or posterior corridors may be precluded by retroperitoneal scarring, visceral adhesions, or heightened risk to neural elements. In this scenario, the lateral lumbar interbody fusion (LLIF) technique offers a minimally invasive alternative that enables access to the disc space while minimizing disruption to vascular and visceral structures[4,5].

This report presents a rare case of symptomatic lumbar DDD developing nearly two decades after a gunshot wound, in which the projectile remained lodged adjacent to the L3–L4 disc. Given anatomical constraints imposed by prior abdominal surgery, a lateral approach was selected to achieve decompression and interbody stabilization. The successful use of LLIF in this delayed, post-traumatic setting—sparsely addressed in the current literature—highlights both the feasibility and potential advantages of this technique in anatomically complex scenarios[5].

CASE PRESENTATION

The patient is a 43-year-old male (born July 19, 1980) who presented with progressively worsening low back pain. His relevant past medical history includes a GSW to the lumbar region sustained 20 years prior to presentation. The initial trauma necessitated an exploratory laparotomy due to abdominal perforation, but did not require a colostomy. The projectile was not removed at the time and remained lodged near the L3-L4 spinal segment. Remarkably, the patient remained asymptomatic concerning his lumbar spine for nearly two decades following the injury, reporting no significant back pain or neurological deficits during this period. The recent onset of progressive lombalgia prompted further investigation (Table 1).

Diagnostic evaluation centered on the CT scan performed in October 2023. The imaging revealed several key findings: 1. A comminuted fracture of the superior endplate of the L4 vertebra. 2. A retained metallic projectile situated in the right juxta-foraminal region at the L3-L4 level. 3. Significant degenerative changes at the L3-L4 intervertebral disc space, consistent with advanced DDD. 4. An

Table 1. Timeline of clinical events, diagnostic procedures, interventions, and outcomes.

Time	Event
20 years prior to surgery	Sustained GSW to the lumbar spine with retained projectile near L3-L4; underwent exploratory laparotomy.
19 years after injury (prior to Oct 2023)	Long asymptomatic period regarding spinal symptoms.
19 years after injury (prior to Oct 2023)	Onset of progressive, debilitating low back pain.
October 2023	Computed Tomography (CT) scan of the lumbar spine performed for diagnostic evaluation.
May 2024	Underwent L3-L4 LLIF procedure with projectile extraction and cage implantation.
post-operation	Complete remission of low back pain symptoms observed; no neurological deficits noted.
Until 6 month follow up	Patient reported steady symptomatic improvement

associated disc-osteophyte complex at the L4-L5 level, noted to be protruding into the left foramen and contacting the exiting L4 nerve root on that side (although the primary symptoms appeared related to L3-L4) (Figure 1).

The decision-making process for surgical intervention considered the patient's incapacitating symptoms and the imaging findings. The choice of surgical approach involved careful deliberation. A posterior approach was deemed high-risk due to the need for potential dural sac retraction and nerve root manipulation in the vicinity of the projectile and degenerated disc. An anterior lumbar interbody fusion (ALIF) approach, while offering good visualization for projectile extraction, was contraindicated by the access surgery team due to the patient's history of exploratory laparotomy. The potential for significant retroperitoneal adhesions increased the risk of vascular injury with an anterior approach. Consequently, the LLIF approach was selected as the optimal strategy, providing direct lateral access to the L3-L4 disc space while minimizing manipulation of neural elements posteriorly and avoiding the risks associated with the scarred anterior retroperitoneal plane[4,5].

The patient underwent an LLIF procedure at the L3-L4 level in May 2024. The surgery was performed utilizing a minimally invasive lateral, retroperitoneal, transpsoas approach. Crucially, the procedure was conducted with the assistance of a vascular surgeon specialized in access to the spine to ensure safe navigation through the retroperitoneal space and psoas muscle. During the procedure, the degenerated L3-L4 disc material was removed, and the retained projectile lodged in the juxta-foraminal region was successfully identified and extracted. Following discectomy and projectile removal, an appropriately sized interbody cage was implanted into the L3-L4 disc space to restore disc height, provide stability, and facilitate eventual fusion. The LLIF technique allowed for adequate visualization and instrumentation of the target level while avoiding the specific risks associated with the posterior and anterior alternatives in this particular patient.

The patient experienced a favorable post-operative course without immediate complications. A significant and complete remission of the pre-operative low back pain was reported in the immediate post-operative period. No new motor or sensory deficits were observed. Immediate post-operative radiographic evaluation confirmed satisfactory positioning of the LLIF cage, adequate restoration of the L3-L4 disc height, and improvement in segmental lumbar lordosis (Figure 2). Over the course of six months, the patient reported gradual and sustained improvement in symptoms (Figure 3).

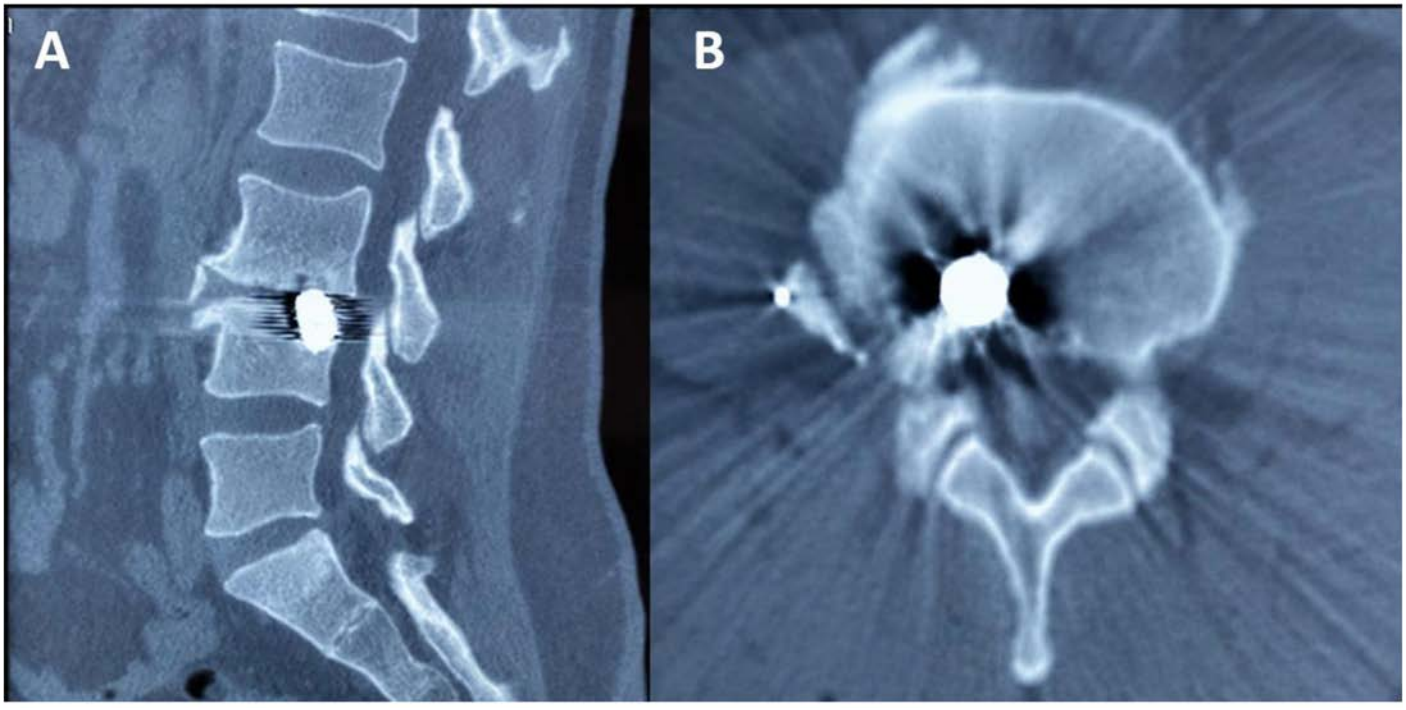

Figure 1. Pre-operative CT scan images demonstrating the L4 endplate fracture, retained projectile, and L3-L4 DDD - Placeholder for image insertion.

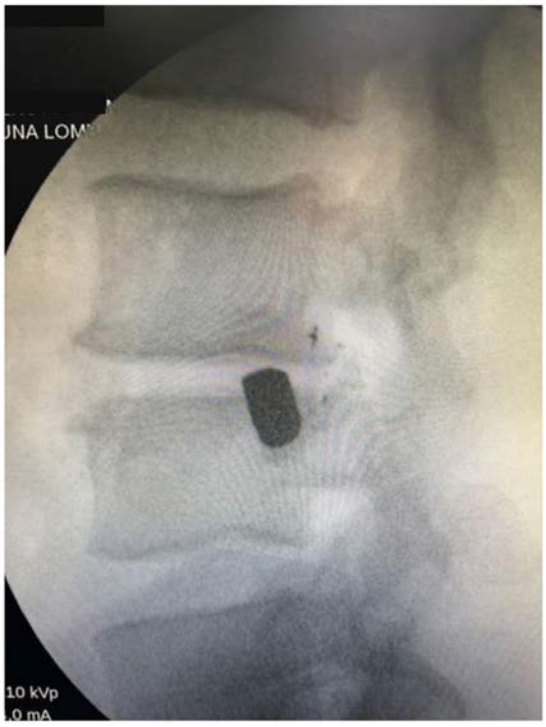

Figure 2. Intraoperative images.

DISCUSSION

The degenerative cascade following spinal trauma is often multifactorial and protracted, particularly when a retained projectile acts as a persistent source of biomechanical and biochemical disruption. Chronic inflammation, altered disc loading, impaired nutrient diffusion, and extracellular matrix degradation are key mechanisms implicated in trauma-induced disc degeneration[2]. These processes may remain subclinical for years, eventually culminating in segmental instability, neural compression, or debilitating axial pain[1,2].

In the present case, imaging revealed localized disc collapse, Modic endplate changes, and reactive sclerosis adjacent to the retained bullet fragment at the L3–L4 level. These features are consistent with advanced degenerative disc disease and segmental overload, suggestive of chronic mechanical and inflammatory insult. As highlighted by Scarcia et al., DDD is not merely a loss of disc height but reflects a broader spectrum of radiological and

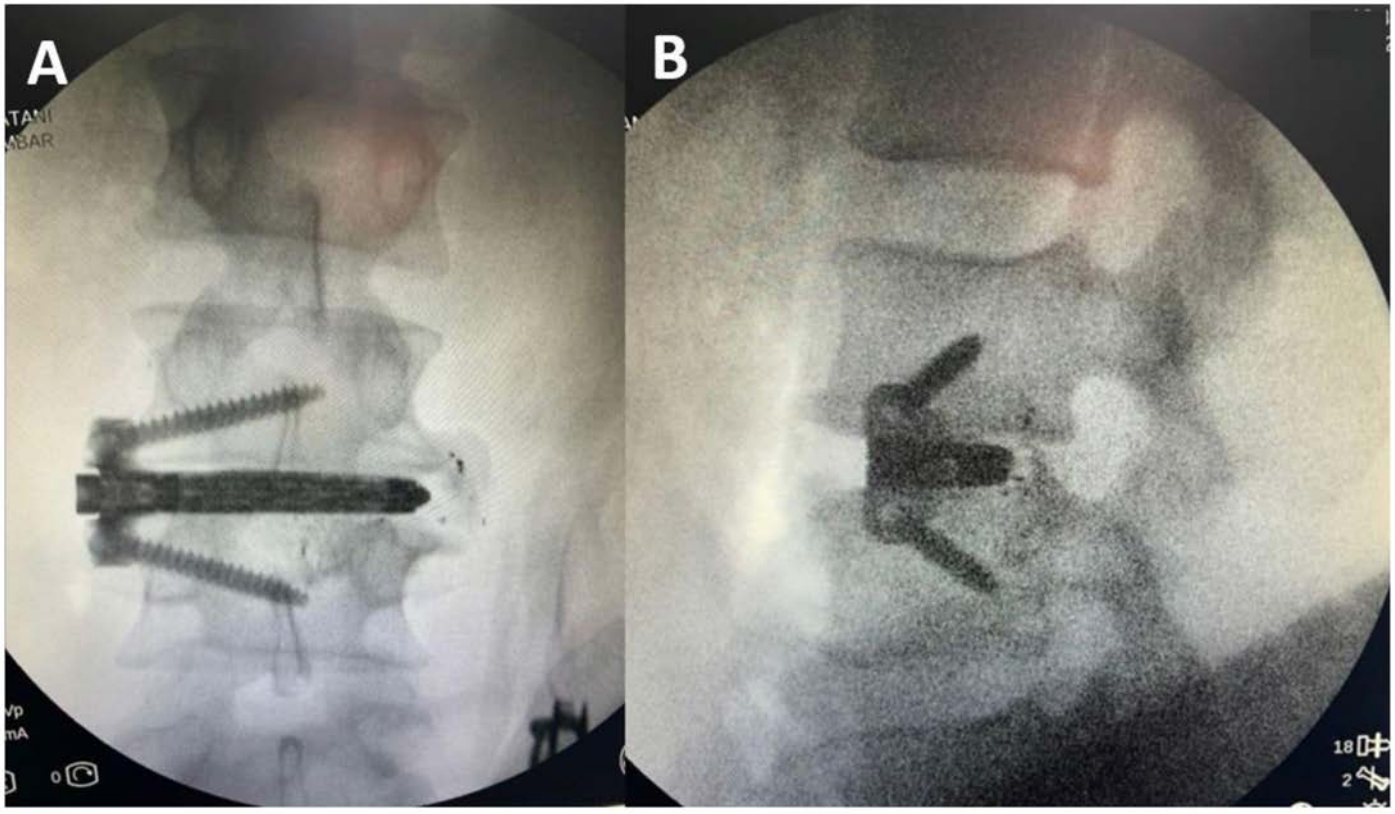

Figure 3. Post-operative radiographic images demonstrating cage position and spinal alignment - Placeholder for image insertion.

morphological alterations—many of which were evident in this patient[6]. Conservative management had been exhausted, and the persistence of disabling axial pain with radiological progression supported the indication for surgical stabilization.

The choice of surgical approach in lumbar interbody fusion must balance biomechanical goals with patient-specific anatomical constraints. In this case, prior laparotomy rendered an anterior retroperitoneal corridor suboptimal due to expected adhesions and increased vascular risk. While posterior approaches such as PLIF or TLIF are widely utilized, they carry a higher risk of dural sac manipulation and neural irritation—especially in cases with distorted anatomy. LLIF offered a compromise: indirect decompression and robust segmental support through a minimally invasive lateral corridor[4,5]. As documented by Salzmann et al., LLIF is associated with lower blood loss and shorter operative times in selected patients[4], while Gianoli et al. have demonstrated its feasibility even in trauma settings[5]. Furthermore, Teng et al.'s meta-analysis supports LLIF as a biomechanically sound alternative with favorable fusion rates when compared to other interbody techniques[7].

Whether to remove retained bullet fragments from the spine remains a subject of debate. Some authors argue that asymptomatic projectiles may be safely left in situ, especially when removal entails significant surgical risk. However, others have emphasized the potential for delayed complications—including lead toxicity, migration, or infectious processes—as valid indications for extraction[8,9]. In our case, the fragment was intimately associated with the degenerated L3–L4 disc and situated within the surgical field, offering a unique opportunity for safe retrieval. The presence of disabling symptoms and localized structural deterioration further supported the rationale for removal as part of the decompressive and stabilizing procedure.

This case underscores the importance of individualized surgical planning in post-traumatic lumbar pathology, particularly when conventional corridors are anatomically compromised. Beyond the technical aspects, it illustrates how delayed sequelae of penetrating spinal injury can culminate in surgically remediable pathology—even decades later. Although generalizability is inherently limited in single-patient reports, this case contributes to the growing body of evidence supporting LLIF as a feasible and strategically advantageous approach in select trauma-related degenerative scenarios.

CONCLUSION

LLIF proved to be a viable and anatomically strategic solution in the management of delayed, post-traumatic lumbar DDD adjacent to a retained projectile. In this anatomically challenging scenario, the lateral approach enabled decompression and stabilization while minimizing surgical morbidity—affirming its role as a valuable alternative when traditional access routes are contraindicated.

REFERENCES

1. Kos N, Gradisnik L, Velnar T. A brief review of the degenerative intervertebral disc disease. Med Arch. 2019;73(6):421-4. https://doi.org/10.5455/medarh.2019.73.421-424. PMid:32082013.

2. Kirnaz S, Capadona C, Lintz M, et al. Pathomechanism and biomechanics of degenerative disc disease: features of healthy and degenerated discs. Int J Spine Surg. 2021;15(s1):10-25. https://doi.org/10.14444/8052. PMid:34376493.

3. Platt A, El Dafrawy MH, Lee MJ, Herman MH, Ramos E. Gunshot wounds to the lumbosacral spine: systematic review and meta-analysis. Global Spine J. 2022;12(6):1247-53. https://doi.org/10.1177/21925682211030873. PMid:34275384.

4. Salzmann SN, Shue J, Hughes AP. Lateral lumbar interbody fusion: outcomes and complications. Curr Rev Musculoskelet Med. 2017;10(4):539-46. https://doi.org/10.1007/s12178-017-9444-1. PMid:29038952.

5. Gianoli D, Bättig L, Bertulli L, Forster T, Martens B, Stienen MN. Lateral lumbar and thoracic interbody fusion (LLIF) for thoracolumbar spine trauma. N Am Spine Soc J. 2024;19:100534. https://doi.org/10.1016/j.xnsj.2024.100534. PMid:39257670.

6. Scarcia L, Pileggi M, Camilli A, et al. Degenerative disc disease of the spine: from anatomy to pathophysiology and radiological appearance. J Pers Med. 2022;12(11):1810. https://doi.org/10.3390/jpm12111810. PMid:36579533.

7. Teng I, Han J, Phan K, Mobbs R. A meta-analysis comparing ALIF, PLIF, TLIF and LLIF. J Clin Neurosci. 2017;44:11-7. https://doi.org/10.1016/j.jocn.2017.06.013. PMid:28676316.

8. Velmahos GC, Demetriades D. Gunshot wounds of the spine: should retained bullets be removed to prevent infection? Ann R Coll Surg Engl. 1994;76(2):85-7. PMid:8154819.

9. de los Cobos D, Powers A, Behrens JP, Mattei TA, Salari P. Surgical removal of a migrating intraspinal bullet: illustrative case. J Neurosurg Case Lessons. 2021;1(22):CASE21132. https://doi.org/10.3171/CASE21132. PMid:35855464.

CORRESPONDING AUTHOR

Aécio Rubens Dias Pereira Filho, MD
Instituto de Acessos à Coluna Aécio Dias – IAAD
São Paulo, SP, Brazil
E-mail: cientifico.iaad@gmail.com

Funding: *nothing to disclose.*
Conflicts of interest: *nothing to disclose.*
Ethics Committee Approval: *approved by Prevent Senior Committee (CAAE: 90628925.3.0000.8114).*

CRediT

Aécio Rubens Dias Pereira Filho: Investigation, Writing – Original Draft. Rubens Hajime Aratani: Investigation, Writing – Original Draft. Eduardo Fernandes Arruda: Investigation, Writing – Original Draft. Edjaimes Geitenes: Investigation, Writing – Review & Editing. Maria Paula Loureiro de Oliveira Pereira: Investigation, Writing – Review & Editing. Francisco Cialdine Frota Carneiro Júnior: Formal Analysis, Writing – Review & Editing.

JBNC
JORNAL BRASILEIRO DE NEUROCIRURGIA
BRAZILIAN JOURNAL OF NEUROSURGERY

Occult Rupture-Related Pseudoaneurysm Associated with a Ruptured Middle Cerebral Artery Aneurysm Diagnosed During Microsurgical Clipping

Pseudoaneurisma Oculto Associado a Aneurisma Roto de Artéria Cerebral Média Diagnosticado Durante Clipagem Microcirúrgica

Jose Luis Quelho Filho[1]
Paulo Eduardo Albuquerque Zito Raffa[1]
Leonardo Vieira Nunes[1]
Gabriel Ribas Nascimento de Melo[1]
Rodrigo Shibaki[2]
Lucas Crociati Meguins[3]

ABSTRACT

Introduction: *Rupture-related pseudoaneurysm formation secondary to true intracranial aneurysm rupture is an exceptionally rare vascular phenomenon. These lesions are characterized by the absence of a true arterial wall and are composed of organized hematoma and fibrous tissue communicating with the parent vessel lumen. Radiological findings are frequently nonspecific or absent with diagnosis being challenging.* **Case Presentation:** *A 54-year-old man presented with poor-grade aneurysmal subarachnoid hemorrhage following generalized tonic-clonic seizures associated with cocaine use. Computed tomography angiography demonstrated a ruptured bilobulated aneurysm arising from the left middle cerebral artery bifurcation. Emergency microsurgical clipping was performed through a standard pterional approach. Intraoperatively, a previously unrecognized rupture-related pseudoaneurysm adjacent to the aneurysm dome and presumed rupture site was identified. Complete clip reconstruction of both the true aneurysm and pseudoaneurysmal cavity was achieved. Despite a long and complex postoperative course, the patient achieved complete neurological recovery.* **Conclusion:** *Rupture-related pseudoaneurysms may remain entirely occult on preoperative vascular imaging and become evident only during microsurgical exploration. Neurosurgeons should maintain a high index of suspicion when treating irregular or multilobulated ruptured aneurysms, as recognition of the pseudoaneurysmal component may significantly alter surgical planning, facilitate complete lesion exclusion, and reduce the risk of intraoperative rupture and postoperative rebleeding.*

Keywords: *Rupture-related pseudoaneurysm; Intracranial pseudoaneurysm; Middle cerebral artery aneurysm; Aneurysmal subarachnoid hemorrhage; Microsurgical clipping*

RESUMO

Introdução: *A formação de pseudoaneurisma relacionado à ruptura de aneurisma intracraniano verdadeiro é um fenômeno vascular excepcionalmente raro. Essas lesões são caracterizadas pela ausência de uma parede arterial verdadeira, sendo compostas por hematoma organizado e tecido fibroso em comunicação com o vaso parental. Os achados radiológicos são frequentemente inespecíficos, tornando o diagnóstico desafiador.* **Descrição do Caso:** *Um homem de 54 anos apresentou hemorragia subaracnoidea após crises convulsivas tônico-clônicas generalizadas associadas ao uso de cocaína. A angiotomografia computadorizada demonstrou um aneurisma bilobulado roto, originado na bifurcação da artéria cerebral média esquerda. Foi realizada clipagem microcirúrgica via pterional. No intraoperatório, identificou-se um pseudoaneurisma, previamente não reconhecido. Obteve-se a reconstrução completa com clipagem tanto do aneurisma verdadeiro quanto da cavidade pseudoaneurismática. Apesar de uma evolução pós-operatória longa e complexa, o paciente obteve recuperação neurológica completa.* **Conclusão:** *Os pseudoaneurismas relacionados à ruptura podem permanecer completamente ocultos aos exames de imagem vascular pré-operatórios, tornando-se evidentes apenas durante a exploração microcirúrgica. Neurocirurgiões devem manter um alto índice de suspeição ao tratar aneurismas rotos irregulares ou multilobulados, uma vez que o reconhecimento do componente pseudoaneurismático pode alterar significativamente o planejamento cirúrgico, facilitar a exclusão completa da lesão e reduzir o risco de ruptura intraoperatória e ressangramento pós-operatório.*

Palavras-Chave: *Pseudoaneurisma relacionado à ruptura; Pseudoaneurisma intracraniano; Aneurisma de artéria cerebral média; Hemorragia subaracnoidea aneurismática; Clipagem microcirúrgica*

[1]Department of Neurosurgery, Faculdade de Medicina de São José do Rio Preto – FAMERP, São José do Rio Preto, SP, Brasil.
[2]Faculdade de Medicina de São José do Rio Preto – FAMERP, São José do Rio Preto, SP, Brasil
[3]Fundação Faculdade Regional de Medicina de São José do Rio Preto – FUNFARME, Hospital de Base, São José do Rio Preto, SP, Brasil.

Received Jul 18, 2026
Corrected Aug 4, 2026
Accepted Aug 8, 2026

INTRODUCTION

Intracranial pseudoaneurysms are rare vascular lesions accounting for approximately 1% of all intracranial aneurysms. Unlike true aneurysms, which retain varying degrees of normal arterial wall architecture, pseudoaneurysms lack a complete vessel wall and consist primarily of organized hematoma, thrombus, and fibrous tissue that remain in communication with the parent artery. As a result, these lesions exhibit extreme structural fragility and are associated with substantially higher rates of rupture, rebleeding, morbidity, and mortality than conventional intracranial aneurysms[1].

Most intracranial pseudoaneurysms arise secondary to traumatic vascular injury, iatrogenic arterial damage, infection, radiation exposure, or underlying connective tissue disorders[1]. In contrast, pseudoaneurysm formation following rupture of a true intracranial aneurysm represents an exceptionally uncommon phenomenon that has been documented only in isolated case reports and small case series[2-7]. Consequently, its true incidence, natural history, and optimal treatment strategies remain poorly defined.

The currently accepted pathophysiological mechanism involves rupture of the aneurysm dome with blood extravasation into the surrounding cisternal or parenchymal spaces. When the hemorrhage becomes locally contained, a peri-aneurysmal hematoma may remain in communication with the aneurysm lumen. Progressive organization of this hematoma can subsequently result in the formation of a fibrous cavity devoid of normal arterial wall layers, creating a rupture-related pseudoaneurysm adjacent to the original lesion[3-7]. Several terms have been used to describe this process, including ghost aneurysm, mixed aneurysm, and rupture-related pseudoaneurysm[2-6].

Diagnosis remains particularly challenging because angiographic findings are frequently subtle, nonspecific, or entirely absent. Reported radiological features include delayed contrast filling, delayed contrast washout, contrast retention, daughter-sac morphology, multilobulated configuration, snowman-shaped appearance, and interval aneurysm enlargement on serial imaging studies[1,3-8]. However, none of these findings are pathognomonic, and many lesions remain angiographically occult. Consequently, definitive diagnosis often relies on repeat vascular imaging, direct intraoperative inspection, or histopathological evaluation[1,3-8].

Recognition of rupture-related pseudoaneurysms has important clinical implications. Failure to identify the pseudoaneurysmal component may increase the risk of catastrophic intraoperative rupture, incomplete aneurysm exclusion, and postoperative rebleeding[1,4-6]. Furthermore, the presence of a pseudoaneurysm may substantially alter microsurgical anatomy and influence clip reconstruction strategy.

Herein, we report a rare case of a ruptured middle cerebral artery bifurcation aneurysm associated with an occult rupture-related pseudoaneurysm that was not identified on preoperative computed tomography angiography and became evident only during microsurgical clipping. To our knowledge, reports describing intraoperative diagnosis of an occult rupture-related pseudoaneurysm associated with a ruptured middle cerebral artery aneurysm remain exceedingly uncommon[5,6]. In addition, we provide a narrative review of the available literature regarding the pathophysiology, radiological characteristics, diagnostic challenges, and therapeutic implications of this uncommon vascular entity.

CASE PRESENTATION

A 54-year-old man with a history of recent cocaine use presented after experiencing a generalized tonic-clonic seizure associated with urinary incontinence. Several hours later, while being evaluated at an outside emergency department, he developed a second generalized tonic-clonic seizure followed by progressive neurological deterioration and severe psychomotor agitation, ultimately requiring endotracheal intubation for airway protection.

Upon transfer to our institution, the patient remained sedated and mechanically ventilated. Neurological assessment prior to sedation interruption was consistent with poor-grade aneurysmal subarachnoid hemorrhage, corresponding to Hunt-Hess grade V and World Federation of Neurosurgical Societies (WFNS) grade V.

Non-contrast head computed tomography demonstrated diffuse subarachnoid hemorrhage involving the basal cisterns, bilateral sylvian fissures, anterior interhemispheric fissure, and cortical sulci. Associated intraventricular hemorrhage and acute hydrocephalus were present, corresponding to modified Fisher grade IV hemorrhage (Figure 1 A-B).

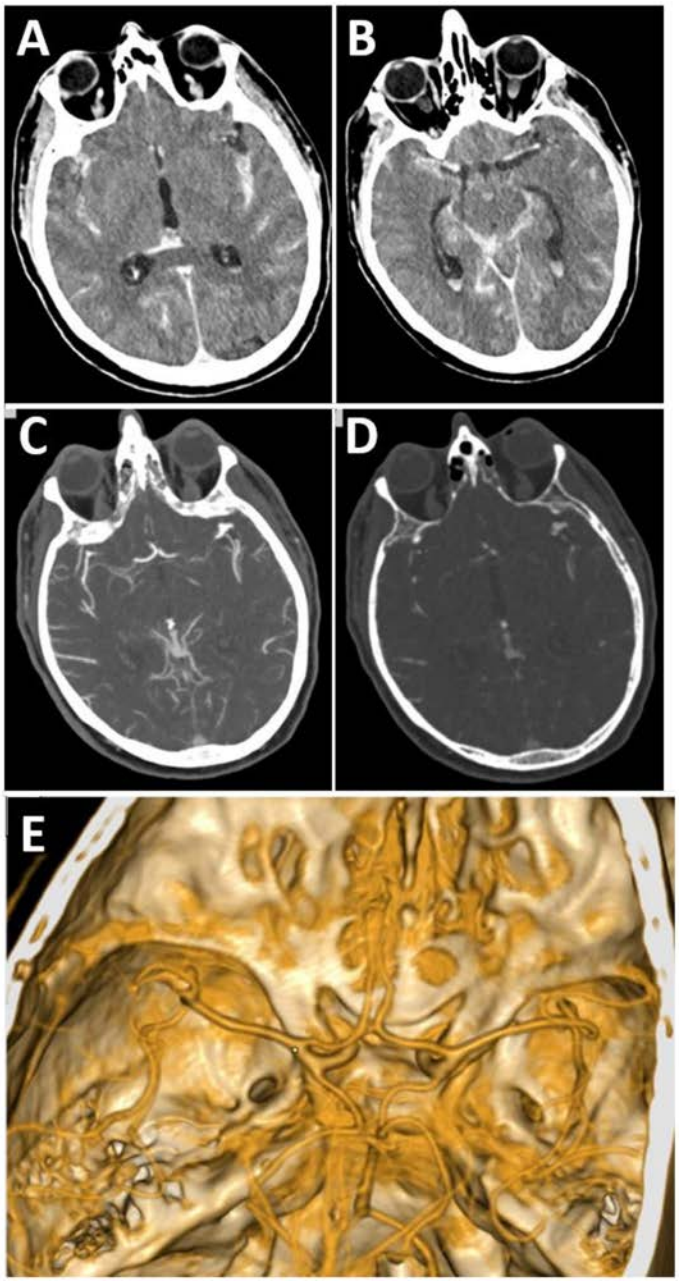

Figure 1. A, B. Preoperative imaging demonstrating aneurysmal subarachnoid hemorrhage and a ruptured left middle cerebral artery bifurcation aneurysm. Non-contrast head computed tomography shows diffuse subarachnoid hemorrhage involving the basal cisterns and bilateral sylvian fissures, with associated intraventricular hemorrhage and acute hydrocephalus, corresponding to modified Fisher grade IV hemorrhage. **C, D, E**. Axial computed tomography angiography images and three-dimensional vascular reconstruction demonstrate a multilobulated aneurysm arising from the left middle cerebral artery bifurcation with incorporation of an M2 branch. No pseudoaneurysmal component was identified on preoperative vascular imaging.

Computed tomography angiography revealed a multilobulated aneurysm arising from the bifurcation of the left middle cerebral artery with incorporation of an inferior M2 branch (Figure 1 C-E). No radiological findings suggestive of pseudoaneurysm formation were identified.

Given the presence of a ruptured middle cerebral artery aneurysm associated with poor-grade aneurysmal subarachnoid hemorrhage, emergency microsurgical treatment was undertaken.

A standard left pterional craniotomy was performed. Following wide sylvian fissure dissection, proximal control of the M1 segment was obtained. Careful microsurgical exploration of the aneurysm complex unexpectedly revealed a second cavity adjacent to the aneurysm dome and presumed rupture site, a finding not appreciated on preoperative vascular imaging (Figure 2).

This structure exhibited a dark-red appearance, irregular morphology, and an extremely friable wall without recognizable

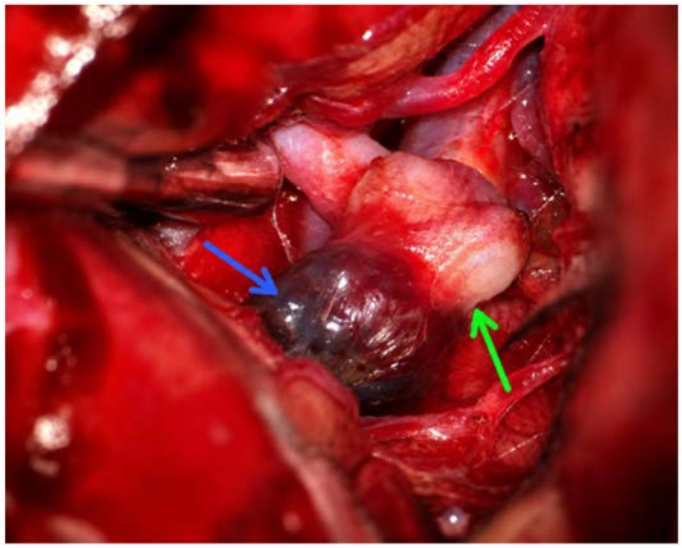

Figure 2. Intraoperative identification of an occult rupture-related pseudoaneurysm associated with a ruptured middle cerebral artery aneurysm. Microscopic intraoperative view demonstrates the true aneurysm arising from the left middle cerebral artery bifurcation and an adjacent rupture-related pseudoaneurysmal cavity located near the presumed rupture site. The pseudoaneurysm exhibited a dark-red appearance, irregular morphology, and a friable wall highly suggestive of an organized peri-aneurysmal hematoma communicating with the aneurysm lumen. This lesion was not evident on preoperative computed tomography angiography and was recognized only during microsurgical dissection.

arterial layers. Intraoperative findings were highly suggestive of a rupture-related pseudoaneurysm formed by an organized peri-aneurysmal hematoma communicating with the aneurysm lumen.

Temporary clipping of the M1 segment allowed circumferential dissection of the lesion complex. Because the pseudoaneurysmal cavity represented the most fragile portion of the lesion, special attention was directed toward complete exclusion of both the true aneurysm and the pseudoaneurysm. Definitive clip reconstruction was achieved using four permanent clips while preserving all incorporated M2 branches and maintaining satisfactory parent vessel geometry. No intraoperative rupture or other surgical complications occurred.

Following aneurysm exclusion, an intraparenchymal intracranial pressure monitor was inserted through a right frontal Kocher point. The patient was subsequently transferred to the neurocritical care unit for postoperative management.

Postoperative computed tomography demonstrated expected surgical findings with persistent subarachnoid and intraventricular blood products. New cortico-subcortical hypodense lesions involving both frontal lobes and the left temporal pole were identified and were considered compatible with delayed cerebral ischemia secondary to cerebral vasospasm (Figure 3).

The postoperative course was complicated by multiple systemic events, including neurogenic myocardial injury, aspiration pneumonia, bacterial meningitis, acute kidney injury, pulmonary thromboembolism requiring therapeutic anticoagulation, and transient urinary retention. Despite these complications, serial neuroimaging demonstrated progressive resolution of the hemorrhage without hydrocephalus progression or evidence of recurrent bleeding.

Neurological recovery was gradual but remarkable. The patient was successfully weaned from mechanical ventilation and vasopressor support and progressively regained full neurological function. At the time of discharge, he was awake, alert, fully oriented, and demonstrated a Glasgow Coma Scale score of 15. No focal motor deficits were identified, and he was able to ambulate independently and perform all activities of daily living without assistance.

DISCUSSION

Pathophysiology of rupture-related pseudoaneurysm formation

Rupture-related pseudoaneurysms represent a distinct pathological entity that differs fundamentally from conventional intracranial

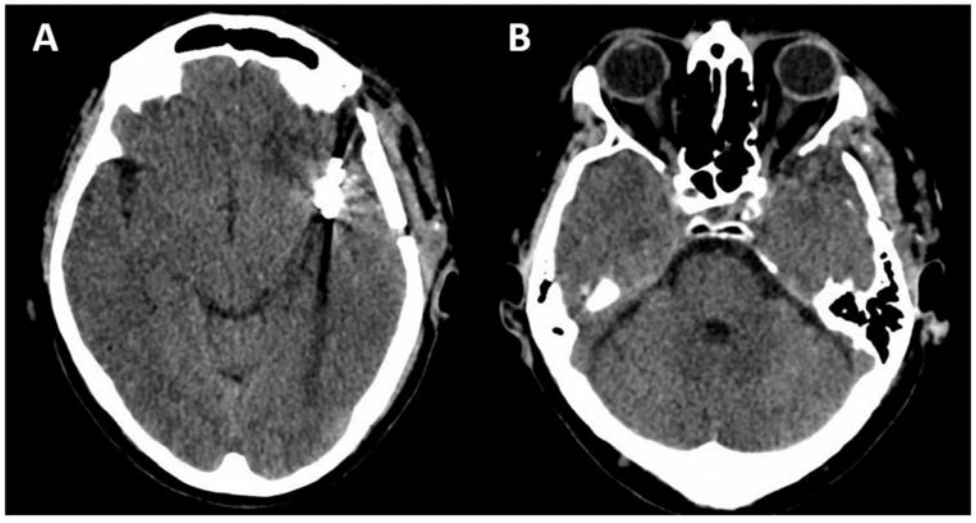

Figure 3. A. Postoperative imaging following microsurgical clip reconstruction. Axial postoperative computed tomography images demonstrate expected postoperative findings after clip reconstruction of the left middle cerebral artery aneurysm complex, with multiple clips visible in the left sylvian region. **B.** Follow-up imaging showed no evidence of recurrent hemorrhage, significant mass effect, or hydrocephalus progression.

aneurysms. Unlike true aneurysms, which arise through progressive degeneration of the arterial wall, rupture-related pseudoaneurysms develop secondary to rupture of an existing saccular aneurysm[3-6].

The most widely accepted mechanism involves disruption of the aneurysm dome with blood extravasation into the surrounding cisternal or parenchymal spaces. When the hemorrhage becomes locally contained, a peri-aneurysmal hematoma may remain in communication with the aneurysm lumen. Progressive clot organization and fibrosis subsequently create a cavity devoid of normal arterial wall layers. This newly formed cavity behaves as a pseudoaneurysm and remains highly vulnerable to recurrent rupture because it is composed primarily of organized thrombus and fibrous tissue rather than native vascular structures[3-6].

Several authors have proposed different terminologies for this phenomenon. Mori et al.[3] introduced the term "ghost aneurysm" to describe a transient pseudoaneurysmal cavity visualized after aneurysm rupture. Crusius et al.[2] subsequently proposed the designation "mixed aneurysm" to emphasize the coexistence of a true aneurysm and a pseudoaneurysmal component within the same lesion. Despite differences in nomenclature, these descriptions likely represent different manifestations of the same underlying pathological process.

The extreme fragility of the pseudoaneurysmal wall explains the increased risk of rebleeding and intraoperative rupture reported in the literature. Furthermore, the pseudoaneurysm frequently corresponds to the actual rupture site, making its identification particularly important during definitive treatment[3-6].

Literature review findings

A review of the available literature demonstrates the rarity of rupture-related pseudoaneurysms associated with true intracranial aneurysms. Most published reports consist of isolated case reports or small case series, highlighting the limited understanding of this phenomenon (Table 1)[2-7].

Reported aneurysm locations include the middle cerebral artery, posterior communicating artery, anterior communicating artery, and other anterior circulation vessels[4-6,9]. Diagnosis has been established through digital subtraction angiography, repeat vascular imaging demonstrating interval morphological changes, intraoperative inspection, or histopathological examination[3-8].

Several recurring imaging characteristics have been described, including snowman morphology, multilobulated configuration, daughter-sac appearance, delayed contrast filling, delayed contrast washout, and contrast retention (Table 2)[1,3-8]. However, these findings are inconsistent and may be absent even in confirmed cases.

Treatment strategies reported in the literature include microsurgical clipping, endovascular coiling, stent-assisted

Table 1. Published Reports of Rupture-Related Intracranial Pseudoaneurysms Associated with Ruptured True Aneurysms.

Author	Year	Location	Diagnosis Timing	Treatment	Outcome
Nomura et al.[4]	2000	Irregular intracranial aneurysm	Angiography and intraoperative findings	Microsurgical clipping	Favorable
Mori et al.[3]	2004	Ruptured cerebral aneurysm ("ghost aneurysm")	Angiography	Microsurgical clipping	Favorable
Nomura et al.[6]	2015	Middle cerebral artery	CT angiography and surgery	Microsurgical clipping	Favorable
Crusius et al.[2]	2017	Mixed aneurysm	Angiography	Microsurgical treatment	Favorable
Nomura et al.[5]	2017	Multiple intracranial locations (case series)	Angiography, surgery, and follow-up imaging	Microsurgical and endovascular treatment	Variable
Kim et al.[9]	2018	Posterior communicating artery	Digital subtraction angiography	Endovascular coiling	Favorable
Tsukiyama et al.[7]	2020	Ruptured intracranial aneurysm	Serial angiographic evaluation	Microsurgical treatment	Favorable
Present case	2026	Middle cerebral artery bifurcation	Intraoperative diagnosis during microsurgical clipping	Microsurgical clipping	Complete neurological recovery (GCS 15, no focal deficits)

Abbreviations: CT, computed tomography; GCS, Glasgow Coma Scale.

Table 2. Proposed Radiological Clues Suggestive of Rupture-Related Pseudoaneurysm.

Imaging Feature	Proposed Mechanism
Snowman morphology	True aneurysm plus pseudoaneurysm cavity
Daughter-sac appearance	Rupture site organization
Delayed contrast filling	Slow inflow into pseudoaneurysm
Delayed contrast washout	Restricted outflow
Contrast retention	Stagnant flow within pseudoaneurysm
Multilobulated morphology	Mixed aneurysm formation
Interval aneurysm enlargement	Progressive pseudoaneurysm development
Dynamic morphological change	Evolution after aneurysm rupture

coiling, and flow-diversion techniques[1,5,9]. Outcomes appear largely dependent on the severity of the initial hemorrhage rather than the pseudoaneurysm itself.

Diagnostic challenges

Preoperative diagnosis remains particularly challenging because radiological findings are frequently subtle, nonspecific, or entirely absent[1,3-8].

Nomura et al.[4-6] demonstrated that pseudoaneurysms may remain angiographically occult and become evident only after repeat vascular imaging or direct surgical inspection. Similarly, Tsukiyama et al.[7] reported dynamic aneurysm morphology changes following rupture that strongly suggested progressive pseudoaneurysm formation.

Surgical implications

Recognition of a rupture-related pseudoaneurysm may substantially alter operative strategy[1,4-6].

Failure to recognize the pseudoaneurysm may result in incomplete lesion exclusion and persistent risk of postoperative hemorrhage[1,4-6].

The present case highlights one of the principal advantages of microsurgical treatment. Direct visualization of the aneurysm complex allowed identification of pathological structures that were not appreciated on preoperative imaging.

Microsurgical treatment remains particularly advantageous for middle cerebral artery bifurcation aneurysms because it allows direct visualization of the rupture site, preservation of branch anatomy, and complete reconstruction of complex lesions, outcomes consistently reported in contemporary microsurgical series[8,10].

Although endovascular techniques continue to evolve, rupture-related pseudoaneurysms remain challenging lesions because of their irregular morphology, absence of a true wall, and dynamic evolution[1,9]. The principal pathological, radiological, and surgical differences between true aneurysms and rupture-related pseudoaneurysms are summarized in Table 3[1,9].

Lessons from the present case

Another notable aspect of the present case was the patient's remarkable neurological recovery despite presenting with poor-grade aneurysmal subarachnoid hemorrhage (Hunt-Hess V, WFNS V, modified Fisher IV)[11-15]. Although poor-grade aneurysmal subarachnoid hemorrhage is traditionally associated with high morbidity and mortality, aggressive multidisciplinary management may still result in favorable outcomes in selected patients[12,14].

To our knowledge, this represents one of the few reported cases of an occult rupture-related pseudoaneurysm associated with a ruptured middle cerebral artery bifurcation aneurysm diagnosed exclusively during microsurgical clipping.

Collectively, the available literature suggests that rupture-related pseudoaneurysms represent dynamic lesions that may evolve rapidly

Table 3. Comparison Between True Intracranial Aneurysms and Rupture-Related Pseudoaneurysms.

Characteristic	True Aneurysm	Rupture-Related Pseudoaneurysm
Wall composition	Attenuated arterial wall	Fibrous tissue and organized hematoma
Histology	Intima, media, and adventitia remnants	No true arterial wall
Pathogenesis	Degenerative vascular remodeling	Secondary to rupture of a pre-existing aneurysm
Rupture risk	Elevated	Extremely high
Rebleeding risk	Moderate	High
Imaging appearance	Usually stable morphology	Dynamic and irregular morphology
Angiographic behavior	Immediate filling and washout	Delayed filling and contrast retention may occur
Intraoperative appearance	Defined aneurysm wall	Friable cavity with poorly defined borders
Surgical manipulation	Standard aneurysm dissection and clipping	High-risk dissection due to wall fragility
Diagnostic certainty	Usually established radiologically	Frequently established intraoperatively
Need for repeat imaging	Uncommon	May be required due to dynamic evolution
Treatment objective	Exclusion of aneurysm sac	Exclusion of both aneurysm and pseudoaneurysm
Risk of intraoperative rupture	Elevated	Markedly increased
Clinical significance	Common cerebrovascular lesion	Rare but potentially underrecognized complication of aneurysm rupture

Abbreviation: CT, computed tomography.

after aneurysm rupture and frequently remain underrecognized. The present case reinforces previous observations that angiographic findings may be absent despite the presence of a clinically significant pseudoaneurysmal component. Consequently, definitive diagnosis may depend on meticulous microsurgical inspection, emphasizing the continued value of microsurgical expertise in the management of complex aneurysmal disease.

Limitations

This report has several limitations. First, it describes a single patient and therefore does not allow definitive conclusions regarding incidence, natural history, or optimal treatment strategies. Second, histopathological confirmation of the pseudoaneurysmal cavity was not available, and diagnosis was based on characteristic intraoperative findings. Third, postoperative digital subtraction angiography was not performed, limiting radiological confirmation of complete lesion exclusion. Finally, the available literature consists predominantly of isolated case reports and small case series, restricting the strength of evidence regarding this uncommon vascular entity.

CONCLUSION

Rupture-related pseudoaneurysm formation secondary to rupture of a true intracranial aneurysm represents a rare but clinically significant vascular phenomenon. As demonstrated in the present case, these lesions may remain entirely occult on preoperative vascular imaging and become apparent only during direct microsurgical exploration.

Recognition of the pseudoaneurysmal component is essential because it frequently corresponds to the rupture site and represents the most fragile portion of the lesion, carrying an increased risk of intraoperative rupture and postoperative rebleeding. Consequently, neurosurgeons should maintain a high index of suspicion when treating irregular or multilobulated ruptured aneurysms, even in the absence of specific radiological findings.

This case highlights the diagnostic value of direct microsurgical inspection, the importance of meticulous clip reconstruction addressing both aneurysmal and pseudoaneurysmal components, and the continued role of microsurgical expertise in

the management of complex cerebrovascular pathology. Further studies are necessary to better define the incidence, radiological characteristics, and optimal treatment strategies for rupture-related pseudoaneurysms associated with intracranial aneurysms.

REFERENCES

1. Zheng Y, Lu Z, Shen J, Xu F. Intracranial pseudoaneurysms: evaluation and management. Front Neurol. 2020;11:582. https://doi.org/10.3389/fneur.2020.00582. PMid:32733358.

2. Crusius CU, Aguiar PH, Crusius MU. Mixed aneurysm: a new proposed nomenclature for a rare condition. Surg Neurol Int. 2017;8:29. PMid:28303209.

3. Mori K, Yamamoto T, Nakao Y, Esaki T. Ghost aneurysm associated with rupture of a cerebral aneurysm. Neurosurg Rev. 2004;27(3):208-12.

4. Nomura M, Mori K, Kawamura H. Pseudoaneurysm formation in a thrombus located at the rupture site of an irregularly shaped aneurysm. J Neurosurg. 2000;93(6):998-1000. https://doi.org/10.3171/jns.2000.93.6.0998. PMid:11117874.

5. Nomura M, Mori K, Tamase A, et al. Pseudoaneurysm formation due to rupture of intracranial aneurysms: case series and literature review. Neuroradiol J. 2017;30(2):129-37. https://doi.org/10.1177/1971400916684667. PMid:28059632.

6. Nomura M, Tamase A, Kamide T, Mori K, Seki S, Yanagimoto K. Pseudoaneurysm formation in intracerebral hematoma due to ruptured middle cerebral artery aneurysm. Surg J (NY). 2015;1(1):e47-9. https://doi.org/10.1055/s-0035-1567877. PMid:28824972.

7. Tsukiyama A, Yoshimoto Y, Watanabe M, Kuga Y, Takahashi H, Nakazato Y. Morphological change of cerebral aneurysm with possible pseudoaneurysm formation after rupture: case report and literature review. Neurol Med Chir (Tokyo). 2020;60(6):314-9.

8. Rodríguez-Hernández A, Sughrue ME, Akhavan S, Habdank-Kolaczkowski J, Lawton MT. Current management of middle cerebral artery aneurysms: surgical results and literature review. World Neurosurg. 2013;79(1):143-50. PMid:23022651.

9. Kim BM, Chang CH, Oh SY, Kim DJ, Kim DI, Suh SH. A pseudoaneurysm associated with a ruptured cerebral aneurysm and successful coil embolization. J Cerebrovasc Endovasc Neurosurg. 2018;20(1):24-9. https://doi.org/10.7461/jcen.2018.20.1.24. PMid:30370236.

10. Dasenbrock HH, Smith TR, Gormley WB, et al. Hospital and surgeon volume-outcome relationships in clipping and coiling of cerebral aneurysms in the United States. Neurosurgery. 2016;79(3):354-64. PMid:26901145.

11. Connolly ES Jr, Rabinstein AA, Carhuapoma JR, et al. Guidelines for the management of aneurysmal subarachnoid hemorrhage. Stroke. 2012;43(6):1711-37. https://doi.org/10.1161/STR.0b013e3182587839. PMid:22556195.

12. Hoh BL, Ko NU, Amin-Hanjani S, et al. 2023 guideline for the management of patients with aneurysmal subarachnoid hemorrhage: a guideline from the American Heart Association/American Stroke Association. Stroke. 2023;54(7):e314-70. https://doi.org/10.1161/STR.0000000000000436. PMid:37212182.

13. Lawton MT, Vates GE. Subarachnoid hemorrhage. N Engl J Med. 2017;377(3):257-66. https://doi.org/10.1056/NEJMcp1605827. PMid:28723321.

14. Macdonald RL, Schweizer TA. Spontaneous subarachnoid haemorrhage. Lancet. 2017;389(10069):655-66. https://doi.org/10.1016/S0140-6736(16)30668-7. PMid:27637674.

15. Molyneux AJ, Kerr RSC, Yu LM, et al. International Subarachnoid Aneurysm Trial (ISAT) of neurosurgical clipping versus endovascular coiling in 2143 patients with ruptured intracranial aneurysms: a randomised comparison of effects on survival, dependency, seizures, rebleeding, subgroups, and aneurysm occlusion. Lancet. 2005;366(9488):809-17. https://doi.org/10.1016/S0140-6736(05)67214-5. PMid:16139655.

CORRESPONDING AUTHOR

José Luis Quelho Filho, MD
Faculdade de Medicina de São José do Rio Preto – FAMERP
Department of Neurosurgery
São José do Rio Preto, São Paulo, Brasil
E-mail: jquelho73@gmail.com

Funding: *nothing to disclose.*
Conflicts of interest: *nothing to disclose.*
Institution: *Hospital de Base de São José do Rio Preto.*

CRediT

Jose Luis Quelho Filho: conceptualization, data curation, formal analysis, investigation, methodology, validation, visualization, writing – original draft, writing – review & editing, supervision, project administration. Paulo Eduardo Albuquerque Zito Raffa: conceptualization, data curation, formal analysis, investigation,

methodology, validation, visualization, writing – original draft, writing – review & editing. Leonardo Vieira Nunes: conceptualization, data curation, formal analysis, investigation, methodology, validation, visualization, writing – original draft, writing – review & editing, supervision. Gabriel Ribas Nascimento de Melo: conceptualization, data curation, formal analysis, investigation, methodology, validation, visualization, writing – original draft, writing – review & editing. Rodrigo Shibaki: formal analysis, investigation, methodology, visualization, writing – original draft, writing – review & editing. Lucas Crociati Meguins: conceptualization, data curation, formal analysis, investigation, methodology, validation, visualization, writing – review & editing, supervision, project administration

GAMMA HOSPITAL INC KNIFE

Tratamento de diversas doenças cerebrais é possível com o Gamma Knife Perfexion®

Utiliza até 192 feixes de radiação

Gamma Knife, **cirurgia cerebral** sem corte nem internamento.

Patologias tratadas:

Metástases cerebrais
Outros tumores benignos e malignos
Neuralgia do trigêmeo
Malformações arteriovenosas
Tremor essencial e Parkinson
Casos selecionados de epilepsia

Indique o seu paciente

Diretor técnico: Dr. Daniel Benzecry CRM PR 15845 RQE Nº: 6982

JBNC
JORNAL BRASILEIRO DE NEUROCIRURGIA
BRAZILIAN JOURNAL OF NEUROSURGERY

Case Report

Parafalcine Chondrosarcoma: clinical and surgical evaluation of a rare case

Condrossarcoma Parafalcino: avaliação clínica e cirúrgica de um caso raro

Muhammed Şamil Sağlam[1]
Hüda Eroğlu[1]
Hacı Hasan Esen[2]
Mehmet Fatih Erdi[1]

ABSTRACT

Introduction: *Intracranial chondrosarcomas are exceedingly rare malignant tumors of cartilaginous origin, accounting for less than 0.15% of all primary intracranial neoplasms. They typically arise from skull base synchondroses, whereas meningeal locations such as the falx cerebri are uncommon.* **Case presentation**: *A 72-year-old woman presented with progressive headache and right lower extremity weakness for two months. Neuroimaging revealed a 5 × 4 cm extra-axial parafalcine mass with irregular calcifications and minimal contrast enhancement, initially suggestive of meningioma. CT angiography demonstrated an avascular lesion. The patient underwent gross total resection via left central craniotomy with neuronavigation and intraoperative neuromonitoring. Histopathological evaluation confirmed a grade 2 chondrosarcoma. Postoperative imaging showed no residual tumor. Adjuvant radiotherapy was not administered, and close clinical and radiological follow-up was recommended.* **Conclusion**: *This case highlights an atypical presentation in advanced age and emphasizes the importance of including chondrosarcoma in the differential diagnosis of calcified, dural-based intracranial lesions.*

Keywords: *Sarcoma; Chondrosarcoma; Parafalx*

RESUMO

Introdução: *Condrosarcomas intracranianos são tumores malignos extremamente raros de origem cartilaginosa, representando menos de 0,15% de todas as neoplasias intracranianas primárias. Normalmente surgem de sincrondrosas na base do crânio, enquanto locais meníngeos como a falx cerebri são incomuns.* **Descrição do caso**: *Uma mulher de 72 anos apresentou dor de cabeça progressiva e fraqueza no membro inferior direito por dois meses. Estudos de neuroimagem revelaram massa parafalcina extra-axial de 5 × 4 cm com calcificações irregulares e aumento mínimo de contraste, inicialmente sugestivo de meningioma. A angiografia computadorizada demonstrou lesão avascular. A paciente foi submetida a ressecção total via craniotomia central esquerda com neuronavegação e neuromonitoramento intraoperatório. A avaliação histopatológica confirmou condrosarcoma grau 2 e as imagens pós-operatórias não mostraram tumor residual. Não foi administrada a radioterapia adjuvante, e recomendado acompanhamento clínico e radiológico rigoroso.* **Conclusão**: *Este caso destaca uma apresentação atípica na idade avançada e enfatiza a importância de incluir o condrosarcoma no diagnóstico diferencial de lesões intracranianas calcificadas baseadas em durais.*

Palavras-Chave: *Sarcoma; Condrosarcoma; Parafalcino*

[1]Department of Neurosurgery, Necmettin Erbakan University Meram Faculty of Medicine, Konya, Türkiye.
[2]Department of Pathology, Necmettin Erbakan University Meram Faculty of Medicine, Konya, Türkiye.

Received Aug 6, 2026
Accepted Aug 13, 2026

INTRODUCTION

Intracranial chondrosarcomas are rare malignant tumors of cartilaginous origin in the central nervous system, accounting for less than 0.15% of all primary intracranial neoplasms[1-3] These tumors most commonly arise from cartilaginous synchondroses at the skull base. However, in rare cases, they may originate from the meninges along the falx cerebri, tentorium, or cerebral convexity[3,4].

Although their pathogenesis has not been fully elucidated, it has been suggested that they may arise from embryonic cartilaginous remnants, metaplasia of meningeal fibroblasts, or multipotent mesenchymal cells[5]. Intracranial chondrosarcomas pose significant diagnostic challenges because of their rarity and wide spectrum of radiological findings. These lesions are frequently confused with meningioma, chondroma, or meningeal metastases, and definitive diagnosis is most often established through histopathological examination[6].

In this study, we present a case of intracranial chondrosarcoma with parafalcine localization that radiologically mimicked a calcified meningioma, and its clinical, radiological, and histopathological features in light of the literature is discussed.

CASE PRESENTATION

A 72-year-old female patient presented with progressively worsening headache, weakness, and fatigue in the right leg, which had been ongoing for two months. The patient had no prior brain imaging studies. Her medical history included diabetes mellitus, hypertension, and previous nephrectomy. She had no known pre-existing brain pathology or history of radiotherapy. Neurological examination revealed limited cooperation and right lower extremity muscle strength of 4/5.

Cranial computed tomography (CT) showed an approximately 5 × 4 cm mass lesion at the vertex level in the interhemispheric region. The lesion was considered extra-axial and contained irregular peripheral calcifications. CT angiography revealed an avascular lesion (Figure 1). Contrast-enhanced cranial magnetic resonance imaging (MRI) showed an extra-axial mass located medially in the left posterior parietal region, adjacent to the superior sagittal sinus wall, without significant contrast enhancement. No marked peritumoral edema was observed (Figure 2). Written informed consent was obtained from the patient for the surgical procedure and for publication of this case report and accompanying images. All procedures were performed in accordance with the Declaration of Helsinki.

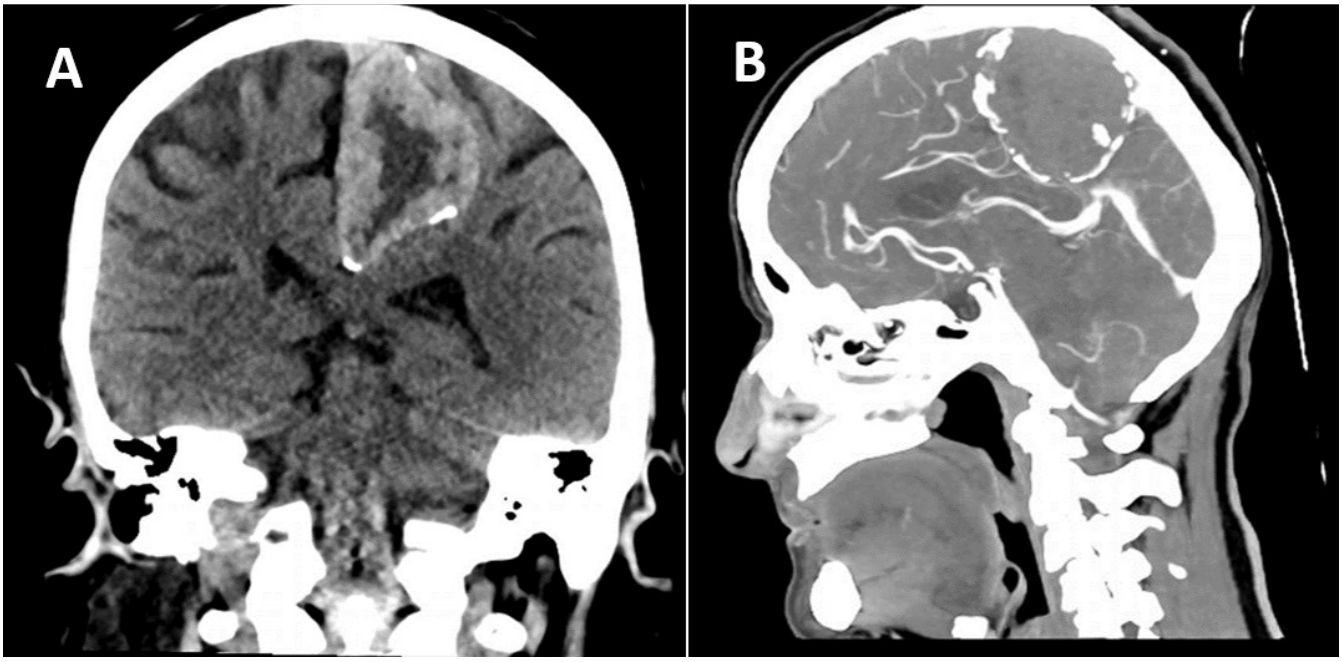

Figure 1. Preoperative CT images. **A**. Irregular calcifications in the coronal CT section. **B**. Avascular nature of the mass in the sagittal CT section.

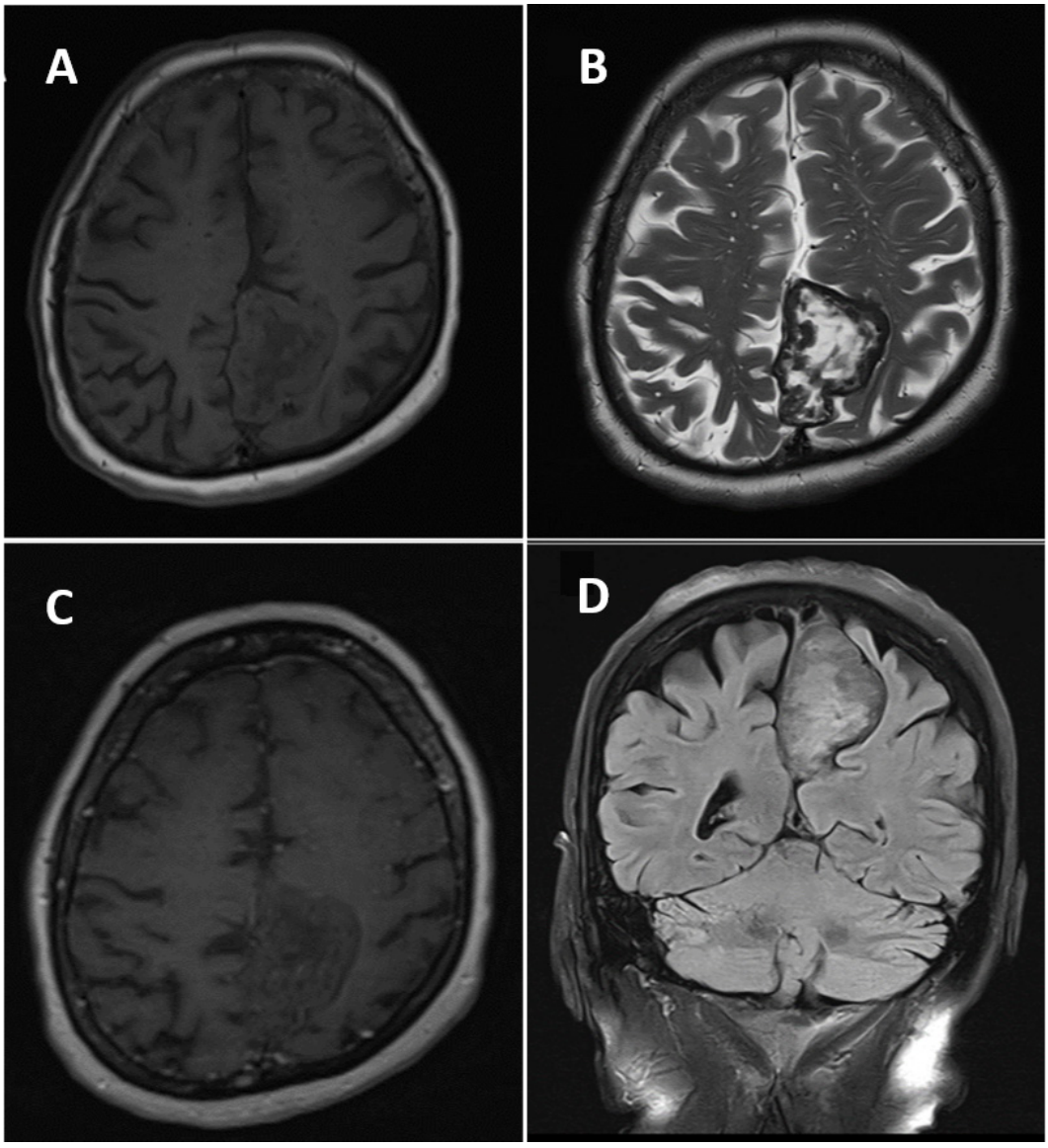

Figure 2. Preoperative MRI images. **A**. Axial T1-weighted MRI. **B**. Axial T2-weighted MRI. **C**. Axial contrast-enhanced T1-weighted MRI. **D**. Coronal T1-weighted MRI.

The patient underwent surgical treatment. Through a left central craniotomy, a firm mass with a clear cleavage plane from the surrounding brain tissue was totally excised using an ultrasonic aspirator (UST-2001, Stryker, Kalamazoo, MI, USA). Because of the proximity of the lesion to the motor cortex, neuronavigation was used intraoperatively to confirm localization, and neuromonitoring was employed to preserve functional areas.

Histopathological evaluation revealed negative SSTR2A and pancytokeratin immunohistochemical staining, supporting the diagnosis of grade 2 chondrosarcoma (Figure 3). Postoperative contrast-enhanced MRI showed no evidence of residual tumor (Figure 4). The patient underwent evaluation by the Department of Radiation Oncology. Close follow-up was recommended, with no indication for adjuvant radiotherapy.

At the first postoperative month, the patient had right hemiparesis with muscle strength of 3/5. She was oriented and cooperative. The patient was transferred to a palliative care unit for physical therapy and rehabilitation. During follow-up, no evidence of tumor recurrence was detected.

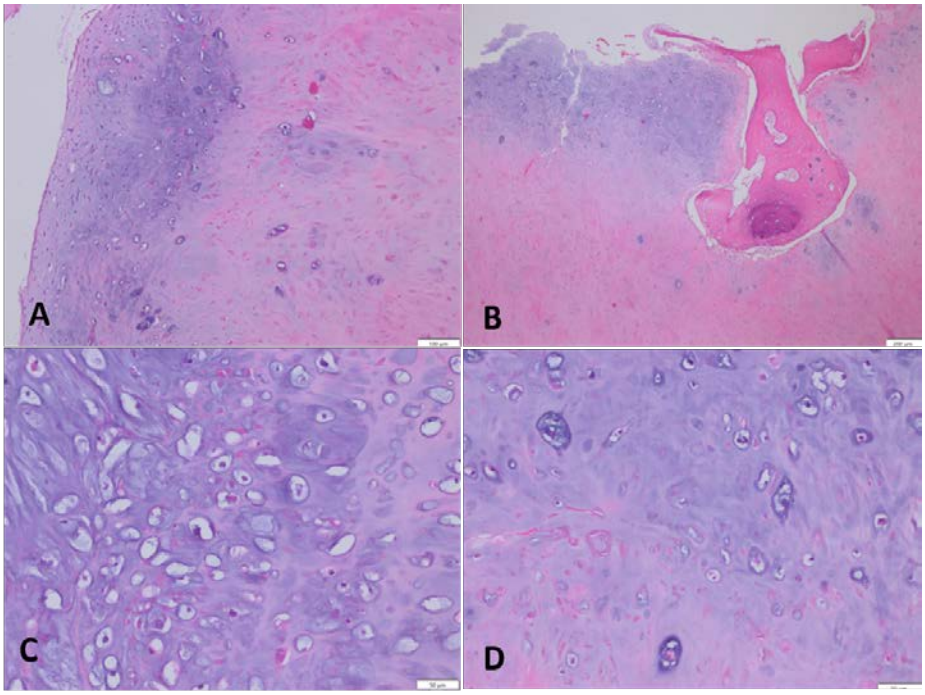

Figure 3. Histopathological images: **A**. Tumor structure with variable cellularity, containing hyaline and myxoid areas. **B**. Image surrounding the skull bone. **C**. and **D**. Image of chondrocytes with atypical clear cytoplasm.

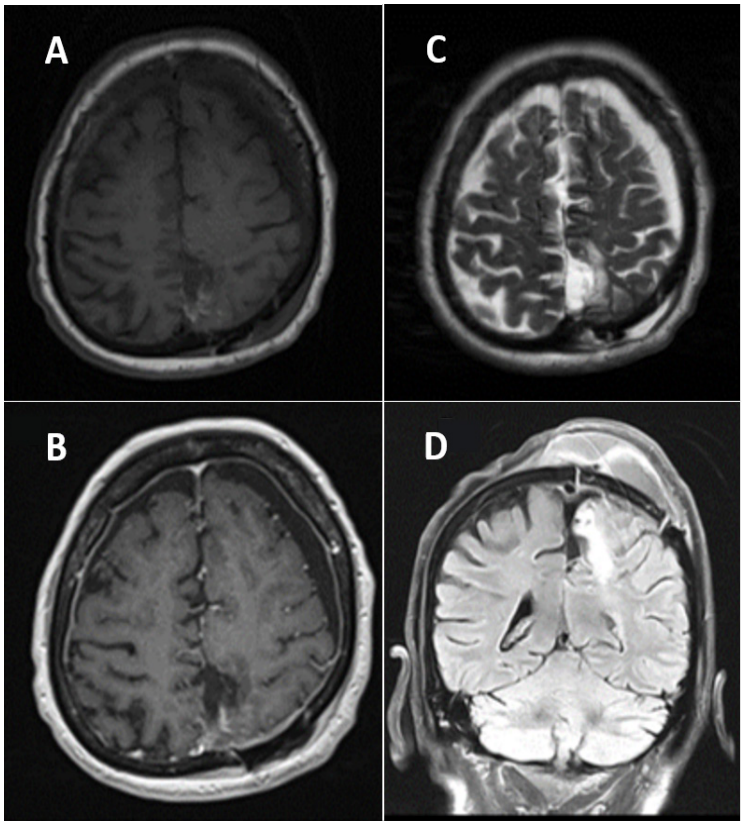

Figure 4. Postoperative MRI images. **A.** Axial T1-weighted MRI. **B.** Axial T2-weighted MRI. **C.** Axial contrast-enhanced T1-weighted MRI. **D.** Coronal T1-weighted MRI.

DISCUSSION

Intracranial chondrosarcomas are extremely rare malignant tumors, accounting for less than 0.15% of all primary intracranial neoplasms[1,2]. Although their histogenesis has not been fully clarified, it has been suggested that they originate from pluripotent mesenchymal cells in the dura mater or from cells derived from embryonic cartilaginous remnants[5]. Although intracranial chondrosarcomas most commonly occur at the skull base, localization along the falx, tentorium, and cerebral convexity meninges is quite rare[3,4]. In this context, the parietal parafalcine localization of the lesion in the present case represents one of the less commonly reported atypical sites and supports the meningeal origin hypothesis.

Histopathologically, chondrosarcomas are classified into classical, mesenchymal, and myxoid subtypes, which exhibit significant differences in clinical behavior and prognosis[6]. The classical type is generally well differentiated and associated with a better prognosis, whereas the mesenchymal type demonstrates a more aggressive course with a high potential for recurrence and metastasis[7]. It has been reported that the mesenchymal subtype is more frequently observed in parasagittal and falcine tumors[7]. Classical chondrosarcomas are low-grade tumors characterized by a well-developed cartilaginous matrix and minimal anaplasia. In contrast, mesenchymal chondrosarcomas are defined by highly cellular anaplastic mesenchymal cells and poorly differentiated cartilaginous components, exhibiting more aggressive biological behavior. Myxoid chondrosarcomas are characterized by uniform chondrocytes arranged in cords and strands within an abundant myxoid stroma and have intermediate malignant potential[2,6]. Prognosis is closely related to histological subtype, extent of surgical resection, use of adjuvant therapy, and particularly the presence of local recurrence[1]. Local recurrence is considered one of the most important determinants of mortality[1].

The condition typically manifests between the ages of 10 and 30 years[8]. The present case, occurring in a 72-year-old patient, represents a marked deviation from the expected age distribution, thereby underscoring the exceptional nature of this presentation. Clinical manifestations generally vary depending on tumor location and size, with headache, focal neurological deficits, and symptoms related to increased intracranial pressure being the most commonly reported findings.

Radiologically, these lesions typically appear iso- or mildly hyperdense on CT scan and may contain varying degrees of calcification. On MRI, they are usually hypointense on T1-weighted images and mildly hyperintense on T2-weighted images, often demonstrating heterogeneous contrast enhancement[9]. Despite their large size, significant peritumoral edema and necrosis are generally not observed[8]. Angiographic studies typically reveal low vascularity, especially in mesenchymal subtypes[10]. However, because of their rarity and heterogeneous imaging characteristics, differential diagnosis is often challenging. The most common differential diagnoses include meningioma, hemangiopericytoma, chondromyxoid fibroma, metastatic lesions, and arteriovenous malformations[6]. In the present case, the lesion radiologically mimicked a meningioma because of the presence of irregular calcifications and the absence of significant contrast enhancement. However, the avascular nature of the lesion on CT angiography was consistent with the literature.

In light of these findings, radiological modalities appear to have limited specificity in differential diagnosis. Definitive diagnosis is most often established through histopathological examination following surgical resection. Histologically, the coexistence of hyaline cartilage islands and small undifferentiated mesenchymal cells is characteristic[1]. Immunohistochemically, these tumors typically show positivity for S-100 and vimentin and negativity for EMA and cytokeratin[11]. In the present case, the principal histopathological differential diagnoses included chordoid meningioma and chordoma. These entities were immunohistochemically excluded by the absence of SSTR2A and pancytokeratin expression. Furthermore, PHH3 immunohistochemistry demonstrated a single mitotic figure, allowing accurate assessment of mitotic activity (Figure 3).

Although currently there is no standardized treatment guideline, the mainstay of treatment is maximal safe surgical resection. It has been reported that recurrence rates are lower in cases in which gross total resection is achieved[2,11]. Chemotherapy has no established role in treatment. However, adjuvant radiotherapy has been shown to significantly improve survival, particularly in cases with subtotal resection or high-grade tumors[12]. Nevertheless, because of the rarity of the disease, data regarding optimal treatment strategies and long-term outcomes remain limited.

CONCLUSION

Intracranial chondrosarcomas are rare malignant tumors that pose significant diagnostic challenges because of their variable radiological features. They should be considered in the differential diagnosis of dural-based, calcified extra-axial lesions. Definitive diagnosis relies on histopathological evaluation, and maximal safe surgical resection remains the cornerstone of treatment. The present case is noteworthy because of its occurrence in an elderly patient, interhemispheric parafalcine location, and absence of marked contrast enhancement, features that differ from those commonly reported in the literature. Therefore, intracranial chondrosarcoma should be considered in the differential diagnosis of lesions with similar radiological characteristics.

REFERENCES

1. Bloch OG, Jian BJ, Yang I, et al. A systematic review of intracranial chondrosarcoma and survival. J Clin Neurosci. 2009;16(12):1547-51. https://doi.org/10.1016/j.jocn.2009.05.003. PMid:19796952.

2. Salcman M, Scholtz H, Kristt D, Numaguchi Y. Extraskeletal myxoid chondrosarcoma of the falx. Neurosurgery. 1992;31(2):344-8. https://doi.org/10.1227/00006123-199208000-00021. PMid:1513440.

3. Lee YY, van Tassel P, Raymond AK. Intracranial dural chondrosarcoma. AJNR Am J Neuroradiol. 1988;9(6):1189-93. PMid:3143243.

4. Roy S, Chopra P, Prakash BB, Tandon PN. Chondrosarcoma of the meninges. Acta Neuropathol. 1972;22(3):272-4. https://doi.org/10.1007/BF00684531. PMid:4637009.

5. Volpe NJ, Liebsch NJ, Munzenrider JE, Lesseill S. Neuro-ophthalmologic findings in chordoma and chondrosarcoma of the skull base. Am J Ophthalmol. 1993;115(1):97-104. https://doi.org/10.1016/S0002-9394(14)73531-7. PMid:8420385.

6. Nagata S, Sawada K, Kitamura K. Chondrosarcoma arising from the falx cerebri. Surg Neurol. 1986;25(5):505-9. https://doi.org/10.1016/0090-3019(86)90092-3. PMid:3961667.

7. Safaee M, Clark AJ, Tihan T, Parsa AT, Bloch O. Falcine and parasagittal chondrosarcomas. J Clin Neurosci. 2013;20(9):1232-6. https://doi.org/10.1016/j.jocn.2013.01.004. PMid:23759737.

8. Chu J, Ma H, Wang Y, Li K, Liao C, Ding Y. CT and MRI findings of intracranial extraskeletal mesenchymal chondrosarcoma: a case report and literature review. Transl Cancer Res. 2022;11(9):3409-15. https://doi.org/10.21037/tcr-21-2547. PMid:36237268.

9. Oruckaptan HH, Berker M, Soylemezoglu F, Ozcan OE. Parafalcine chondrosarcoma: an unusual localization for a classical variant: case report and review of the literature. Surg Neurol. 2001;55(3):174-9. https://doi.org/10.1016/S0090-3019(01)00329-9. PMid:11311919.

10. Chandler JP, Yashar P, Laskin WB, Russell EJ. Intracranial chondrosarcoma: a case report and review of the literature. J Neurooncol. 2004;68(1):33-9. https://doi.org/10.1023/B:NEON.0000024728.72998.7d. PMid:15174519.

11. Bourgouin PM, Tampieri D, Robitaille Y, et al. Low-grade myxoid chondrosarcoma of the base of the skull: CT, MR, and histopathology. J Comput Assist Tomogr. 1992;16(2):268-73. https://doi.org/10.1097/00004728-199203000-00017. PMid:1545025.

12. Isaacson B, Kutz JW, Roland PS. Lesions of the petrous apex: diagnosis and management. Otolaryngol Clin North Am. 2007;40(3):479-519, viii. https://doi.org/10.1016/j.otc.2007.03.003. PMid:17544693.

CORRESPONDING AUTHOR

Muhammed Şamil Sağlam, MD
Necmettin Erbakan University Meram Faculty of Medicine
Department of Neurosurgery
Selçuklu, Konya, Türkiye
E-mail: saglamsamil@gmail.com

Funding: *nothing to disclose.*
Conflicts of interest: *nothing to disclose.*
Ethics Committee Approval: *waived.*

CRediT

Muhammed Şamil Sağlam: Investigation, Data Curation, Writing – Original Draft. Hüda Eroğlu: Investigation, Literature Review, Data Curation, Resources, Writing – Original Draft. Hacı Hasan Esen: Investigation, Validation, Writing – Review & Editing. Mehmet Fatih Erdi: Conceptualization, Supervision, Writing – Review & Editing, Project Administration.

When Blooming Matters: bilateral cavernous sinus cavernoma mimicking macroadenoma

Quando o Blooming Importa: cavernoma bilateral do seio cavernoso mimetizando macroadenoma hipofisário

Andrey Fillip Thomaz Ribeiro[1]
Pedro Bernardo Berriel[1]
Nathalie Henriques Silva Canedo[1]
Nina Ventura Wilner[1]
Sérgio Ferreira Alves Júnior[1]

ABSTRACT

Cavernous sinus cavernomas are rare vascular lesions that may mimic pituitary macroadenomas. We report the case of a 40-year-old woman presenting with headache and generalized seizures. Computed tomography demonstrated bilateral hyperdense cavernous sinus lesions, while magnetic resonance imaging revealed parasellar masses with marked blooming artifact on susceptibility-weighted imaging, suggesting vascular content. Despite these findings, the initial diagnosis favored pituitary macroadenoma with cavernous sinus extension. During transsphenoidal surgery, the lesion proved highly vascular, with significant intraoperative bleeding preventing safe resection. Histopathological analysis confirmed cavernoma. This case highlights the importance of susceptibility-sensitive magnetic resonance imaging sequences in the preoperative diagnosis of parasellar vascular lesions and surgical planning.

Keywords: *Cavernous sinus; Central nervous system vascular malformations; Magnetic resonance imaging*

RESUMO

Cavernomas do seio cavernoso são lesões vasculares raras que podem mimetizar macroadenomas hipofisários. Relatamos o caso de uma mulher de 40 anos apresentando cefaleia e crises convulsivas. A tomografia computadorizada demonstrou lesões hiperdensas bilaterais nos seios cavernosos, enquanto a ressonância magnética evidenciou lesões parasselares com acentuado efeito blooming em sequência ponderada por susceptibilidade magnética, sugerindo conteúdo vascular. Apesar desses achados, o diagnóstico inicial favoreceu macroadenoma hipofisário com extensão para os seios cavernosos. Durante a cirurgia transesfenoidal, a lesão mostrou-se altamente vascularizada, com sangramento intraoperatório significativo, impedindo a ressecção segura. A análise histopatológica confirmou cavernoma. Este caso destaca a importância das sequências de ressonância magnética sensíveis à susceptibilidade magnética no diagnóstico pré-operatório de lesões vasculares parasselares e no planejamento cirúrgico.

Palavras-Chave: *Seio cavernoso; Malformações vasculares do sistema nervoso central; Ressonância magnética*

[1]Universidade Federal do Rio de Janeiro – UFRJ, Rio de Janeiro, RJ, Brazil.

Received Jun 4, 2026
Accepted Jun 25, 2026

CLINICAL IMAGES

The differential diagnosis of parasellar and cavernous sinus lesions includes pituitary adenomas, meningiomas, schwannomas, aneurysms, inflammatory lesions, and vascular malformations. Cavernous sinus cavernomas are rare lesions that may mimic pituitary macroadenomas on imaging studies, making preoperative diagnosis challenging[1,2]. Unlike intra-axial cavernous malformations, extra-axial cavernous sinus lesions often lack the classic "popcorn" appearance and may demonstrate nonspecific enhancement patterns on magnetic resonance imaging (MRI)[3].

Recognition of these lesions is particularly important because surgical manipulation may result in significant intraoperative bleeding due to their highly vascular nature and close relationship with the internal carotid arteries and cranial nerves within the cavernous sinus. We report a rare case of bilateral cavernous sinus cavernoma initially diagnosed as a nonfunctioning pituitary macroadenoma.

Case presentation

A 40-year-old woman presented with progressive headache, bilateral periorbital edema, and sporadic generalized tonic-clonic seizures. She denied symptoms suggestive of pituitary hormonal dysfunction. Neurological examination demonstrated no focal deficits, although the patient reported occasional blurred vision and retro-orbital discomfort.

Initial non-contrast computed tomography (CT) demonstrated bilateral spontaneously hyperdense expansile lesions centered within the cavernous sinuses, without calcifications or acute intracranial hemorrhage (Figure 1).

Subsequent MRI revealed bilateral parasellar lesions showing hypointense signal on T1-weighted images and heterogeneous hyperintensity on T2-weighted and FLAIR sequences, with mild heterogeneous contrast enhancement (Figure 1). The larger left-sided lesion measured up to 2.7 cm, while the right-sided lesion measured up to 1.5 cm. Both lesions were closely related to the cavernous segments of the internal carotid arteries, causing

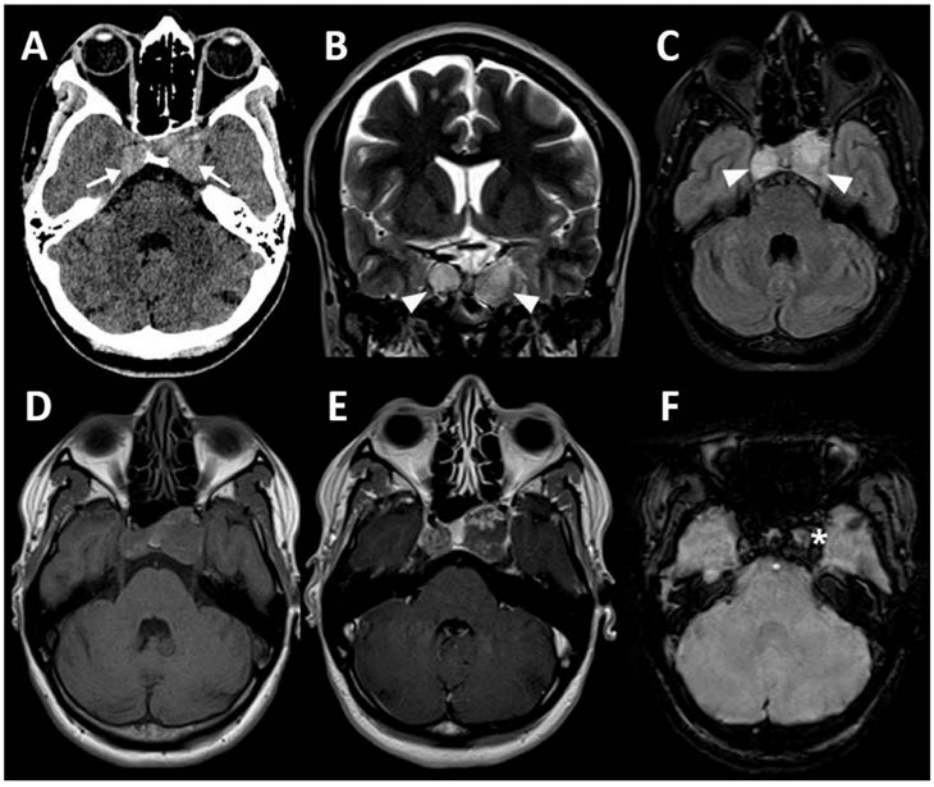

Figure 1. Brain computed tomography and magnetic resonance imaging scans revealing expansile lesions in both cavernous sinuses, hyperdense on CT (white arrows in **A**), with hyperintensity on T2-weighted and FLAIR sequences (white arrowheads in **B** and **C**), showing a reticulated pattern of enhancement (**D/E**) and blooming effect on SWI (asterisk in **F**).

lateral displacement without significant luminal narrowing. Mild expansion of the cavernous sinuses was observed without relevant sellar floor destruction or optic chiasm compression.

Susceptibility-weighted imaging (SWI) demonstrated marked blooming artifact in both lesions, suggesting hemorrhagic and vascular components (Figure 1). Despite this finding, the initial radiological impression favored a nonfunctioning pituitary macroadenoma with bilateral cavernous sinus extension, given the parasellar location and the rarity of alternative diagnoses.

Endocrinological evaluation demonstrated no hormonal abnormalities. After 12 months of follow-up, during which the patient remained symptomatic, elective transsphenoidal surgery was performed.

Intraoperatively, the lesion proved extremely friable and highly vascular, with profuse bleeding after initial manipulation, preventing safe resection. The procedure was therefore limited to hemostasis and incisional biopsy.

Histopathological analysis demonstrated dilated vascular spaces lined by flattened endothelial cells without atypia, associated with areas of previous hemorrhage and focal thrombosis. Immunohistochemistry demonstrated CD34 positivity, confirming the diagnosis of cavernoma (Figure 2).

Given the elevated surgical risk and postoperative neurological stability, conservative management with serial imaging follow-up was elected.

DISCUSSION

Cavernous sinus cavernomas are rare vascular lesions that may mimic invasive pituitary macroadenomas and other parasellar tumors. Bilateral involvement is exceptionally uncommon, with only a few cases reported in the literature. Headache, cranial neuropathies, diplopia, and visual disturbances are the most common clinical manifestations, usually resulting from mass effect on adjacent neurovascular structures.

MRI plays a central role in the diagnosis of cavernous sinus cavernomas. Spontaneous hyperdensity on CT and marked blooming artifact on susceptibility-sensitive sequences are important imaging findings suggestive of a vascular and/or hemorrhagic lesion[4]. Blooming artifact corresponds to marked hypointensity on susceptibility-sensitive sequences caused by magnetic susceptibility effects, resulting in an apparent increase in lesion size compared with conventional MRI sequences. In the present case, the pronounced susceptibility artifact was atypical for pituitary macroadenoma and, in retrospect, could have suggested the diagnosis of cavernoma.

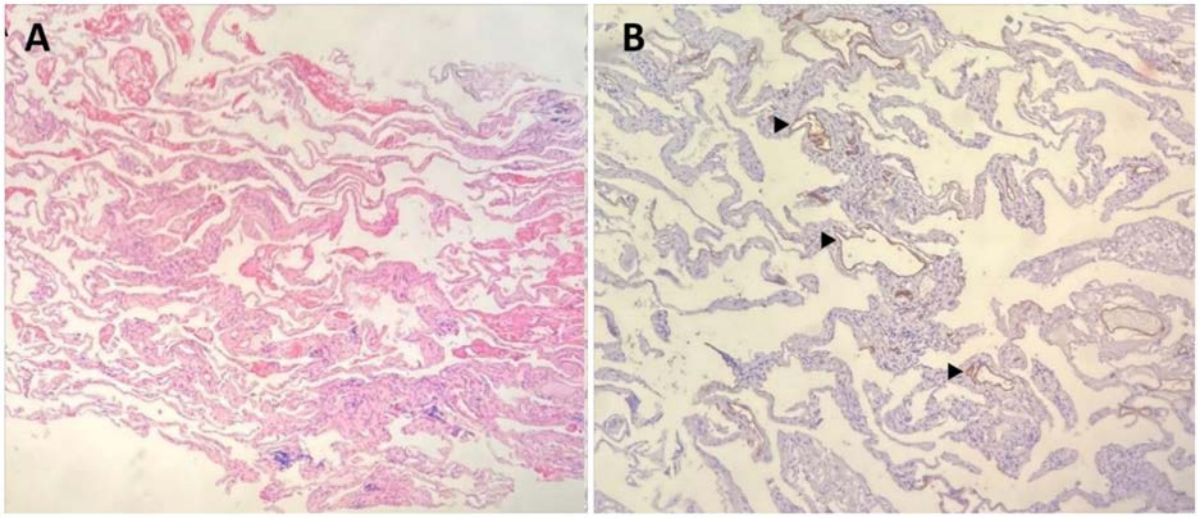

Figure 2. Hematoxylin–eosin–stained histological section at 100x magnification demonstrating extensive branching vascular channels (**A**). Immunohistochemical section at 200x magnification showing endothelial immunopositivity for CD34 (black arrowheads in **B**). This constellation of findings is consistent with the diagnosis of cavernoma.

Surgical management remains challenging because these lesions are highly vascular and closely related to critical neurovascular structures. Unexpected intraoperative hemorrhage may significantly increase morbidity and limit safe resection. Consequently, conservative management or stereotactic radiosurgery may be considered in selected cases[5].

CONCLUSION

Cavernous sinus cavernoma should be considered in the differential diagnosis of parasellar lesions, particularly when marked susceptibility artifact is present on MRI. Accurate preoperative recognition is essential for surgical planning because these lesions may present substantial intraoperative bleeding risk and may benefit from less aggressive therapeutic strategies.

REFERENCES

1. Razek AAK, Castillo M. Imaging lesions of the cavernous sinus. AJNR Am J Neuroradiol. 2009;30(3):444-52. https://doi.org/10.3174/ajnr.A1398. PMid:19095789.

2. Mahalingam HV, Mani SE, Patel B, et al. Imaging spectrum of cavernous sinus lesions with histopathologic correlation. Radiographics. 2019;39(3):795-819. https://doi.org/10.1148/rg.2019180122. PMid:30978149.

3. Hassanzadeh S, Gao L, Alvarado AM, Camarata PJ, Lakis NS, Haeri M. Extra-axial cavernous angioma: a case report and review of the literature. Neurol Int. 2024;16(1):162-85. https://doi.org/10.3390/neurolint16010010. PMid:38251058.

4. Mendonça JLF, Viana SL, Matsumine M, Silva RFE, Viana MACB, Freitas FMO. Cavernous angioma of the cavernous sinus: imaging findings. Arq Neuropsiquiatr. 2004;62(4):1004-7. https://doi.org/10.1590/S0004-282X2004000600013. PMid:15608959.

5. Benson JC, Eschbacher KL, Raghunathan A, Johnson D, Kim DK, Van Gompel J. Cavernous sinus vascular venous malformation. AJNR Am J Neuroradiol. 2022;43(1):19-23. https://doi.org/10.3174/ajnr.A7343. PMid:34764085.

CORRESPONDING AUTHOR

Andrey Fillip Thomaz Ribeiro, MD
Universidade Federal do Rio de Janeiro – UFRJ
Rio de Janeiro, Rio de Janeiro, Brazil
E-mail: andreyftribeiro@gmail.com

Funding: *nothing to disclose.*
Conflicts of interest: *nothing to disclose.*
Institution: *Universidade Federal do Rio Janeiro.*

CRediT

Andrey Fillip Thomaz Ribeiro: Data Curation. Andrey Fillip Thomaz Ribeiro; Pedro Bernardo Berriel: Writing - Original Draft. Sérgio Ferreira Alves Júnior; Nina Ventura Wilner; Nathalie Henriques Silva Canedo: Writing - Review & Editing.

Sérgio Ferreira Alves Júnior; Nina Ventura Wilner: Supervision. Andrey Fillip Thomaz Ribeiro; Sérgio Ferreira Alves Júnior: Project administration.

HOSPITAL INC
INSTITUTO DE NEUROLOGIA DE CURITIBA

Responsável Técnico
Dr. André Giacomelli Leal
CRM-PR 21874

CENTRO DE FORMAÇÃO
RESIDÊNCIA MÉDICA

RECONHECIDAS PELO MEC

NEUROCIRURGIA*
NEUROLOGIA
ANESTESIOLOGIA
CARDIOLOGIA
CIRURGIA CARDÍACA

DKG KREBSGESELLSCHAFT

CENTRO INTERNACIONAL DE NEURO-ONCOLOGIA

International Fellowship Program – World Federation of Neurosurgical Societies

*Parcerias internacionais – Federación LatinoAmericana de Sociedades de Neurocirugía & Universitätsklinikum Tübingen

hospitalinc.com.br

Cerebral Vulnerability to Re-injury in Traumatic Brain Injury and Medical Pathologies: definition and proposal of classification

Vulnerabilidad Cerebral a la Reinjuria en el Traumatismo Craneoencefálico y Las Patologías Médicas: definición y propuesta de clasificación

Luis Rafael Moscote-Salazar[1]
Tariq Janjua[2]
Amit Agrawal[3]
Pratiksha Baliga[4]

Dear Editor,

Traumatic brain injury (TBI) is a leading cause of morbidity and mortality worldwide in all ages. While much is known about the acute and subacute phases of TBI, a critical dimension remains underexplored: the brain's vulnerability to re-injury[1,2], particularly in individuals with preexisting brain damage, either due to prior trauma or underlying medical conditions. Emerging evidence suggests that traumatic brain injury induces persistent neuroinflammatory, glymphatic, and neurovascular alterations that may increase susceptibility to subsequent neurological insults[3-5]. In clinical practice, some patients present not only with a new neurotrauma but with a brain that has already been structurally or functionally compromised. The interaction between the prior insult and a new traumatic event may lead to disproportionate neurological deterioration, delayed recovery, or persistent deficits[1,2]. Persistent axonal injury, chronic microglial priming, and impaired metabolic clearance may amplify secondary injury cascades even after relatively minor trauma[6-8]. Yet, current neurotrauma guidelines rarely address this vulnerability. This paper aims to introduce and define the concept of "vulnerability to re-injury" in neurotrauma, propose a classification framework, and discuss its implications for prevention, monitoring, and clinical decision-making.

Definition of Cerebral vulnerability

We define Cerebral vulnerability as a condition characterized by an increased susceptibility of the brain to further damage following prior injury and pathological changes due to exposure to a new harmful factor (e.g., physical trauma and other adverse conditions) because of previous injury or pathology. Such a condition means that the brain does not respond to the negative impact as it usually would; the ability to use protective and restorative responses is reduced. Recent experimental research shows that brain injury leads to significant changes in the regulation of neuroprotection and neuroimmune and glymphatic functions. The result is decreased brain resistance, and therefore increased chances of developing more serious problems after a new injury[3,5,7]. Thus, the idea of decreased cerebral reserve comes into play[4,5]. This definition takes into consideration both subjects with TBI history and patients suffering from diseases affecting their central nervous system, creating a basis for categorizing and managing these unique groups of patients. We present a conceptual model classifying cerebral vulnerability to repeated brain injuries into two categories based on the causes of brain damage. The model is beneficial in assessing and managing the risk of re-injury among patients with neurotrauma (Table 1). Brain diseases such as neurodegeneration and microvascular changes could be associated with low levels of cerebral reserve and adaptation to neuroprotective stimuli, resulting in rapid degeneration when exposed to secondary injuries[9-11].

[1]Department of Neurosurgery, AV Healthcare Innovators, LLC; Madison, WI, United States.
[2]The National Brain Aneurysm & Tumor Center, Minneapolis, United States.
[3]Department of Neurosurgery, All India Institute of Medical Sciences, Bhopal, Madhya Pradesh, India.
[4]Neurosurgery Research, Mahatma Gandhi Mission Institute of Health Sciences, Maharashtra, Mumbai, India.

Received Aug 3, 2026
Accepted Aug 6, 2026

Table 1. Types of cerebral vulnerability to re-injury.

Type	Definition	Underlying Condition	Key Features	Clinical Implication
Type I-Post-Traumatic Cerebral Vulnerability	Brain susceptibility due to a previous TBI	History of traumatic brain injury (any severity)	- Persistent axonal injury - Neurovascular dysregulation - Glial scarring - Metabolic fragility - Chronic neuroinflammatory priming	Increased risk of disproportionate damage after minor trauma (e.g., second-impact syndrome)
Type II-Medical Cerebral Vulnerability	Brain susceptibility due to non-traumatic medical conditions	Hepatic encephalopathy, small vessel disease, neurodegenerative disorders, metabolic or autoimmune encephalopathies	- Impaired baseline neuroprotection - Structural and functional vulnerability - Reduced recovery potential	Lower threshold for damage, rapid deterioration even after moderate trauma

Pathophysiological Rationale

Type I and Type II cerebral vulnerability likely share overlapping pathophysiological mechanisms, including excitotoxicity, chronic neuroinflammation, impaired glymphatic clearance, mitochondrial dysfunction, and neurovascular uncoupling, all of which may amplify secondary injury cascades after subsequent trauma[7,8]. Identification of the early stage of cerebral vulnerability may have significant clinical importance. Individuals suffering from either Type I or Type II cerebral vulnerability must be identified in advance, irrespective of their preserved Glasgow Coma Scale, owing to their tendency towards deterioration. Advanced monitoring using either invasive or non-invasive techniques may be necessary even in mild cases. An individualized approach to therapy, including early neuroprotection and better hemodynamic management, can positively impact the results. Identification of the stage of cerebral vulnerability can help design a personalized neurocritical management strategy, especially in geriatric individuals, professional athletes with repetitive brain injuries, and individuals with neurodegenerative and cerebrovascular diseases[1,11,12]. Consideration must be made regarding a more prolonged rehabilitation period and cognitive disabilities.

Case Illustrations

Type I: Post-Traumatic Cerebral Vulnerability

A 48-year-old man, who had suffered from moderate traumatic brain injury (TBI) four years ago, is brought to the emergency department because of an episode of a mild fall at home. No abnormality is found on initial computed tomography. However, 48 hours later, the patient manifests symptoms of acute confusion, imbalance, and seizures episodes. Magnetic resonance imaging indicates diffuse axonal injury (DAI)-like changes without hemorrhagic signs. Notwithstanding the minor extent of the secondary injury, there is a disproportionate neurological impairment probably caused by ongoing microstructural and neurophysiological damage. This scenario represents Type I cerebral vulnerability[1,2]. This kind of deterioration could be related to ongoing microstructural susceptibility and neurophysiological dysfunction that occurred in response to repeated TBI[1,12].

Type II: Medical Cerebral Vulnerability

A 72-year-old woman with type 2 diabetes and chronic small vessel disease presents after a minor head bump sustained while rising from bed. Her husband brought her to the emergency department.

Upon arrival, she was alert and oriented with a GCS of 15. Twelve hours later, she becomes lethargic and develops right-sided weakness. CT and MRI reveal no mass lesion, but show periventricular white matter changes and cerebral atrophy. The presence of existing neurological impairment in the patient, specifically autoregulatory impairment and microcirculatory disturbance, may have influenced her susceptibility and resulted in type II brain injury. Reduced cerebrovascular reserve and chronic white matter injury may lower the threshold for clinical decompensation after otherwise minor traumatic events[5,9]. We believe that developing clinical screening tools will help identify patients with heightened susceptibility to re-injury (prior TBI or underlying neurological conditions). Current guidelines on trauma management must include this concept for proper patient assessment, monitoring criteria, and management strategies.

In summary, cerebral susceptibility to secondary brain injury is a less appreciated but relevant clinical concept within neurotrauma medicine. Our introduction of the dichotomy between post-traumatic vulnerability (Type I) and medical vulnerability (Type II) will allow health care professionals to adopt patient-specific treatment approaches during the entire care process from triage through rehabilitation. Awareness of cerebral vulnerability may be a critical step toward customized neurotrauma management, providing for risk-based surveillance, targeted treatment protocols, and enhanced neurological outcomes.

REFERENCES

1. Longhi L, Saatman KE, Fujimoto S, et al. Temporal window of vulnerability to repetitive experimental concussive brain injury. Neurosurgery. 2005;56(2):364-74, discussion 364-74. https://doi.org/10.1227/01.NEU.0000149008.73513.44. PMid:15670384.

2. Laurer HL, Bareyre FM, Lee VM, et al. Mild head injury increasing the brain's vulnerability to a second concussive impact. J Neurosurg. 2001;95(5):859-70. https://doi.org/10.3171/jns.2001.95.5.0859. PMid:11702878.

3. Yang Z, Li P, Wei J. Perceiving traumatic brain injury from glymphatic system. Mol Psychiatry. 2025;30(11):5546-62. https://doi.org/10.1038/s41380-025-03126-6. PMid:40745390.

4. Kaniuk JK, Kumar D, Mazurek C, et al. From acute injury to chronic neurodegeneration: molecular mechanisms linking secondary brain injury to long-term pathology. Int J Mol Sci. 2025;26(15):7191. https://doi.org/10.3390/ijms26157191. PMid:40806328.

5. Katramadou A, Bender ES, Kanakis D. from traumatic brain injury to Alzheimer's disease: multilevel biomechanical, neurovascular, and molecular mechanisms with emerging therapeutic directions. Int J Mol Sci. 2026;27(3):1570. https://doi.org/10.3390/ijms27031570. PMid:41683989.

6. Bi D, Gao B, Shen Y, Dai Z, Yang S, Wang L. Traumatic brain injury and neurodegenerative diseases: the role of axonal injury and amyloid-β. Brain Res. 2025;1865:149873. https://doi.org/10.1016/j.brainres.2025.149873. PMid:40784618.

7. Zhu L, Huang S, Chen W, Li K, Sheng J. Cytokines and related signaling pathways in traumatic brain injury. Front Immunol. 2026;17:1738589. https://doi.org/10.3389/fimmu.2026.1738589. PMid:41756282.

8. Barker RB, Karakaya E, Baran D, et al. The glymphatic and meningeal lymphatic systems may converge, connecting traumatic brain injury progression with chronic traumatic encephalopathy onset. Mol Cell Neurosci. 2025;134:104031. https://doi.org/10.1016/j.mcn.2025.104031. PMid:40713001.

9. Simmonds E, Han J, Kirov G, Sharp DJ, Massey TH, Escott-Price V. Dementia risk due to traumatic brain injury in subtypes of dementia in the welsh population. Neurology. 2025;105(3):e213866. https://doi.org/10.1212/WNL.0000000000213866. PMid:40609060.

10. Edwards S, Corrigan F, Collins-Praino L. Lasting impact: exploring the brain mechanisms that link traumatic brain injury to Parkinson's Disease. Mol Neurobiol. 2025;62(6):7421-44. https://doi.org/10.1007/s12035-025-04706-x. PMid:39891816.

11. Howarth NE, Ji C, Batten J, et al. Neurodegenerative Disease and Association Football (NDAF): systematic review and meta-analysis. Int J Environ Res Public Health. 2025;22(5):806. https://doi.org/10.3390/ijerph22050806. PMid:40427919.

12. Brett BL, Sullivan ME, Asken BM, Terry DP, Meier TB, McCrea MA. Long-term neurobehavioral and neuroimaging outcomes in athletes with prior concussion(s)and head impact exposure. Clin Neuropsychol. 2025;39(8):2220-48. https://doi.org/10.1080/13854046.2024.2442427. PMid:39797596.

CORRESPONDING AUTHOR

Pratiksha Baliga, MD
Neurosurgery Research
Mahatma Gandhi Mission Institute of Health Sciences
Maharashtra, Mumbai, India
E-mail: drpratikshabaliga@gmail.com

Funding: *nothing to disclose.*
Conflicts of interest: *The authors declare that they have no conflict of interest.*

CRediT

Pratiksha Baliga, Amit Agrawal, Luis Rafael Moscote-Salazar: Conceptualization. Tariq Janjua: Data Curation. Luis Rafael Moscote-Salazar: Formal Analysis. Luis Rafael Moscote-Salazar: Methodology. Amit Agrawal: Project Administration. Tariq Janjua: Visualization. Pratiksha Baliga, Amit Agrawal, Luis Rafael Moscote-Salazar: Writing – Original Draft: Writing – Original Draft. Pratiksha Baliga: Writing – Review & Editing.

HOSPITAL INC

O único hospital do Paraná entre os melhores do Brasil.

(Eleito por médicos na pesquisa DataFolha 2025)

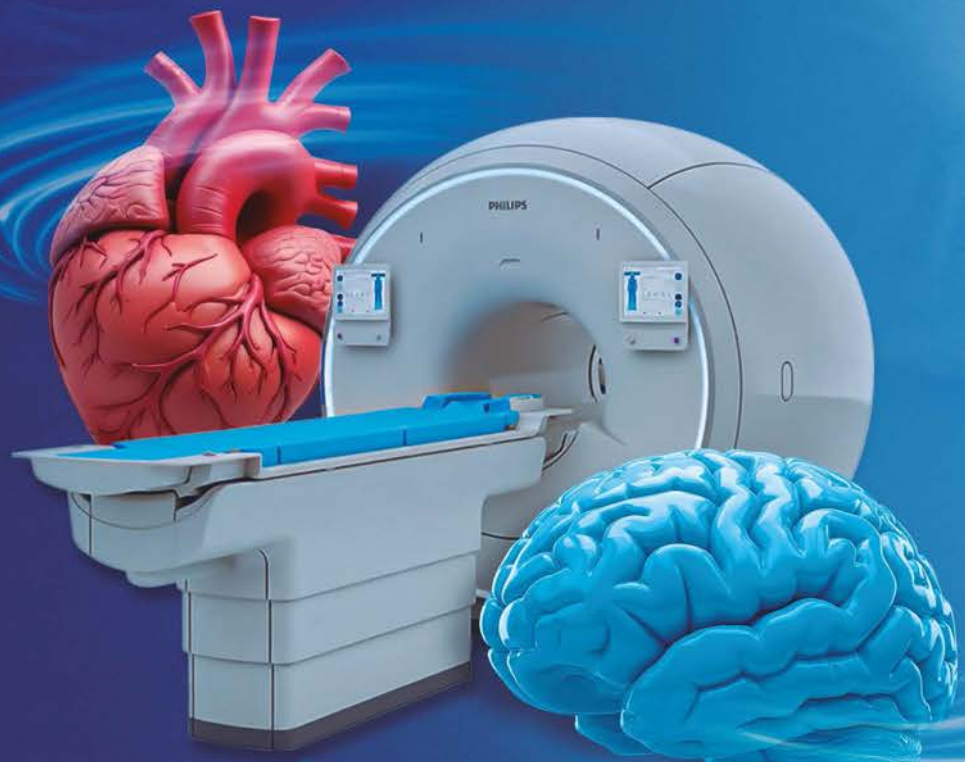

NEUROLOGIA

NEUROCIRURGIA

CARDIOLOGIA

CIRURGIA DA COLUNA

CENTRO DIAGNÓSTICO POR IMAGEM

E MUITO MAIS.

ESCOLHA O HOSPITAL QUE **OS MÉDICOS CONFIAM.**

HOSPITAL INC
INSTITUTO DE NEUROLOGIA DE CURITIBA

SEDE INC ECOVILLE

Rua Jeremias Maciel Perreto, 300,
Campo Comprido, Curitiba/PR

Diretor Técnico Médico: André Giacomelli Leal - CRM - PR 21874

Agende seu exame